Christian-Albrechts-Universität zu Kiel

Graduate School "Human Development in Landscapes"

CRC 1266: "Scales of Transformation - Human-Environmental Interaction in Prehistoric and Archaic Societies"

Human-environment dynamics across the Bronze Age in northern Italy: method testing and multi-proxy approaches

Dissertation

in fulfilment of the requirements for the degree of "Dr. rer. nat."

of the Faculty of Mathematics and Natural Sciences

at Kiel University

submitted by

Marco Zanon

Kiel, 2020

First referee: Prof. Dr. Wiebke Kirleis

Second referee: Prof. Dr. Ingmar Unkel

Date of oral examination: March 23, 2020

Table of Contents

Sworn declaration

I hereby confirm that the following statements are true and correct:

- apart from the supervisor's guidance, the content and design of the thesis are solely a product of Marco Zanon's own work,
- this thesis has not been previously submitted, either partially or as a whole, to another examining body as part of a different doctoral project. Sections of this thesis have been published in peer-reviewed journals in fulfillment of the requirements for the production of a cumulative dissertation. These already-published sections are clearly identified as such in the body of the dissertation,
- this production of this thesis was conducted in accordance to the Rules of Good Scientific Practice of the German Research Foundation,
- Marco Zanon never incurred in the withdrawal of any academic degree.

Abstract

Besides technological innovations and new typological features, the transition into the Bronze Age in northern Italy is marked by the adoption of distinctive settlement strategies. Prominent differences with previous periods are represented not only by higher numbers and density of settlements, but also by a widespread preference for wetland areas. These phenomena are particularly evident in the Lake Garda region, where a rising number of lacustrine pile-dwelling settlements is documented since the Bronze Age onset (approximately 4150 years cal. BP). The pile-dwelling phenomenon lasted approximately for one millennium, approximately until 3150 years cal. BP). At the end of the Late Bronze Age, this settlement system collapsed, leaving the area largely depopulated. Widespread settlement abandonment did not affect only the surroundings of Lake Garda. In the neighboring central Po Plain, a dense network of riverine villages developed since approximately 3500 years cal. BP. These moat-and-rampart villages, locally termed "terramare", abruptly disappeared together with the last pile dwellings. The reasons behind the rise and demise of these extensive lacustrine and riverine settlement networks remain currently open for discussion. Palaeoecological studies conducted in the area focused mostly on developing qualitative land-use narratives for the Bronze Age. As a result, multiple questions remain to be addressed concerning the determination of local climate trajectories. Similarly, quantitative land-cover approaches are left largely unexplored. Given these premises, this project aims at improving the available knowledge concerning both the role of climate and land use dynamics in northern Italy across the Bronze Age and neighboring periods, with a special focus on the pile-dwelling phenomenon in the southern Lake Garda region. The results are presented in the form of a cumulative dissertation composed of three published papers. The first of these three contributions focuses on the sedimentary record of Bande di Cavriana, a drained wetland in the Lake Garda area. Here, palynological and geochemical analysis provided new evidences that the rise of the Bronze Age pile-dwelling phenomenon occurred under a rapidly changing climate. The second paper focuses on the collapse of Bronze Age settlement networks. Pollen-based temperature and precipitation models obtained from Northern Italian sites depict increasingly arid conditions towards the end of the Bronze Age. This reconstruction is in agreement with the current archaeological narrative, which attributes the end of the central Po Plain settlement networks to a combination of landscape overexploitation and to the emergence of unsuitable climatic conditions. The third contribution serves primarily a methodological role within this project. It provided the opportunity to test extensively a landscape reconstruction algorithm based on pollen data and remote sensing. The application of this method to pollen sequences from Lake Garda provided a very first quantitative reconstruction of land cover changes across the Copper Age- Bronze Age transition, in connection with the establishment of the first pile-dwelling settlements.

Zusammenfassung

In Norditalien ist der Übergang in die Bronzezeit neben technologischen Innovationen und neuen typologischen Merkmalen durch die Einführung veränderter Siedlungsstrategien gekennzeichnet. Auffällige Unterschiede zu früheren Perioden zeigen sich nicht nur in einer erhöhten Anzahl und Dichte der Siedlungen, sondern auch durch eine weit verbreitete Präferenz für Feuchtgebiete. Besonders deutlich werden diese Phänomene in der Region des Gardasees, wo seit Beginn der Bronzezeit (ca. 4150 Jahre cal. BP) zunehmend Pfahlbausiedlungen an Seeufern dokumentiert sind. Das Pfahlbauphänomen dauerte etwa ein Jahrtausend, bis 3150 Jahre cal. BP). Am Ende der späten Bronzezeit brach dieses Siedlungssystem zusammen, so dass das Gebiet weitgehend entvölkert blieb. Die weit verbreitete Siedlungsaufgabe betraf nicht nur die Umgebung des Gardasees. In der benachbarten zentralen Po-Ebene entstand seit etwa 3500 Jahren cal? BP ein dichtes Netz von an Flussufern gelegenen Dörfern. Diese mit Wassergraben und Wall eingefassten Dörfer, bekannt als "Terramare", verschwanden abrupt zusammen mit den letzten Pfahlbauten der nördlcih angrenzenden Region. Die Gründe für das Aufkommen und den Zusammenbruch dieser ausgedehnten Siedlungsnetze an See- und Flussufern stehen derzeit noch zur Diskussion. Paläoökologische Studien, die in diesem Gebiet durchgeführt wurden, konzentrierten sich vor allem auf die Entwicklung qualitativer Landnutzungsnarrative für die Bronzezeit. Welchen Einfluß lokale Klimaphänomene hatten, mussnoch geklärt werden. Ebenso bleiben quantitative Landnutzungsansätze weitgehend unerforscht. Die hier vorgestellten Forschungen zielen darauf ab, das verfügbare Wissen zur Rolle der Klima- und Landnutzungsdynamik in Norditalien über die Bronzezeit und benachbarte Perioden hinweg zu verbessern, wobei ein besonderer Schwerpunkt auf das Pfahlbauphänomen in der südlichen Gardasee-Region gelegt wird. Die Ergebnisse werden in Form einer kumulativen Dissertation präsentiert, die wesentlich auf drei bereits veröffentlichten Artikeln basiert. Der erste dieser drei Beiträge konzentriert sich auf die Auswertung und Interpretation von Sedimentsequenzen von Bande di Cavriana, einem entwässerten Feuchtgebiet in der Gardaseeregion. Hier liefern palynologische und geochemische Analysen neue Belege dafür, dass der Aufstieg des bronzezeitlichen Pfahlbauphänomens unter einem sich schnell verändernden Klima erfolgte. Der zweite Artikel konzentriert sich auf den Zusammenbruch der bronzezeitlichen Siedlungsnetzwerke. Pollenbasierte Temperatur- und Niederschlagsmodelle von norditalienischen Standorten zeigen zunehmend trockene Bedingungen gegen Ende der Bronzezeit an. Diese Rekonstruktion steht im Einklang mit der aktuellen archäologischen Bewertung, die das Ende der zentralen Siedlungsnetzwerke der Po-Ebene auf eine Kombination von Übernutzung der Landschaftund einen Wechsel zu ungünstigen Klimabedingungen zurückführt. Der dritte Beitrag dient in erster Linie der Methodenentwicklung. Hier wird einn Algorithmus zur Landschaftsrekonstruktion auf der Grundlage von Pollendaten und Fernerkundung ausgiebig getested. Die Anwendung dieser Methode auf Pollensequenzen aus der Gardasee-Region liefert eine erste quantitative Rekonstruktion der Landnutzungsänderungen am Übergang Kupferzeit-Bronzezeit im Zusammenhang mit der Errichtung der ersten Pfahlbausiedlungen.

List of Figures

Part III

Part IV

Part V

Appendix I

Appendix II

Appendix III

List of Tables

PART I

SETTING THE FRAME: THE BRONZE AGE PILE-DWELLING PHENOMENON IN NORTHERN ITALY

The core of this research project is centered on the investigation of human-environment interactions within a relatively well-constrained time-window and study region: the Bronze Age in the southern Lake Garda area (Northern Italy; Figs. 1.1-1.2). The reason behind this choice lies in the highly peculiar archaeological record of this period compared to the situations that immediately preceded and followed it.

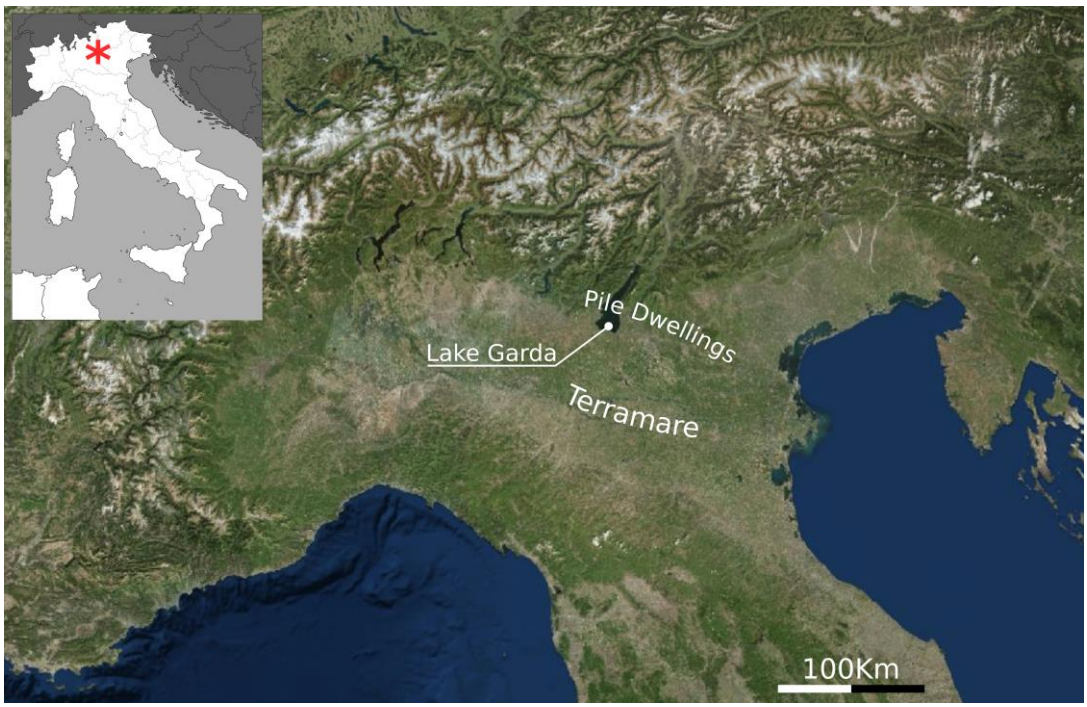

Figure 1.1. *Location of Lake Garda within northern Italy and main Bronze Age settlement networks (pile-dwellings and Terramare) between Lake Garda and the Apennine foothills (de Marinis, 2010). Map source: Italian National Geoportal (http://www.pcn.minambiente.it).*

The transition between Copper and Bronze Age in the Lake Garda area -conventionally set at 4150 years cal. BP (2200 years BC; de Marinis, 1999; Leonardi et al., 2015)- is accompanied by a marked shift in settlement patterns, building techniques and density of archaeological finds. With limited exceptions, the local Neolithic and Copper Age records are characterized by rather rare archaeological traces (predominantly sparse flint tools and pottery sherds; de Marinis, 2000). In contrast, about 50 dwelling sites have been documented for the Bronze Age (de

Marinis, 2010; Fig. 1.3). This increase in site density is apparently accompanied by a preference for damp locations. More than 30 wetland settlement sites are recorded in the area, either along the shores of Lake Garda itself, or within the many smaller water bodies scattered in its vicinities (de Marinis, 2010; Poggiani Keller et al., 2005). Most notably, new villages were established in the form of pile dwellings. The adoption of pile-dwelling building techniques was a common feature during the Neolithic across different circum-alpine regions (e.g. Menotti, 2015). Yet, in northern Italy this phenomenon is limited to few sites before its widespread rise during the Bronze Age (Baioni et al., 2014).

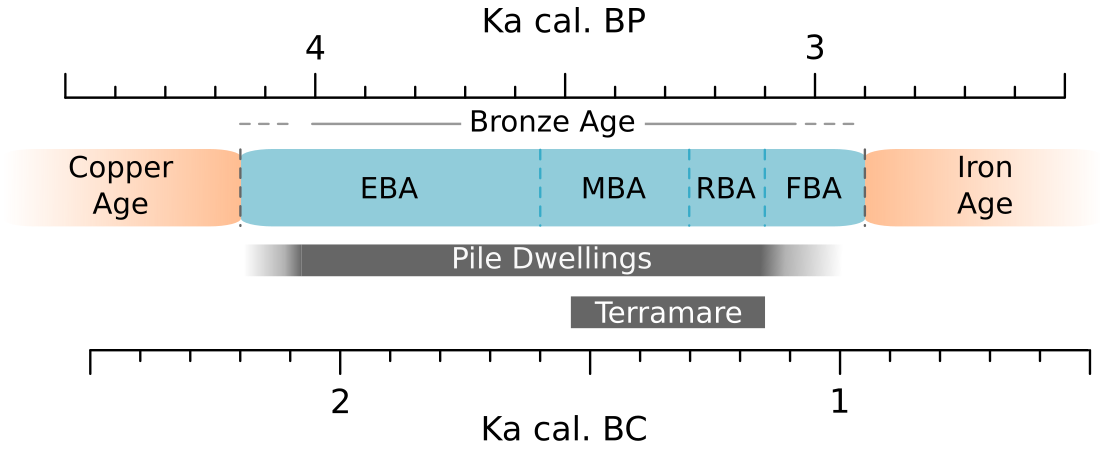

Figure 1.2. *Chronological contextualization of the Bronze Age pile-dwelling and Terramare phenomena. EBA: Early Bronze Age, MBA: Middle Bronze Age, RBA: Recent Bronze Age, FBA: Final Bronze Age. The chronological subdivision follows de Marinis (1999) and de Marinis (2010).*

Small lakes and wetlands are particularly abundant in the study area due to its geomorphological configuration. The southern shores of Lake Garda are surrounded by a series of concentric moraine belts produced by multiple episodes of advance and retreat of the Garda glacier during the Pleistocene (Ravazzi et al., 2014). Following the glacier's retreat, inter-moraine depressions were occupied by water bodies, thus forming a tightly clustered lacustrine network that apparently proved attractive to Bronze Age settlers. Many of these lakes and wetlands survived across the Holocene, in multiple cases being drained only in recent times for agricultural purposes or peat exploitation. The combination of stable waterlogged conditions and gradual sediment accumulation over the past millennia allowed for an excellent preservation of wooden settlement structures and other organic remains located within these basins, with Bronze Age pile-dwellings being a foremost example.

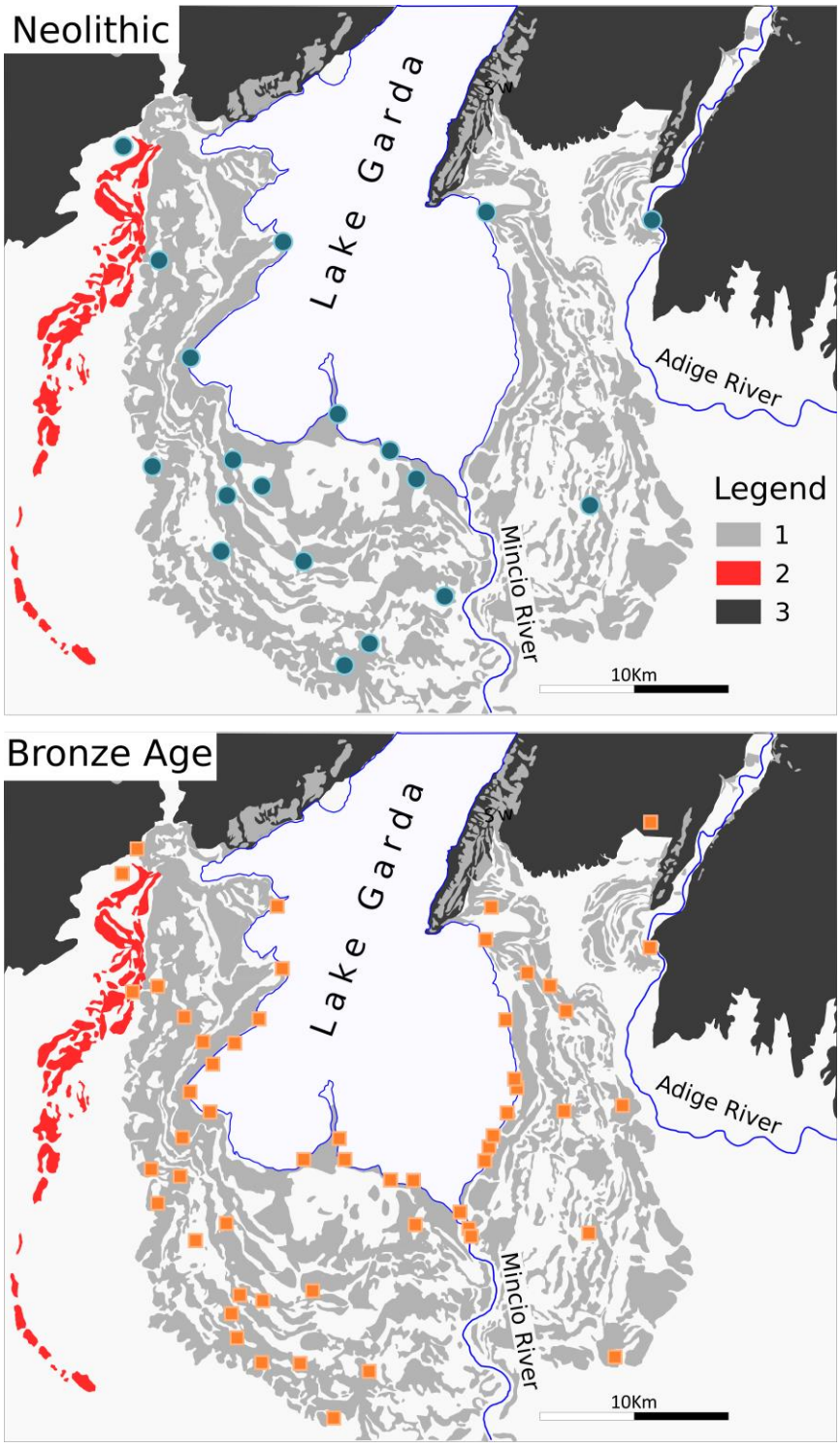

Figure 1.3. *Neolithic (circles) and Bronze Age (squares) sites in the southern Lake Garda area. Modified from de Marinis (2000), with additional data from Poggiani Keller, 2014 and Poggiani Keller et al., 2005. The contours of the topographic features are based on Venzo (1965). Legend: 1) Late Pleistocene moraines (Cremaschi, 1987; Ravazzi et al., 2014). 2) Mid-Pleistocene moraines (Venzo, 1965). 3) Alpine foothills.*

The quality and amount of archaeological information stored in these wetland deposits allows to reconstruct prehistoric craftsmanship and subsistence strategies with a level of detail not achievable on dryland sites. In recognition of this rather exceptional trove of information, a selection of Lake Garda pile-dwelling settlements were included in the UNESCO World Heritage serial site "Prehistoric Pile Dwellings around the Alps" (World Heritage Committee, 2011), together with multiple wetland sites dated between the Neolithic and the Iron Age from different circum-alpine countries.

Importantly, pile-dwellings did not constitute the only distinctive settlement system active during the Bronze Age in northern Italy. From approximately 3500 years cal. BP (1550 years BC), during the Middle Bronze Age, a different network of villages rose in the central Po Plain, south of Lake Garda (Fig. 1.1). These new settlements, termed *Terramare* (singular: *Terramara*), were surrounded by earthen ramparts and moats directly connected to nearby rivers (Cardarelli, 2010). Numerous palaeoenvironmental studies have been conducted on the development and environmental impact of Terramare sites (e.g. Dal Corso et al., 2016; Mercuri et al., 2015, 2006; Ravazzi et al., 2004) and now constitute organic components of local archaeological narratives (e.g. Cardarelli, 2010; Cremaschi, 2009; Cremaschi et al., 2016, 2006; Dalla Longa et al., 2019). Given the geographical proximity of pile-dwelling and Terramare areas, as well as their cultural connections, information emerging from the latter is occasionally used within this dissertation to better contextualize changes observed in the former.

The emergence of the Bronze Age pile-dwellings, while not necessarily abrupt (Baioni et al., 2015), represents a marked shift from any preceding cultural pattern. The peculiarity of this phenomenon is furtherly accentuated by its sudden demise, which occurred approximately 1000 years after the onset of the Bronze Age. After approximately 3150/3100 years cal. BP (1200/1150 years BC), the settlement system in the Lake Garda area largely came to an end, leaving a visible discontinuity in the archaeological record (Fig. 1.4). The Final Bronze Age (Fig. 1.2) is represented only by stray finds (de Marinis, 2010). This widespread settlement collapse was not limited to the Lake Garda region. The Terramare network was affected too. A cultural break is visible in the plain north of the Po River, where new settlement patterns emerged (Fig. 1.4). More dramatic was the situation in the southern Po Plain, which remained largely depopulated until the Iron Age (Cardarelli, 2010; de Marinis, 2010).

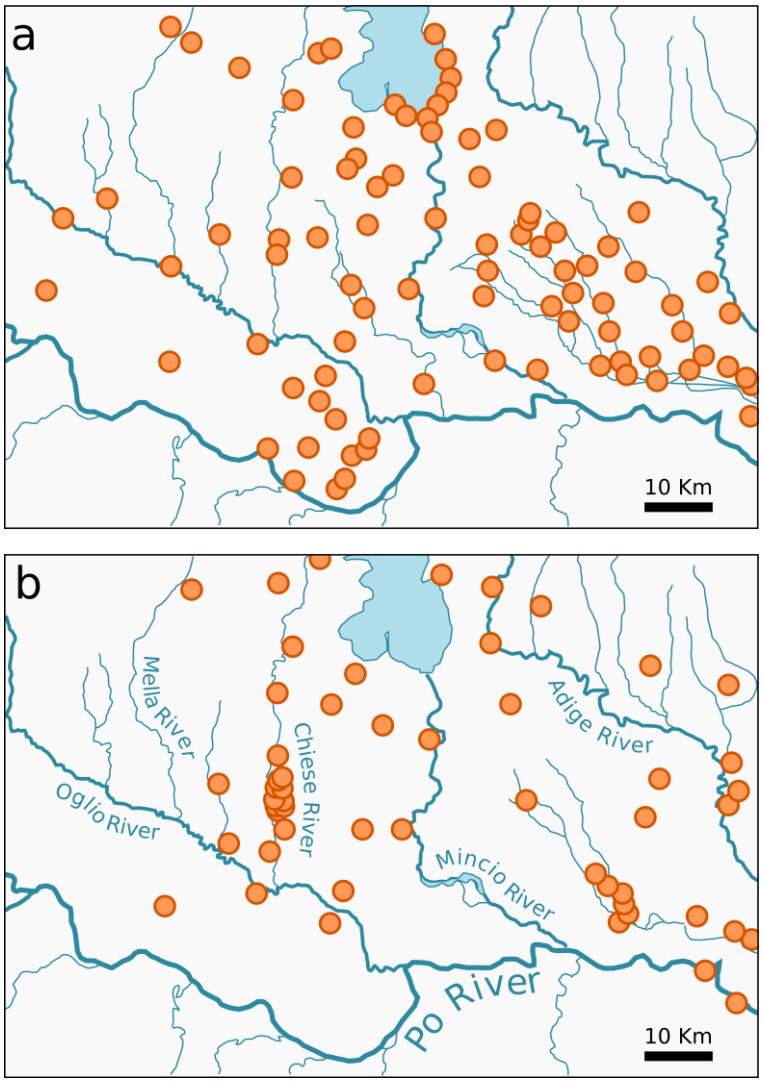

Figure 1.4. *Distribution of Recent Bronze Age (a) and Final Bronze Age (b) sites between the Lake Garda and Po River. Modified from de Marinis (2010).*

Tackling socio-environmental triggers: ongoing hypothesis and data availability

The reasons behind the rise of the pile-dwelling phenomenon and its subsequent decline remain open to debate. The preference for wetland contexts has been interpreted as a necessity to protect people and livestock from external threats, such as forest fires or -given the presence of perimetral palisades- other human communities (de Marinis, 2000). A climatic component was considered too, suggesting that widespread lake level declines might have exposed areas with soft and fertile sediments. Compared to forested areas, these peri-lacustrine belts would have been easier to cultivate, making them preferred locations to establish new settlements

(de Marinis, 2000). Climate is currently considered an important driver in the determination of local-to-regional settlement dynamics. As an example, the vertical wooden posts supporting the Lavagnone pile dwelling show signs of structural failure (all beams display a ~45° bend in one direction) approximately between 3850 and 3750 years cal. BP (1900-1800 years BC). The same situation was recognized at the pile-dwelling sites of Bande di Cavriana, Barche di Solferino and Lucone di Polpenazze (de Marinis, 2000; Piccoli, 1986). This common feature was interpreted as the possible result of a regional dry event, which would have caused a significant drop in lake levels and a subsequent destabilization of the lake sediments in which the foundations of the pile-dwellings were infixed (de Marinis, 2000). Climate is also considered a determinant co-factor in the final collapse of north Italian Bronze Age networks. In the Terramara settlement of Santa Rosa, located ca. 60 km south of Lake Garda, a sequence of wells dug at increasing depths appears to suggest a significant lowering of the water table towards the end of the Bronze Age (Cremaschi et al., 2006). At the same time, the dense network of villages points to a growing demographic pressure on the environments. Increasingly arid condition and over-exploitation of natural resources might have then caused water and food shortages (Cremaschi et al., 2016), fatally lowering the carrying capacity of local environments.
Importantly, any inclusion of climatic triggers in local archaeological narratives is often only loosely supported by proper comparisons between cultural data and local palaeoclimatic information. As an example, de Marinis (2000) briefly compares Bronze Age settlement patterns in the Lake Garda area with lake-level trends from France and Switzerland (Magny, 1995). The same argument was mentioned more recently in Rapi (2013). A more comprehensive comparison between archaeological data and extra-local palaeoclimatic proxies is presented by Cremaschi et al. (2016) concerning the end of the Terramare network. Cremaschi et al. (2016) compare central Po Plain archaeological dynamics with alpine glacier fluctuations (Lockwood, 2001), changes in solar activity (Blaauw et al., 2004) and lake-level reconstructions from alpine and central Italian lakes (Magny et al., 2012). A common pattern across the available literature is the lack of palaeoclimatic time series located directly within the study area. A notable exception is represented by the isotopic record of Lake Frassino (southern Lake Garda area, Baroni et al., 2006), which nonetheless lacks sufficient chronological resolution and dating accuracy across the Bronze Age. Any comparison against extra-local proxies is indeed justified, since small study regions can without any doubt be affected by continental- or global-scale climate change. Nonetheless, it would be equally important to obtain palaeoclimatic reconstructions

located closer to the area under investigation, in order to evaluate to which extent local dynamics are comparable to wider-scale trends. Few more palaeoclimatic information from the southern Lake Garda and central Po Plain do exist, yet they occur as rather constrained stratigraphic information. The most recent example comes from the Terramara site of Fondo Paviani (ca. 60 km SE of Lake Garda), where a short-lived arid phase occurring towards the end of the Bronze Age (ca. 3200 years cal. BP; 1250 years BC) was identified through the presence of gypsum crystals in a near-site sedimentary sequence (Dal Corso, 2018; Dalla Longa et al., 2019). Earlier evidences for a dry phase in the second half of the Bronze Age come from the pile-dwelling site of Lavagnone. Here, the presence of burrowing-bee nests dug in the basin infilling has been connected to a desiccation trend occurring after ca. 3400-3300 years cal. BP (1450-1350 years BC; Perego et al., 2011).

Climate forcing and population resilience are not the only pressing research questions when it comes to human-environment interactions in the pile-dwelling area. The sudden increase in site density recorded during the Bronze Age, paired with the large amount of wooden structures emerging from archaeological excavations, raises also multiple questions concerning the environmental impact of the lake-dwelling phenomenon. As an example, a major change in building techniques is recorded in the Lavagnone sequence. Here, before approximately 3900 years cal. BP (1950 years BC), pile-dwelling structures were built upon long poles deeply infixed into the lake floor. Afterwards, this solution was replaced by shorter poles stabilized through horizontal basal plates (de Marinis et al., 2005), possibly suggesting a diminished availability of appropriately-sized trees. Besides archeological evidence, qualitative information on landscape exploitation comes primarily from pollen diagrams. Within the southern Lake Garda area, published data is available from the wetland sites of Lucone (Badino et al., 2011; Valsecchi et al., 2006), Lavagnone (Arpenti et al., 2007; de Marinis et al., 2005; Perego, 2015) and Castellaro Lagusello (Dal Corso, 2018). These diagrams show a marked decline in arboreal species in connection with the establishment of Bronze Age settlements, generally interpreted as widespread logging for building materials. The contemporaneous rise of anthropogenic species (e.g. cereals, disturbance-resistant herbaceous taxa) is linked to an expansion of croplands and pastures. These patterns are consistent across multiple sites, and are radically different from Neolithic and Copper Age vegetation dynamics, ultimately suggesting that Bronze Age societies did have an unprecedented impact on the landscape. Still, these pollen diagrams offer only a markedly qualitative perspective on land cover and land use changes. Transitioning from qualitative pollen information to quantitative

land cover data is a notoriously complex task requiring careful calibration procedures, yet addressing this issue might help to understand how local communities were managing forest resources and whether they contributed to their own demise through landscape overexploitation.

Research rationale and structure of this PhD thesis

The available data depicts the Bronze Age as a period extremely rich in environmental and cultural transformations. At the same time, it is also clear that additional studies are needed to capture the complexity of these human-environment interactions. A first point that needs to be addresses is the lack of local palaeoclimatic records. Obtaining this piece of information represents a necessary step in order to understand if comparisons with extra-local proxies are appropriate, or if the southern Lake Garda region -which now represents a peculiar sub-Mediterranean enclave between the Alps and the Po Plain- displays more resilient or completely independent patterns. The second key issue is represented by our still limited understanding of Bronze Age land-use dynamics. Claiming that wetland settlements had an impact on the environment represents a reasonable assumption. Furthermore, the available palynological studies, while not numerous, depict very coherent environmental transformations at the transition into the Bronze Age. The (at least apparent) homogeneity of this situation suggests that ecological studies in this area should be taken one step further, moving from qualitative approaches to quantitative reconstructions. This task is admittedly complicated by different interfering factors, such as the complete lack of true off-site records (i.e. pollen sequences reasonably not affected by "non-natural" pollen deposition, like waste disposal from nearby pile-dwellings). In addition, vegetation modeling has not been attempted before in any capacity in the study area, rising the necessity to properly test any land-cover modeling procedure.

Given these premises, this PhD project aims at testing existing archaeological and environmental narratives in the southern Lake Garda area by integrating published information with new analysis. This objective is pursued a) through the production of new vegetational data and climatic models, which are then evaluated against existing proxies, and b) by testing the performance of landscape reconstruction algorithms and their applicability to the study area. Vegetation assemblages and environmental parameters are primarily reconstructed via pollen analysis of wetland sediments and pollen-based quantitative modeling. Additional geochemical proxies

are also used to achieve a deeper insight into local dynamics by looking at similar drivers (e.g. temperature/precipitation trends) under multiple points of view.

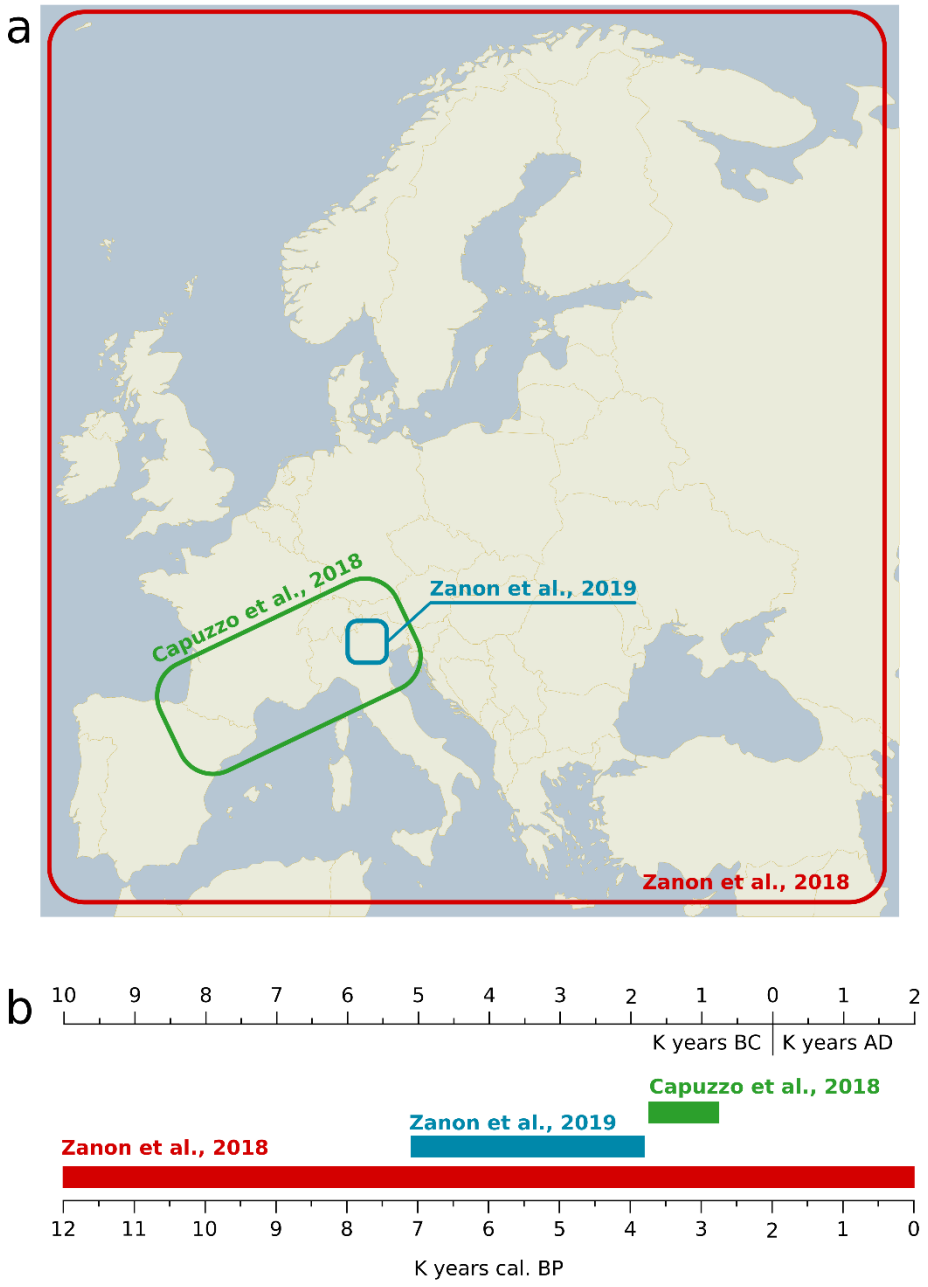

Figure 1.5. *Spatial (a) and chronological (b) windows covered by each research paper produced within this PhD project.*

The main conclusions of this project are collected in three peer-reviewed publications, which variously contribute to address the different research issues identified so far:

1. **Zanon M.**, Unkel I., Andersen N., Kirleis W., 2019. *Palaeoenvironmental dynamics at the southern Alpine foothills between the Neolithic and the Bronze Age onset. A multi-proxy study from Bande di Cavriana (Mantua, Italy)*. Quaternary Science Reviews, 221.
2. Capuzzo G., **Zanon M.**, Dal Corso M., Kirleis W., Barceló J.A., 2018. *Highly diverse Bronze Age population dynamics in Central-Southern Europe and their response to regional climatic patterns*. PLOS ONE, 13.
3. **Zanon M.**, Davis B.A.S., Marquer L., Brewer S., Kaplan J.O., 2018. *European Forest Cover During the Past 12,000 Years: A Palynological Reconstruction Based on Modern Analogs and Remote Sensing*. Frontiers in Plant Science, 9.

As it is evident from the papers' titles, they variously exceed the spatial and chronological limits of the study area. Figure 1.5 provides a concise overview of the extent covered by each research article. The first paper (Zanon et al., 2019) is the only one that remains well within the northern Italian borders. Its primary focus consists in addressing the climatic and land cover context in the millennia that precede the Bronze Age onset. This time span is not properly addressed by previous publications dealing with the southern Lake Garda area, and represents a necessary piece of information to contextualize the rise of the pile-dwelling phenomenon.
The second article (Capuzzo et al., 2018) covers instead the end of the Bronze Age and the transition into the Iron Age, thus addressing the collapse of the pile-dwelling and Terramare networks. This paper makes an extensive use of modeling approaches. Socio-environmental dynamics are explored through a comparison between radiocarbon-based population curves and pollen-based climate reconstructions. The Bande di Cavriana pollen sequence, discussed in Zanon et al. (2019), does not cover the end of the Bronze Age, and therefore is not included in this paper. Climate modeling in Capuzzo et al. (2018) is instead performed using previously published pollen sequences from the central Po Plain and northwestern Italy. Within this paper, the same modeling techniques are also applied to other European regions ranging from the Swiss Plateau to the northeastern Iberian coast. Producing independent demographic and climatic reconstructions across different regions allowed to highlight how different trajectories occurred at the same time in neighboring areas. More importantly, this approach extended the testing ground for the demographic

and climate models, leading to a better understanding of their strengths and weaknesses.

The third paper (Zanon et al., 2018) serves primarily a methodological purpose within this PhD project. It addresses the need to extensively test a modeling algorithm prior to proceeding with land-cover reconstructions in the study area. The widely-used landscape reconstruction model REVEALS (Sugita, 2007) depends on local vegetation parameters (i.e. pollen productivity estimates) to be tested properly. This information is currently not available for the southern alpine area and is notoriously labor-intensive to obtain and validate (Broström et al., 2008). For this reason, the modeling effort in Zanon et al. (2018) is based on a more readily applicable and testable method which makes use of modern pollen analogues and remote sensing data. With limited exceptions (Williams et al., 2011), this modern analogue technique (MAT) lacks proper testing on European vegetation assemblages. Given the need to explore its capabilities across a wide range of land cover types (e.g. pre-agriculture and agricultural landscapes), it was directly tested at a continental scale and across the whole Holocene. This wide spatial and chronological reach allowed also to test the MAT-based reconstructions against other existing REVEALS-based models for different European areas, thus ensuring a rather in-depth evaluation of the method.

Each research article is reported in full within this dissertation: Zanon et al. (2019) is presented in Part II; Capuzzo et al. (2018) in Part III and Zanon et al. (2018) in part IV. The papers are not presented in order of publication. Zanon et al. (2019) is introduced first, since it deals with the transition into the Bronze Age. It is then followed by Capuzzo et al. (2018), which addresses the end of the Bronze Age. Zanon et al. (2018) is presented last, since its methodological focus is not specifically centered on the southern Lake Garda area. The content of each paper is reported exactly as published, with the exception of figure and table numbers, which have been adapted to the structure of this dissertation, and minor typos. All articles are preceded by an introductory section, which provides further information on the role of each paper within this project.

Bibliography

Arpenti, E., Ravazzi, C., Deaddis, M., 2007. Il Lavagnone di Desenzano del Garda: analisi pollinica ed informazioni paleoecologiche sui depositi lacustri durante le prime fasi d'impianto dell'abitato (antica età del Bronzo). Notizie Archeologiche Bergomensi 10 (2002), 35–54.

Badino, F., Baioni, M., Castellano, L., Martinelli, N., Perego, R., Ravazzi, C., 2011. Foundation, development and abandoning of a Bronze Age pile-dwelling ("Lucone d", Garda Lake) recorded in the palynostratigraphic sequence of the pond offshore the settlement. Il Quaternario e Italian Journal of Quaternary Sciences 24.

Baioni, M., Grassi, B., Mangani, C., Martinelli, N., 2014. Pile-dwelling villages of northern Italy: research and finds, in: Archaeology of Lake Settlements, IV–II Mill. BC: Chronology of Cultures, Environment and Palaeoclimatic Rhythm. Materials of International Conference Dedicated the Semi-Centennial Anniversary of the Researches of Lake Dwellings in North-Western Russia Saint-Petersburg, 13–15 November 2014. pp. 311–316.

Baioni, M., Longhi, C., Mangani, C., Martinelli, N., Nicosia, C., Ruggiero, M.G., Salzani, P., 2015. La palafitta del Corno di Sotto (Desenzano del Garda, Brescia) nell'ambito dello sviluppo dei primi insediamenti palafitticoli del lago di Garda, in: Leonardi, G., Tiné, V. (Eds.), Preistoria e protostoria del Veneto, Studi di preistoria e protostoria. Istituto italiano di preistoria e protostoria ; Soprintendenza per i beni archeologici del Veneto : Università degli studi di Padova, Firenze : Padova.

Baroni, C., Zanchetta, G., Fallick, A.E., Longinelli, A., 2006. Mollusca stable isotope record of a core from Lake Frassino, northern Italy: hydrological and climatic changes during the last 14 ka. The Holocene 16, 827–837. https://doi.org/10.1191/0959683606hol975rp

Blaauw, M., van Geel, B., van der Plicht, J., 2004. Solar forcing of climatic change during the mid-Holocene: indications from raised bogs in The Netherlands. The Holocene 14, 35–44. https://doi.org/10.1191/0959683604hl687rp

Broström, A., Nielsen, A.B., Gaillard, M.-J., Hjelle, K., Mazier, F., Binney, H., Bunting, J., Fyfe, R., Meltsov, V., Poska, A., Räsänen, S., Soepboer, W., von Stedingk, H., Suutari, H., Sugita, S., 2008. Pollen productivity estimates of key European plant taxa for quantitative reconstruction of past vegetation: a review. Vegetation History and Archaeobotany 17, 461–478. https://doi.org/10.1007/s00334-008-0148-8

Cardarelli, Andrea, 2010. The collapse of the terramare culture and growth of new economic and social system during the Late Bronze Age in Italy, in: Cardarelli, A, Cazzella, A., Frangipane, M., Peroni, R. (Eds.), Scienze Dell'Antichità. Storia Archeologia Antropologia 15 (2009). Atti Del Convegno Internazionale "Le Ragioni Del Cambiamento/Reasons for Change". Roma, 15-17 Giugno 2006. Edizioni Quasar.

Cremaschi, M., 2009. Foreste, terre coltivate e acque : l'originalità del progetto terramaricolo, in: Bernabò Brea, M., Cremaschi, M. (Eds.), Acqua e civiltà nelle terramare: la vasca votiva di Noceto. Università degli studi di Milano, Skirà, Milano.

Cremaschi, M., 1987. Paleosols and Vetusols in the Central Po Plain (Northern Italy). A study in Quaternary Geology and Soil development. Unicopli.

Cremaschi, M., Mercuri, A.M., Torri, P., Florenzano, A., Pizzi, C., Marchesini, M., Zerboni, A., 2016. Climate change versus land management in the Po Plain (Northern Italy) during the Bronze Age: New insights from the VP/VG sequence of the Terramara Santa Rosa di Poviglio. Quaternary Science Reviews 136, 153–172. https://doi.org/10.1016/j.quascirev.2015.08.011

Cremaschi, M., Pizzi, C., Valsecchi, V., 2006. Water management and land use in the terramare and a possible climatic co-factor in their abandonment: The case study of the terramara of Poviglio Santa Rosa (northern Italy). Quaternary International 151, 87–98. https://doi.org/10.1016/j.quaint.2006.01.020

Dal Corso, M., 2018. Environmental history and development of the human landscape in a northeastern Italian lowland during the Bronze Age: a multidisciplinary case-study (PhD Thesis). Kiel University.

Dal Corso, M., Nicosia, C., Balista, C., Cupitò, M., Dalla Longa, E., Leonardi, G., Kirleis, W., 2016. Bronze Age crop processing evidence in the phytolith assemblages from the ditch and fen around Fondo Paviani, northern Italy. Vegetation History and Archaeobotany. https://doi.org/10.1007/s00334-016-0573-z

Dalla Longa, E., Dal Corso, M., Vicenzutto, D., Nicosia, C., Cupitò, M., 2019. The Bronze Age settlement of Fondo Paviani (Italy) in its territory. Hydrography, settlement distribution, environment and in-site analysis. Journal of Archaeological Science: Reports 28, 102018. https://doi.org/10.1016/j.jasrep.2019.102018

de Marinis, R., 2000. Il Museo civico archeologico Giovanni Rambotti di Desenzano del Garda una introduzione alla preistoria del lago di Garda. Città di Desenzano del Garda, Assessorato alla Cultura, Desenzano del Garda.

de Marinis, R., 1999. Towards a Relative and Absolute Chronology for the Bronze Age in Northern Italy. Notizie Archeologiche Bergomensi 7, 23–100.

de Marinis, R.C., 2010. Continuity and discontinuity in northern Italy from the Recent to the Final Bronze Age: a view from north-western Italy, in: Cardarelli, A., Cazzella, A., Frangipane, M., Peroni, R. (Eds.), Scienze Dell'Antichità. Storia Archeologia Antropologia 15 (2009). Atti Del Convegno Internazionale "Le Ragioni Del Cambiamento/Reasons for Change". Roma, 15-17 Giugno 2006. Edizioni Quasar, pp. 535–545.

de Marinis, R.C., Rapi, M., Ravazzi, C., Arpenti, E., Deaddis, M., Perego, R., 2005. Lavagnone (Desenzano del Garda): new excavations and palaeoecology of a Bronze Age pile dwelling site in northern Italy, in: Della Casa, Ph., Trachsel, M. (Eds.), Wetland Economies and Societies. Proceeding of the International Conference in Zurich, Zurich, 10-13 March 2004. Collectio Archæologica 3, 221-232.

Leonardi, G., Cupitò, M., Baioni, M., Longhi, C., Martinelli, N., 2015. Northern Italy around 2200 cal BC – From Copper Age to Early Bronze Age: continuity and/or discontinuity?, in: Meller, H., Arz, H.W., Jung, R., Risch, R. (Eds.), 2200 BC – A Climatic Breakdown as the Cause for the Collapse of the Old World. 7th Archaeological Conference of Central Germany, October 23–26, 2014 in Halle (Saale). Tagungen Des Landesmuseums Für Vorgeschichte Halle, Band 12/I. pp. 283–304.

Lockwood, J.G., 2001. Abrupt and sudden climatic transitions and fluctuations: a review. International Journal of Climatology 21, 1153–1179. https://doi.org/10.1002/joc.630

Magny, M., 1995. Une histoire du climat: des derniers mammouths au siècle de l'automobile. Éds. Errance.

Magny, M., Joannin, S., Galop, D., Vannière, B., Haas, J.N., Bassetti, M., Bellintani, P., Scandolari, R., Desmet, M., 2012. Holocene palaeohydrological changes in the northern Mediterranean borderlands as reflected by the lake-level record of Lake Ledro, northeastern Italy. Quaternary Research 77, 382–396. https://doi.org/10.1016/j.yqres.2012.01.005

Menotti, F., 2015. The lake-dwelling phenomenon: myth, reality and...archaeology, in: Menotti, F. (Ed.), The End of the Lake-Dwellings in the Circum-Alpine Region. Oxbow Books.

Mercuri, A.M., Accorsi, C.A., Mazzanti, M.B., Bosi, G., Cardarelli, A., Labate, D., Marchesini, M., Grandi, G.T., 2006. Economy and environment of Bronze Age settlements – Terramaras – on the Po Plain (Northern Italy): first results from the archaeobotanical research at the Terramara di Montale. Vegetation History and Archaeobotany 16, 43–60. https://doi.org/10.1007/s00334-006-0034-1

Mercuri, A.M., Montecchi, M.C., Pellacani, G., Florenzano, A., Rattighieri, E., Cardarelli, A., 2015. Environment, human impact and the role of trees on the Po plain during the Middle and Recent Bronze Age: Pollen evidence from the local influence of the terramare of Baggiovara and Casinalbo. Review of Palaeobotany and Palynology 218, 231–249. https://doi.org/10.1016/j.revpalbo.2014.08.009

Perego, R., 2015. Contribution to the development of the Bronze Age plant economy in the surrounding of the Alps: an archaeobotanical case study of two Early and Middle Bronze Age sites in northern Italy (Lake Garda region). University of Basel.

Perego, R., Badino, F., Deaddis, M., Ravazzi, C., Vallè, F., Zanon, M., 2011. L'origine del paesaggio agricolo pastorale in nord Italia: espansione di Orlaya grandiflora (L.) Hoffm. nella civiltà palafitticola. Notizie Archeologiche Bergomensi 19, 161–173.

Piccoli, A., 1986. Aspetti generali e particolari delle strutture e delle stratigrafie dell'insediamento preistorico di Bande di Cavriana (MN), in: Carancini, G.L. (Ed.), Atti Dell'incontro Di Acquasparta 1985. "Gli Insediamenti Perilacustri Dell'età Del Bronzo e Della Prima Età Del Ferro: Il Caso Dell'antico Lacus Velinus" - Palazzo Cesi, 15-17 Novembre 1985.

Poggiani Keller, R. (Ed.), 2014. Contadini, allevatori e artigiani a Tosina di Monzambano (Mn) tra V e IV millennio a.C. - Una comunità neolitica nei circuiti padani e veneti. Grafiche Tagliani Stampa e Comunicazione per Acherdo Edizioni, Calcinato (Bs).

Poggiani Keller, R., Leva, M.A.B., Menotti, E.M., Roffia, E., Pacchieni, T., Baioni, M., Martinelli, N., Ruggiero, M.G., Bocchio, G., 2005. Siti d'ambiente umido della Lombardia: rilettura di vecchi dati e nuove ricerche, in: Della Casa, Ph., Trachsel, M. (Eds.), Wetland Economies and Societies. Proceeding of the International Conference in Zurich, Zurich, 10-13 March 2004. Collectio Archæologica 3, 233-250.

Rapi, M., 2013. Dall'età del Rame all'età del Bronzo. I primi villaggi palafitticoli e la cultura di Polada., in: de Marinis, R.C. (Ed.), L'Età Del Rame. La Pianura Padana e Le Alpi

al Tempo Di Ötzi. Compagnia della Stampa, Massetti Rodella Editori, Roccafranca (Brescia), pp. 69–86.

Ravazzi, C., Cremaschi, M., Forlani, L., 2004. Studio archeobotanico della Terramara di S. Rosa di Poviglio (RE). Nuovi dati e analisi floristica e sintassonomica della vegetazione nell'eta del Bronzo. Gli scavi nell'abitato piccolo della Terramara Santa Rosa di Poviglio (Reggio nell'Emilia). Edizioni All'Insegna del Giglio, Firenze 703–736.

Ravazzi, C., Pini, R., Badino, F., De Amicis, M., Londeix, L., Reimer, P.J., 2014. The latest LGM culmination of the Garda Glacier (Italian Alps) and the onset of glacial termination. Age of glacial collapse and vegetation chronosequence. Quaternary Science Reviews 105, 26–47. https://doi.org/10.1016/j.quascirev.2014.09.014

Sugita, S., 2007. Theory of quantitative reconstruction of vegetation I: pollen from large sites REVEALS regional vegetation composition. The Holocene 17, 229–241. https://doi.org/10.1177/0959683607075837

Valsecchi, V., Tinner, W., Finsinger, W., Ammann, B., 2006. Human impact during the Bronze Age on the vegetation at Lago Lucone (northern Italy). Vegetation History and Archaeobotany 15, 99–113. https://doi.org/10.1007/s00334-005-0026-6

Venzo, S., 1965. Rilevamento geologico dell'anfiteatro morenico frontale del Garda dal Chiese all'Adige con carta a colori 1:40000. Memorie della Società Italiana di Scienze Naturali e del Museo Civico di Storia Naturale di Milano 14, 82.

Williams, J.W., Tarasov, P., Brewer, S., Notaro, M., 2011. Late Quaternary variations in tree cover at the northern forest-tundra ecotone. Journal of Geophysical Research 116. https://doi.org/10.1029/2010JG001458

World Heritage Committee, 2011. Decisions adopted by the World Heritage Committee at its 35th session (No. WHC-11/35.COM/20). UNESCO, Paris.

Zanon, M., Davis, B.A.S., Marquer, L., Brewer, S., Kaplan, J.O., 2018. European Forest Cover During the Past 12,000 Years: A Palynological Reconstruction Based on Modern Analogs and Remote Sensing. Front. Plant Sci. 9. https://doi.org/10.3389/fpls.2018.00253

Zanon, M., Unkel, I., Andersen, N., Kirleis, W., 2019. Palaeoenvironmental dynamics at the southern Alpine foothills between the Neolithic and the Bronze Age onset. A multi-proxy study from Bande di Cavriana (Mantua, Italy). Quaternary Science Reviews 221, 105891. https://doi.org/10.1016/j.quascirev.2019.105891

PART II

ENVIRONMENTAL CONDITIONS TOWARDS THE ONSET OF THE BRONZE AGE PILE-DWELLING PHENOMENON

As mentioned in the introductory section, the Lake Garda region is particularly rich in wetland deposits compared to surrounding areas, yet this potential for palaeoecological investigations has been so far only partially explored. The study of sedimentary archives from Lucone (Badino et al., 2011; Valsecchi et al., 2006), Lavagnone (Arpenti et al., 2007; de Marinis et al., 2005; Perego, 2015) and Castellaro Lagusello (Dal Corso, 2018) offered precious insights into environmental conditions in connection with the establishment of Bronze Age pile-dwellings. The primary scope of these investigations consisted in reconstructing human impact on the landscape though pollen and plant macroremain data. A limited effort has been so far directed towards the reconstruction of co-occurring climate dynamics and their potential influence on cultural patterns. The geographically closest palaeoclimatic record is represented by the stable isotope measurements from Lake Frassino (Baroni et al., 2006), which nonetheless does not appear suitable to trace sub-centennial temperature/precipitation fluctuations due to its relatively coarse resolution and age-depth model. The lake-level records of Lake Ledro and Lake Accesa, in northern and north-central Italy respectively, are often cited when discussing northern Italian palaeoclimate (e.g. Cremaschi et al., 2016). Lake Ledro lies in the southern Alps, approximately 50 km north of our study area and at an elevation of ca. 650 m a.s.l. Its catchment area includes mountains ranging from 1500 to 2250 m (Joannin et al., 2014, 2013). Compared to Lake Ledro, the southern Lake Garda moraines (ca. 100-200 m a.s.l.) have milder winters, warmer summers and lower precipitations (Brunetti et al., 2012). Lake Accesa lies ca. 280 km south of Lake Garda, from which it is separated by the Po Plain and the Apennine mountain range. Geographical distance and different modern temperature/precipitations patterns do not automatically exclude the use of Lake Ledro and Lake Accesa as reference palaeoclimatological records for the southern Lake Garda area. Yet, it would be appropriate to verify first to what extent all these areas follow comparable climatic patterns.

The absence of palaeoclimatic information from within the southern Lake Garda area was addressed with the investigation of a new sedimentary record. The site chosen for this task, the drained basin of Bande di Cavriana, lies close to the southern margin of the Lake Garda moraine complex. Like many wetland sites in the area, Bande di

Cavriana hosts the remains of a Bronze Age pile dwelling. This settlement was established several decades after the onset of the Early Bronze Age (ca. 3955 ± 10 years cal. BP; 2005 ± 10 years BC), while other settlements in the area were already active. As an example, the oldest dendrochronological dating within the study area comes from the Lavagnone pile dwelling, with 4027 ± 10 years cal. BP (2077 ± 10 years BC; Baioni et al., 2015; de Marinis et al., 2005). As such, Bande di Cavriana represents a valuable archive where natural sedimentation at the transition between Copper Age and Bronze Age is not disturbed by on- or near-site anthropic activities. This favorable situation allowed to extract climatic information right at the onset of the pile-dwelling phenomenon.

The sedimentary sequence investigated at Bande di Cavriana covers approximately three millennia, from ca. 7150 to 3800 years cal. BP (5200-1850 years BC), thus covering a period spanning from the Neolithic to the Early Bronze Age. Afterwards, the sedimentary infilling of the basin appears to be truncated, probably due to desiccation, terrestrialization, or peat extraction. Climate information across this interval was extracted by evaluating multiple proxy evidence, primarily stable isotope from mollusks, X-Ray Fluorescence and Carbon-Nitrogen ratios. The results of these investigations are presented in Zanon et al. (2019) and reported in their entirety below. This study provides evidence that climate patterns in the southern Lake Garda region show visible similarities with supra-regional dynamics across the Copper Age – Bronze Age transition. Further considerations on the supra-regional significance of the Bande di Cavriana record are presented in Part V.

As a further note, it should be pointed out that Bande di Cavriana was not the only site investigated within this project. Intensive fieldwork and further pollen analysis were conducted at other locations too within the southern Lake Garda area. Additional information on these sites, including the reasons why they were eventually not included in any publication, is reported in Appendix I.

Palaeoenvironmental dynamics at the southern Alpine foothills between the Neolithic and the Bronze Age onset. A multi-proxy study from Bande di Cavriana (Mantua, Italy)

Marco Zanon[a], Ingmar Unkel[b], Nils Andersen[c], Wiebke Kirleis[a]

a. Institute of Pre- and Protohistoric Archaeology, Christian-Albrechts-Universität zu Kiel, Johanna-Mestorf-Str. 2-6, D-24118, Kiel, Germany
b. Institute for Ecosystem Research, Christian-Albrechts-Universität zu Kiel, Olshausenstr. 75, D-24118, Kiel, Germany
c. Leibniz Laboratory for Radiometric Dating and Stable Isotope Research, Max-Eyth-Str. 11-13, Christian Albrechts-Universität zu Kiel, D-24118, Kiel, Germany

Original research article published on *Quaternary Science Reviews* 221 (2019).
https://doi.org/10.1016/j.quascirev.2019.105891

ABSTRACT

The onset of the Bronze Age (approximately 4150 years cal. BP) in the southern Lake Garda region (N-Italy) is marked by an increase in the number of settlements and by the widespread adoption of pile-dwelling building techniques. The prominence of this phenomenon polarized the attention of local palaeoenvironmental investigations. As a result, pre-Bronze Age landscape and climate dynamics have been investigated to a lesser degree. In an attempt to address this disparity, our contribution focuses on the period between ~7100 and ~3800 years cal. BP, i.e. approximately between Early Neolithic and Early Bronze Age. The location of our analysis is the former lake of Bande di Cavriana (Mantua). Multi-proxy investigations highlight few major climatic shifts prior to the Bronze Age onset. A first transition into more warm/dry conditions is recorded between ~6300 and 6100 years cal. BP. Similar conditions occur again after ~4600 years cal. BP, peaking at ~4300 years cal. BP. Speculatively, taking into account dating uncertainties, this second shift might represent the local expression of the '4.2Ka' event. A marked transition into a colder/more humid situation occurs then after ~4300 years cal. BP and persists into the Bronze Age. Major vegetational changes begin during the Neolithic with the steady rise of *Carpinus betulus* pollen (from ~5700 years cal. BP). A more rapid expansion of this taxon after ~5100 years cal. BP might reflect shifts in forest exploitation strategies during the Copper Age (e.g. coppicing) or changes in the ruminant fauna (e.g. grazing vs. browsing habits), arguably due to human intervention. Nonetheless, pollen grains of anthropogenic indicators appear with consistent

frequency only since the Bronze Age. The establishment of the Bande di Cavriana pile dwelling (~3950 years cal. BP) is marked by declining arboreal pollen values and growing anthropogenic taxa. This behavior likely reflects a more intense landscape exploitation (deforestation, expansion of arable fields and meadows), although an influx of herbaceous pollen from near-site activities (e.g. cereal processing, garbage dumping) should not be overlooked.

INTRODUCTION

The southern border of Lake Garda (N-Italy) is surrounded by a series of concentric end-moraines (Fig. 2.1) deposited by multiple glacial advances during the Pleistocene epoch (Ravazzi et al., 2014). Traces of human presence are attested in the area since the Paleolithic (de Marinis, 2000), yet archaeological evidences are rather sparse up until the onset of the Bronze Age (conventionally set at ~4150 years cal. BP; de Marinis, 2000, 1999). The transition into the Bronze Age is marked by a prominent increase in site density and by a widespread adoption of settlement strategies based on pile dwellings. Over 30 wetland settlements are recorded in the Lake Garda area, either in proximity of the lake shores or within the many smaller water bodies scattered in between the moraine ridges (de Marinis, 2010; Poggiani Keller et al., 2005). A selection of these sites has been recently included in the UNESCO World Heritage serial site "Prehistoric Pile Dwellings around the Alps" (World Heritage Committee, 2011). Determinant for the inclusion in the World Heritage List is the excellent level of preservation of their waterlogged organic remains, which allows for a detailed insight into Bronze Age craftsmanship and subsistence strategies.

Given the archaeological prominence of the pile-dwelling phenomenon, most efforts to characterize the Holocene landscape history in the study area focused primarily on the environmental impact of these lakeside settlements. Published palynological and carpological data are available from the wetland sites of Lucone (Badino et al., 2011; Valsecchi et al., 2006), Lavagnone (Arpenti et al., 2007; de Marinis et al., 2005; Perego, 2015) and Castellaro Lagusello (Dal Corso, 2018; location of all sites presented in Fig. 2.1). Within these studies, limited space is devoted to the discussion of land cover dynamics in the centuries and millennia that precede the Bronze Age onset. A more detailed understanding of pre-Bronze Age environmental dynamics is certainly valuable. It would allow not only to assess the local impact of early agricultural societies, but also to unravel any climatic or land use trend that might have contributed to the emergence of the pile-dwelling phenomenon itself. For this reason,

here we focus on the vegetational and climatic history of the southern Lake Garda region between ~7100 and ~3800 years cal. BP, thus covering a time-window spanning approximately from the Early Neolithic to the Early Bronze Age. We conducted our investigations on sediment cores from the former lake of Bande di Cavriana (Figs. 2.1 and 2.2), now a drained wetland. Our study makes use of geochemical data from sediment samples, stable isotopes from freshwater mollusks and pollen analysis. All these palaeoenvironmental proxies contributed to define potential changes in land cover and climate before the onset of the Bronze Age, and to describe the environmental context during the local spread of piled-welling settlements.

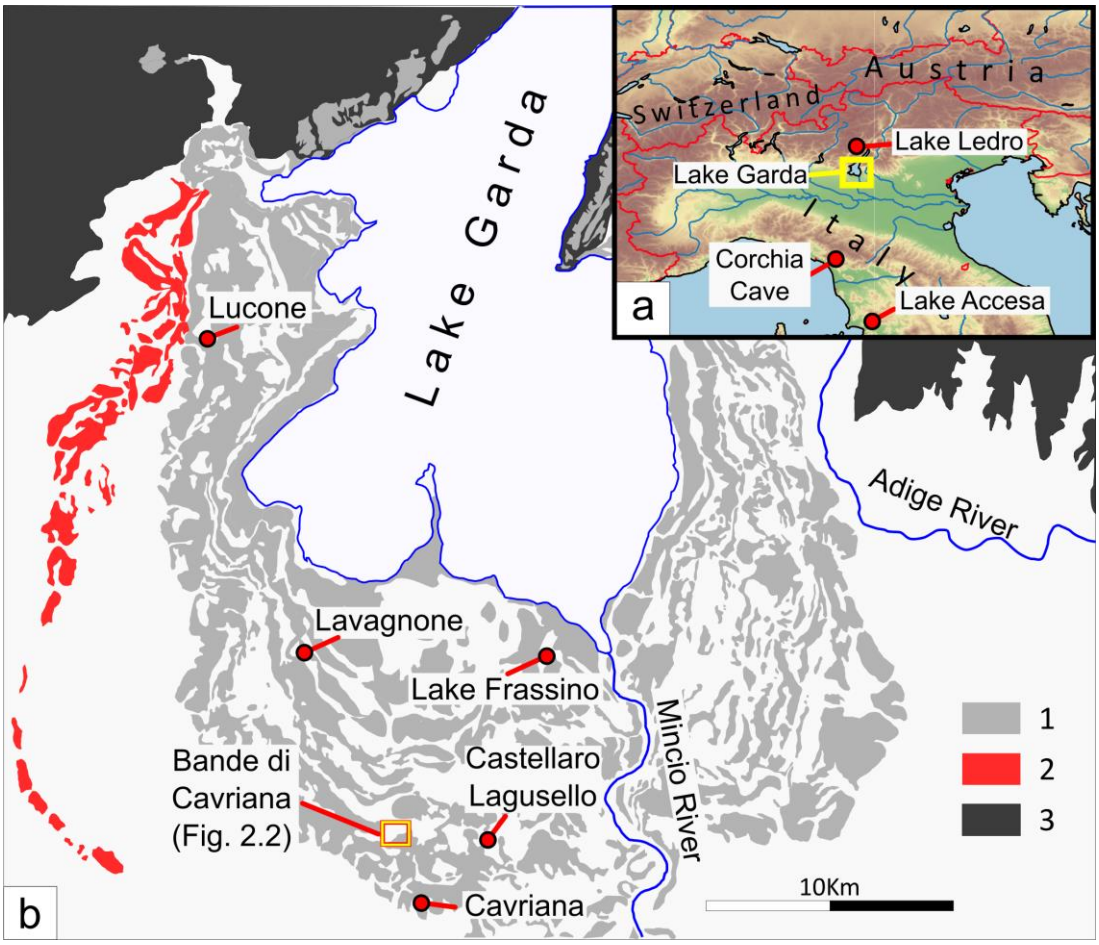

Figure 2.1. *Position of Bande di Cavriana and other sites mentioned in the text. Overview of northern and central Italy (a) and location of the study site within the Garda Lake glacial moraines (b). The contours of the topographic features in (b) are based on Venzo (1965). Legend: 1) Late Pleistocene moraines (Cremaschi, 1987; Ravazzi et al., 2014). 2) Mid-Pleistocene moraines (Venzo, 1965). 3) Alpine foothills.*

STUDY SITE: BANDE DI CAVRIANA

Object of the present work is a former wetland located within two moraine ridges in the southern Lake Garda area (Figs. 2.1-2.2). The site itself does not have its own toponym; in literature it is commonly named after the nearby location of Bande, within the municipality of Cavriana (e.g. Piccoli, 1974). The basin was occupied by a marsh or a seasonally inundated meadow until the excavation of a drainage channel (named "Fossa Can(n)a", allegedly dug during the Middle Ages) allowed the economic exploitation of the area. Bande di Cavriana is primarily known for its Bronze Age remains. Sparse Neolithic artefacts are documented within the municipality of Cavriana (e.g. Biagi and Piccoli, 1979), but not from this basin. The presence of a Bronze Age pile dwelling was first described in the late 19th century, while the first research work began after 1950 (World Heritage Nomination, 2009). The most recent excavations have been carried out between 1967 and 1983 under the supervision of Museo Archeologico dell'Alto Mantovano (Piccoli, 1986a). The Early Bronze Age settlement layers were supported by vertical oak poles deeply driven into the basin infilling (Piccoli, 1986a, 1986b, 1982, 1974). A major change in building techniques occurred within the Middle Bronze Age (approximately after 3550 years cal. BP). During this period, portions of the damp littoral zone were reclaimed by dumping layers of sand, plant remains and waste materials (Piccoli, 1986a, 1974). These dump layers were held in place by wooden support elements, sometimes in the shape of box-like structures (Piccoli, 1986a). The settlement was probably active during the Recent Bronze Age too (approximately before 3100 years cal. BP), as suggested by typological analysis of few ceramic finds (Piccoli, 1986a). Absolute datings for the settlement are available only for the Early Bronze Age, where dendrochronological analysis revealed felling dates between ~3955 ± 10 and ~3909 ± 10 years cal. BP (Martinelli, 2007). The presence of open waters, at least during parts of the Early Bronze Age, is attested by the presence of few logboats, although only one of these was recovered during a proper archaeological investigation (Piccoli, 1980). Due to the remarkable condition of its waterlogged organic remains, the Bronze Age site of Bande di Cavriana was among the locations included in 2011 in the serial UNESCO World Heritage site "Prehistoric Pile Dwellings around the Alps". Our investigations are concentrated in the area south of the drainage channel (Fig. 2.2). According to local knowledge, any attempt to cultivate this portion of the basin with modern machinery failed due to ground instability, ultimately suggesting that deep plowing did not affect the stratigraphy.

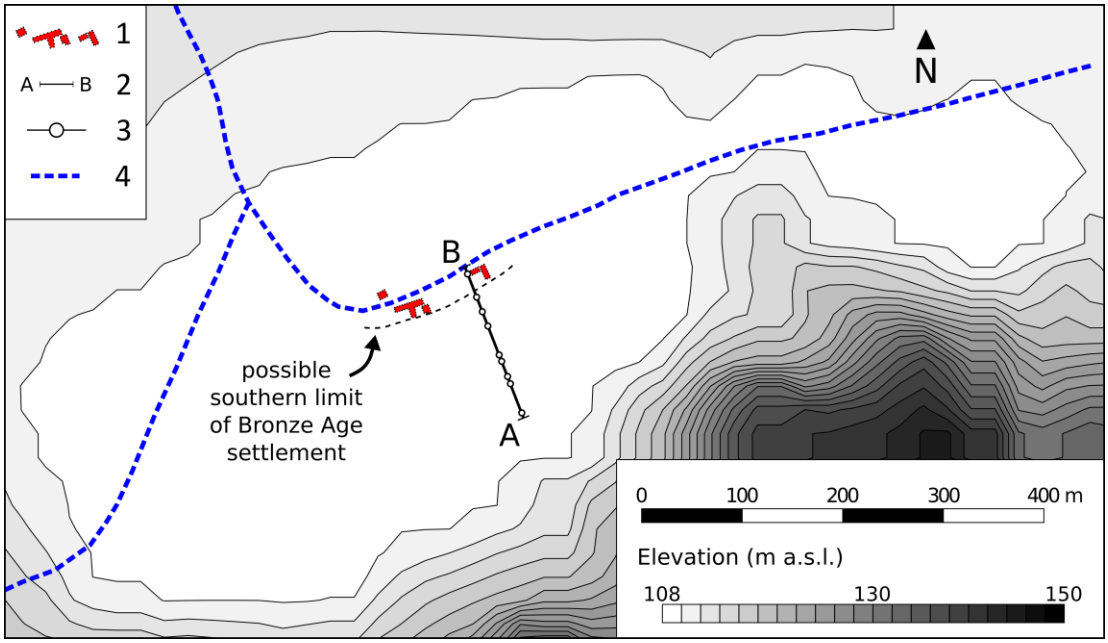

Figure 2.2. *Topography of the Bande di Cavriana basin. Legend: 1) Approximate location of the archaeological excavation trenches, from Piccoli (1986b, 1986a, 1982). 2) Extent of the coring transect and 3) coring locations (Fig. 2.3). 4) Drainage ditch ("fossa Cana"). The topographic relief is based on a 20 m resolution DTM obtained from the regional geoportal www.geoportale.regione.lombardia.it.*

MATERIALS AND METHODS

Corings and stratigraphy

The stratigraphy of the Bande di Cavriana basin was probed through a series of corings collected along a N-S transect (Figs. 2.2-2.3). The surface topography of the transect was logged using a Topcon GPT-3000N total station. All cores were collected through a Usinger piston corer (Mingram et al., 2007). A maximum depth of 3.5 m was reached with core CAV4, which was selected as reference sequence for further analysis. Its sedimentary record can be simplified down to five main stratigraphic units (SU) in order to facilitate any comparison with other cores (Fig. 2.3):

SU 1. 350-170 cm: Compact mud with distinct elastic texture and sulfur smell. Pale pink/light brown color with unevenly distributed, slightly darker bands of variable thickness. Visible faunal remains are rare and appear to be limited to cfr. *Unio* sp. shells. Scattered *Najas marina* seeds are present too. A thick band of dark brown, organic-rich mud (detritus gyttja) is located between 242 and 237 cm. The sediment type comprising SU 1 is locally known as "polmone" (Italian for "lung"), due to its texture arguably resembling lung tissue (cf. Piccoli, 1974).

SU 2. 170-118 cm: Carbonate mud. The variable concentration of fine organic sediment results in an irregular banding pattern, ranging in color from light

brown/pale pink to dark brown. The transition between this unit and the previous one appears to be gradual and not easily traceable, as the two sedimentary units share similar colors. Compared to SU 1, this unit is visibly richer in shell fragments and acquires a gradually less rubbery texture with decreasing depth.

SU 3. 118-79 cm: Carbonate lake marl, comparable in composition to SU 2 but with a distinct light yellow-grey color. Darker bands are visible between 87 and 80 cm at the interface with the following unit. In CAV4, the transition between SU 2 and SU 3 appears sharp and jagged, rising suspicion that it might be the result of a hiatus in the sedimentation. The absence of pronounced discontinuities in pollen percentages and the relative linearity of the age-depth model (sections "Pollen record" and "Chronological assessment") do not appear to support the presence of a (sustained) sedimentary hiatus. Such sharp transition was not observed in other cores.

SU 4. 79-62 cm: Dark brown detritus gyttja. Visible presence of small charcoal fragments (length up to 1 cm). Layer of black compressed detritus gyttja between 74 and 70 cm. Bioturbations are visible across this SU and partly along the upper limit of the previous one. Particular care was taken in removing bioturbated portions before sampling. Considerations concerning the presence of possible contaminants are reported in section "Chronological assessment".

SU 5. 62-0 cm: Topsoil composed of sand, gravel and pebbles (max diameters up to 3-4 cm) in a clayish matrix.

The remaining cores were limited to a maximum depth of 1-2m in order to focus on the sedimentary transitions between SU 2, 3 and 4. The stratigraphic units SU 2-5 described for CAV4 were also found in cores CAV 13b, CAV8, CAV12 and CAV9 (Fig. 2.3). In cores CAV15 and CAV11, SU 3 is lacking. In core CAV15, SU 2 is followed by a lacustrine marl layer richer in fine brown organic matter; this layer merges into a band of detritus gyttja, which in turn merges again into carbonate mud. In core CAV11, SU 2 is directly followed by SU 4.

Cores CAV10, CAV11, CAV15, and the first meter of CAV12 were extremely compressed as a result of the coring operations, losing up to ca. 50% of their total length. Notably, core sections composed by lake marl (e.g. core CAV12 between 1 and 2m depth) were not affected by compression, suggesting that this issue occurs only in organic-rich layers (i.e. detritus gyttja and topsoil). Following this observation, in Fig. 2.3 we propose a restored version of cores CAV10, CAV11 CAV12 and CAV15 after correcting for the compression of SU 4 and SU 5 within each core, assuming that this phenomenon occurred evenly along these units. The southernmost core, CAV14 was collected approximately 25 m south of CAV13b. An additional

sedimentary unit, here termed **SU 0**, was found only in this core. SU 0 is composed of compact pink/light orange clay and is then followed by light grey lake marl comparable to SU 3, and by topsoil (SU 5).

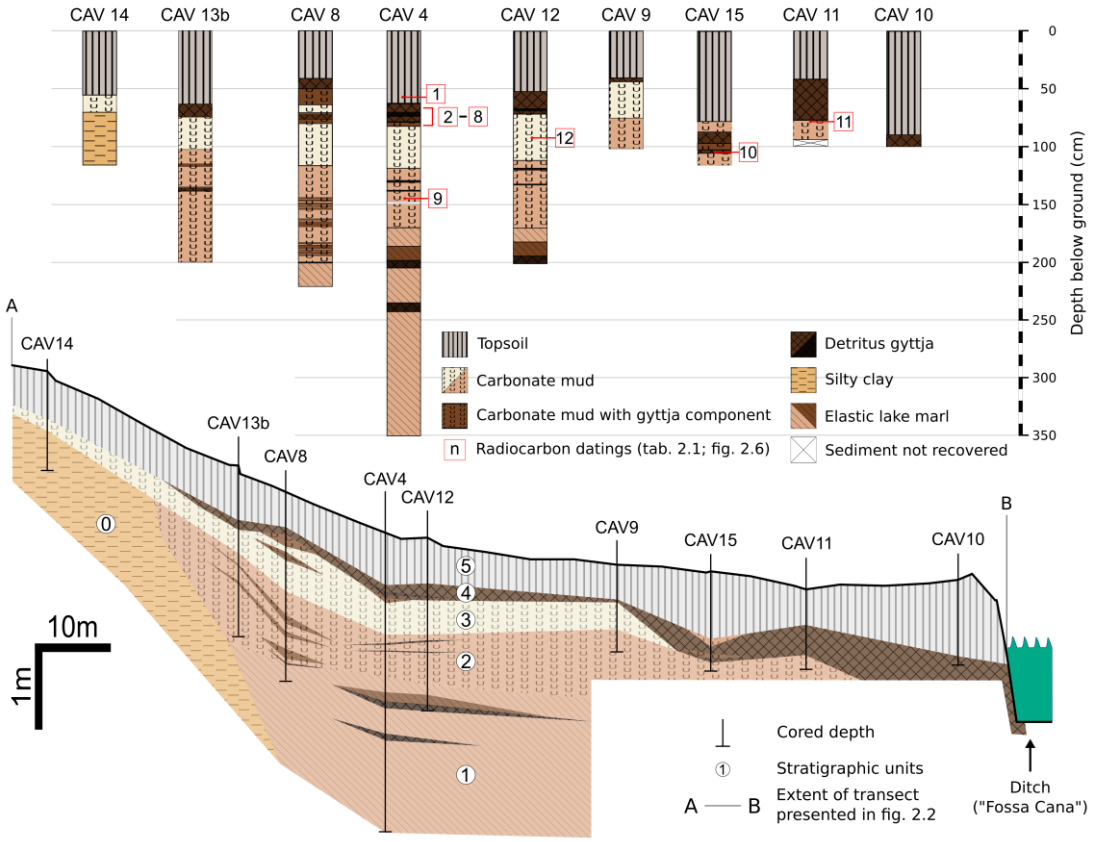

Figure 2.3. *Simplified lithology of all CAV corings and inferred stratigraphy of the basin.*

Sample selection

Exploratory pollen samples on core CAV 4 allowed to identify the Copper Age/Bronze Age boundary around the transition between SU 3 and SU 4 (see section "Chronological assessment" for considerations on the relevant biostratigraphic markers). For this reason, geochemical and further palynological investigations were primarily concentrated between a depth of ca. 150 and 50 cm along this core. The position of all samples extracted for each analysis is show in Supplementary Fig. S2.1 (Appendix II).

Geochemical analysis

Loss on ignition. Core CAV4 was sampled every 1 cm between 146 and 53 cm for loss on ignition (LOI) analysis. Sediment samples measuring 1 cm^3 were first

desiccated at 105 °C for 12 h, and then heated at 550 °C for 3 h and at 950 °C for 2 h. Each sample was individually weighted before and after each heating step.

X-ray fluorescence (XRF). Continuous XRF scanning was performed on core CAV4 at a 1 cm resolution using an Aavatech XRF core scanner equipped with a Rhodium X-ray source. In the present paper, we focus on a limited number of elements: calcium (Ca), titanium (Ti), rubidium (Rb), strontium (Sr), zirconium (Zr). The abundance of Ca and Ti was obtained with a tube voltage of 10 kV and an exposure time of 20 s. A voltage of 30 kV and 30 s exposure time was used for Rb, Sr, Zr. The XRF scanning data is provided as element intensities in total counts per second (tcps). Element counts depend not only on element concentration, but also on matrix effects and the scanner setup (Tjallingii et al., 2007). We present single elements either normalized against tcps, or preferably as log-ratios, that can be interpreted as changes in relative concentration of an element pair, in order to avoid statistical analysis of data sensitive to the closed sum effect and asymmetric element ratios (Weltje and Tjallingii, 2008).

Carbon/nitrogen ratio. Total organic carbon (TOC) and total nitrogen (TN) were measured on 31 dried and homogenized samples using a Euro EA Elemental Analyzer. To assess the amount of terrestrial versus aquatic organic matter, C:N (TOC:TN) ratios were calculated (Meyers, 2003).

Stable isotopes. After sampling for palynological and geochemical analysis, core CAV4 was subdivided into 2-3 cm thick slices and sieved to extract animal and plant macro-remains. Being the most abundant and well-preserved freshwater gastropod along the core, 35 samples of *Valvata piscinalis* (Girod et al., 1980; Welter-Schultes, 2012) were selected for $\delta^{18}O$ and $\delta^{13}C$ analysis. Between 2 and 10 complete individuals were selected for each sample, depending on the availability of well preserved shells (see Supplementary Fig. S2.1, Appendix II). Prior to isotopic analysis, the shell remains were cleaned with demineralized water in an ultrasonic bath to remove sediment traces. The samples were then left to dry at room temperature and eventually crushed in an agate mortar. Two bulk samples composed of powdered individuals collected at different depths were also analyzed by X-ray diffraction (XRD).

Pollen analysis

A total of 26 samples (1-4 cm^3) were analyzed from core CAV4 between a depth of 144 and 62 cm. Sampling occurred every 4 cm between 144 and 84 cm and mostly every 2 cm between 84 and 62 cm. Samples were treated with HCl 10% and KOH 5% in order to remove carbonates and humic acids. Filters with a mesh of 200 and 6 μm were used to remove particles outside pollen size range. Pollen grains were stained via acetolysis (cf. Erdtman, 1960) and preserved in glycerin. Taxa identification was carried out using dichotomic keys (Beug, 2004; Clarke and Jones, 1977; Moore et al., 1991) and by comparison with the reference collection of the Institute of Pre- and Protohistory of Christian-Albrechts University in Kiel. The counting process was aided by the software Countpol 3.3, developed by I. Feeser (Kiel University, Germany). A minimum of 1000 pollen grains of terrestrial taxa were counted for each sample. Pollen concentrations are not part of the present contribution. Nonetheless, *Lycopodium* tablets were added to the samples prior to the chemical treatment (Stockmarr, 1971) in order to allow their inclusion in future studies. The pollen diagram was drawn using Tilia v1.7.16. The calculation of pollen and NPPs percentages is based on the sum of trees, shrubs and upland herbs. Diagram zonation was performed using the built-in cluster analysis function available in Tilia v1.7.16 (CONISS; Grimm, 1987). Edwards & Cavalli Sforza's chord distance was selected as a coefficient of dissimilarity, using only terrestrial taxa whose presence reaches at least 1% of the pollen sum at any point in the diagram.

Temperature modeling

Semi-quantitative annual temperature estimates for the studied sequence were inferred from pollen data via modern analogue technique (MAT; Mauri et al., 2015; Overpeck et al., 1985). Squared Chord Distance was chosen as dissimilarity index (Gavin et al., 2003). The European Modern Pollen database (Davis et al., 2013b, 2013a) was used as a calibration data set, coupled with climatic parameters extracted from the Worldclim 1.4 data set (Hijmans et al., 2005). The reconstructions are based on the weighted average of the closest 9 analogs. The methodology used follows Capuzzo et al., (2018). H-block cross-validation (h = 300 km) was applied to the training set in order to evaluate the influence of spatial autocorrelation on the model (Telford and Birks, 2009). All calculations were performed using R v3.5.0 (R Core Team, 2015) with packages rioja v0.9-21 (Juggins, 2019) and fields v.9.7 (Nychka et al., 2019). The MAT was applied only to samples below 79 cm (SU 2-3). The pollen content of zone SU 4 is likely affected by the nearby establishment of the pile dwelling

during the Bronze Age (see section "Transition into the Bronze Age"). A not easily quantifiable part of the pollen load within this SU likely results from human activities taking place few meters away from the coring location (e.g. cereal pollen dispersal through threshing, winnowing and sieving; e.g. Bower, 1992) and is therefore not representative of "natural" pollen dispersal and deposition dynamics.

Radiocarbon dating and age-depth modeling

Plant fragments for radiometric dating were recovered from cores CAV4, CAV11, CAV12 and CAV15 (Fig. 2.3, Table 2.1). No suitable material was found in the remaining cores. Samples were dated at the laboratories of Kiel (code KIA) and Poznan (code Poz). The age-depth model for core CAV4 was build using the software Oxcal v4.3 (Bronk Ramsey, 2009) with the IntCal13 calibration dataset (Reimer et al., 2013). A single P-sequence with k = 2 was used for the whole core, with boundary commands set at the transitions between each SU to separate different sedimentary environments.

RESULTS AND INTERPRETATION

Sediment geochemistry

The distinction of different stratigraphic units within core CAV 4 presented in section "Corings and stratigraphy" was primarily based on a visual and tactile analysis of the sediment. The geochemical characterization of the core via LOI and XRF largely supports this initial subdivision.

LOI. In the interval 146-118 cm, falling within SU 2, organic matter (OM) content does not show a regular trend but fluctuates from a minimum of ~14% to a maximum of ~43%. The most prominent OM peaks correspond to well visible layers of darker sediment or concentrations of aquatic plant remains. The following zone, comprised between 117 and 80 cm and corresponding to SU 3, is characterized by a remarkable stability of all three LOI curves. The OM content is in the range ~17.5 ± 2%. The carbonatic fraction is stable at ~35 ± 1.5% and the unburnt residue lies at ~48 ± 2%. Samples in SU 4 (79-61 cm) show a variety of trends. Carbonates content drops abruptly, remaining then fairly stable at around ~6.5 ± 1.5%. The residue displays a more gradual negative trend that corresponds to a sharper increase in OM content. From 77 to 71 cm, OM is the main component of the sediment. It reaches its highest values in the whole core (~73-74%) at a depth of 71-73 cm, corresponding to a layer of black, compressed detritus gyttja. After this point, the content of OM drops sharply, matched by the opposite behavior of the residue.

Table 2.1. *Complete list of radiocarbon-dated material from CAV cores. The numbers in the leftmost column refer to dating numbers in Fig. 2.3. Samples marked with the symbol '*' were excluded from age-depth modeling (see section "Chronological assessment").*

N°	Lab ID	Core	Depth (cm)	Material	Weight (g)	Age ^{14}C	Remarks	Mean calibrated/modeled age cal. BP (1σ)		
								from	to	median
1*	Poz-69225	CAV4	52-54.5	Seeds of Caryophyllaceae and cf. *Solanum nigrum*.	0.009	102.78 ± 0.35 pMC	0.4mgC	modern/contaminant		
2	KIA 51881	CAV4	72.5-74.5	Charcoal	>0.01	3601 ± 27		3956	3873	3907
3*	Poz-75788	CAV4	72.5-74.5	Seeds of Caryophyllaceae; seed of *Setaria pumila*; charred cereal spikelet fragment.	0.0035	615 ± 30		modern/contaminant		
4*	KIA 50276	CAV4	74.5-76	Charcoal	>0.01	3838 ± 21		4288	4159	4238
5	KIA 51882	CAV4	76-78	Charcoal	>0.01	3647 ± 26		3954	3922	3938
6*	KIA 50277	CAV4	78-80	Charcoal (Oak)	>0.01	3884 ± 22		4405	4290	4333
7	KIA 51883	CAV4	78-80	Charcoal (Oak)	>0.01	3665 ± 28		3970	3945	3958
8*	Poz-75790	CAV4	80-82	Seeds of Caryophyllaceae.	0.0026	101.72 ± 0.34 pMC	0.6mgC	modern/contaminant		
9	KIA 50432	CAV4	144 - 147	Bark fragment	0.006	6145 ± 35		7154	6953	7038
10	Poz-75791	CAV15	104-108	*Rubus* sp. seeds; Solanum nigrum seed; *Triticum monococcum* charred spikelet fragment.	0.003	3655 ± 35	Lower boundary of SU 4	4073	3914	3977
11	Poz-75792	CAV11	77-79	*Rubus* sp. seeds	0.01	3715 ± 35	Upper boundary of SU 2	4143	3986	4050
12	Poz-76077	CAV12	90-95	Wood fragment	0.038	4260 ± 40	0.4mgC	4867	4743	4838

The negative trend of OM continues in the most superficial zone, SU 5 (60-53 cm), eventually reaching the lowest value in the whole core (~8%) at 54 cm. The unburnt residue values rise in the top half of SU 4, then stabilizing around ~75 ± 2% in SU 5. The carbonatic component displays here a weak positive trend.

XRF. The relationships between elemental trends are expressed using Pearson's correlation coefficient and presented as a correlation matrix (Table 2.2).

These comparisons reveal the presence of two main and opposite patterns, exemplified in Fig. 2.4 by the curves of Calcium (Ca/tcps) and Titanium (Ti/tcps). The behavior of Calcium closely retraces the LOI-derived carbonate curve, displaying a relative stability through SU 2 and SU 3, followed by a sharp drop at the transition between SU 3 and SU 4. These trends are broadly shared by Strontium, as suggested by a (weak) positive correlation between the two curves ($r = 0.33$, $p < 0.05$, Table 2.2). Titanium is a rather immobile element with low participation in biological activities, and therefore often used as a detrital input indicator. The Ti curve presents a solid neutral trend along SU 2 and SU3, rising then sharply at the transition into SU 4. This visible increase at the transition into SU 4 defines the negative correlation with Ca ($r = -0.9$, $p < 0.001$). The behavior of Ti is shared by other elements connected with detrital input (Rb and Zr; correlation with Ti: $r = 0.94$, 0.95 respectively; $p <$ 0,001. Correlation of these elements with Ca: -0.8, -0.83 respectively; $p < 0.001$). The correlation between Ca and Sr is explainable by their chemical affinity. Sr can substitute Ca in the deposition of carbonates, specifically playing an important role in the formation of aragonite crystals (Sunagawa et al., 2007).

Table 2.2*. Correlation matrix (Pearson's correlation coefficient) for CAV4 elemental data (XRF analysis). P-values for each elemental pair are reported in brackets.*

	Ca	**Sr**	**Rb**	**Ti**
Sr	0.33 (<0.05)			
Rb	-0.8 (<0.001)	0.17 (0.1)		
Ti	-0.9 (<0.001)	0.01 (0.9)	0.94 (<0.001)	
Zr	-0.83 (<0.001)	0.14 (0.2)	0.99 (<0.001)	0.95 (<0.001)

Changes in Ca:Sr have been previously used to infer variations in biogenic carbonates vs. detrital carbonate deposition (Hodell et al., 2008) relying on the assumptions that biogenic carbonates precipitate mostly in the form of aragonite (Brown et al., 1992). Yet, in core CAV 4 the substantial drop in Ca presence appears to be primarily driven by a sudden change in lithology (transition from Carbonates to detritus gyttja, SU 3 to SU 4). The Ca:Sr curve distinctively retraces the Ca trajectory, suggesting that it might be heavily affected by the same lithological change.

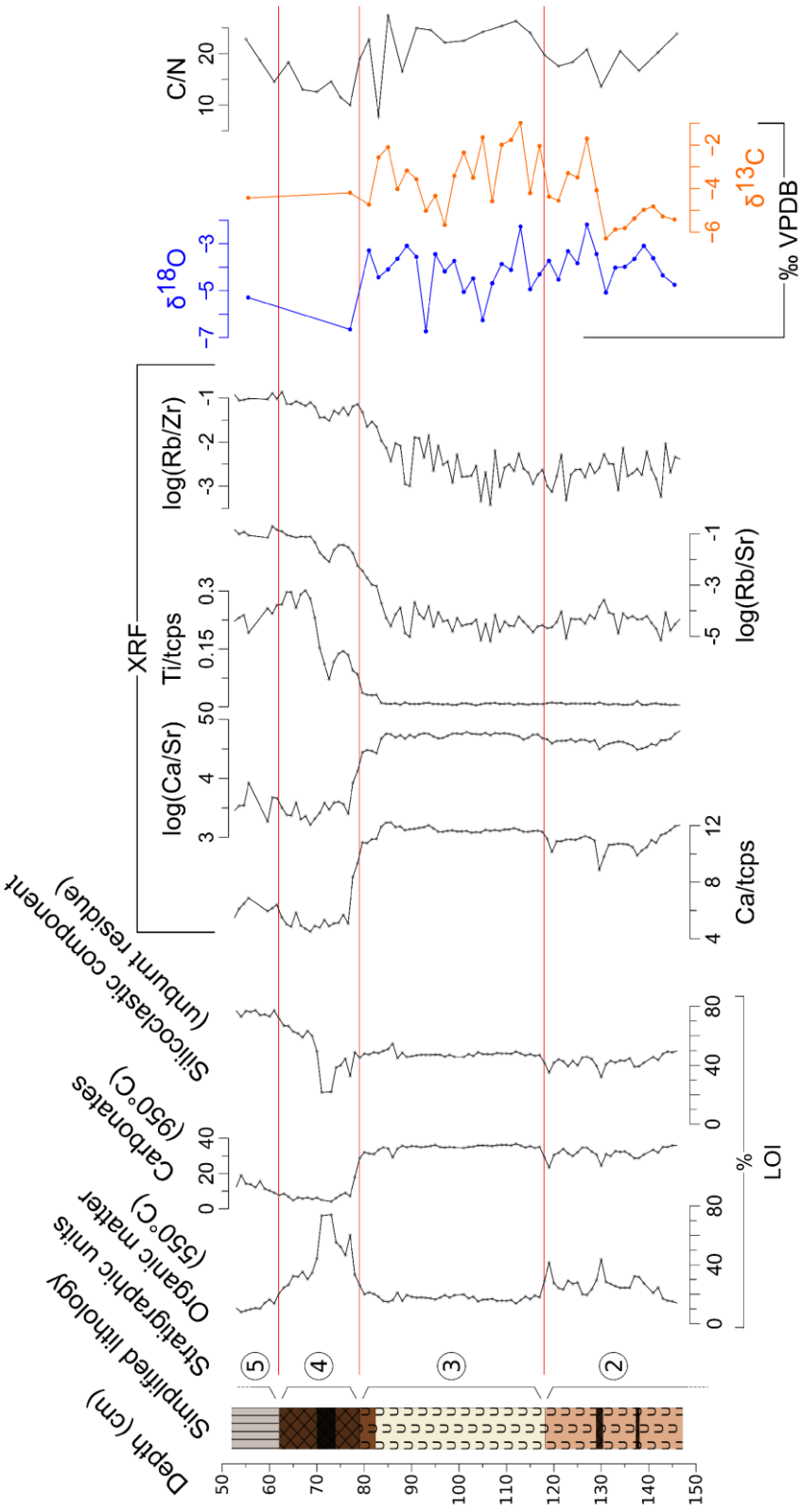

Figure 2.4. *Results of the geochemical and isotope analysis conducted on core CAV 4.*

The value of this elemental ratio as an indicator of biogenic vs. detrital carbonates in this context remains therefore dubious. The Rb:Zr and Rb:Sr curves show comparable behaviors: a rather neutral trend between ca. 146 and 85 cm, a sharp increase between ca. 85 and 75 cm and a return to a neutral or mildly positive trend after ca. 75 cm. Rb tends to substitutes K in mineral lattices and is primarily linked to easily-weathered phyllosilicates. Zr is a common component of coarse, more weathering-resilient silt and sand. An increase in Rb:Zr has been therefore linked to a higher influx of fine-grained mineral particles (clay/fine silt; Berntsson et al., 2015). Beside biogenic carbonates, Sr is also found in weathering-resistant magmatic and metamorphic rocks (e.g. plagioclase). In CAV4, Rb:Sr and Rb:Zr show a strong correlation, with $r = 0.95$ ($p < 0.001$), ultimately supporting the notion that both curves might be tracking the same signal.

Carbon-nitrogen ratio. The elemental ratio between Carbon and Nitrogen isotopes has been used as an indicator to trace sources of organic matter in lake sediments (e.g. Kaushal and Binford, 1999; Thevenon et al., 2012). In these contexts, organic carbon is regarded as deriving primarily from terrestrial sources, as cellulose and lignin are Nitrogen-poor, while an enrichment in Nitrogen would point towards a stronger algal contribution (Talbot, 2001). For reference, nonvascular lacustrine vegetation yields C:N ratios between 4 and 10, while the value for humus lies in the 10-20 range and terrestrial vascular plant reach values well above 20 (Håkanson and Jansson, 1983; Meyers and Ishiwatari, 1993). Yet macrophytic vegetation is enriched in Carbon and can display C:N ratios >10 (Cloern et al., 2002; Hunter, 1976; Wang et al., 2015). Fluctuations of C:N ratios in sediment samples might then depend on a series of factors, including erosion rates within the watershed (contribution of mobilized terrestrial biomass) and lake level changes (varying distance of near-shore aquatic vegetation from the coring point). Both mechanisms are potentially important in small basins such as Bande di Cavriana. Concerning the CAV4 record, C:N values below ~125 cm are characterized by large fluctuations between consecutive samples, with values moving between ~13 and 24. More stable trends are visible between ~125 and ~90 cm. Notably, C:N values rise steadily from ~17.5 to ~26 between 121 and 112 cm, declining then down to ~22 between 112 and 97 cm. Wide fluctuations occur once again between ~91 and ~77 cm. The highest (~27) and lowest (~8) values occur in this section and belong to adjacent samples (85 and 83 cm respectively). A generally positive trend characterizes the samples above 77 cm, with values going from ~10 to ~22.

Stable oxygen and carbon isotopes. Stable isotope data are continuous across SU 2 and 3. In SU 4, only level 77 cm contained well preserved *V. piscinalis* shells. Intact specimens were also recovered and analyzed from level 55.5 cm in SU 5. The results from SU 4 and 5 are included in Fig. 2.4 for completeness but will not be commented further. The XRD analysis of bulk samples resulted in pure aragonite, suggesting that no recrystallization process interfered with the original isotopic signal. The $\delta^{18}O$ curve exhibits a major positive shift between 131 and 127 cm, transitioning seamlessly from ~-5.1‰ to ~ -2.2‰ within the space of three consecutive samples. After 127 cm, it appears to be dominated by a predominantly negative trend until 105 cm (~-6.3‰), interrupted by a positive spike at 113 cm (~-2.3‰). The $\delta^{13}C$ curve appears to display a more erratic behavior. The overall correlation between $\delta^{18}O$ and $\delta^{13}C$ is quite low ($r = 0.2$, $p > 0.05$). Yet a section characterized by a closer agreement is visible between the bottom of the sequence and ~107 cm ($r = 0.53$, $p < 0.05$), where both curves share prominent episodes of enrichment and depletion. Particularly notable for $\delta^{13}C$ too is the 131-127 cm interval already noted above, where values shifts from ~-6.3‰ to ~ -1.7‰. On the overall, $\delta^{18}O$ values in SU 2, 3 and 4 lie between ~ -6.8‰and ~-2.2‰ (mean: ~-4.1 ± 1), while $\delta^{13}C$ is between ~ -6.3‰ and ~-1‰ (mean: ~-3.9 ± 1.4). Stable Isotope values for the southern Lake Garda area have been previously investigated by Baroni et al. (2006) using *V. piscinalis* shells too. The authors determined also that local meteoric precipitation is the main source of water for Lake Frassino and Lake Castellaro (~9 km NE and ~4 km E of Bande di Cavriana respectively, Fig. 2.1). We assume this statement to hold true for Bande di Cavriana as well, since the site lies in the same geological context and appears to be lacking inlets or outlets beside its artificial drainage channel. The $\delta^{18}O$ and $\delta^{13}C$ values recorded along core CAV4 are in line with the Holocene data from Lake Frassino (Baroni et al., 2006). We avoid any precise comparison between the two sequences given the potential uncertainties in the Lake Frassino age-depth model (i.e. dating primarily based on bulk sediment samples).

Pollen record

The results of the palynological analysis conducted on core CAV4 are shown in Fig. 2.5. Pollen data are introduced before the chronological assessment of the sequence, since a description of the pollen flora is necessary to contextualize the construction of the CAV4 age-depth model.

The five Pollen Assemblage Zones (PAZ) identified through cluster analysis are defined as follows:

PAZ CV-1 (144-118 cm) is dominated by *Corylus*, deciduous *Quercus* and *Alnus glutinosa*-type, whose pollen grains represent between ~75 and ~85% of the pollen sum. Peak values of ~50% are recorded for *Corylus* at the bottom of the zone, followed by a steady decline resulting in a 20% loss. The negative trend of *Corylus* is matched by an increase in deciduous *Quercus*, while the remaining taxa appear to be uninfluenced by these dynamics. Herbaceous taxa constitute only ~2-4% of the pollen sum. Primary anthropogenic indicators (e.g. Cerealia, *Orlaya grandiflora*) are absent or limited to isolated pollen grains.

PAZ CV-2 (118-90 cm) shows a composition initially comparable to the previous PAZ. Deciduous *Quercus* is the most abundant taxon, with values ranging from 30% to 40%. *Corylus* (range: ~18-24%) is few percentage points above *Alnus glutinosa*-type (range: 13-20%). The presence of herbaceous taxa peaks at ~6%, while the sum of all anthropogenic indicators does not reach 0.5% of the pollen sum. The steady positive trend of *Carpinus betulus*, raising from ~3% to ~18%, is the main event differentiating this zone from CV-1. The expansion of this taxon sees a contemporary decrease in the abundance of *Alnus glutinosa*-type, Poaceae and, subsequently, deciduous *Quercus* and *Corylus*.

PAZ CV-3a (90-83 cm) is characterized by the highest abundance of arboreal species registered in the pollen diagram. Both *Alnus glutinosa*-type and *Carpinus betulus* reach their peak values in this zone (~35% and 23% respectively), bringing the total arboreal pollen to a maximum of ~82%. With the addition of shrub pollen (range: ~15-18%. Primarily *Corylus*), non-herbaceous taxa reach a maximum of ~97%.

PAZ CV-3b (83-79 cm) shares the same composition of CV-3a in terms of broad distribution of main taxa and total arboreal pollen abundance. The distinction of CV-3b as a separate zone is justified by the beginning of a continuous curve for different non-arboreal taxa (e.g. Chenopodiaceae, *Anthemis*-type, Cichorioideae, *Centaurea nigra*-type, Cerealia, *Orlaya grandiflora*) formerly absent from the pollen record or present only as scattered finds.

PAZ CV-4a (79-73 cm) differentiates itself from all previous zones because of a sharp positive trend of several non-arboreal taxa. As an example, the presence of *Aster*-type rises from an average value of ~0.5% in PAZs CV-3a + CV-3b to ~4.5% in CV-4a. Cichorioideae rise from <0.5% to ~1%. Dipsacaceae go from <0.5% to ~4%. Poaceae rise from ~2% to ~11%. *Centaurea nigra*-type goes from <0.1% to ~1.5%. Cerealia-type goes from <0.5% to ~2%. *Orlaya grandiflora* rises from <0.1% to ~2%.

Ranunculus acris-type goes from <0.5% to ~3%. Pollen belonging to upland herbaceous taxa increases from ~5% to ~35%. A visible rise is registered also for *Hedera* (from ~0.5% to ~2.5%) and *Vitis* (from~0.5% to ~2%). The expansion of these taxa occurs mostly at the expenses of deciduous *Quercus* (from ca. 20% to ca. 9%) and *Carpinus betulus* (from ~18% to ~11%).

PAZ CV-4b (73-62 cm) maintains a strong herbaceous presence, but is marked by a partial recovery of deciduous *Quercus* (~7% increase) and by peak values of *Pinus sylvestris/mugo* (maximum value: ~7%). Noticeable is the presence of few *Juglans* pollen grains.

Chronological assessment

The sediment samples collected from Bande di Cavriana proved to be invariably poor of terrestrial material suitable for radiocarbon dating. For this reason, our interpretation of the chronology of the basin relies on multiple dates collected from different cores. Visual aids to identify the position of each dating are presented in Figs. 2.3 and 2.6. The bottom of the studied sequence (~146.5 cm, deepest XRF sample) is dated to approx. 7150 years cal. BP, falling therefore within the Early Neolithic period (Starnini et al., 2018). Due to visible stratigraphic similarities between cores CAV4 and CAV12 (Fig. 2.3), we opted to incorporate dating Poz-76077 (CAV12) into the age-depth model of core CAV4. The thickness of SU 3, equivalent between the two cores, was used as a main reference point to correlate the two levels. The depth of dating Poz-76077 along CAV12 (90-95 cm) would then correspond to ca. 96-101 cm along CAV4 (the discrepancy between the two depths depends predominantly on the topsoil, which is thicker in CAV 4). Poz-76077 inserts itself seamlessly in the modeled trajectory between KIA 51883 and KIA 50432 (Fig. 2.6), suggesting that at the very least its inclusion is not detrimental for the overall model quality. The visible lithological change that constitutes the transition from SU 3 to SU 4, accompanied by an equally important shift in palynological composition, provides an additional reference point to date core CAV4. Comparable transitions from lacustrine carbonates to fine detritus gyttja, associated with a sharp increase in anthropogenic pollen, have been identified in the nearby basins of Lavagnone, Lucone and Castellaro Lagusello (Arpenti et al., 2007; Badino et al., 2011; Dal Corso, 2018; de Marinis et al., 2005; Perego et al., 2011. See location in Fig. 2.1). These lithological and palynological evidences are unambiguously associated with the establishment of a Bronze Age pile dwelling in the immediate vicinity of the coring locations.

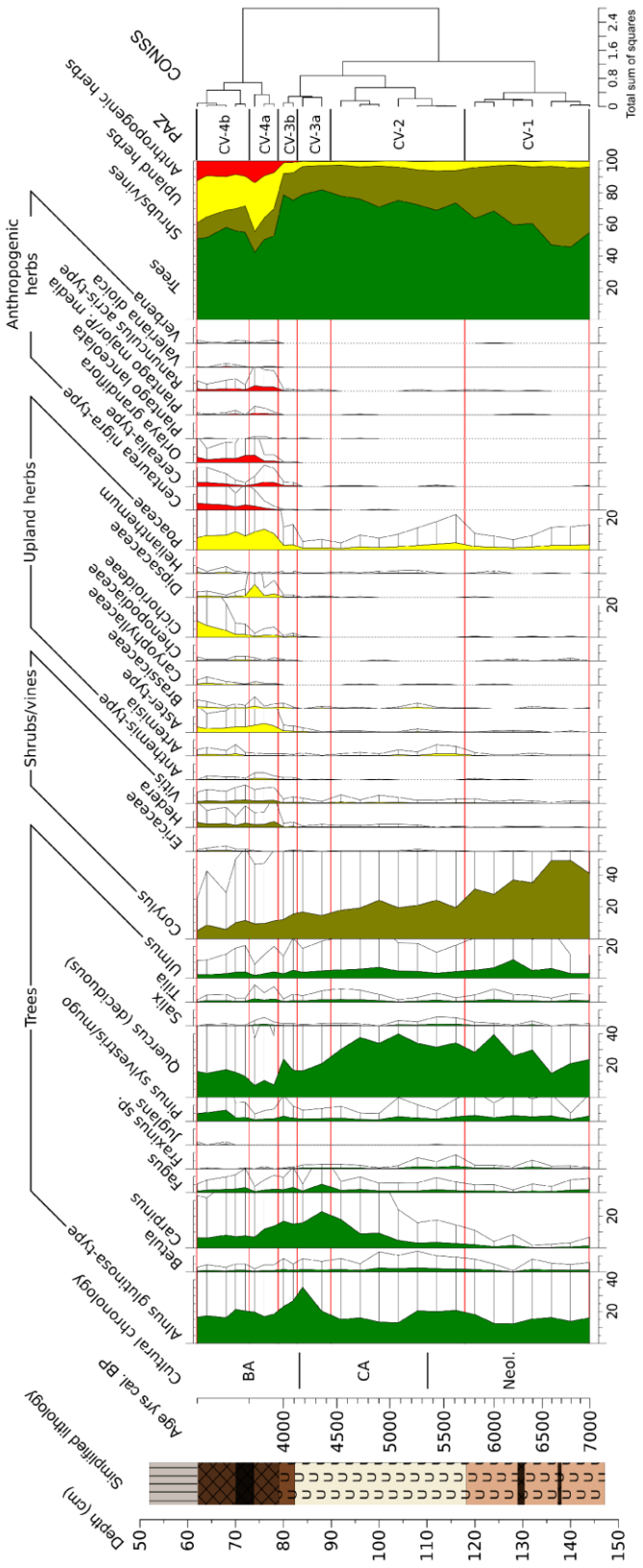

Figure 2.5. *Core CAV4. Selected upland pollen types (percentage values) with added 5x exaggeration factor and CONISS-based zonation. BA = Bronze Age; CA = Copper Age; Neol. = Neolithic. The transitions between Neolithic, Copper Age and Bronze Age follow de de Marinis and Pedrotti (1997) and de Marinis (1999).*

Consistently with these interpretations, we infer that the boundary between SU 3 and SU 4, corresponding to the limit between PAZ CV-3b and CV-4a, represents the establishment of the Bande di Cavriana pile dwelling. The correspondence between these sedimentary and palynological events and the establishment of the settlement is supported by additional radiocarbon and dendrochronological datings available for this site. Dating Poz-75792, collected along core CAV11 at the top of SU 3, returned a median date of ~4050 years cal. BP, while the lower boundary of SU 4 in core CAV 15 produced a median date of ~3980 years cal. BP (Poz-75791). These age ranges are consistent with the earliest available dendrochonological age for Bande di Cavriana, which returned a felling date of 3955 ± 10 years cal. BP (Martinelli, 2007). This dendrochronological date is included in the CAV 4 age-depth model at the base of SU 4. The dating of SU 4 was initially attempted via two oak charcoal fragments extracted from core CAV4 (KIA 50277 and KIA 50276). Both samples resulted in median ages (4330 and 4240 years cal. BP respectively) considerably older than both the establishment of the pile dwelling (3955 ± 10 years cal. BP; Martinelli, 2007) and the estimated local onset of the Bronze Age (ca. 4150 years cal. BP; de Marinis, 1999), initially suggesting a pronounced old-wood effect.

Table 2.3. *Limits of CAV4 pollen zones.*

PAZ	Depth (cm)	Age (years cal. BP)
CV-4b	73-62	~3900-3800
CV-4a	79-73	~3960-3900
CV-3b	83-79	~4130-3960
CV-3a	90-83	~4450-4130
CV-2	118-90	~5700-4450
CV-1	144-118	~7000-5700

With the specific intention to verify these results, additional datings were performed on leftover terrestrial material from core CAV4 (Poz-75790, Poz-75788 and Poz-69225). Sample Poz-75790 was entirely composed of Caryophyllaceae seeds. Sample Poz-69225 was predominantly composed of Caryophyllaceae seeds plus a single seed fragment (<1 mg) of cf. *Solanum nigrum*. Caryophyllaceae seeds accounted for over half the weight of sample Poz-75788 too, with the remaining portion constituted by a single *Setaria pumila* seed and by an unidentifiable charred spikelet fragment. Both samples Poz-75790 and Poz-69225 resulted to be of modern origin. The age of Poz-75788 can be likely attributed to a mixture of modern Caryophyllaceae seeds and older

material. Consequently, we regard these Caryophyllaceae seed as modern contaminants. The vectors that led to their presence in core CAV4 remains to be ascertained, although a link to the bioturbation observed in the core cannot be excluded.

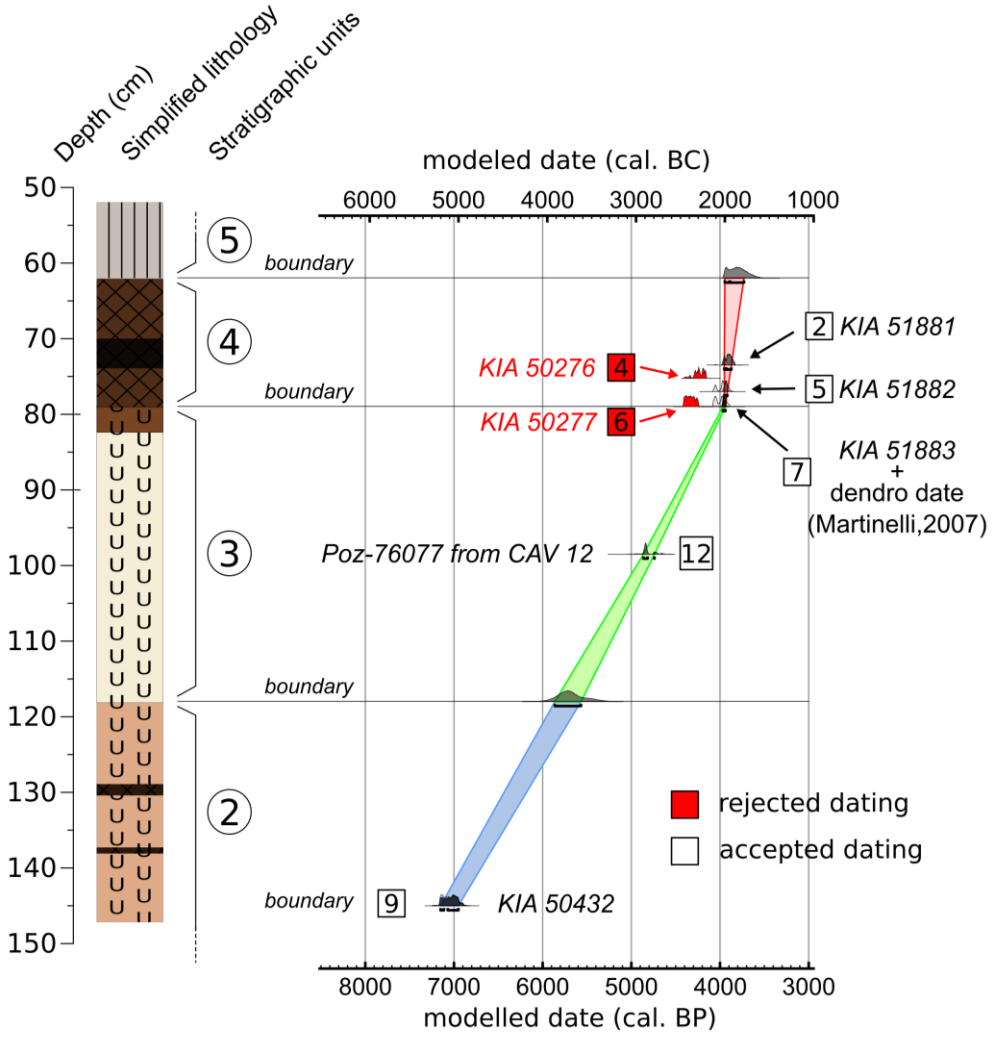

Figure 2.6. *Age-depth model for core CAV 4. Dating numbers refer to their position in Table 2.1. Datings 1-3-8 in Table 2.1 are considered affected by modern contaminations and are not included in the model or in this figure. Graph created with Oxcal v4.3 (see section "Chronological assessment"). Image editing (addition of lithology, dating identifiers, improved legibility) carried out with Inkscape 0.91 (inkscape.org).*

Still, it should be noted that the composition of any pollen sample along the core remains consistent with pre-iron age plant assemblages. A possible exception is constituted by few *Juglans* pollen grains identified in SU 4, since the introduction of this taxon in the Po Plain can be ascribed to the Iron Age (Ravazzi et al., 2013).

Nonetheless, sparse *Juglans* grains have also been documented within the Bronze Age levels of Castellaro Lagusello (Dal Corso, 2018), and linked to long-distance transport. Easily identifiable taxa that expanded in the area after the Iron Age (such as *Castanea* or *Secale*; Ravazzi et al., 2013), or in more recent times (such as *Ambrosia* or *Zea mays*) were not detected during pollen analysis. While their absence does not constitute a definitive proof, it appears to reinforce the attribution of SU 4/PAZ CV-4 to a period ranging from the Early Bronze Age to the Iron Age. The similarities between CAV4 and multiple independent records (e.g. comparisons discussed in section "Discussion") support this conclusion. Furthermore, following the emergence of potentially inaccurate datings (Meadows et al., 2015), the Leibniz laboratory in Kiel offered to test a second time charcoal samples from SU 4/PAZ CV-4. The results of the new datings (KIA 51881, KIA 51882, and KIA 51883) are in line with the pollen-inferred chronology for this core section (Table 2.1; Fig. 2.6). Following the age-depth model presented in Fig. 2.6, the chronological limits of the CAV4 pollen zones are reported in Table 2.3.

Temperature reconstructions

The temperature curve is provided with the intention to synthesize multiple pollen curves into a single palaeoenvironmental indicator, thus easing comparisons with other proxies. After applying h-block cross-validation, the model retained a satisfactory predictive power (r^2 = 0.62 and RMSEP = 3.4 °C, with a standard deviation of the training set = 5.5 °C). The resulting T_{ann} curve (Fig. 2.7) shows a dominant positive slope between the bottom of the sequence and 116 cm, followed then by a negative trend.

DISCUSSION

Notable climatic events

The palaeoenvironmental analysis available for core CAV4 provide multiple perspectives on the mechanisms that influenced sediment deposition at Bande di Cavriana. The combined interpretation of multiple proxies reveals different combinations of seemingly contrasting patterns, likely emerging from the ambiguity of some signal sources (e.g. reactions to cold and/or wet shifts). A few selected scenarios are described below and highlighted in Fig. 2.7. Between approx. 6300 and 6100 years cal. BP (Fig. 2.7, 'a') all proxies appear to display a convincing level of agreement towards a warmer/drier episode, possibly preceded by a cold/wet downturn. This interpretation is inferred from the XRF-based Rb:Sr and Rb:Zr ratios

as indicators for erosion (decreasing values = less precipitations), and a matching $\delta^{18}O$ and $\delta^{13}C$ enrichment which suggests a transition towards warmer conditions that enhanced lake productivity. A more than 5 point increase in C:N goes in the same direction, pointing towards lower lake levels and an expansion of peri-littoral terrestrial vegetation towards the coring location. In contrast, the situation between ~5700 and 5430 years cal. BP (Fig. 2.7, 'b') reveals an apparent contradiction between the Rb:Sr and Rb:Zr data, which point towards higher erosion, and the peak in $\delta^{18}O$ values, which would suggest a warmer/drier climate. Maintaining that Rb:Zr and Rb:Sr represent changes in erosion/precipitation, it is possible that the sharp $\delta^{18}O$ enrichment visible here is specifically a product of higher temperatures rather than a decrease in precipitation. An increase in $\delta^{18}O$ associated with co-varying $\delta^{13}C$ might in fact results from a higher proportion of summer precipitation, which is richer in $\delta^{18}O$ relative to winter values, and would point to a longer summer period (Drummond et al., 1995). Consistently, the generally positive trend of $\delta^{13}C$ values denotes conditions favorable for lake productivity. A peak in the pollen based temperature curve appears to support this general interpretation. Within this time window, C:N reaches one of the highest values in the whole sequence, suggesting that the overall lake level was negatively affected by a prevailing evaporation (terrestrialization of lake shores) and/or that the growing erosion led to a higher input in terrestrial matter. It should also be noted that human pressure too can act as an independent driver behind changes in Rb:Zr and Rb:Sr. Yet, given the near absence of anthropogenic indicators, a large-scale human impact on erosion rates appears currently unlikely (see section "Land cover changes" for further considerations). The warmer and wetter ~5700-5430 years cal. BP interval is then followed by a diametrically opposite situation (~5430-5100 years cal. BP; Fig. 2.7, 'c'). A decrease in precipitation, inferred from the Rb:Sr and Rb:Zr trends, is matched by the most prominent $\delta^{18}O$ drop in the whole sequence, which loses almost 4‰ in the span of few samples. Colder conditions are also supported by declining pollen-based temperature values. In this context, a negative C:N trend could be a product of diminishing erosion over time, reflecting a lower input of terrestrial matter rather than a higher lake productivity. Around 5100-5200 years cal. BP, the joint behavior of $\delta^{18}O$ and $\delta^{13}C$ curves ends. As noted for the ~5700 and 5430 years cal. BP interval, co-variance between $\delta^{18}O$ and $\delta^{13}C$ values might result from changes in the length of the summer period or proportion of summer precipitations (Drummond et al., 1995).

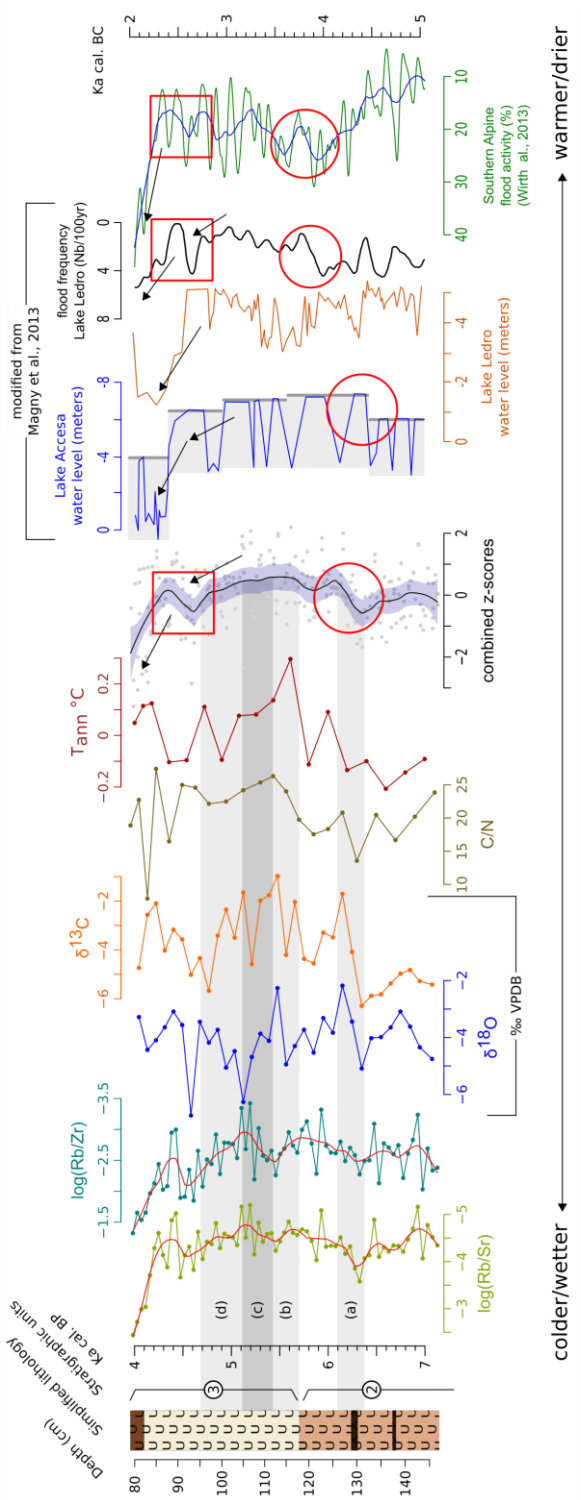

Figure 2.7*. Palaeoenvironmental proxies for core CAV4 plotted according to sample ages.* T_{ann} *is expressed as deviation from the mean value of the sequence. Rb:Sr and Rb:Zr have been LOESS smoothed for ease of interpretation (smooth factor = 0.15). The shaded area enveloping the z-score curve delimits the 95% confidence interval of the regression. Black arrows, red circles and red squares are meant to highlight possible similarities between major trend changes in the combined z-scores curve and other proxies.*

Their distinctively opposite behavior within the 5100-4700 years cal. BP section of the core (Fig. 2.7, 'd') could then suggest a marked change in seasonal temperature/precipitation patterns. These few examples are meant to illustrate how a single proxy curve might respond to different drivers of change through time. Such a detailed interpretation is undoubtedly desirable, and represents an attempt to capture the complexity inherent to ecological systems. Yet, since any combination of trends could be attributed to a seemingly reasonable narrative, the risk of over-interpretation increases proportionally to the number of "climatic events" identified in a given sequence. In an attempt to mitigate this risk, we opted to focus on broader climate trends shared among different proxies. All (unsmoothed) curves from CAV4 presented in Fig. 2.7 were converted to z-scores in such way that growing values correspond to warmer/drier/less erosive conditions. Conversely, decreasing z-scores correspond to colder/wetter/more erosive ones. The z-scores of all proxies were then combined and LOESS smoothed (smooth factor = 0.2). This approach is meant to highlight any situation where stable isotopes, XRF and pollen-based curves generally agree towards one of two possible simple trajectories: warm/dry vs. cold/wet. The resulting curve is then compared against independent reconstructions from sites between the southern Alpine area and central Italy. Data from Lake Ledro, Lake Accesa (Magny et al., 2013) and the stacked southern-Alpine flood record (Wirth et al., 2013) are presented in Fig. 2.7. The southern-Alpine synthesis includes the Lake Ledro data too, yet the flood curve from Ledro is also presented separately due to its relative geographical proximity to Bande di Cavriana (Fig. 2.1). The combined CAV4 z-scores curve presents a few notable features. The first one is represented by a dynamic change in trajectories between ~6500 and 6000 years cal. BP. Here, the initial cold/wet trend is interrupted by a marked shift in the opposite direction (~6300-6100 years cal. BP). As noted above (example 'a'; Fig. 2.7), this change results from all proxies transitioning towards a warm and dry trajectory. A similar and approximately contemporaneous shift into drier conditions is arguably visible at Lake Accesa, where the lowermost limits of the reconstructed lake levels drops by more than 1m after ~6400 years cal. BP (Fig. 2.7, red circle). A comparably clear drop is not visible in the Ledro lake level curve (Fig. 2.7), yet the Ledro flood record shows an intriguingly similar shift into more arid conditions ~500 years later (Fig. 2.7, red circle). A major trend change occurs at the same time within the S-Alpine flood record too. Any correspondence between these transitions is currently just presented as a noteworthy similarity. Even ignoring local hydrological differences, assuming that all these events are depicting the same warm/arid shift would still imply a fundamental disagreement

between age-depth models. In this regard, it is certainly true that the dating of SU 2 would benefit from additional chronological constraints. The same time interval al Lake Accesa appears to be dated more reliably, although its age-depth model is partly built upon radiocarbon datings from bulk sediment. A second notable feature of the z-scores curve is represented by a sequence of events similar to the ~6500-6000 years cal. BP situation. A mild negative trend dominates the curve after ~5500 years cal. BP, dropping more sharply after ~4800 years cal. BP. This decidedly cold/wet drop is then interrupted between 4600 and 4300 years cal. BP by a temporary shift to more warm/arid conditions. After ~4300 years cal. BP, the rapid cold/wet trajectory resumes, lasting until the end of the sequence. This pattern, arguably resulting mostly from the strong gradients in the XRF proxies, can be partly retraced in the other reconstructions too. The warm/dry shift is recorded in the Ledro flood record and possibly in the more noisy S-Alpine flood synthesis. It is absent from the lake level curves of Ledro and Accesa, yet all these reconstructions invariably agree towards a sharp cold/wet downturn after 4400-4300 years cal. BP. These pronounced cold/wet trends have been linked to a more southerly position of the of the circum-North Atlantic circulation system. In this context, the negative NAO (North Atlantic Oscillation) would have caused strong winds and moisture to enter the Mediterranean Sea, leading to an increase in precipitation frequency in Northern/Central Italy (Magny et al., 2013; Wirth et al., 2013).

Of particular interest is the 4600-4300 years cal. BP warm/arid shift. Very tentatively, and taking into account dating uncertainties, this event might be ascribed to a local expression of the rather elusive '4.2ka' arid event (Bini et al., 2019). Beside the flood record of Ledro, a comparable drier period is documented in the isotopic record of Corchia cave (4500-4100 years cal. BP. Location shown in Fig. 2.1) likely in connection with a short-lived more positive NAO (Isola et al., 2019).

Land cover changes

Pre-Bronze Age woodland dynamics: the expansion of *Carpinus betulus*. Together with the extinction of *Abies* (Wick and Möhl, 2006), the expansion of *Carpinus betulus* is probably the most notable vegetational event to occur along the southern Alpine foothills during the late mid-Holocene (Ravazzi and Pini, 2013). At Bande di Cavriana, the rise of this taxon (*C. betulus sensu* Beug, 2004) begins between pollen zones CV-1 and CV-2, approximately from 5700 years cal. BP (Fig. 2.5). The same long-tailed rise is visible at Lucone, Lavagnone and Castellaro Lagusello, although a precise comparison is hindered by chronological uncertainties. *C. betulus*

expanded in northern Italy from the Venetian Plain (Magri et al., 2015), arguably following a slow migration from its glacial refugia in the Balkans (Grivet and Petit, 2003). Expanding into dense-canopy forests should in theory not constitute an obstacle for this species, which tolerates full sunlight as well as strongly shaded environments (San-Miguel-Ayanz et al., 2016). Its superior height would probably put it in an advantaged position against *Corylus*, which could explain the apparent competition between these two taxa in the CAV4 diagram. The suppression of *Corylus* populations has been noted also in connection with *Fagus* expansion (Gardner and Willis, 1999). While the latter is not abundant in the study area, this observation is in line with the CAV4 data, supporting the sensitivity of *Corylus* toward a growing presence of taller species with shade-tolerant saplings. The damaging capabilities of *C. betulus* have been recently observed in Białowieża forest (Poland), where the 20th century invasion of this species is connected with lower light levels on the forest ground and with a decline in biodiversity (Kwiatkowska and Wyszomirski, 1988). Yet the expansion of *C. betulus* during the Holocene was evidently slower when compared to other tree species. This delay might stem from multiple factors. *C. betulus* seeds are primarily wind disseminated, with a reported dispersal distance <150 m (Coart et al., 2005). Conversely, seeds of *Quercus* and *Corylus* are dispersed by animals, thus improving both germination chances (Kollmann and Schill, 1996) and potential dispersal range. In the case of *C. betulus*, aggravating factors might also include a long stratification time (up to 1 year; Savill, 2013), relatively low seed viability (~45% germination rates; Savill, 2013), and reported difficulties to germinate in oak-leaf litter (Kwiatkowska et al., 1997). For comparison, outdoor tests showed that >80% of *Corylus* nuts sown in autumn germinated during the following spring (Pipinis et al., 2018). Being a strong resprouter, *C. betulus* can withstand severe coppicing and pollarding (San-Miguel-Ayanz et al., 2016), and might be favored by fire activity against less reactive taxa (Kaltenrieder et al., 2010). These regenerative capabilities arguably promoted its expansion in connection with anthropogenic disturbance (Küster, 1997). A marked increase in *C. betulus* percentages occurs in the Lake Garda area after ~5350 years cal. BP, during the Copper Age (Ravazzi and Pini, 2013). At Bande di Cavriana, this phenomenon is visible after ~5100 years cal. BP (Fig. 2.5). Ravazzi and Pini (2013) suggest a connection between rising *C. betulus* percentages and the introduction of metal axes. Copper axes are documented in the regional archaeological record from approximately the second half of the 6th millennium BP (e.g. Artioli et al., 2017). An earlier availability of polished stone axes is attested too. Within the southern Lake Garda area, typological comparisons place the earliest stone

axe finds between early/middle (Lo Vetro, 2014) and middle/late Neolithic (de Marinis, 2000), i.e. roughly between mid-8th and 6th millennium BP. The performances of comparable stone tools have been tested experimentally, supporting their effectiveness in felling trees (Lunardi, 2008). If the increase of *C. betulus* is linked to human activities, it might then be less dependent on the available technology and more on the adoption of new woodland exploitation strategies. Neolithic settlements were certainly active in the area before the transition into the Bronze Age (e.g. most notably the settlement of Tosina, ~7.5 km East of Bande di Cavriana, Poggiani Keller, 2014). Yet, the archaeological evidences during this period remain generally diluted both in space and in time. On-site pollen analysis reveal typical high levels of herbaceous and anthropogenic taxa (Zanon, 2014), but far from major settlements almost no palynological traces of human activities are visible (e.g. pollen zones CV-1, CV-2, CV-3a within this study; Zanon, 2010). These differences may be at least in part caused by inadequate sampling resolutions, but they nonetheless appear to exclude widespread and long lasting anthropic disturbance on the landscape. Whether the region-wide expansion of *C. betulus* is to be attributed to scattered Neolithic/Copper age human groups or not, it remains to be ascertained. As noted in section "Notable climatic events", SU 2 encompasses a series of potentially diverse temperature/precipitation patterns. If *C. betulus* dynamics are linked to these variable climatic trends, it is unclear which mechanisms consistently promoted this taxon against other thermophilous/mesophilous taxa. An additional explanation for the Copper Age rise of *C. betulus* is suggested by the recent '*Carpinus* invasion' recorded at Białowieża (Kwiatkowska et al., 1997). In this context, a reduction in the population of browsers (red deer), and the reintroduction of grazers (European bison) possibly led to a lower control in the density of *C. betulus* saplings. A similar situation might be applicable to the Cavriana region. The Neolithic and following periods are associated with a growing importance of herding activities (i.e. grazing fauna) and a lower reliance on hunting (Bona, 2014). This pattern might speculatively depend on a preference for a more stable meat supply, but could also suggest a decreasing game density in human populated areas. The rise in *C. betulus* could then depend on a gradually lower presence of wild browsers over a long time period, accompanied by the rising importance of domestic grazers. This situation could have been furtherly tilted in *C. betulus*' favor by the relatively lower nutritional value of its leaves compared to those of other local species (Hejcmanová et al., 2014). In addition, a higher grazing pressure might have also promoted the germination of *C. betulus* seeds by reducing herb and litter cover (Kwiatkowska et al., 1997).

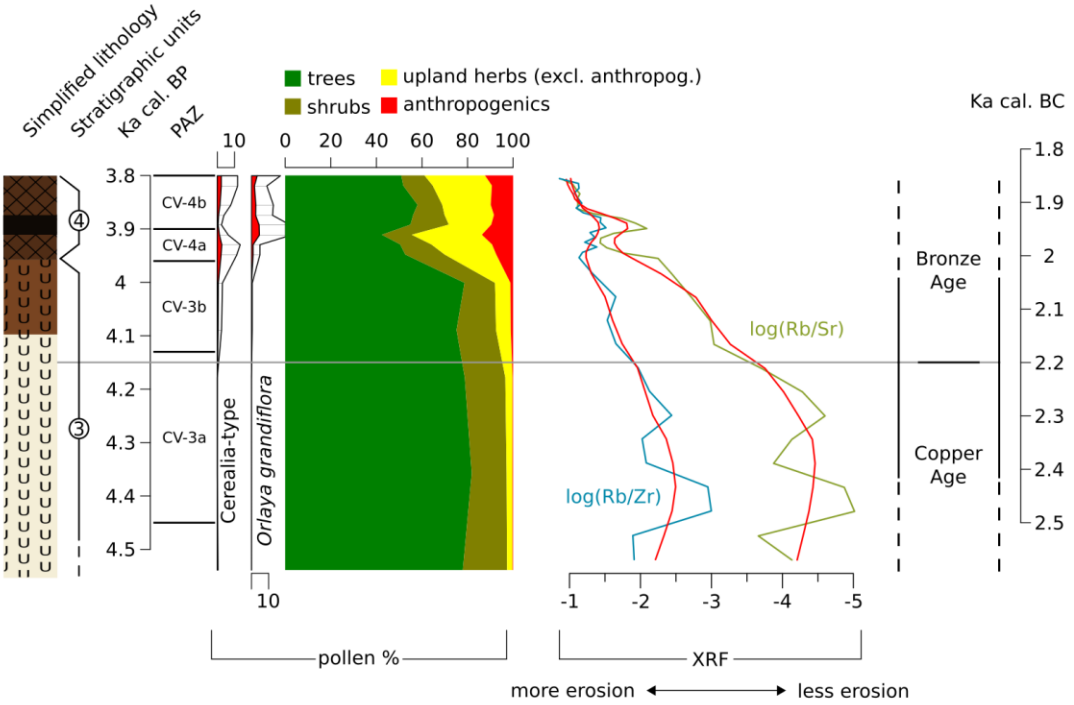

Figure 2.8. *Selected pollen curves and erosion indicators from core CAV4 around the Copper Age-Bronze Age transition. Rb:Sr and Rb:Zr have been LOESS smoothed (red curves) for ease of interpretation (smooth factor = 0.15).*

Transition into the Bronze Age. The transition between Copper and Bronze age is a fluid phenomenon, whose limit is conventionally set at 4150 years cal. BP (Baioni et al., 2015; de Marinis, 1999). Beside the development of bronze metallurgy, this phenomenon is prominently marked by a shift in settlement strategies. Neolithic and Copper Age evidences in the Garda Lake area are mostly dominated by scattered finds (de Marinis, 2000; particularly notable is the funerary complex of Manerba del Garda, e.g. Barfield et al., 2010), possibly ascribed to relatively short-lived dwelling phases. In contrast with this pattern, nearly 50 Bronze Age settlements have been described in the area, with the majority of them (as is the case for Bande di Cavriana) located along water bodies (de Marinis, 2010). As mentioned in section "Chronological assessment", the colonization of lakes and wetlands is associated with a distinct impact on stratigraphic and pollen profiles. The increase in anthropogenic indicators and herbaceous taxa likely reflects landscape exploitation in the vicinities of the settlement (e.g. areas dedicated to crops and pastures). The decline in arboreal pollen is commonly interpreted as the result of widespread deforestation events (e.g. Badino et al., 2011). Forest resources were clearly employed in the construction of pile dwellings (e.g. more than 200 wooden posts were documented at Lavagnone within a 90m^2 excavation, de Marinis, 2000), yet it is currently not clear if logging for

timber and fuel exceeded forest regeneration rates. The use of alternatives to wood, such as dung employed as a fuel source (e.g. Miller, 1984), has currently been excluded given the available data (Perego, 2015). Notably, the beginning of an uninterrupted Cerealia-type curve in core CAV4 begins approximately after 4100 years cal. BP (Fig. 2.8), which is compatible with the conventional date for the Bronze Age onset in the area. Between this date and the establishment of the Bande di Cavriana pile dwelling, anthropogenic species are continuously present even though with low values, possibly hinting at a stable human presence outside of the study site. For reference, severe anthropic disturbance begins ~4200 years cal. BP in the Lavagnone sequence (lower limit of pollen zone LVG21, Perego, 2015), and ~4100 years cal. BP at Castellaro Lagusello (lower limit of zone CL11.5, Dal Corso, 2018). A shift towards higher erosion (rising Rb:Sr and Rb:Zr values) occurs after ~4300 years cal. BP, before the beginning of the Bronze Age (Fig. 2.8). In the "Notable climatic events" section, we interpreted this shift as a transition into cooler/wetter conditions. Human exploitation of the landscape can affect erosion rates too, and should be regarded as a potential driver behind Rb:Sr and Rb:Zr trends. In this specific context, the sparse archaeological record and lack of anthropogenic indicators before the Bronze Age, as well as comparable wet shifts seen in independent proxies (Fig. 2.7), appear to support a climate-oriented interpretation. Ultimately, the reasons that led Bronze Age dwellers to prefer lakeside locations remain inscrutable. Yet, the CAV4 sequence supports the hypothesis that the widespread adoption of pile-dwelling settlement strategies in the Garda Lake area occurred under a changing climate. Perego (2015) reports on the presence of dung pellets in dwelling layers from Lucone and Lavagnone, pointing out how their presence could enrich the pollen load of the surrounding sediment with both arboreal and non-arboreal pollen. Similarly, at least part of the Cerealia-type pollen could derive from on-site processing activities. A high amount of pollen remains in fact trapped in the glumes and may be dispersed during, for example, threshing and winnowing (Bower, 1992). Pollen data collected near dwelling layers should then be interpreted with due caution, since a potentially significant part of their pollen load could be independent from 'natural' atmospheric deposition. In this regard, we limit our discussion of the Bronze Age CAV 4 section to few notes on *Orlaya grandiflora*. This xerophytic taxon thrives on dry meadows and before the Bronze Age was likely relegated to marginal niches. Consequently, its rising percentages possibly suggest increasing topsoil depletion and the subsequent expansion of well-drained areas with exposed coarse glacial deposits (Perego et al., 2011). In the pollen record of Bande di Cavriana, the initial establishment of a

continuous *Orlaya* curve with values generally <1% is followed by a noticeable rise towards higher percentages. The same pattern is visible at the sites of Lavagnone and Castellaro Lagusello. This marked percentage increase occurs ~4000 years cal. BP at Castellaro Lagusello (within pollen zone CL11.5, Dal Corso, 2018), ~3900 years cal. BP at Bande di Cavriana (Fig. 2.8) and ~3800 years cal. BP at Lavagnone (lower limit of pollen zone LVG23, Perego, 2015). *Orlaya* is present at Lucone with lower percentages compared to the other sites, and expands only after ~3700 years cal. BP (pollen zone LD24, Furlanetto, 2013). Taken at face value, these dates appear to describe a South-East to North-West vector. New data and improved age-depth models might help to evaluate the solidity of this pattern which, given the zoochorous dispersal of this species (Perego et al., 2011), could prove useful to test for itinerant pastoral activities.

CONCLUSIONS

In the present paper we provide a synthesis of multiple environmental proxies from the site of Bande di Cavriana. Our investigations span the interval between Early Neolithic and Early Bronze Age, approximately between ~7100 and 3800 years cal. BP. The combined analysis of stable isotopes, XRF and pollen data revealed the presence of at least three major shifts in temperature/precipitation before the transition into the Bronze Age. The first one occurs approximately between 6300 and 6100 years cal. BP and marks a long lasting transition into warmer/more arid conditions. The second shift begins at ~4600 years cal. BP and peaks at ~4300 years cal. BP. It represents a new short-lived return to warm/arid conditions after a gradual recovery from the 6300-6100 years cal. BP transition. Arguably, this episode could represent the local expression of the '4.2ka' event. Future investigations might help to ascertain if these events represent actual supra-regional patterns or if they reflect more localized hydrological changes. The third major shift occurs after ~4300 years cal. BP, when the Bande di Cavriana record shows a marked trajectory towards colder/wetter conditions. This trend is more consistently recorded in multiple independent proxies, and suggests that the transition into the Bronze Age (approximately ~4150 years cal. BP) occurred under a fast changing climate. Caution must nonetheless be applied when interpreting palaeoclimatic indicators, as tracking human activity before the establishment of the Bronze Age pile-dwellings remains complicated. Neolithic and Copper Age finds in the study region are present but relatively diluted, and convincing palynological indicators of widespread, sustained human disturbance are largely absent before the Bronze Age. Still, our interpretation

concerning the Copper Age expansion of *Carpinus betulus* (after ~5100 years cal. BP at Bande di Cavriana) involves a possible growing importance of herding activities, as well as new forest exploitation strategies. This connection remains to be tested. If proven true, it would also prompt a contextual re-interpretation of different geochemical proxies, since they might variously respond to landscape exploitation as well as to shifting climate patterns. Currently, given the available evidences, we suggest a dominant climatic control over local wetland dynamics before the Bronze Age.

ACKNOWLEDGEMENTS

This contribution is part of a PhD research project developed within the Graduate School "Human Development in Landscapes" (Christian-Albrechts-Universität zu Kiel) and funded by the German Research Foundation (DFG). The paper further evolved through discussions in the DFG Collaborative Research Center (CRC) 1266 "Scales of Transformations, Human-Environmental Interaction in Prehistoric and Archaic Societies" at Kiel University (DFG - Projektnummer 2901391021 e SFB 1266). Maria Giuseppina Ruggiero (Soprintendenza Archeologia, Belle Arti Paesaggio per le province di Como, Lecco, Monza e Brianza, Pavia, Sondrio e Varese) and Adalberto Piccoli (Museo Archeologico dell'alto Mantovano) provided invaluable support with obtaining access to the study site and during fieldwork operations. Their help is greatly appreciated. The authors also wish to thank two anonymous reviewers for their helpful comments, corrections and suggestions.

Bibliography

Arpenti, E., Ravazzi, C., Deaddis, M., 2007. Il Lavagnone di Desenzano del Garda: analisi pollinica ed informazioni paleoecologiche sui depositi lacustri durante le prime fasi d'impianto dell'abitato (antica età del Bronzo). Notizie Archeologiche Bergomensi 10 (2002), 35–54.

Artioli, G., Angelini, I., Kaufmann, G., Canovaro, C., Dal Sasso, G., Villa, I.M., 2017. Long-distance connections in the Copper Age: New evidence from the Alpine Iceman's copper axe. PLOS ONE 12, e0179263. https://doi.org/10.1371/journal.pone.0179263

Badino, F., Baioni, M., Castellano, L., Martinelli, N., Perego, R., Ravazzi, C., 2011. Foundation, development and abandoning of a Bronze Age pile-dwelling ("Lucone d", Garda Lake) recorded in the palynostratigraphic sequence of the pond offshore the settlement. Il Quaternario e Italian Journal of Quaternary Sciences 24.

Baioni, M., Longhi, C., Mangani, C., Martinelli, N., Nicosia, C., Ruggiero, M.G., Salzani, P., 2015. La palafitta del Corno di Sotto (Desenzano del Garda, Brescia) nell'ambito dello sviluppo dei primi insediamenti palafitticoli del lago di Garda, in: Leonardi, G., Tiné, V. (Eds.), Preistoria e protostoria del Veneto, Studi di preistoria e protostoria. Istituto italiano di preistoria e protostoria ; Soprintendenza per i beni archeologici del Veneto : Università degli studi di Padova, Firenze : Padova.

Barfield, L.H., Manning, S.W., Valzolgher, E., Higham, T.F., 2010. A wiggle-matched date for the Copper Age cemetery at Manerba del Garda, northern Italy. Radiocarbon 52, 984–1001.

Baroni, C., Zanchetta, G., Fallick, A.E., Longinelli, A., 2006. Mollusca stable isotope record of a core from Lake Frassino, northern Italy: hydrological and climatic changes during the last 14 ka. The Holocene 16, 827–837. https://doi.org/10.1191/0959683606hol975rp

Berntsson, A., Jansson, K.N., Kylander, M.E., Vleeschouwer, F.D., Bertrand, S., 2015. Late Holocene high precipitation events recorded in lake sediments and catchment geomorphology, Lake Vuoksjávrátje, NW Sweden. Boreas 44, 676–692. https://doi.org/10.1111/bor.12127

Beug, H.-J., 2004. Leitfaden der Pollenbestimmung für Mitteleuropa und angrenzende Gebiete. Verlag Dr. Friedrich Pfeil.

Biagi, P., Piccoli, A., 1979. Stazione della Cultura dei Vasi a Bocca Quadrata a Cavriana (Mn) - (Monte Tondo, Corte Galeazzo), in: Atti Del Convegno Archeologico Benacense - Cavriana, 10 Settembre 1978, Annali Benacensi - Rassegna Di Studi Paletnologici Ed Archeologici. pp. 141–149.

Bini, M., Zanchetta, G., Perşoiu, A., Cartier, R., Català, A., Cacho, I., Dean, J.R., Di Rita, F., Drysdale, R.N., Finnè, M., Isola, I., Jalali, B., Lirer, F., Magri, D., Masi, A., Marks, L., Mercuri, A.M., Peyron, O., Sadori, L., Sicre, M.-A., Welc, F., Zielhofer, C., Brisset, E., 2019. The 4.2 ka BP Event in the Mediterranean region: an overview. Climate of the Past 15, 555–577. https://doi.org/10.5194/cp-15-555-2019

Bona, F., 2014. La fauna del sito di Tosina, in: Poggiani Keller, R. (Ed.), Contadini, Allevatori e Artigiani a Tosina Di Monzambano (Mn) Tra V e IV Millennio a.C. - Una Comunità Neolitica Nei Circuiti Padani e Veneti. Grafiche Tagliani Stampa e Comunicazione per Acherdo Edizioni, Calcinato (Bs).

Bower, M., 1992. Cereal Pollen Dispersal: A Pilot Study. Cambridge Archaeological Journal 2, 236–241. https://doi.org/10.1017/S0959774300000615

Bronk Ramsey, C., 2009. Bayesian Analysis of Radiocarbon Dates. Radiocarbon 51, 337–360. https://doi.org/10.1017/S0033822200033865

Brown, B.E., Fassbender, J.L., Winkler, R., 1992. Carbonate production and sediment transport in a marl lake of southeastern Wisconsin. Limnology and Oceanography 37, 184–191. https://doi.org/10.4319/lo.1992.37.1.0184

Brunetti, M., Lentini, G., Maugeri, M., Nanni, T., Simolo, C., Spinoni, J., 2012. Projecting North Eastern Italy temperature and precipitation secular records onto a high-resolution grid. Physics and Chemistry of the Earth, Parts A/B/C, The Climate of Venetia and Northern Adriatic 40–41, 9–22. https://doi.org/10.1016/j.pce.2009.12.005

Capuzzo, G., Zanon, M., Dal Corso, M., Kirleis, W., Barceló, J.A., 2018. Highly diverse Bronze Age population dynamics in Central-Southern Europe and their response to regional climatic patterns. PLOS ONE 13, e0200709. https://doi.org/10.1371/journal.pone.0200709

Clarke, G.C.S., Jones, M.R., 1977. Plantaginaceae. Review of Palaeobotany and Palynology 24, 129–154. https://doi.org/10.1016/0034-6667(77)90051-3

Cloern, J.E., Canuel, E.A., Harris, D., 2002. Stable carbon and nitrogen isotope composition of aquatic and terrestrial plants of the San Francisco Bay estuarine system. Limnology and Oceanography 47, 713–729. https://doi.org/10.4319/lo.2002.47.3.0713

Coart, E., Glabeke, S.V., Petit, R.J., Bockstaele, E.V., Roldán-Ruiz, I., 2005. Range wide versus local patterns of genetic diversity in hornbeam (Carpinus betulus L.). Conservation Genetics 6, 259–273. https://doi.org/10.1007/s10592-004-7833-7

Cremaschi, M., 1987. Paleosols and Vetusols in the Central Po Plain (Northern Italy). A study in Quaternary Geology and Soil development. Unicopli.

Cremaschi, M., Mercuri, A.M., Torri, P., Florenzano, A., Pizzi, C., Marchesini, M., Zerboni, A., 2016. Climate change versus land management in the Po Plain (Northern Italy) during the Bronze Age: New insights from the VP/VG sequence of the Terramara Santa Rosa di Poviglio. Quaternary Science Reviews 136, 153–172. https://doi.org/10.1016/j.quascirev.2015.08.011

Dal Corso, M., 2018. Environmental history and development of the human landscape in a northeastern Italian lowland during the Bronze Age: a multidisciplinary case-study (PhD Thesis). Kiel University.

Davis, B.A.S., Zanon, M., Collins, P., Mauri, A., Bakker, J., Barboni, D., Barthelmes, A., Beaudouin, C., Birks, H.J.B., Bjune, A.E., Bozilova, E., Bradshaw, R.H.W., Brayshay, B.A., Brewer, S., Brugiapaglia, E., Bunting, J., Connor, S.E., de Beaulieu, J.-L., Edwards, K.J., Ejarque, A., Fall, P., Florenzano, A., Fyfe, R., Galop, D., Giardini, M., Giesecke, T., Grant, M.J., Guiot, J., Jahns, S., Jankovská, V., Juggins, S., Kahrmann, M., Karpińska-Kołaczek, M., Kołaczek, P., Kühl, N., Kuneš, P.,

Lapteva, E.G., Leroy, S.A.G., Leydet, M., Sáez, J.A.L., Masi, A., Matthias, I., Mazier, F., Meltsov, V., Mercuri, A.M., Miras, Y., Mitchell, F.J.G., Morris, J.L., Naughton, F., Nielsen, A.B., Novenko, E., Odgaard, B., Ortu, E., Overballe-Petersen, M.V., Pardoe, H.S., Peglar, S.M., Pidek, I.A., Sadori, L., Seppä, H., Severova, E., Shaw, H., Święta-Musznicka, J., Theuerkauf, M., Tonkov, S., Veski, S., van der Knaap, P., van Leeuwen, J.F.N., Woodbridge, J., Zimny, M., Kaplan, J.O., 2013a. Erratum to: The European Modern Pollen Database (EMPD) project. Vegetation History and Archaeobotany 22, 531–531. https://doi.org/10.1007/s00334-013-0408-0

Davis, B.A.S., Zanon, M., Collins, P., Mauri, A., Bakker, J., Barboni, D., Barthelmes, A., Beaudouin, C., Bjune, A.E., Bozilova, E., Bradshaw, R.H.W., Brayshay, B.A., Brewer, S., Brugiapaglia, E., Bunting, J., Connor, S.E., Beaulieu, J.-L. de, Edwards, K., Ejarque, A., Fall, P., Florenzano, A., Fyfe, R., Galop, D., Giardini, M., Giesecke, T., Grant, M.J., Guiot, Jöel, Jahns, S., Jankovská, V., Juggins, S., Kahrmann, M., Karpińska-Kołaczek, M., Kołaczek, P., Kühl, N., Kuneš, P., Lapteva, E.G., Leroy, S.A.G., Leydet, M., Guiot, José, Jahns, S., Jankovská, V., Juggins, S., Kahrmann, M., Karpińska-Kołaczek, M., Kołaczek, P., Kühl, N., Kuneš, P., Lapteva, E.G., Leroy, S.A.G., Leydet, M., Sáez, J.A.L., Masi, A., Matthias, I., Mazier, F., Meltsov, V., Mercuri, A.M., Miras, Y., Mitchell, F.J.G., Morris, J.L., Naughton, F., Nielsen, A.B., Novenko, E., Odgaard, B., Ortu, E., Overballe-Petersen, M.V., Pardoe, H.S., Peglar, S.M., Pidek, I.A., Sadori, L., Seppä, H., Severova, E., Shaw, H., Święta-Musznicka, J., Theuerkauf, M., Tonkov, S., Veski, S., Knaap, W.O. van der, Leeuwen, J.F.N. van, Woodbridge, J., Zimny, M., Kaplan, J.O., 2013b. The European Modern Pollen Database (EMPD) project. Veget Hist Archaeobot 22, 521–530. https://doi.org/10.1007/s00334-012-0388-5

de Marinis, R., 2000. Il Museo civico archeologico Giovanni Rambotti di Desenzano del Garda una introduzione alla preistoria del lago di Garda. Città di Desenzano del Garda, Assessorato alla Cultura, Desenzano del Garda.

de Marinis, R., 1999. Towards a Relative and Absolute Chronology for the Bronze Age in Northern Italy. Notizie Archeologiche Bergomensi 7, 23–100.

de Marinis, R.C., 2010. Continuity and discontinuity in northern Italy from the Recent to the Final Bronze Age: a view from north-western Italy, in: Cardarelli, A., Cazzella, A., Frangipane, M., Peroni, R. (Eds.), Scienze Dell'Antichità. Storia Archeologia Antropologia 15 (2009). Atti Del Convegno Internazionale "Le Ragioni Del Cambiamento/Reasons for Change". Roma, 15-17 Giugno 2006. Edizioni Quasar, pp. 535–545.

de Marinis, R.C., Pedrotti, A., 1997. L'età del rame nel versante italiano delle Alpi centro-occidentali, in: Atti Della XXXI Riunione Scientifica IIPP "La Valle d'Aosta Nel Quadro Della Preistoria e Protostoria Dell'arco Alpino Centro-Occidentale" - Courmayeur, 2-5 Giugno 1994.

de Marinis, R.C., Rapi, M., Ravazzi, C., Arpenti, E., Deaddis, M., Perego, R., 2005. Lavagnone (Desenzano del Garda): new excavations and palaeoecology of a Bronze Age pile dwelling site in northern Italy, in: Della Casa, Ph., Trachsel, M. (Eds.), Wetland Economies and Societies. Proceeding of the International Conference in Zurich, Zurich, 10-13 March 2004. Collectio Archæologica 3, 221-232.

Drummond, C.N., Patterson, W.P., Walker, J.C.G., 1995. Climatic forcing of carbon-oxygen isotopic covariance in temperate-region marl lakes. Geology 23, 1031. https://doi.org/10.1130/0091-7613(1995)023<1031:CFOCOI>2.3.CO;2

Erdtman, G., 1960. The Acetolysis Method: a revised description. Svensk Botanisk Tidskrift 54, 561–564.

Furlanetto, G., 2013. Storia della vegetazione dell'anfiteatro benacense negli ultimi 3000 anni. Analisi pollinica dei depositi lacustri del Lucone di Polpenazze. (Università degli Studi di Milano, academic year 2011/2012. Unpublished master's thesis).

Gardner, A.R., Willis, K.J., 1999. Prehistoric farming and the postglacial expansion of beech and hornbeam: a comment on Küster. The Holocene 9, 119–121.

Gavin, D.G., Oswald, W.W., Wahl, E.R., Williams, J.W., 2003. A statistical approach to evaluating distance metrics and analog assignments for pollen records. Quaternary Research 60, 356–367. https://doi.org/10.1016/S0033-5894(03)00088-7

Girod, A., Bianchi, I., Mariani, M., 1980. Gasteropodi I. Guide per il riconoscimento delle specie animali delle acque interne italiane. CNR AQ/1/44, 7: 1-85, Roma.

Grimm, E.C., 1987. CONISS: a FORTRAN 77 program for stratigraphically constrained cluster analysis by the method of incremental sum of squares. Computers & Geosciences 13, 13–35.

Grivet, D., Petit, R.J., 2003. Chloroplast DNA phylogeography of the hornbeam in Europe: Evidence for a bottleneck at the outset of postglacial colonization. Conservation Genetics 4, 47–56.

Håkanson, L., Jansson, M., 1983. Principles of lake sedimentology. The Blackburn Press, New Jersey.

Hejcmanová, P., Stejskalová, M., Hejcman, M., 2014. Forage quality of leaf-fodder from the main broad-leaved woody species and its possible consequences for the Holocene development of forest vegetation in Central Europe. Vegetation History and Archaeobotany 23, 607–613. https://doi.org/10.1007/s00334-013-0414-2

Hijmans, R.J., Cameron, S.E., Parra, J.L., Jones, P.G., Jarvis, A., 2005. Very high resolution interpolated climate surfaces for global land areas. International Journal of Climatology 25, 1965–1978. https://doi.org/10.1002/joc.1276

Hodell, D.A., Channell, J.E.T., Curtis, J.H., Romero, O.E., Röhl, U., 2008. Onset of "Hudson Strait" Heinrich events in the eastern North Atlantic at the end of the middle Pleistocene transition (~640 ka)? Paleoceanography 23. https://doi.org/10.1029/2008PA001591

Hunter, R.D., 1976. Changes in carbon and nitrogen content during decomposition of three macrophytes in freshwater and marine environments. Hydrobiologia 51, 119–128. https://doi.org/10.1007/BF00009827

Isola, I., Zanchetta, G., Drysdale, R.N., Regattieri, E., Bini, M., Bajo, P., Hellstrom, J.C., Baneschi, I., Lionello, P., Woodhead, J., Greig, A., 2019. The 4.2 ka event in the central Mediterranean: new data from a Corchia speleothem (Apuan Alps, central Italy). Climate of the Past 15, 135–151. https://doi.org/10.5194/cp-15-135-2019

Joannin, S., Magny, M., Peyron, O., Vanniere, B., Galop, D., 2014. Climate and land-use change during the late Holocene at Lake Ledro (southern Alps, Italy). The Holocene 24, 591–602. https://doi.org/10.1177/0959683614522311

Joannin, S., Vannière, B., Galop, D., Peyron, O., Haas, J.N., Gilli, A., Chapron, E., Wirth, S.B., Anselmetti, F., Desmet, M., Magny, M., 2013. Climate and vegetation changes during the Lateglacial and early–middle Holocene at Lake Ledro (southern Alps, Italy). Climate of the Past 9, 913–933. https://doi.org/10.5194/cp-9-913-2013

Juggins, S., 2019. rioja: Analysis of Quaternary Science Data.

Kaltenrieder, P., Procacci, G., Vanniere, B., Tinner, W., 2010. Vegetation and fire history of the Euganean Hills (Colli Euganei) as recorded by Lateglacial and Holocene sedimentary series from Lago della Costa (northeastern Italy). The Holocene 20, 679–695. https://doi.org/10.1177/0959683609358911

Kaushal, S., Binford, M.W., 1999. Relationship between C:N ratios of lake sediments, organic matter sources, and historical deforestation in Lake Pleasant, Massachusetts, USA. Journal of Paleolimnology 22, 439–442. https://doi.org/10.1023/A:1008027028029

Kollmann, J., Schill, H.-P., 1996. Spatial patterns of dispersal, seed predation and germination during colonization of abandoned grassland by Quercus petraea and Corylus avellana. Vegetatio 125, 193–205. https://doi.org/10.1007/BF00044651

Küster, H., 1997. The role of farming in the postglacial expansion of beech and hornbeam in the oak woodlands of central Europe. The Holocene 7, 239–242.

Kwiatkowska, A.J., Spalik, K., Michalak, E., Palinska, A., Panufnik, D., 1997. Influence of the size and density of Carpinus betulus on the spatial distribution and rate of deletion of forest-floor species in thermophilous oak forest. Plant Ecology 129, 1–10.

Kwiatkowska, A.J., Wyszomirski, T., 1988. Decline of Potentillo albae-Quercetum phytocoenoses associated with the invasion ofCarpinus betulus. Vegetatio 75, 49–55. https://doi.org/10.1007/BF00044625

Lo Vetro, D., 2014. Le industrie litiche di Tosina: un contributo alla definizione dell'identità culturale della Lagozza, in: Poggiani Keller, R. (Ed.), Contadini, Allevatori e Artigiani a Tosina Di Monzambano (Mn) Tra V e IV Millennio a.C. - Una Comunità Neolitica Nei Circuiti Padani e Veneti. Grafiche Tagliani Stampa e Comunicazione per Acherdo Edizioni, Calcinato (Bs).

Lunardi, A., 2008. Experimental testing with polished green stone axes and adzes: technology and use. Prehistoric Technology 40, 369–373.

Magny, M., Combourieu-Nebout, N., de Beaulieu, J.L., Bout-Roumazeilles, V., Colombaroli, D., Desprat, S., Francke, A., Joannin, S., Ortu, E., Peyron, O., Revel, M., Sadori, L., Siani, G., Sicre, M.A., Samartin, S., Simonneau, A., Tinner, W., Vannière, B., Wagner, B., Zanchetta, G., Anselmetti, F., Brugiapaglia, E., Chapron, E., Debret, M., Desmet, M., Didier, J., Essallami, L., Galop, D., Gilli, A., Haas, J.N., Kallel, N., Millet, L., Stock, A., Turon, J.L., Wirth, S., 2013. North–south palaeohydrological contrasts in the central Mediterranean during the Holocene: tentative synthesis and working hypotheses. Clim. Past 9, 2043–2071. https://doi.org/10.5194/cp-9-2043-2013

Magri, D., Agrillo, E., Di Rita, F., Furlanetto, G., Pini, R., Ravazzi, C., Spada, F., 2015. Holocene dynamics of tree taxa populations in Italy. Review of Palaeobotany and Palynology 218, 267–284. https://doi.org/10.1016/j.revpalbo.2014.08.012

Martinelli, N., 2007. Dendrocronologia delle palafitte dell'area gardesana: situazione delle ricerche e prospettive. Contributi di archeologia in memoria di Mario Mirabella Roberti. Atti del XVI Convegno Archeologico Benacense (Cavriana, 15–16 October 2005). Annali Benacensi XIII–XIV 103–20.

Mauri, A., Davis, B.A.S., Collins, P.M., Kaplan, J.O., 2015. The climate of Europe during the Holocene: a gridded pollen-based reconstruction and its multi-proxy evaluation. Quaternary Science Reviews 112, 109–127. https://doi.org/10.1016/j.quascirev.2015.01.013

Meadows, J., Hüls, M., Schneider, R., 2015. Accuracy and Reproducibility of 14C Measurements at the Leibniz-Labor, Kiel: A First Response to Lull et al., "When 14C Dates Fall Beyond the Limits of Uncertainty: An Assessment of Anomalies in Western Mediterranean Bronze Age 14C Series." Radiocarbon 57, 1041–1047. https://doi.org/10.2458/azu_rc.57.18569

Meyers, P.A., 2003. Applications of organic geochemistry to paleolimnological reconstructions: a summary of examples from the Laurentian Great Lakes. Organic Geochemistry 34, 261–289. https://doi.org/10.1016/S0146-6380(02)00168-7

Meyers, P.A., Ishiwatari, R., 1993. Lacustrine organic geochemistry—an overview of indicators of organic matter sources and diagenesis in lake sediments. Organic Geochemistry 20, 867–900. https://doi.org/10.1016/0146-6380(93)90100-P

Miller, N.F., 1984. The Use of Dung as Fuel : an Ethnographic Example and an Archaeological Application. Paléorient 10, 71–79. https://doi.org/10.3406/paleo.1984.941

Mingram, J., Negendank, J.F.W., Brauer, A., Berger, D., Hendrich, A., Köhler, M., Usinger, H., 2007. Long cores from small lakes—recovering up to 100 m-long lake sediment sequences with a high-precision rod-operated piston corer (Usinger-corer). J Paleolimnol 37, 517–528. https://doi.org/10.1007/s10933-006-9035-4

Moore, P.D., Webb, J.A., Collison, M.E., 1991. Pollen analysis. Blackwell scientific publications.

Nychka, D., Furrer, R., Paige, J., Sain, S., 2019. fields: Tools for Spatial Data, R-Package.

Overpeck, J.T., Webb, T., Prentice, I.C., 1985. Quantitative interpretation of fossil pollen spectra: Dissimilarity coefficients and the method of modern analogs. Quaternary Research 23, 87–108. https://doi.org/10.1016/0033-5894(85)90074-2

Perego, R., 2015. Contribution to the development of the Bronze Age plant economy in the surrounding of the Alps: an archaeobotanical case study of two Early and Middle Bronze Age sites in northern Italy (Lake Garda region). University of Basel.

Perego, R., Badino, F., Deaddis, M., Ravazzi, C., Vallè, F., Zanon, M., 2011. L'origine del paesaggio agricolo pastorale in nord Italia: espansione di Orlaya grandiflora (L.) Hoffm. nella civiltà palafitticola. Notizie Archeologiche Bergomensi 19, 161–173.

Piccoli, A., 1986a. Aspetti generali e particolari delle strutture e delle stratigrafie dell'insediamento preistorico di Bande di Cavriana (MN), in: Carancini, G.L. (Ed.), Atti Dell'incontro Di Acquasparta 1985. "Gli Insediamenti Perilacustri Dell'età Del Bronzo e Della Prima Età Del Ferro: Il Caso Dell'antico Lacus Velinus" - Palazzo Cesi, 15-17 Novembre 1985.

Piccoli, A., 1986b. Nuovi aspetti strutturali e stratigrafici da Bande di Cavriana, in: 2° Convegno Archeologico Regionale - Atti - 13-14-15 Aprile 1984 - Como, Villa Olmo.

Piccoli, A., 1982. Bande di Cavriana (MN) - 1982 - Indagine d'emergenza. Sibrium XVI.

Piccoli, A., 1980. Considerazioni sul rinvenimento di una piroga preistorica a Bande di Cavriana (Mantova), in: Mirabella Roberti, M. (Ed.), Atti Del Convegno Su Archeologia e Storia a Milano e Nella Lombardia Orientale (Province Di Bergamo, Brescia e Mantova). Villa Monastero Di Varenna, Lago Di Como (5-6 Giugno 1971 - 10-11 Giugno 1972).

Piccoli, A., 1974. Strutture lignee dell'abitato preistorico di Bande di Cavriana, in: Aspetti e Problemi Dell'età Del Bronzo Nell'entroterra Benacense. Atti Del Convegno Di Cavriana - 25 Marzo 1973.

Pipinis, E., Stampoulidis, A., Milios, E., Kitikidou, K., Akritidou, S., Theodoridou, S., Radoglou, K., 2018. Effects of seed moisture content, stratification and sowing date on the germination of Corylus avellana seeds. J. For. Res. https://doi.org/10.1007/s11676-018-0852-x

Poggiani Keller, R. (Ed.), 2014. Contadini, allevatori e artigiani a Tosina di Monzambano (Mn) tra V e IV millennio a.C. - Una comunità neolitica nei circuiti padani e veneti. Grafiche Tagliani Stampa e Comunicazione per Acherdo Edizioni, Calcinato (Bs).

Poggiani Keller, R., Leva, M.A.B., Menotti, E.M., Roffia, E., Pacchieni, T., Baioni, M., Martinelli, N., Ruggiero, M.G., Bocchio, G., 2005. Siti d'ambiente umido della Lombardia: rilettura di vecchi dati e nuove ricerche, in: Della Casa, Ph., Trachsel, M. (Eds.), Wetland Economies and Societies. Proceeding of the International Conference in Zurich, Zurich, 10-13 March 2004. Collectio Archæologica 3, 233-250.

R Core Team, 2015. R: A Language and Environment for Statistical Computing. R Foundation for Statistical Computing, Vienna, Austria.

Ravazzi, C., Marchetti, M., Zanon, M., Perego, R., Quirino, T., Deaddis, M., De Amicis, M., Margaritora, D., 2013. Lake evolution and landscape history in the lower Mincio River valley, unravelling drainage changes in the central Po Plain (N-Italy) since the Bronze Age. Quaternary International 288, 195–205. https://doi.org/10.1016/j.quaint.2011.11.031

Ravazzi, C., Pini, R., 2013. Clima, vegetazione forestale e alpeggio tra la fine del Neolitico e l'inizio dell'età del Bronzo nelle Alpi e in Pianura Padana, in: de Marinis, R.C. (Ed.), L'Età Del Rame. La Pianura Padana e Le Alpi al Tempo Di Ötzi. Compagnia della Stampa, Massetti Rodella Editori, Roccafranca (Brescia), pp. 69–86.

Ravazzi, C., Pini, R., Badino, F., De Amicis, M., Londeix, L., Reimer, P.J., 2014. The latest LGM culmination of the Garda Glacier (Italian Alps) and the onset of glacial termination. Age of glacial collapse and vegetation chronosequence. Quaternary Science Reviews 105, 26–47. https://doi.org/10.1016/j.quascirev.2014.09.014

Reimer, P.J., Bard, E., Bayliss, A., Beck, J.W., Blackwell, P.G., Bronk Ramsey, C., Buck, C.E., Cheng, H., Edwards, R.L., Friedrich, M., Grootes, P.M., Guilderson, T.P., Haflidason, H., Hajdas, I., Hatté, C., Heaton, T.J., Hoffmann, D.L., Hogg, A.G., Hughen, K.A., Kaiser, K.F., Kromer, B., Manning, S.W., Niu, M., Reimer, R.W., Richards, D.A., Scott, E.M., Southon, J.R., Staff, R.A., Turney, C.S.M., van der

Plicht, J., 2013. IntCal13 and Marine13 radiocarbon age calibration curves 0-50,000 years cal BP 55, 1869–1887. https://doi.org/10.2458/azu_js_rc.55.16947

San-Miguel-Ayanz, J., De Rigo, D., Caudullo, G., Houston Durrant, T., Mauri, A. (Eds.), 2016. European atlas of forest tree species. Publications Office of the European Union, Luxembourg.

Savill, P.S., 2013. The Silviculture of Trees Used in British Forestry. CABI.

Starnini, E., Biagi, P., Mazzucco, N., 2018. The beginning of the Neolithic in the Po Plain (northern Italy): Problems and perspectives. Quaternary International 470, 301–317. https://doi.org/10.1016/j.quaint.2017.05.059

Stockmarr, J.A., 1971. Tablets with spores used in absolute pollen analysis. Pollen spores 13, 615–621.

Sunagawa, I., Takahashi, Y., Imai, H., 2007. Strontium and aragonite-calcite precipitation. Journal of Mineralogical and Petrological Sciences 102, 174–181. https://doi.org/10.2465/jmps.060327a

Talbot, M.R., 2001. Nitrogen Isotopes in Palaeolimnology, in: Last, W.M., Smol, J.P. (Eds.), Tracking Environmental Change Using Lake Sediments: Physical and Geochemical Methods, Developments in Paleoenvironmental Research. Springer Netherlands, Dordrecht, pp. 401–439. https://doi.org/10.1007/0-306-47670-3_15

Telford, R.J., Birks, H.J.B., 2009. Evaluation of transfer functions in spatially structured environments. Quaternary Science Reviews 28, 1309–1316. https://doi.org/10.1016/j.quascirev.2008.12.020

Thevenon, F., Adatte, T., Spangenberg, J.E., Anselmetti, F.S., 2012. Elemental (C/N ratios) and isotopic ($\delta^{15}N_{org}$, $\delta^{13}C_{org}$) compositions of sedimentary organic matter from a high-altitude mountain lake (Meidsee, 2661 m a.s.l., Switzerland): Implications for Lateglacial and Holocene Alpine landscape evolution. The Holocene 22, 1135–1142. https://doi.org/10.1177/0959683612441841

Tjallingii, R., Röhl, U., Kölling, M., Bickert, T., 2007. Influence of the water content on X-ray fluorescence core-scanning measurements in soft marine sediments. Geochemistry, Geophysics, Geosystems 8. https://doi.org/10.1029/2006GC001393

Valsecchi, V., Tinner, W., Finsinger, W., Ammann, B., 2006. Human impact during the Bronze Age on the vegetation at Lago Lucone (northern Italy). Vegetation History and Archaeobotany 15, 99–113. https://doi.org/10.1007/s00334-005-0026-6

Venzo, S., 1965. Rilevamento geologico dell'anfiteatro morenico frontale del Garda dal Chiese all'Adige con carta a colori 1:40000. Memorie della Società Italiana di Scienze Naturali e del Museo Civico di Storia Naturale di Milano 14, 82.

Wang, W.Q., Sardans, J., Wang, C., Zeng, C.S., Tong, C., Asensio, D., Peñuelas, J., 2015. Ecological stoichiometry of C, N, and P of invasive Phragmites australis and native Cyperus malaccensis species in the Minjiang River tidal estuarine wetlands of China. Plant Ecology 216, 809–822. https://doi.org/10.1007/s11258-015-0469-5

Welter-Schultes, F.W., 2012. European Non-Marine Molluscs, a Guide for Species Identification: Bestimmungsbuch für europäische Land-und Süsswassermollusken. Planet Poster Editions.

Weltje, G.J., Tjallingii, R., 2008. Calibration of XRF core scanners for quantitative geochemical logging of sediment cores: Theory and application. Earth and Planetary Science Letters 274, 423–438. https://doi.org/10.1016/j.epsl.2008.07.054

Wick, L., Möhl, A., 2006. The mid-Holocene extinction of silver fir (Abies alba) in the Southern Alps: a consequence of forest fires? Palaeobotanical records and forest simulations. Vegetation History and Archaeobotany 15, 435–444. https://doi.org/10.1007/s00334-006-0051-0

Wirth, S.B., Glur, L., Gilli, A., Anselmetti, F.S., 2013. Holocene flood frequency across the Central Alps – solar forcing and evidence for variations in North Atlantic atmospheric circulation. Quaternary Science Reviews 80, 112–128. https://doi.org/10.1016/j.quascirev.2013.09.002

World Heritage Committee, 2011. Decisions adopted by the World Heritage Committee at its 35th session (No. WHC-11/35.COM/20). UNESCO, Paris.

World Heritage Nomination, 2009. Prehistoric Pile Dwellings around the Alps. Executive Summary. Volume II (No. IT-LM-07).

Zanon, M., 2014. Prime analisi palinologiche, in: Poggiani Keller, R. (Ed.), Contadini, Allevatori e Artigiani a Tosina Di Monzambano (Mn) Tra V e IV Millennio a.C. - Una Comunità Neolitica Nei Circuiti Padani e Veneti. Grafiche Tagliani Stampa e Comunicazione per Acherdo Edizioni, Calcinato (Bs).

Zanon, M., 2010. L'ambiente naturale e l'impatto antropico nel bacino infra-morenico del Lavagnone di Desenzano del Garda tra VI e IV millennio a.C. Università degli Studi di Milano , academic year 2008/2009. Unpublished master's thesis.

PART III

POPULATION COLLAPSE AND CLIMATE DYNAMICS AT THE END OF THE BRONZE AGE

The primary research questions concerning the end of Bronze Age networks is not so different from the issues just discussed about their initial emergence: did climate variability play any role in influencing settlement dynamics? The situation described in Part II applies to Part III as well: given that current archaeological narratives are primarily based on extra-regional climate proxies, our current understanding of climate dynamics in the northern Italian lowlands and across the southern alpine margin would greatly benefit from the inclusion of more localized climatic reconstructions.

The Bande di Cavriana record, presented in Part II, provides new evidence concerning unstable climatic conditions at the onset of the Bronze Age. These results share multiple similarities with independent palaeoenvironmental records from northern and central Italy, confirming that the network of small lakes and wetlands in the southern Lake Garda area was responding in a measurable way to supra-regional climatic patterns. Yet this sequence does not extend past the Early Bronze Age and, consequently, does not allow to verify if this local sensitivity persisted through the Bronze Age collapse. For this reason, a different approach was adopted in order to investigate human-environment dynamics across the Bronze Age-Iron Age transition (between ca. 3100 and 2800 years cal. BP; 1150-850 years BC).

Instead of relying on newly produced data, temperature and precipitation patterns were reconstructed using previously published palynological records from northern Italy. Raw pollen data was converted into climate parameters using an analogue-based modeling algorithm already tested across Europe (Mauri et al., 2015), which allowed to bypass the still-standing lack of geochemistry-based climate proxies. Most notably, a cooperation with G. Capuzzo (University of Barcelona, Spain, and Université Libre de Bruxelles, Belgium) allowed to extend the scope of this exercise by coupling the pollen-based climate curves with population models derived from radiocarbon datings. The pollen sites involved in the climate reconstructions were specifically selected due to their proximity to the sites included in the demographic reconstruction. This requirement allowed to maintain the close connection between archaeological data and environmental proxies that is regarded as a primary characteristic of this doctoral project.

The results of this multifaceted modeling exercise are published in Capuzzo et al. (2018), which is reported in its entirety below. The same demographic and climatic models applied to northern Italy are also extended to different European regions within the same paper, highlighting not only a wide variety of demographic patterns within neighboring areas, but also equally diverse combinations of temperature and precipitation trends.

Highly diverse Bronze Age population dynamics in Central-Southern Europe and their response to regional climatic patterns

Giacomo Capuzzo[a,b], Marco Zanon[c,d], Marta Dal Corso[d], Wiebke Kirleis[c,d], Juan A. Barceló[b]

a. Laboratory of Anthropology and Human Genetics, Faculty of Science, Université Libre de Bruxelles, Brussels, Belgium,
b. Quantitative Archaeology Lab (LAQU), Department of Prehistory, Autonomous University of Barcelona, Faculty of Arts and Humanities, Bellaterra (Barcelona), Spain,
c. Graduate School "Human Development in Landscapes", Kiel University, Kiel, Germany,
d. Institute of Pre- and Protohistoric Archaeology, Kiel University, Kiel, Germany

Original research article published on *PLoS ONE* 13(8), 2018.
https://doi.org/10.1371/journal.pone.0200709

ABSTRACT

The reconstruction of past demographic patterns is a fundamental step towards a better understanding of human-environment relations, especially in terms of quantifiable anthropic impact and population susceptibility to environmental changes. The recently developed Summed Calibrated Probability Distributions (SCPD) approach, based on large collections of archaeological radiocarbon dates, provides a new tool to obtain continuous prehistoric population curves suitable for comparison with palaeoenvironmental time series. Despite a wide application in Mesolithic and Neolithic contexts worldwide, the use of the SCPD method remains rare for post-Neolithic societies. Our aim is to address this visible gap and apply the SCPD approach to South European archeological contexts between the Bronze Age and the transition into the Iron Age (1800-800 cal. BC), then evaluating these results against local archeological narratives and palaeoecological data. We first test the SCPD method at a supra regional scale, ranging from the Ebro to the Danube rivers, and subsequently in five selected regions within this area. We then compare the regional population curves to climate data reconstructed from local palynological records. Our results highlight the contrast between a stable supra regional demographic trend and more dynamic regional patterns. We do not observe any convincing long-term correlations between population and climate, but localized episodes of demographic stagnation or decline are present in conjunction with climatic shifts or extremes. Nevertheless, climate change as a triggering factor should

be considered with caution, especially in peripheral areas where the archaeological data is faint, or where local evidence points to contemporaneous, ongoing landscape overexploitation.

INTRODUCTION

The reconstruction of past population size and density has always been a major challenge for archaeological research. Early attempts were based on the analysis of settlement sizes and funerary contexts, leading to the hypothesis that there was a significant population increase over a large part of Europe during the Late Bronze Age (Earle and Kristiansen, 2010; Kristiansen, 2015, 2000). One well-known case study cites the rise in the number of barrows and an increase in burial wealth at around 1200 BC in Northern Europe, and a visible increase in the number of necropolises in Poland from 1500-1400 BC (Kristiansen, 2000; Stepniak, 1986). Archaeologists also observed a peak in the number of lakeside settlements in Switzerland during the same period (Primas, 1990). The hypothesis that there was a population increase during the Late Bronze Age (Kristiansen, 2000) was strengthened further by geostatistical analysis of site densities in the landscape (Zimmermann, 2012; Zimmermann et al., 2009). Yet, the European Bronze Age was also characterized by episodes of crisis, leading to the end of some settlement systems and to phases of widespread depopulation (Kneisel et al., 2012). A major example in our study area is the end of the lake-dwelling settlement system in the Circum-Alpine region. The pile-dwelling phenomenon expanded to its maximum during the first phases of the Bronze Age, covering a wide area ranging from Eastern France to Slovenia (Harding and Fokkens, 2013; Menotti, 2004). An abrupt abandonment phase is then recorded north of the Alps in partial connection with high lake level stands (1400-1150 BC). Conversely, the settlement network south of the Alps was relatively stable through most of the Bronze Age, eventually peaking in population density with the development of the Terramare culture in the neighboring Po Plain (Bernabò Brea et al., 1997; Cardarelli, 2010). The southern Alpine pile-dwelling/Terramare culture collapsed around 1150 BC, probably due to a combination of factors including unsustainable landscape exploitation and climatic change (Cremaschi et al., 2016, 2006; Dal Corso, 2018). In recent years, the creation of large databases of radiocarbon dates has enabled the use of SCPDs to infer relative population dynamics. The number of datable archeological contexts can be a direct function of human pressure on the landscape (e.g. Hinz et al., 2012). Consequently, frequency fluctuations in a series of SCPDs can be interpreted as a reflection of past population trends. Archaeologists have given

particular attention to the Neolithic period (Collard et al., 2010; Crombé and Robinson, 2014; Hinz et al., 2012; Isern et al., 2014; Kolář et al., 2016; Shennan, 2013, 2009; Shennan et al., 2013; Shennan and Edinborough, 2007) using SCPDs to track population dynamics in connection with the spread of agricultural practices. However, this methodology has been rarely applied to the so-called 'metal ages'. Notable examples for the European Bronze Age appear to be limited to the works of Armit et al. (2014, 2013), focusing on the reconstruction of Irish population trends in connection with the Subboreal-Subatlantic transition, and Balsera et al. (2015) on the demography of prehistoric Iberia from 7000 to 2000 BC.

In the present paper, we use the SCPD method to track human activity from the Ebro to the Danube Rivers, including the Northeastern Iberian Peninsula, Central and Southern France, Northern Italy, Switzerland, Austria, and Southern Germany (Fig. 3.1).

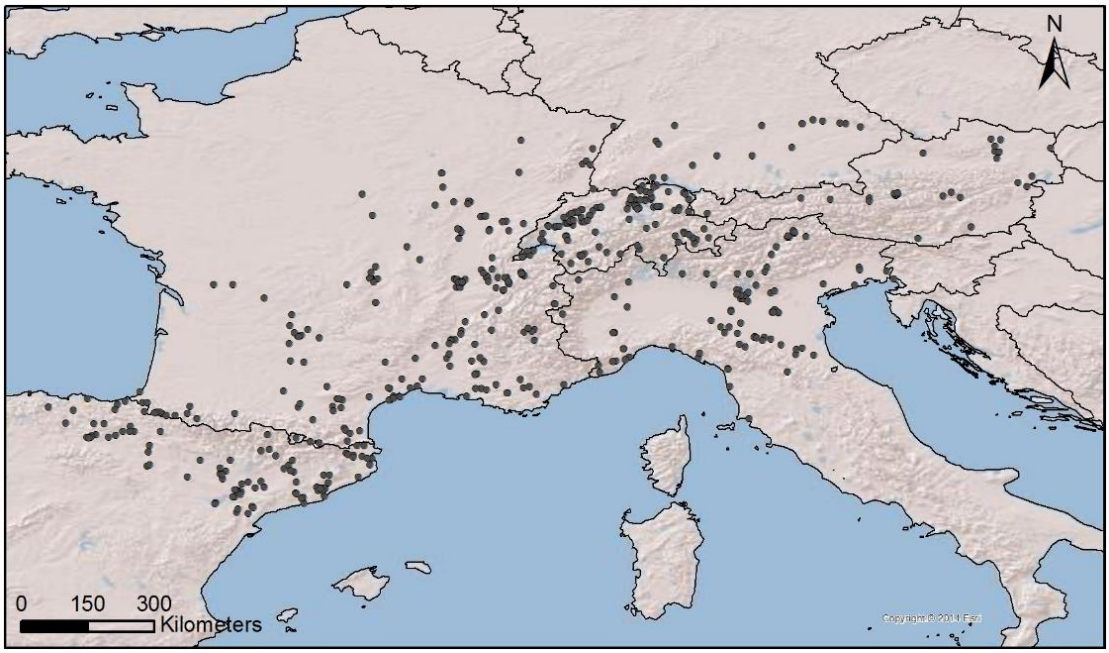

Figure 3.1. *Overview of the study area. The black dots show the spatial distribution of the archaeological sites included in the EUBAR database and used to derive population data (Software: ArcGIS10.3).*

We focus our reconstructions on 1800-800 BC, broadly covering most of the Bronze Age and the transition into the Iron Age. This larger area is subsequently divided into five regions (the Swiss Plateau, the Po Plain, the Massif Central, the Southern French coast, and the Northeastern Iberian Peninsula, Fig. 3.2) in order to track more specific trends and inter-regional dynamics. The regional demographic trends are then compared with semi-quantitative climatic curves reconstructed from local pollen

archives. We use the Modern Analogue Technique (MAT; Davis et al., 2003; Mauri et al., 2015) to reconstruct summer temperature and precipitation from different pollen archives selected in the five regions and their immediate vicinities. The temperature and precipitation reconstructions for each group of sites within a region are then combined into two respective LOESS-smoothed curves. The resulting highly localized synthesis offered by these two climatic parameters allows for a geographically consistent comparison with the demographic data. The continuous, semi-quantitative, and localized nature of these reconstructions offer an independent testing ground for established regional palaeoenvironmental narratives based on combinations of discrete, qualitative, and extra-regional data.

MATERIALS AND METHODS

Demographic reconstructions

Several techniques have been used to estimate the probable size of a human population based on archaeological data, such as the study of settlement size, house dimensions, and site catchment areas, as well as the measurement of the rates of exploitation, consumption, and discard of raw materials and artifacts (Chamberlain, 2009). Similarly, the analysis of funerary contexts and human skeletons has been used to estimate past population size through the inference of age-specific mortality from assemblages of human skeletal remains (Katzenberg and Saunders, 2011). A recent tool developed in this field focuses on the use of summed calibrated probability distributions (SCPD) of radiocarbon dates from archaeological sites in order to track trends in human presence. The originality of calibrating ^{14}C data to infer population structure (and use the pooled mean of the "dates as data" to do so) comes from K. Edinborough's 2005 PhD thesis (Edinborough, 2009, 2005). The SCPD method is based on the reasonable assumption that as the number of people increases, so does the strength of their archaeological signal. Consequently, changes in the relative temporal frequency of radiocarbon dated depositional events are interpreted as reflections of demographic trends.

In the present paper, we adopt the SCPD method to infer past demographic fluctuations during the Bronze Age and towards the transition into the Iron Age. We produced the general South European demographic reconstruction by combining 1233 calibrated radiocarbon dates selected from the EUBAR database (Capuzzo et al., 2014), openly accessible online at http://www.telearchaeology.org/EUBAR and at https://figshare.com/s/be0d5df7df1fff96f7bb. Subsequently, we composed separate SCPD curves for each one of the selected regions using subsections of the

EUBAR dataset. All related analyses have been carried out through the software OxCal 4.3 (Bronk Ramsey, 2009) using the IntCal13 calibration curve (Reimer et al., 2013).

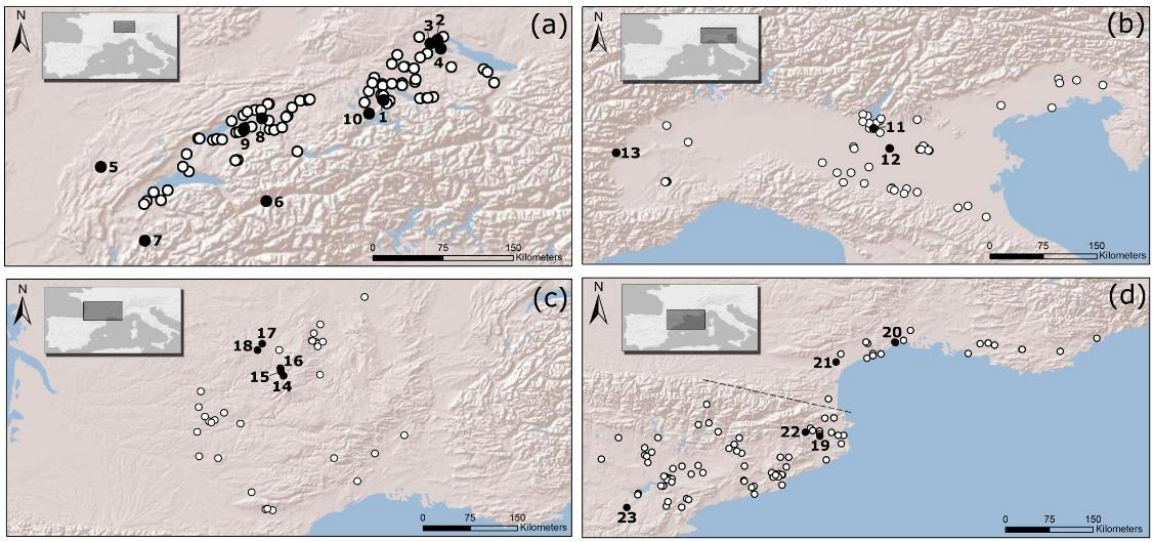

Figure 3.2. *Regions investigated in the present study: (a) Swiss Plateau; (b) Po Plain; (c) Massif Central; (d) Southern French coast and North-eastern Iberian Peninsula. The latter two regions are also jointly referred to as 'Northwestern Mediterranean' in the present paper. White dots: sites included in the regional SCPDs, selected from the EUBAR dataset. Black dots: sites used for climatic reconstructions (coordinates reported in Table 1). (1) Bibersee; (2) Durchenbergried; (3) Feuenried; (4) Hornstaad/Bodensee; (5) Lac de Clair-vaux; (6) Lac du Mont d'Orge; (7) Lac d'Annecy; (8) Lobsigensee; (9) Montilier; (10) Rotsee; (11) Castellaro Lagusello; (12) For-cello; (13) Lago Piccolo di Avigliana; (14) La Taphanel; (15) Lac du Mont de Belier; (16) Lastioulles; (17) Peyrelevade; (18) Tour-bière de Chabannes; (19) Banyoles; (20) Embouchac; (21) Etang d'Ouveillan; (22) Pla de l`Estany; (23) Salada Pequeña.*

The SCPD approach has been the target of several criticisms (e.g. Contreras and Meadows, 2014; Surovell et al., 2009; Surovell and Brantingham, 2007; Williams, 2012). Interpretative and methodological difficulties in the SCPDs can be divided in three groups: those referring to the systematic bias in the available data, mainly due to different ranges of preservation and to sampling strategies (Armit et al., 2013; Torfing, 2015), those linked to the artificial results generated by the graphical methods of presenting the data (Bronk Ramsey, 2017) and those related to the effect of the calibration process (Crema et al., 2017; Weninger et al., 2015; Williams, 2012). Nonetheless, its wide adoption and testing within several archaeological contexts support its ability to infer past human dynamics (Armit et al., 2014, 2013; Balsera et

al., 2015; Borrell et al., 2015; Crema et al., 2016; Edinborough et al., 2017; Hinz et al., 2012; Johnson and Brook, 2011; Peros et al., 2010; Shennan et al., 2013; Tallavaara et al., 2010; Timpson et al., 2014; Torfing, 2015). In this framework, the EUROEVOL project led by Stephen Shennan at UCL (http://www.ucl.ac.uk/euroevol) deserves to be mentioned for its relevant outcomes (Shennan, 2013; Shennan et al., 2013).

Summing a group of estimates that have different probabilities produces a unique probability density function for a hypothetically defined period, which is the sum of the individual confidence intervals of the radiocarbon dates. Observed positive trends in the SCPD may be interpreted as a sign of increasing population, while decreasing SCPD values would point to demographic declines. Consequently, the steepness of the slope may indicate the speed of increase or decrease.

In the present paper, we combined radiocarbon dates from the same depositional event in order to prevent the non-independence of dated events (Barceló et al., 2014; Bogdanovic et al., 2014). In so doing, we have followed a pre-analytic "binning" procedure, instead of the more usual post-analysis "binning" described in recent contributions (Chaput and Gajewski, 2016; Crema et al., 2017; Downey et al., 2014; French, 2016; Hinz et al., 2012; Palmisano et al., 2017; Shennan et al., 2013; Timpson et al., 2014). We also adopted a range of pre-screening criteria in order to ensure the reliability of our analysis. First, only radiocarbon measurements with a standard deviation of less than 95 years have been taken into account, allowing a reduction in global uncertainty while at the same time maintaining a reasonable sample size. Adopting a stricter cutoff for standard deviations (e.g. 40/50 years) would result in a loss of information, excluding reliable although less precise dates. In this regard, it is worth quoting Shennan (2013, p.305), who maintains that "(the) key point is that even though a single date may have a broad calibrated range, the accumulation of the probability distributions of a large number of dates produces a high degree of chronological resolution making it possible to trace population fluctuations in considerable detail".

Second, we attempted to guarantee an equal representation between sites with only a few radiocarbon dates and multi-dated archaeological contexts. Dates from the same archaeological context and corresponding to the same depositional event (for instance two bones from the same individual in a grave) were tested following Ward and Wilson (1978). When the test was positive, the uncalibrated dates were combined using the tool *R_Combine* of the program OxCal 4.3, then their pooled mean was calibrated (Bronk Ramsey, 2009).

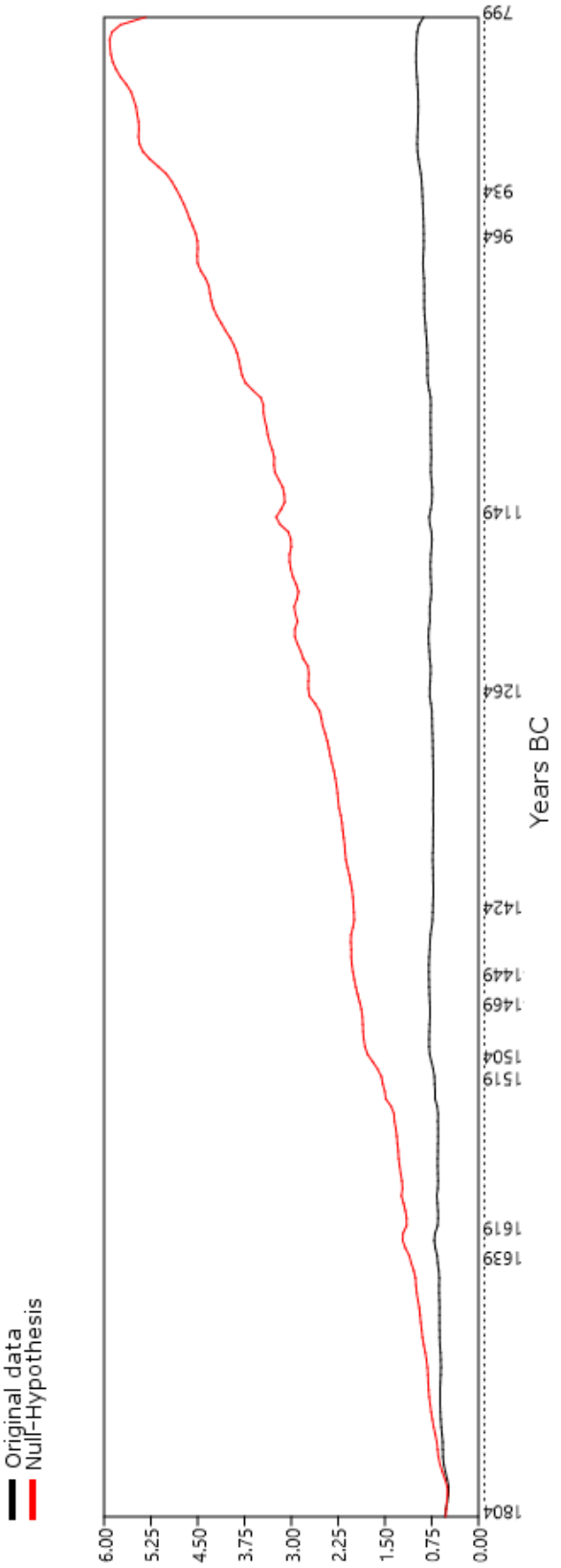

Figure 3.3. *Testing the effect of taphonomic bias on the original SCPD from settlements (Software: PAST 3.18). Black line: Original data; red line: Null-Hypothesis.*

In this way, when summing the radiocarbon estimates resulting from both combined contexts and mono-dated layers, the precision and the accuracy of the SCPDs remarkably improve and the representation of archaeological contexts is not altered. To understand the magnitude of the prescreening criteria adopted in the paper it is meaningful to observe that, on a sample of 1785 radiocarbon dates which compose the EUBAR database, only 852 dates from settlements were retained to construct the SCPD adopted to infer demographic changes at a macro scale. When analyzing the geographical regions separately, we are limited to datasets of less than 500 dates. Although this may be a problem when analyzing very long temporal ranges (more than 5000 years) (Williams, 2012), it is less problematic in shorter temporal ranges -as the 1000 years here studied- and when data density per year and per square kilometer are above critical thresholds. See the discussion section for additional considerations on data density.

On a macroscale, radiocarbon dates from cemeteries and from settlements have been analyzed separately. However, due to the small amount of data at a regional scale, the dates from both contexts have been considered jointly. In order to evaluate whether taphonomic bias may affect the general trend of the temporal series, we followed the approach of Surovell et al. (2009) and tested our data against a null hypothesis based on the equation

$$n_t = 5.726442 \times 10^6 (t + 2176.4)^{-1.3925309}$$

where t has been defined for the interval 1800-800 BC. In Fig. 3.3, the original SCPD data for the period 1800-800 BC (in black) are plotted against a curve derived from the null-hypothesis equation n_t (in red), built upon the assumption that post-depositional bias explains the higher amount of recent ^{14}C samples in terms of higher occurrences of better preserved contexts. The widely different trends of the two curves suggest that our data are not significantly affected by taphonomic bias.

Since the effects of the calibration curve on radiocarbon estimates can alter the shape of the SCPD, we produced a simulated SCPD composed of uniformly distributed radiocarbon dates, under the assumption that the amount of dated archaeological contexts was the same for each year. The shape of the distribution does not change whether the amount of data per year is one or more than one. This was done in order to test a null hypothesis of no relationship between the observed SCPD and the effects of particular sections of the calibration curve, such as plateaus and calendar age steps (Kerr and McCormick, 2014; Weninger et al., 2015; Williams, 2012). A prominent peak in the simulated SCPD is visible at ca. 800 BC (Fig. 3.4),

corresponding to a steep calendar-age step between 860 and 700 BC in the calibration curve. A second peak, of considerably lesser magnitude, is visible at ca. 1420 BC, matching the calendar-age step in the interval 1500-1380 BC. Beside the area around 800 BC, the simulated SCPD curve maintains a reasonably neutral trend, suggesting an overall limited influence of the calibration curve on our study time window.

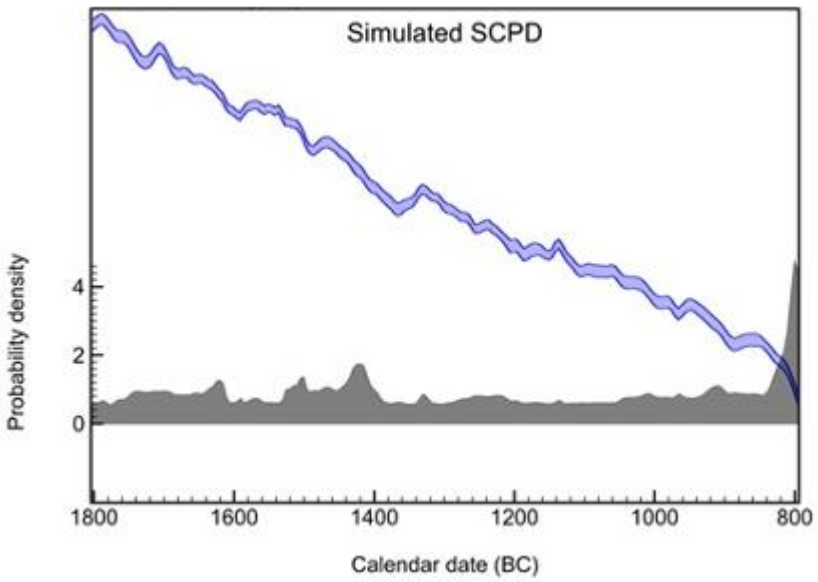

Figure 3.4. *Simulated SCPD (dark grey, same number of dates at each temporal bin) compared with the IntCal13 calibration curve.*

Climatic reconstructions

In order to provide a simple environmental contextualization for the population trends within each region, we coupled the SCPD-based population data with local pollen-based climatic curves. The semi-quantitative reconstructions were performed using the Modern Analogue Technique (MAT) (Guiot, 1990; Overpeck et al., 1985), focusing on two climatic variables: total summer (June, July, and August) precipitations and average summer temperature. The MAT relies on the assumption that pollen samples composed of a similar mixture of taxa are the byproduct of comparable vegetation assemblages. Therefore, given a modern pollen sample, the environmental conditions for its parent plant assemblage can be transferred to any fossil sample sharing a similar palynological composition (Guiot, 2011). The modern pollen samples used to build the calibration data set are derived from the European Modern Pollen Database (EMPD) (Davis et al., 2013).

We performed a basic quality filtering using the available EMPD metadata. Samples with known geolocation errors larger than 5 km were removed from the calibration

data set. Following Mauri et al. (2015), inaccurately georeferenced samples were also identified by comparing their elevation as recorded in the EMPD with elevation data for the same latitude and longitude extracted from a high-resolution Digital Elevation Model (DEM). We excluded all samples where the difference between EMPD and DEM data was higher than 250m (Mauri et al., 2015). Samples collected in riverine or estuarine contexts were removed too due to the presence of waterborne pollen potentially transported over long distances. Furthermore, we applied a minimum threshold of 400 pollen grains belonging to terrestrial species in order to select samples with rather stable taxa percentages (Birks and Birks, 1980, p. 165). It was not possible to apply the same threshold to fossil data due to the limited number of sites available in some regions. Each modern pollen sample was then coupled with local present-day climatic parameters from the WorldClim dataset (Hijmans et al., 2005) using nearest-pixel extraction on the 30 arc-seconds resolution maps. The main source for the fossil archives used in the present paper is the European Pollen Database (EPD; http://europeanpollendatabase.net), which was locally integrated with additional sites. In the present study, we use the EPD version released on May 12, 2016. We constrained the selection of suitable fossil sites within each region by placing a 100 km-wide search window (130 km in the Po plain and Mediterranean areas due to limited data availability) around the location of each EUBAR site, then retaining only the EPD archives falling within its boundaries. No vertical constraint was applied on the Mediterranean region and the Po Plain due to the limited availability of fossil archives. We improved the coverage of these regions by including four additional sites: Banyoles (Revelles et al., 2015, 2014) and Pla de l'Estany (Burjachs, 1994) in the Mediterranean area, and Castellaro Lagusello (Dal Corso, 2018) and Forcello (Ravazzi et al., 2013) on the Po Plain. We applied an upper elevation boundary of 1000 meters in the Massif Central area in order to exclude pollen archives that were located too far from the average elevation of the local EUBAR sites. The high availability of EPD sites in the Swiss plateau region allowed for a stricter constraint; here we selected only archives with the same vertical range of the local EUBAR sites (mean elevation $\pm$ 1σ). The complete list of the pollen archives used within each region is provided in Table 3.1. Semi-quantitative reconstructions were produced for each individual region with the exception of the Southern French coast and the Northeastern Iberian Peninsula. Here, the low number of suitable pollen records prompted us to produce a single set of climate curves - generically termed `Northwestern Mediterranean'- using records from both regions.

Table 3.1. *Name and location of the pollen archives used for climatic reconstructions. Coordinates are expressed in decimal degrees (WGS84 reference system).*

Region	Site name	Latitude	Longitude	Elevation	Num. in Fig. 3.2
Swiss Plateau	Bibersee	47.20694	8.466667	429	1
	Durchenbergried	47.78333	8.983333	432	2
	Feuenried	47.75	8.916667	407	3
	Hornstaad/Bodensee	47.7	9.016667	385	4
	Lac de Clairvaux	46.565	5.749167	525	5
	Lac du Mont d'Orge	46.234	7.338167	640	6
	Lac d'Annecy	45.85667	6.172222	447	7
	Lobsigensee	47.03056	7.298056	514	8
	Montilier	46.935	7.123611	438	9
	Rotsee	47.07583	8.325833	428	10
Po Plain	Castellaro Lagusello	45.36926	10.63631	106	11
	Forcello	45.1114	10.83918	13	12
	Lago Piccolo di Avigliana	45.233	7.388333	356	13
Massif Central	La Taphanel	45.27444	2.679167	975	14
	Lac du Mont de Belier	45.33778	2.643056	860	15
	Lastioulles	45.38611	2.636111	854	16
	Peyrelevade	45.708333	2.383333	780	17
	Tourbière de Chabannes	45.64917	2.310556	800	18
Mediterranean	Banyoles	42.128975	2.752846	173	19
	Embouchac	43.56639	3.916667	1	20
	Etang d'Ouveillan	43.26667	3.00	6	21
	Pla de l`Estany	42.188697	2.531139	520	22
	Salada Pequeña	41.03333	-0.21667	357	23

The age-depth models for every site were obtained from Giesecke et al. (2013) or were produced using the same methodology via Clam 2.2 (Blaauw, 2010). Both modern and fossil pollen counts were converted to percentages based on the sum of terrestrial taxa, then aggregated into plant functional types (PFTs) (Peyron et al., 1998). We preferred the use of PFTs over the selection of indicator taxa, as PFTs reduce the need for taxa-specific modern analogues and can lessen the influence of anthropic disturbance on pollen assemblages (Davis et al., 2003; Mauri et al., 2015; Zanon et al., 2018). Squared Chord Distance was preferred over other dissimilarity metrics due to its better performance in discriminating between vegetation types (Gavin et al., 2003). Climate reconstructions are based on the weighted average of the closest nine analogues. The number of relevant analogues was selected via leave-one-out cross-validation. The resistance of the model to spatial autocorrelation was tested via *h*-block cross-validation, where all samples within *h* kilometers of a test sample are omitted from analogue selection (Telford and Birks, 2009). We opted for a value of $h = 100$ km for both climatic variables, since it should reasonably ensure that pollen source areas between the test sample and its potential analogues do not overlap (as inferable from, e.g., Matthias and Giesecke, 2014; Zhang et al., 2016), while at the same time preventing an excessive depopulation of the analogue pool. Both summer precipitations and temperature retained a satisfactory predictive power for $h = 100$ km, with r^2 accounting for at least 50% of the variance and RMSEP lower than the standard deviations of the training sets (Table 3.2). Temperature and precipitations are expressed as deviations from the mean of all reconstructions across the 1800-800 BC time-window within each region. The reconstructed values for each fossil site were averaged using overlapping windows with a span of 100 years and an increment of 50 years. A synthesis for each climatic parameter was then produced by fitting a LOESS curve to the combined values of every site in each region (smoothing span = 0.06). The age-depth models were used as a base to assess sample quality. Within each site, time windows located more than 1000 years away from the closest radiocarbon-dated point were excluded from the model. Furthermore, the average dating errors were employed as inverse weights in fitting the LOESS curve. All MAT-related analyses were performed using R (R Core Team, 2015) with packages rioja 0.9-9 (Juggins, 2019) and fields 8.4-1 (Nychka et al., 2019). In addition to standard cross-validation techniques, we evaluated the reliability of these climatic reconstructions through a comparison with local, independent palaeoenvironmental proxies (see "Results" section).

Table 3.2. *Performance summary for the h-block cross validation exercise. For each variable, we report the coefficient of determination (r^2), the root of the mean squared error of the prediction (RMSEP) and the standard deviation of the observed climate variables.*

	h-block cross-validation (h=100 km)		Training data set
	r^2	RMSEP	1σ
Summer precipitation	0.60	72.6	114.7
Summer temperatures	0.50	3.27	4.6

RESULTS

At first glance, the general South European demographic reconstruction (Fig. 3.5a) appears to be characterized by mild positive trends between ca. 1800 and 800 BC, interrupted by an apparent stagnation between ca. 1450 and 1050 BC. In the period under investigation, a transition from the inhumation to the cremation rite occurs across several European regions (Barceló et al., 2014; Capuzzo and Barceló, 2015a, 2015b, 2014; De Mulder et al., 2008; Harding and Fokkens, 2013; López-Cachero, 2011; Ruiz Zapatero, 2014a, 2014b). To test the influence of this macroscopic shift in cultural practices on our reconstruction, we produce a second SCPD (Fig. 3.5b) excluding dates from funerary contexts (Fig 3.5c). The resulting demographic curve is similar to Fig. 3.5a -pointing to a limited influence of dates from cemeteries- and displays a more linear positive slope across the whole study window. To evaluate further the effects of the calibration on the SCPD with dates from settlements, the empirical curve (Fig. 3.5b) and the simulated SCPD (Fig. 3.4) have been standardized in order to be compared (Fig. 3.6). The original data coincides mostly with the null-hypothesis of uniform distribution. The peak in the time-span 1639-1619 BC clearly matches a slope in the curve, and cannot be explained in terms of a sudden demographic change. In addition, the interval 1520-1430 BC coincides with two peaks of the calibration curve at approximately 1500 BC and 1430 BC.
However, the changes in the calibration curve at 930 BC and 850 BC do not seem to leave any trace in the series. To minimize the effects of the greater or lesser slope of the IntCal13 calibration curve (Fig. 3.4) on the empirical data, we applied a Locally Weighted Scatterplot Smoothing (LOWESS) (Cleveland, 1979; Cleveland and Devlin, 1988) function that reduces spurious peaks and valleys (Fig. 3.7). A 95% confidence interval has been generated starting from a simulated dataset equivalent in quantity to the number of unique events of the SCPD from settlements, and repeating the interpolation model 500 times. The confidence interval gathers most of these

repetitions, each of them being a "possible demographic history", given certain known sources of error and including the uncertainty in the relative population estimates over time (Downey et al., 2014). In order to mathematically test the hypothesis of population growth within our study time window, we have adopted a statistical approach in which the empirically verified variation is compared to the values that would reflect the null hypothesis, i.e. the absence of population growth. In fact, only if the observed variation proves to be significantly different from the null hypothesis we can accept the existence of a certain pattern of change. In other words, we can stress the existence of a statistically significant demographic growth (or decrease) if the probability at a given point of the curve exceeds the value expected if the null hypothesis were correct. As a consequence, we have curve-fitted the values predicted by the interpolated LOWESS function obtained from SCPD data from settlements, since it minimizes the effects of the calibration process; the null hypothesis to be tested is the neutral growth of the population, expressed in terms of a standard logistic model (Banks, 2013; Panik, 2014) (Fig. 3.8).

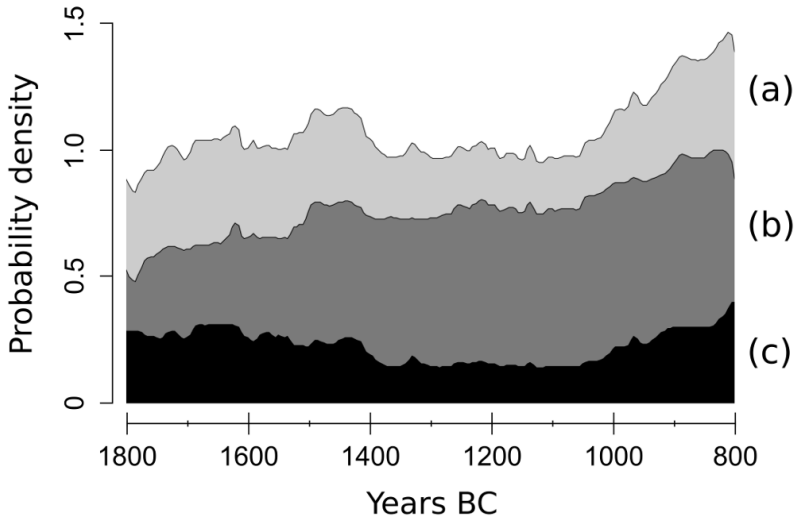

Figure 3.5. *SCPDs of pre-screened radiocarbon dates from the EUBAR database, juxtaposed curves: (a) 1233 dates from the filtered dataset; (b) 852 14C dates from settlements; (c) 283 ^{14}C dates from funerary contexts (IntCal13 calibration curve).*

To make the interpretation of the results easier, the linear trend in the transformed empirical series has been extracted and the linear model has been used as a baseline to detect peaks and valleys in the series (Fig. 3.9). The probability peak around 1450 BC still persists in the transformed series and it is clearly higher than it would be

expected if the null hypothesis were true, indicating one or more episodes of population growth in the time span 1550-1450 BC. The population decrease after around 1470 corresponds to a period of variations in solar activity as attested by the calendar age step in the intervals 1500-1380 BC, as mentioned above. Therefore, it is possible to suppose that there is a link between the two phenomena. More significant seems to be the possible population increase around 1250-1200 BC and the decrease in the probability of dating settlements between 1200 and 1050 BC. The possible population recovery after that time-span allows merely to reach the level of neutral growth, which would be surpassed only after 900 BC. For a better understanding of these phenomena we need to analyze the demographic behavior of the five study regions (Swiss Plateau, the Po Plain, the Massif Central, the Southern French coast, and the Northeastern Iberian Peninsula), which is characterized by various and pronounced episodes of population growth or decline.

Swiss Plateau

The Swiss Plateau SCPD (208 radiocarbon measurements collected from 81 archaeological sites) shows two phases characterized by a general positive trend, extending from the beginning of our study time window to around ca. 1500-1450 BC and from 1100 BC to its end, respectively (Fig. 3.10a). The interposed demographic decline (around 1450-1100 BC) shows a positive correlation with the abandonment of lakeside dwellings in the region (Jennings, 2014; Magny, 2015; Menotti, 2004, 2001). Dwelling abandonment phases in the area appear to correspond with lake-level changes, which in turn have been linked to unfavorable climatic fluctuations (Magny, 2015). The lake-level model presented by Magny (2004) describes a high lake-level (HLL) phase lasting from ca. 1400 to 1150 BC (Fig. 3.10d), possibly linked to the establishment of prevalently wetter and cooler conditions (Magny, 2015). Magny's HLL phases are identified by combining the chronological record of HLL events from multiple sedimentary archives. In the resulting histogram, non-zero Z-scores contribute to define regionally prominent HLL phases (Magny, 2013). An extended negative trend in the SCPD curve appears to support a connection between population decline and the 1440-1150 BC HLL phase. This matching behavior finds only a partial parallel in the pollen-based climatic curves (Fig. 3.10b and 3.10c). At a mere trend level, the summer temperature curve does indeed reach its lowest values between ca. 1400 and 950 BC.

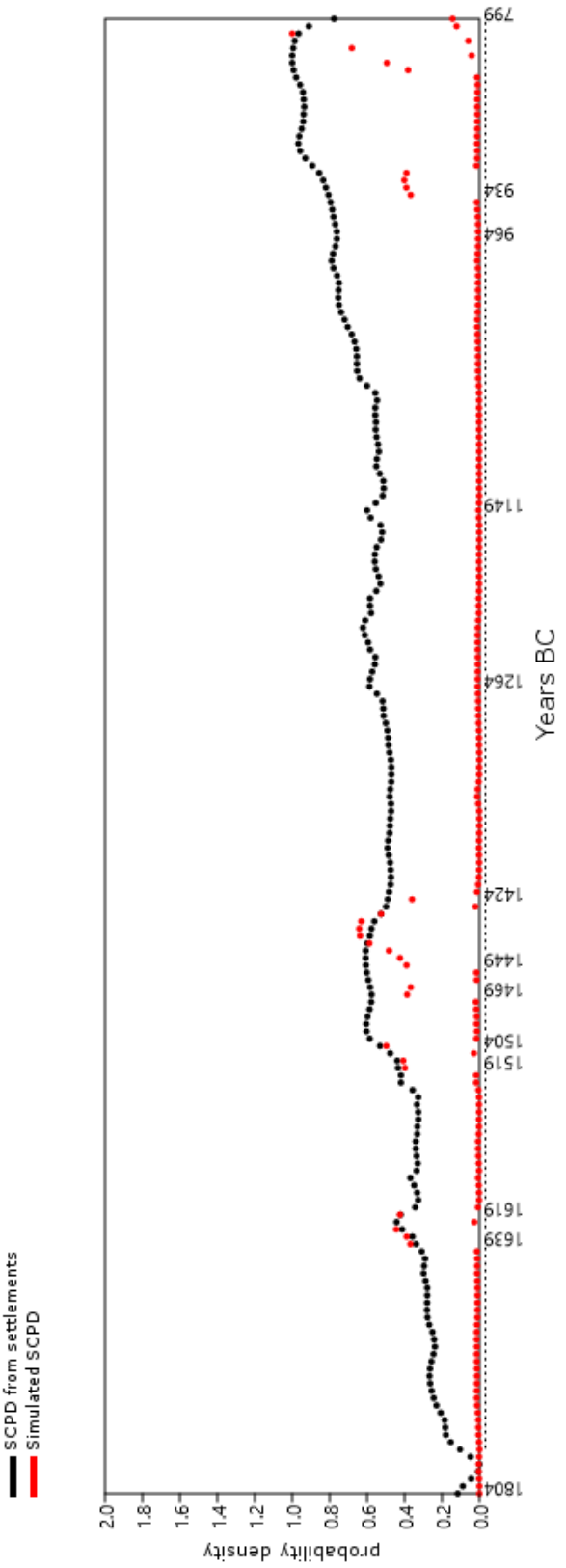

Figure 3.6. *Probability density distributions of the SCPD with dates from settlements (black) and the simulated SCPD (red) after having been standardized (Software: PAST 3.18).*

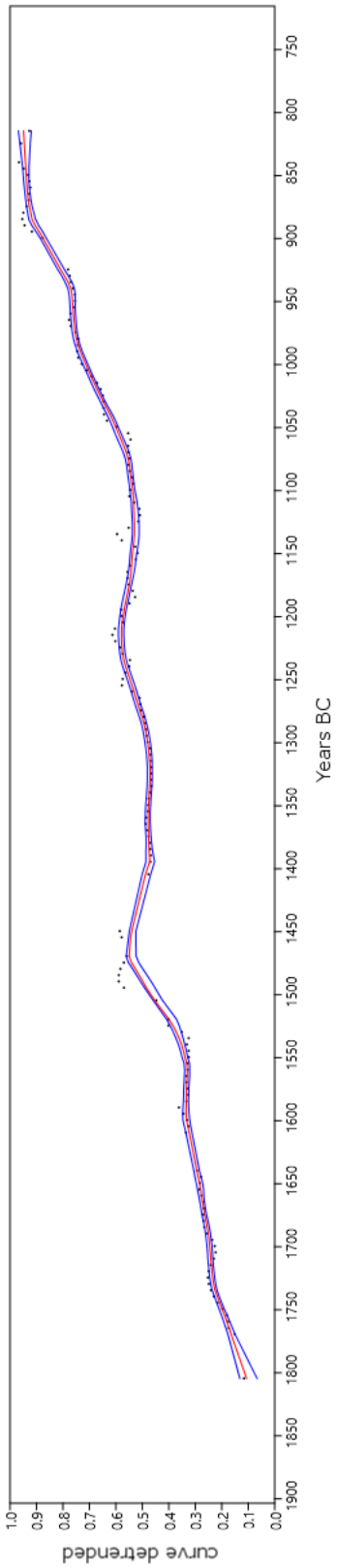

Figure 3.7. *LOWESS function applied to SCPD data from settlements, the 95% confidence interval is marked by the blue lines (Software: PAST 3.18).*

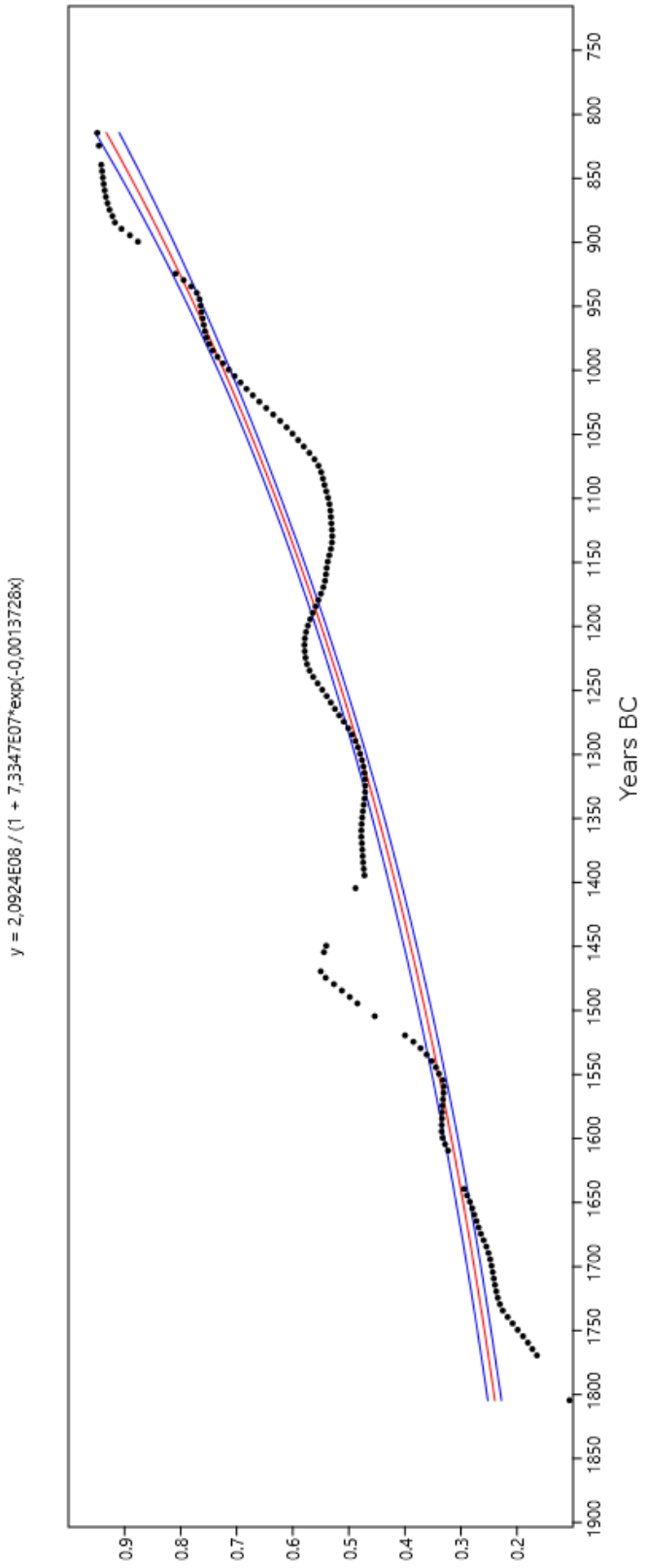

Figure 3.8. *Standard logistic model fitted to the interpolated LOWESS function obtained from the SCPD data from settlements (Software: PAST 3.18).*

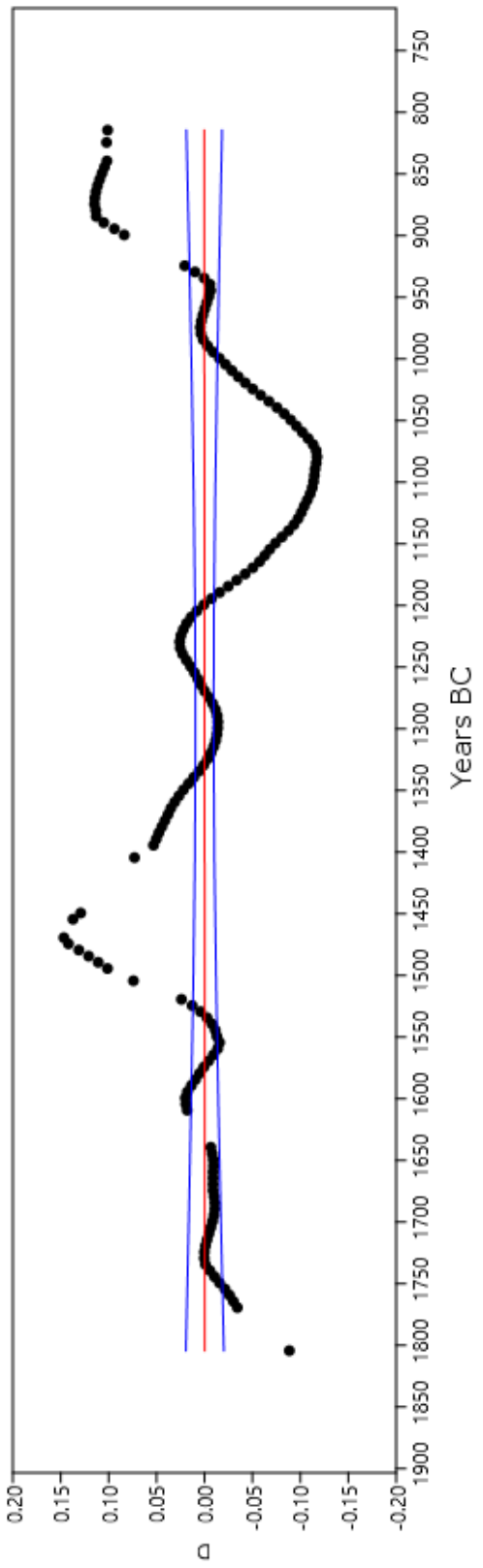

Figure 3.9. *Linear trend of the interpolated LOWESS function obtained from the SCPD data from settlements (Software: PAST 3.18).*

Furthermore, Magny (2015) points out that the sedimentary record of Lake Clairvaux (Jura, France) suggests a climatic downturn in the region as early as 1650-1600 BC, i.e. when temperatures begin to decline in our model. On the other hand, the precipitation curve is characterized by a see-saw pattern that describes an overall neutral trend and displays rather limited similarities with HLL Z-scores. Still, it should be noted that the magnitude of the fluctuations in both pollen-based curves remains rather modest, possibly implying a limited sensitivity of the local plant communities to any climatic factor affecting lake levels.

Po Plain

The SCPD for the Po Plain is based on 134 radiocarbon dates from 46 archaeological sites (Fig. 3.11a). The resulting demographic curve is characterized by a distinct tripartite behavior, displaying notable similarities to both the local archaeological narrative and the climatic reconstructions. The first portion of the curve shows a population increase that eventually peaks at ca. 1500-1450, and is then followed by a severe decline lasting until ca. 1100 BC. The remaining portion of the curve shows low values, reflecting both a sparse human presence and extended demographic stagnation.

During the local transition from the Middle Bronze Age I to the Middle Bronze Age II, ca. 1500 BC according to de Marinis (1999), wetland settlements in the Garda Lake region tended to move to higher grounds and dwellings in the alluvial plain were surrounded by earthen ramparts and ditches, suggesting a general increase in humidity (de Marinis, 2000). Consistently with this interpretation, the precipitation curve (Fig. 3.11b) peaks at 1400 BC, pointing to a higher precipitation phase that is also supported by water level reconstructions for Lake Ledro and Lake Accesa (Fig. 3.11d). Both these lakes, located in the Southern Alps and in Central Italy respectively, show a remarkably similar trend with peaks in water depth around ca. 1500-1400 BC (Magny et al., 2013). The visible decline in population after ca. 1400 BC appears then to match a following gradual transition to drier conditions (Fig. 3.11b and 3.11c), in agreement with the gradual drying up of wetland areas and decline of groundwater levels inferred from independent palaeoecological and archaeological data (Cremaschi et al., 2006; Dal Corso, 2018; Perego et al., 2011; Valsecchi et al., 2006).

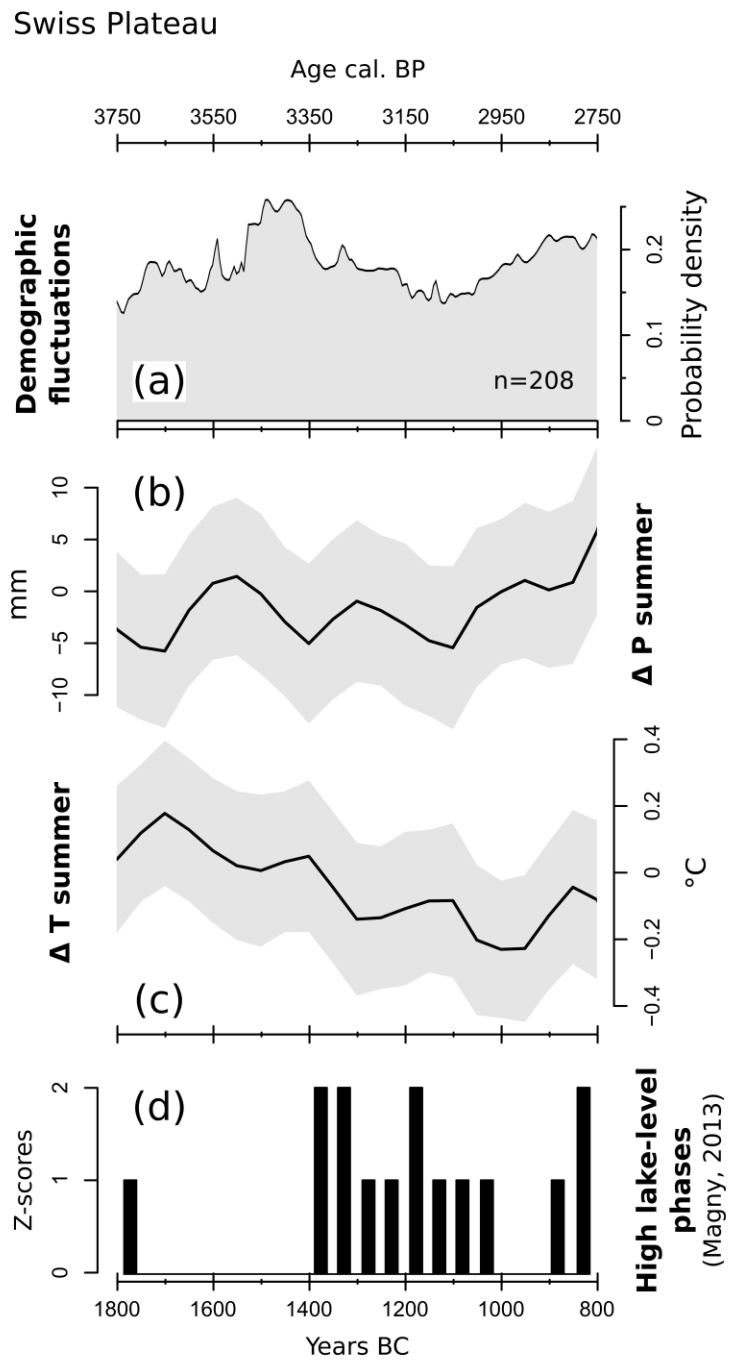

Figure 3.10. *(a) SCPD of 208 ^{14}C dates originating from sites located on the Swiss Plateau; (b) LOESS model of reconstructed summer precipitations; (c) LOESS model of reconstructed summer temperatures; (d) High lake level z-scores digitized from Magny (2013). The shaded areas in (b) and (c) outline the 95 % confidence interval of each LOESS model.*

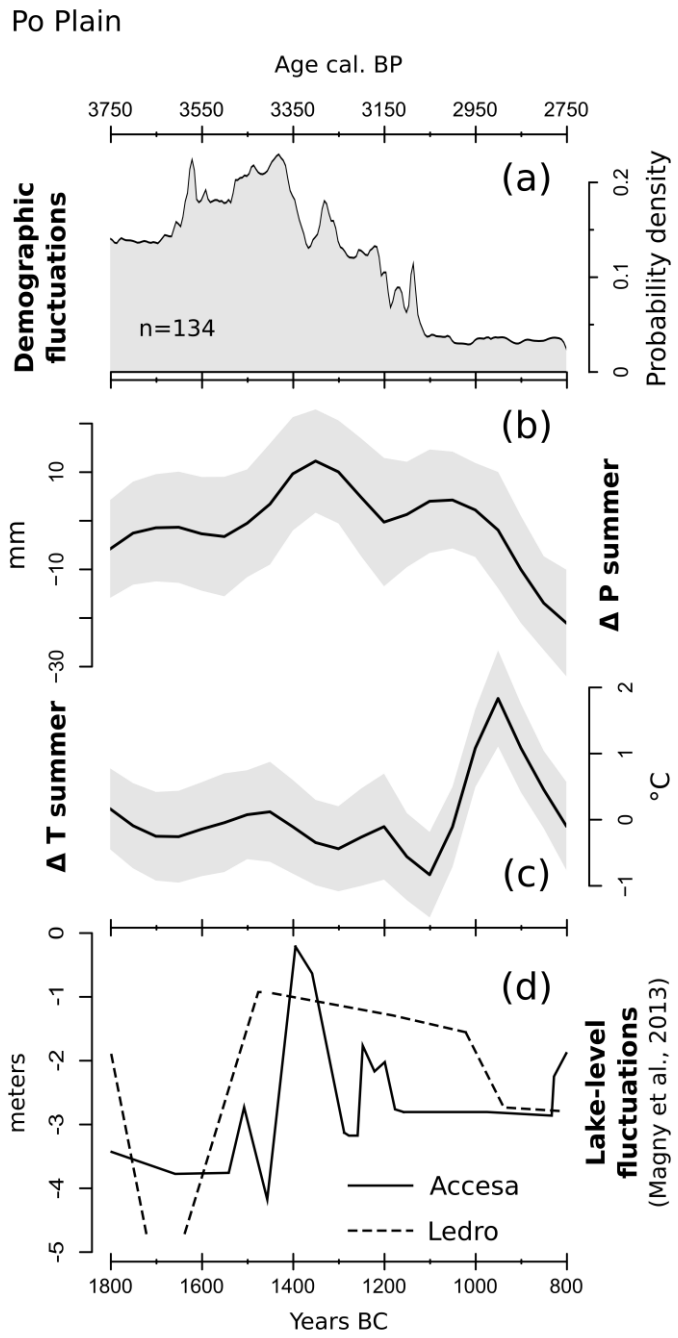

Figure 3.11. *(a) SCPD of 134 ^{14}C dates originating from sites located in the Po Plain; (b) LOESS model of reconstructed summer precipitations; (c) LOESS model of reconstructed summer temperatures; (d) Water level fluctuation for Lake Ledro and Lake Accesa, digitized from Magny et al. (2013). The shaded areas in (b) and (c) outline the 95 % confidence interval of each LOESS model.*

Massif Central

The SCPD for the Massif Central region is based on 57 dates from 33 archaeological sites (Fig. 3.12a). A visual comparison highlights few similarities between the demography and climate, although a cautious interpretation remains necessary due to the limited number of radiocarbon dates composing the SCPD curve. The sharp population increase observed between 1800-1700 BC coincides with a transition to warmer/drier conditions (Fig. 3.12b and 3.12c), and the subsequent general decline (ca. 1700-1400 BC) appears to occur in correspondence with a wet and cold shift. The following climatic fluctuations -most notably a shift towards drier and warmer conditions after ca. 1500 BC- are not met with equally visible demographic changes. On the contrary, the SCPD curve remains rather stable across the most of the study window, pointing to an overall prevailing and long-lasting neutral demographic trend. The notable 1700-1500 BC climatic deterioration finds a first parallel in the high detrital input phase recorded in nearby Lake Aydat between ca. 1650 and 1350 BC (Lavrieux et al., 2013) (Fig. 3.12d), arguably linking wetter/cooler conditions to long-term soil erosion. A predominant climatic trigger for this sediment discharge was suggested especially after ca. 1550 BC (Miras et al., 2015), but local anthropic land use appears to be rather limited throughout the whole Bronze Age (e.g., rare occurrences of cropland/pastoral pollen indicators and coprophilous fungi). The Lake Aydat record is interrupted between ca. 1230 BC and 180 AD due to sediment mixing, thus not covering the minor shift to wetter and cooler conditions visible from 1150-1000 BC in the pollen-based curves. Cubizolle et al. (2012) offer an additional insight on local landscape development through an SCPD-based record of peat formation events for the Eastern Massif Central (Fig. 3.12e). Cubizolle et al. (2012) suggest that anthropic land use was a driving mechanism behind peat initiation, partly basing their hypothesis on climatic reconstructions external to the study area (i.e. Barber et al., 2004; Magny, 2004). A visual comparison between peat formation and demographic trends reveals limited similarities, which nonetheless should not be exceedingly stressed due to the limited number of radiocarbon dates involved. Still, it is worth noting that a visible gap in the peat formation curve (ca. 1400-1200 BC) occurs together with a transition into warmer and drier conditions, and comes to an end after a minor cold and humid shift. These similarities between peat formation events and climate behavior might depend on known wetland expansion trends occurring under cool and moist conditions (Weckström et al., 2010), which would ultimately support the validity of our

reconstructions and possibly point to a prevailing climatic control on local wetland dynamics during the Bronze Age.

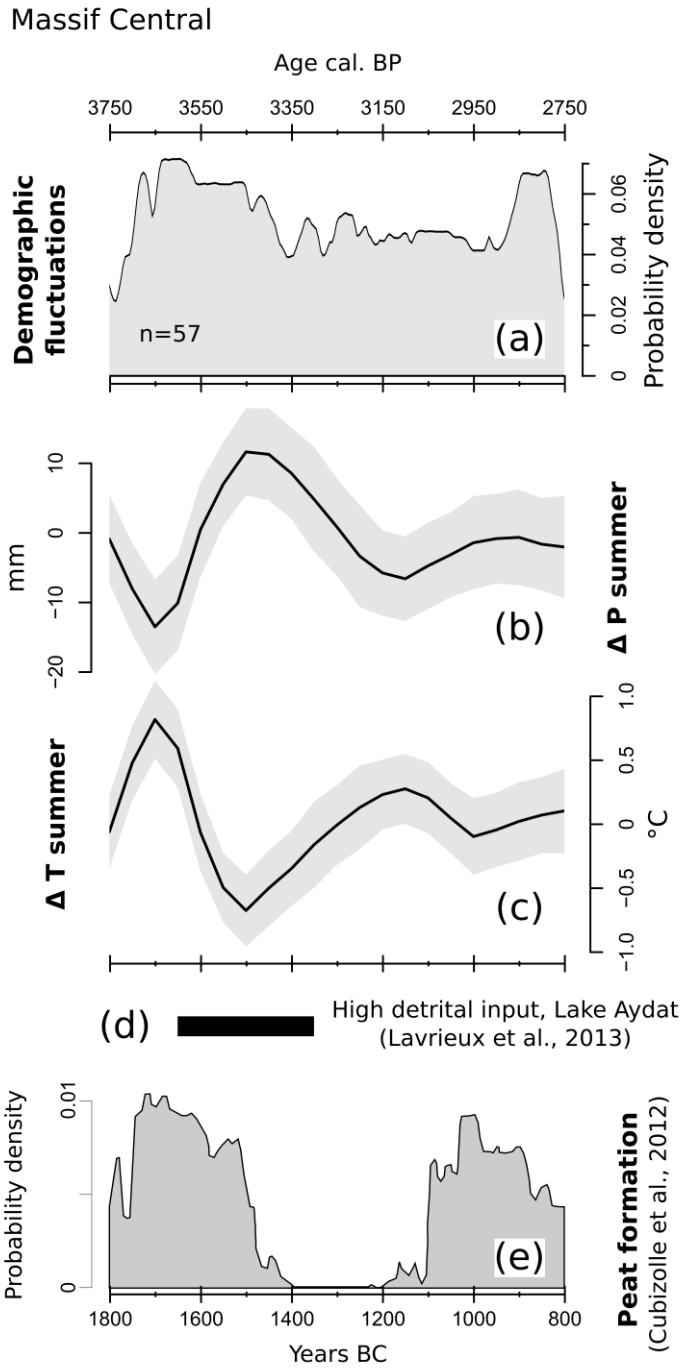

Figure 3.12. *(a) SCPD of 57 ^{14}C dates originating from sites located in the Massif Central; (b) LOESS model of reconstructed summer precipitations; (c) LOESS model of reconstructed summer temperatures; (d) Duration of high detrital phase in Lake Aydat (Lavrieux et al., 2013); (e) SCDP-based peat initiation events digitized from Cubizolle et al. (2012). The shaded areas in (b) and (c) outline the 95 % confidence interval of each LOESS model.*

NW-Mediterranean

The SCPD of the two remaining regions, the Southern French coast and the Northeastern Iberian Peninsula, are discussed together due to their similarities (Fig. 3.13a and 3.13b). As mentioned in section 2.2, a single set of Northwestern Mediterranean temperature and precipitation curves is produced using pollen archives from both areas (Fig. 3.13c and 3.13d). The population curve for Southern France (Fig. 3.13b) is based on 72 dates from 19 archaeological sites located in a buffer zone of 40 km from the Mediterranean coastline. The SCPD curve begins with a negative trend, reaching its lowest point at around 1450 BC. The subsequent population recovery follows an exponential trajectory until ca. 1200 BC, and is then followed by an extended period of stagnation/decline. The Northeastern Iberian dataset is composed of 158 radiocarbon dates from 74 archaeological sites (Fig. 3.13a). The SCPD curve shows visible similarities with the neighboring Southern French coast, but with a lag of ca. 100-200 years. The lowermost values occur between 1400 and 1300 BC, following a rather stable/mildly declining phase. The curve acquires a positive trend until ca. 1000 BC. The remaining portion is then characterized by stable conditions that turn into rapid growth towards the very end of our temporal window. The temperature and precipitation curves display a specular behavior pointing toward an ongoing transition into warmer and drier conditions. A comparable situation, with overall declining annual precipitations and rising annual temperatures between the Middle and Late Bronze Age, was found at the coastal site of Montou (Southern France) based on variations in olive wood anatomy (Terral and Mengüal, 1999) (Fig. 3.13e). These general trends fit well with the gradual aridification process of the Western Mediterranean region, leading from a wetter-than-present mid-Holocene to the current Mediterranean climate (Jalut et al., 2000; Roberts et al., 2011).

DISCUSSION

In the present paper we offer an SCPD-based reconstruction of population dynamics across Central-Southern Europe and within different smaller regions in order to check for any similarity/difference between neighboring areas and evaluate them against existing narratives. As a further exercise, we compare these SCPD-based curves with local, semi-quantitative climatic reconstructions. This comparison aims at identifying the presence or absence of macroscopic matching or specular patterns, in order to evaluate the presence of potential phases of climatic control on human activities.

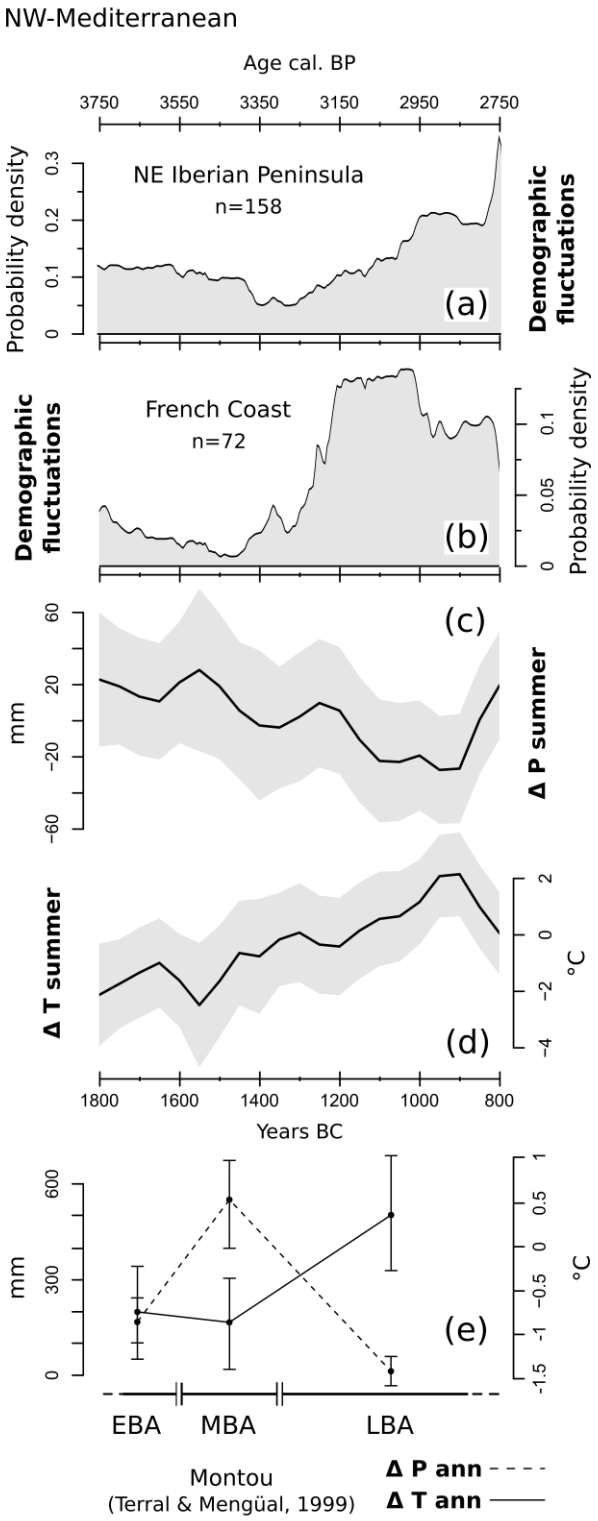

Figure 3.13. *(a) SCPD of 158 14C dates originating from sites located on the northeast Iberian Peninsula; (b) SCPD of 72 ^{14}C dates originating from sites located on the Southern French coast; (c) LOESS model of reconstructed summer precipitations; (d) LOESS model of reconstructed summer temperatures; (e) Annual temperature (ΔT_{ann}) and precipitation (ΔP_{ann}) reconstructions from the site of Montou (SW-France), digitized from Terral and Mengual (1999). The shaded areas in (b) and (c) outline the 95 % confidence interval of each LOESS model.*

We interpret our findings taking into account the available local archaeological and palaeoenvironmental evidence. Nonetheless, we recognize that any schematic comparison can hardly unravel the complex mechanisms behind human population dynamics. Taking into account the potential uncertainties affecting the reconstructions (both demographic and climatic; e.g. combinations of dating accuracy and limited data availability) we opted to avoid a statistically supported (cross-)correlation analysis of our results. We considered a visual comparison between curves appropriate for the available data and the scope of the paper.

Regarding the possible issues on sample size for regional analyses, it is essential to highlight that the one-millennium temporal window considered in the present study is much shorter than the ones commonly adopted in the available literature. The approximate data density (dates/year) for the regional analyses ranges between 0,06 dates/year (Massif Central) and 0,21 dates/year (Swiss Plateau). The geographic framework of the paper spans from the ca. 15000 km^2 of the "Swiss Plateau" region to the ca. 670000 km^2 of the whole area. In terms of spatial density, the lowest value is reached by the Massif Central region with 0,001 dates/km^2 whilst the highest value is recorded in the Swiss Plateau 0,14 dates/Km^2. These values are comparable with those of already published research involving the SCPD method (e.g. literature review in Contreras and Meadows, 2018). Despite a relatively high regional data density per year, it remains important to take into account the limited absolute number of radiocarbon dates available after screening and combination. Instead of the very general recommendations for big datasets (Williams, 2012), we have opted for thresholds based on the temporal range -in this case, 1000 years- and the minimum date for approximating the underlying Poisson distribution with a Gaussian distribution. According to that criterion, the general demographic trend for each region is within such limits. On a macroscale, the European demographic curves (Figs. 3.8 and 3.9) display episodes of distinct population growth (between ca. 1550-1450 BC and after ca. 1050 BC) interrupted by a rather steady negative trend (ca. 1450-1050 BC). This behavior reflects a combination of different and more dynamic regional trajectories.

On the Swiss Plateau, positive SCPD trends (1800-1450 BC; 1050-800 BC) appear to fit well with population recovery periods following phases of settlement discontinuity (2400-2100 BC; 1500-1100 BC; Menotti, 2015a). The reasons behind the population decline from 1500-1100 BC are still debated. The wide spectrum of cultivated crops might have proven to have been an efficient protection against harvest failures, a hypothesis that is supported by the not-increasing role of hunting activities during

unfavorable climatic conditions (Stopp, 2015). Socioeconomic factors might have played a visible role only at a later stage, between the Late Bronze Age and the Early Iron Age, when a significant reduction in the quantity of swords in archaeological contexts could suggest a declining importance of Swiss trade nodes within inter-regional exchange routes (Jennings, 2013; Menotti, 2015b). A combination of cooler conditions and rising lake levels is currently regarded as an important contributing factor behind human displacement events (Menotti, 2015b). Our reconstructions point to only a minor shift towards cooler and wetter conditions, yet they suggest that climate deterioration might have occurred in the area since the end of the 17th century BC. Conversely, population decline occurred only two centuries later according to the archaeological record. This late reaction might point to a high degree of resilience among the local communities to adverse climate events, yet the effective magnitude of this unfavorable climatic trend remains to be more precisely quantified. Only a further harshening of (potentially already) unfavorable conditions might have then resulted in settlement relocation and population decline (namely, the ca. 1500-1100 BC lake-dwelling hiatus), but not in widespread regional abandonment. Even during the coldest phase within our study time window, the area was never completely depopulated, as suggested by the relative abundance of radiocarbon dated archaeological contexts.

The SCPD curve on the Po Plain exhibits changes that are more dramatic. The period between ca. 1650 and 1350 BC marks the maximum development of Bronze Age settlements between the Alps and the Apennines (Bernabò Brea et al., 1997; Bietti Sestieri, 2010; Cardarelli, 2010) corresponding to the population peak observed in the SCPD curve. These overall favorable conditions for population growth are possibly linked to a transition from slash-and-burn forms of agriculture to more productive irrigated croplands (Cremaschi, 2009), even though the direction of causality does not appear to be solvable with the available data. The stable negative SCPD trend after ca. 1400 BC is somewhat in contrast with the traditional interpretation of archaeological data, which points to a sudden abandonment phase only after 1200 BC (de Marinis, 2010). A possible explanation behind this disparity lies in the reorganization of the settlement system in the Terramare area (Eastern Po Plain) after ca. 1450 BC, characterized by population agglomeration in larger settlements -and abandonment of smaller ones- rather than by the establishment of new villages (Cardarelli, 2010). Nonetheless, in agreement with the traditional interpretation, our model shows an extended period of depopulation after ca. 1150 BC in connection with the establishment of warmer and then more arid conditions. Significantly, the

end of the Terramare culture around 1150 BC might have been triggered by a water crisis, as suggested by the lowering of the local water table over time (Cremaschi et al., 2006). This shift towards arid conditions arguably affected an environment already deteriorated by landscape over-exploitation and extensive deforestation (Cremaschi, 2010; Cremaschi et al., 2016, 2006; Dal Corso, 2018; Mercuri et al., 2015). The resulting widespread societal collapse affected the entire Southern Po Plain, which became largely void of settlements until the beginning of the Iron Age (Bernabò Brea et al., 1997; Cupitò et al., 2012; de Marinis, 2010; Mercuri et al., 2012, 2006).

The Massif Central area is the least represented in terms of number of sites. Assuming an adequate coverage and representativeness of the radiocarbon dataset, the low number of data points does suggest a rather diluted human presence within our time window. This situation might primarily reflect difficulties in establishing a durable and extensive occupation in an area characterized by a mountainous landscape (Carozza and Galop, 2008). Consistently, cropland indicators in pollen diagrams are limited to sparse pollen grains, possibly pointing to subsistence strategies more focused on livestock (Miras et al., 2004; Surmely et al., 2009). During the second and the beginning of the first millennium BC, interregional cultural contacts are attested by the presence of specific pottery typologies, such as vessels with handles *ad ascia* attributed to Italic influences transmitted through the Languedoc and Provence (Carozza et al., 2006; Guilaine, 1990). The main trade route in Bronze Age Southern France followed the course of the Rhone River, between the western Alps and the Massif Central, placing the latter in a peripheral but increasingly dynamic situation between the Mediterranean coast and Central France. Despite the patchiness of the radiocarbon record, the fluctuations in the SCPD curve may indeed reflect major regional cultural dynamics. The first peak in human activities (around ca. 1700 BC) occurs during the Early Bronze Age, when the dynamism of the local agro-pastoral communities is testified by regional and interregional cultural contacts, as well as by signs of emerging social stratification (Carozza et al., 2006; Faure, 2012). A change occurs with the transition into the Middle Bronze Age (after ca. 1600 BC), when the archaeological record points to a general abandonment of lowland sites and the use of low and middle mountainous belts (Carozza and Galop, 2008; Faure, 2012). In this context, the contemporaneous transition to colder and wetter conditions, coupled with the sedimentary discharge visible in Lake Aydat, might point to population displacement as a response to increased hydrogeological instability. Nevertheless, both the SCPD curve and the persistence of long-distance contacts in the archaeological record suggest a reorganization of the settlement system towards

increased mobility rather than a complete abandonment of the area (Faure, 2012). A radical landscape transformation is recorded in the region only since the transition into the Iron Age (ca. after 800 BC), with an increasing presence of funeral mounds, the establishment of *oppida* (hilltop sites), and the first large-scale deforestation events (Faure, 2012).

The NW Mediterranean presents a situation clearly distinct from the other regions. The visibly similar trends between the French coast and the NE Iberian Peninsula reflect the commonalities shared by these two regions. Trans-Pyrenean and maritime fluxes of people spread innovations from Southern France to the northeastern Iberian Peninsula, in particular from the Middle Bronze Age onwards. Evidence for these cultural connections can be found in the adoption of specific pottery typologies, such as vessels with handles with vertical expansion (*asas de apéndice de botón*), fluted pottery (*cerámica acanalada*), and the arrival of cremation burials (Capuzzo and Barceló, 2015a, 2015b, 2014; López-Cachero, 2011, 2008; López-Cachero et al., 2014; Ruiz Zapatero, 2014b, 2014a). The NE Iberian area probably played a modest role during the Early/Late Bronze Age when compared with more structured cultural centers located in the southeastern and central parts of the peninsula (Lull et al., 2013a). This peripheral situation appears to be visible in the stagnating SCPD values from ca. 1800-1450 BC, partly overlapping with the widespread abandonment phase that follows the southeastern Argaric collapse (ca. 1550 BC; Lull et al., 2013b). Internal forces or a subsistence crisis are mentioned as leading causes for this sudden cultural shift (Carrión et al., 2007; Lull et al., 2013a). Still, potential connections between these events and the ca. 1400-1300 BC SCPD minimum in NE Iberia remain unclear. The demographic growth registered after this phase matches rather precisely the local emergence of the cremation ritual, possibly suggesting population fluxes from continental Europe (Lull et al., 2013a; Ruiz Zapatero, 2014b, 2014a). The simultaneous transition towards a more arid climate does not appear to hinder population growth. Similarly, positive demographic trends in Southern Iberia in co-occurrence with increasingly arid conditions have already been described between ca. 3550 and 2550 BC (Lillios et al., 2016). Notably, drought resistant barley is the dominant cereal during the entire Bronze Age in Mediterranean Spain (Stika and Heiss, 2013). Of particular interest is the demographic increase registered along the French coast between 1350 and 1200 BC. This phase of demographic growth appears to predate the major cultural phenomenon in the area, i.e. the expansion of the Mailhacien culture around 900 BC (Giraud et al., 2003; Janin, 2009, 2000), which in turn occurs during a period of relative stability in the SCPD curve. In this regard, the

apparent mismatch between the SCPD and the archeological data might depend - at least partially - on cultural differences between the western and the eastern French coast (Gascó, 2011, 2000; Janin, 2000; Mordant, 2013; Vital, 2001, 1999; Vital et al., 2012). A more appropriate intra-regional discussion is currently prevented by the limited number of available radiocarbon dates, which led us to group the French Riviera, Provence and Languedoc-Roussillon under a single SCPD despite their heterogeneous archeological dynamics.

CONCLUSIONS

In the present paper, we use a dataset of archaeological radiocarbon dates to reconstruct demographic trends in Central-Southern Europe between 1800 and 800 BC. On a macroscale, a positive demographic trend is visible until ca. 1450 BC, and is then followed by a phase of population decline lasting until ca. 1050 BC. Until ca. 1050 BC, the macroscale population dynamics appear to be mostly determined by circum-alpine trends. At the beginning of the 16th century BC there was an expansion of the Terramare settlements, in which the entire populated area in the Po Plain tripled in size (Vanzetti, 2013). Similarly, in the French Jura Mountains it is attested a period of population growth around 1500 BC (Pétrequin et al., 2005). Significantly, northern Italy, eastern France, the ore-rich Alpine area were economically the most dynamic regions after 1600 BC in Europe, with clear evidence of a socio-economic growth (Risch and Meller, 2015). The population decrease after ca. 1470 BC coincides then with the crisis of the lake-dwelling settlement system in the Circum-Alpine region (Billamboz, 2013; Menotti, 2015a, 2004, 2001). Similarly, the demographic contraction between 1200 and 1050 BC takes place in a time-span defined by the collapse of the pile-dwelling/Terramare culture around 1150 BC (Cremaschi et al., 2016, 2006; Dal Corso, 2018). A renewed episode of macroscale demographic growth is visible after ca. 1050 BC, likely reflecting both the population peaks recorded along the NW Mediterranean coast and the population recovery trend visible in the Swiss Plateau. Notably, the prominent NW Mediterranean positive trends occur in connection with the local adoption of the cremation ritual, and might imply a demographic influx from central Europe. A potential relation between population trends and climate was visually evaluated by comparing the SCPD curves with semi-quantitative summer temperatures and precipitation curves reconstructed from pollen sequences specific for each region. Climate appears to play a non-dismissible role on the Po Plain, where widespread settlement abandonment occurs in connection with increasingly arid conditions. While independent archaeological and

palaeoenvironmental proxies support this connection, it remains unfeasible to ascertain whether climate represents the main forcing factor leading to the collapse of local Bronze Age societies, or if its effects were exacerbated by additional and cumulating factors, such as an inferred landscape overexploitation. Communities on the Swiss Plateau appear to show a higher degree of resilience to climatic fluctuations, with settlement collapse occurring only during the coolest interval in the temperature curve, after centuries of increasingly cooler conditions. A population drop in the Massif Central occurs in connection with a particularly pronounced cold and wet phase (ca. 1700-1500 BC). Apart from this event, the local communities appear to be largely unaffected by other climatic shifts. The predominant stagnation emerging from the Massif Central SCPD curve seems to reflect a long-term stability rather uncommon among our reconstructions, presumably connected to low demographic density and high mobility deriving from a livestock-based subsistence.

ACKNOWLEDGMENTS

This research is part of the project "Social and Environmental Transitions: Simulating the Past to Understand Human Behaviour", funded by the Spanish Ministry of Education, Culture and Sport, under the program CONSOLIDER-INGENIO 2010, CSD2010-00034 and the project 2014SGR-1169 and 2017SGR-243 funded by the Generalitat de Catalunya. We also acknowledge funds from the Spanish Ministry of Education, Culture and Sport, through the Grant No. HAR2012-31036 and HAR2016-76534-C2-1-R. The authors from Kiel University were supported by the Graduate School "Human Development in Landscapes" (GSC 208/2) and by the DFG Collaborative Research Centre SFB 1266 "Scales of Transformation - Human-Environmental Interaction in Prehistoric and Archaic Societies". The work of the EPD data contributors and of the EPD community is gratefully acknowledged. The authors would like to thank Jordi Revelles and Francesc Burjachs for supplying the pollen data from Banyoles and Pla de l'Estany respectively. We also express our gratitude to the reviewers for their encouraging and constructive comments that improved the quality of the article.

Bibliography

Armit, I., Swindles, G.T., Becker, K., 2013. From dates to demography in later prehistoric Ireland? Experimental approaches to the meta-analysis of large 14C data-sets. Journal of Archaeological Science 40, 433–438. https://doi.org/10.1016/j.jas.2012.08.039

Armit, I., Swindles, G.T., Becker, K., Plunkett, G., Blaauw, M., 2014. Rapid climate change did not cause population collapse at the end of the European Bronze Age. Proceedings of the National Academy of Sciences 111, 17045–17049.

Balsera, V., Díaz-del-Río, P., Gilman, A., Uriarte, A., Vicent, J.M., 2015. Approaching the demography of late prehistoric Iberia through summed calibrated date probability distributions (7000–2000 cal BC). Quaternary International, Palaeolandscapes from Saalian to Weichselian: INQUA TERPRO Commission, Peribaltic International Field Symposium, Lithuania 386, 208–211. https://doi.org/10.1016/j.quaint.2015.06.022

Banks, R.B., 2013. Growth and Diffusion Phenomena: Mathematical Frameworks and Applications. Springer Science & Business Media.

Barber, K., Zolitschka, B., Tarasov, P., Lotter, A.F., 2004. Atlantic to Urals – the Holocene climatic record of Mid-Latitude Europe, in: Battarbee, R.W., Gasse, F., Stickley, C.E. (Eds.), Past Climate Variability through Europe and Africa, Developments in Paleoenvironmental Research. Springer Netherlands, pp. 417–442. https://doi.org/10.1007/978-1-4020-2121-3_20

Barceló, J.A., Capuzzo, G., Bogdanović, I., 2014. Modeling Expansive Phenomena in Early Complex Societies: the Transition from Bronze Iron Age in Prehistoric Europe. J Archaeol Method Theory 21, 486–510. https://doi.org/10.1007/s10816-013-9195-2

Bernabò Brea, M., Cardarelli, A., Cremaschi, M., 1997. Le Terramare, la piu'antica civilta padana. Electa, Modena.

Bietti Sestieri, A.M., 2010. L'Italia nell'età del bronzo e del ferro: dalle palafitte a Romolo (2200-700 aC). Carocci.

Billamboz, A., 2013. Der Standpunkt der Dendroarchäologie zu Auswirkungen der Thera-Eruption nördlich der Alpen, in: Meller, H., Bertemes, F., Bork, H.R., Risch, R. (Eds.), 1600 – Kultureller Umbruch in Schatten Des Thera-Ausbruchs?, Der. 4. Mitteldeutschen Archäologietag, 14–16 Oktober 2011., Tagungen Del Landesmuseums Für Vorgeschichte Halle. Landesamt für Denkmalpflege und Archäologie in Sachsen-Anhalt, Landesmuseum für Vorgeschichte, Halle (Saale), pp. 89–99.

Birks, H.J.B., Birks, H.H., 1980. Quaternary palaeoecology. Edward Arnold London.

Blaauw, M., 2010. Methods and code for 'classical' age-modelling of radiocarbon sequences. Quaternary Geochronology 5, 512–518. https://doi.org/10.1016/j.quageo.2010.01.002

Bogdanovic, I., Capuzzo, G., Mantegari, G., Barceló, J.A., 2014. A DATABASE FOR RADIOCARBON DATES. Some methodological and theoretical issues about its implementation, in: On-Line Papers from the 40th Annual Conference of

Computer Applications and Quantitative Methods in Archaeology (CAA), Southampton, 26-29 March 2012. pp. 457–467.

Borrell, F., Junno, A., Barceló, J.A., 2015. Synchronous Environmental and Cultural Change in the Emergence of Agricultural Economies 10,000 Years Ago in the Levant. PLOS ONE 10, e0134810. https://doi.org/10.1371/journal.pone.0134810

Bronk Ramsey, C., 2017. Methods for Summarizing Radiocarbon Datasets. Radiocarbon 59, 1809–1833. https://doi.org/10.1017/RDC.2017.108

Bronk Ramsey, C., 2009. Bayesian Analysis of Radiocarbon Dates. Radiocarbon 51, 337–360. https://doi.org/10.1017/S0033822200033865

Burjachs, F., 1994. Palynology of the upper Pleistocene and Holocene of the North-East Iberian Peninsula: Pla de l'Estany (Catalonia). Historical Biology 9, 17–33. https://doi.org/10.1080/10292389409380485

Capuzzo, G., Barceló, J.A., 2015a. Cultural changes in the second millennium BC: a Bayesian examination of radiocarbon evidence from Switzerland and Catalonia. World Archaeology 47, 622–641. https://doi.org/10.1080/00438243.2015.1053571

Capuzzo, G., Barceló, J.A., 2015b. Cremation burials in Central and Western Europe: quantifying an adoption of innovation in the 2nd millennium BC, in: Proceedings of the 4th International Open Workshop "Socio-Environmental Dynamics over the Last 12,000 Years: The Creation of Landscapes", Kiel (Germany), March 24-27, 2015.

Capuzzo, G., Barceló, J.A., 2014. La secuencia crono-cultural de la Edad del Bronce-comienzo de la Edad del Hierro en Cataluña. Los contextos arqueológicos fechados por el C14, in: Mercadal, I., Fernàndez, O. (Eds.), La Transició Bronze Final-1ª Edat Del Ferro En Els Pirineus i Territoris Veïns: XV Colloqui Internacional d'Arqueologia de Puigcerdà. Presented at the Congrés Nacional d'Arqueologia de Catalunya. November 17-19, 2011, Puigcerdà (Spain), pp. 659–669.

Capuzzo, G., Boaretto, E., Barceló, J.A., 2014. EUBAR: A Database of 14C Measurements for the European Bronze Age. A Bayesian Analysis of 14C-Dated Archaeological Contexts from Northern Italy and Southern France. Radiocarbon 56, 851–869. https://doi.org/10.2458/56.17453

Cardarelli, A., 2010. The collapse of the terramare culture and growth of new economic and social system during the Late Bronze Age in Italy, in: Cardarelli, A, Cazzella, A., Frangipane, M., Peroni, R. (Eds.), Scienze Dell'Antichità. Storia Archeologia Antropologia 15 (2009). Atti Del Convegno Internazionale "Le Ragioni Del Cambiamento/Reasons for Change". Roma, 15-17 Giugno 2006. Edizioni Quasar.

Carozza, L., Bouby, L., Ballut, C., 2006. Un habitat du Bronze moyen à Cournon-d'Auvergne (Puy-de-Dôme) : nouvelles données sur la dynamique de l'Âge du Bronze moyen sur la bordure méridionale du Massif central. Bulletin de la Société préhistorique française 103, 535–584.

Carozza, L., Galop, D., 2008. Le dynamisme des marges. Peuplement et exploitation des espaces de montagne durant l'âge du Bronze. Villes, villages, campagnes de l'Age du Bronze. Editions Errance.

Carrión, J.S., Fuentes, N., González-Sampériz, P., Sánchez Quirante, L., Finlayson, J.C., Fernández, S., Andrade, A., 2007. Holocene environmental change in a montane

region of southern Europe with a long history of human settlement. Quaternary Science Reviews 26, 1455–1475. https://doi.org/10.1016/j.quascirev.2007.03.013
Chamberlain, A., 2009. Archaeological Demography. Human Biology 81, 275–286. https://doi.org/10.3378/027.081.0309
Chaput, M.A., Gajewski, K., 2016. Radiocarbon dates as estimates of ancient human population size. Anthropocene 15, 3–12. https://doi.org/10.1016/j.ancene.2015.10.002
Cleveland, W.S., 1979. Robust Locally Weighted Regression and Smoothing Scatterplots. Journal of the American Statistical Association 74, 829–836. https://doi.org/10.1080/01621459.1979.10481038
Cleveland, W.S., Devlin, S.J., 1988. Locally Weighted Regression: An Approach to Regression Analysis by Local Fitting. Journal of the American Statistical Association 83, 596. https://doi.org/10.2307/2289282
Collard, M., Edinborough, K., Shennan, S., Thomas, M.G., 2010. Radiocarbon evidence indicates that migrants introduced farming to Britain. Journal of Archaeological Science 37, 866–870. https://doi.org/10.1016/j.jas.2009.11.016
Contreras, D.A., Meadows, J., 2018. Estudios paleodemográficos basados en conjuntos de dataciones radiométricas. Una revisión crítica, in: Barceló, J.A., Morell, B. (Eds.), Métodos Cronométricos En Historia y Arqueología. Dextra.
Contreras, D.A., Meadows, J., 2014. Summed radiocarbon calibrations as a population proxy: a critical evaluation using a realistic simulation approach. Journal of Archaeological Science 52, 591–608. https://doi.org/10.1016/j.jas.2014.05.030
Crema, E.R., Bevan, A., Shennan, S., 2017. Spatio-temporal approaches to archaeological radiocarbon dates. Journal of Archaeological Science 87, 1–9. https://doi.org/10.1016/j.jas.2017.09.007
Crema, E.R., Habu, J., Kobayashi, K., Madella, M., 2016. Summed Probability Distribution of 14C Dates Suggests Regional Divergences in the Population Dynamics of the Jomon Period in Eastern Japan. PLOS ONE 11, e0154809. https://doi.org/10.1371/journal.pone.0154809
Cremaschi, M., 2010. Ambiente, clima ed uso del suolo nella crisi della cultura delle Terramare, in: Cardarelli, A., Cazzella, A., Frangipane, M., Peroni, R. (Eds.), Scienze Dell'Antichità. Storia Archeologia Antropologia 15 (2009). Atti Del Convegno Internazionale "Le Ragioni Del Cambiamento/Reasons for Change". Roma, 15-17 Giugno 2006. Edizioni Quasar, pp. 521–534.
Cremaschi, M., 2009. Foreste, terre coltivate e acque : l'originalità del progetto terramaricolo, in: Bernabò Brea, M., Cremaschi, M. (Eds.), Acqua e civiltà nelle terramare: la vasca votiva di Noceto. Università degli studi di Milano, Skirà, Milano.
Cremaschi, M., Mercuri, A.M., Torri, P., Florenzano, A., Pizzi, C., Marchesini, M., Zerboni, A., 2016. Climate change versus land management in the Po Plain (Northern Italy) during the Bronze Age: New insights from the VP/VG sequence of the Terramara Santa Rosa di Poviglio. Quaternary Science Reviews 136, 153–172. https://doi.org/10.1016/j.quascirev.2015.08.011
Cremaschi, M., Pizzi, C., Valsecchi, V., 2006. Water management and land use in the terramare and a possible climatic co-factor in their abandonment: The case study of

the terramara of Poviglio Santa Rosa (northern Italy). Quaternary International 151, 87–98. https://doi.org/10.1016/j.quaint.2006.01.020

Crombé, P., Robinson, E., 2014. 14C dates as demographic proxies in Neolithisation models of northwestern Europe: a critical assessment using Belgium and northeast France as a case-study. Journal of Archaeological Science 52, 558–566. https://doi.org/10.1016/j.jas.2014.02.001

Cubizolle, H., Fassion, F., Argant, J., Latour-Argant, C., Galet, P., Oberlin, C., 2012. Mire initiation, climatic change and agricultural expansion over the course of the Late-Holocene in the Massif Central mountain range (France): Causal links and implications for mire conservation. Quaternary International 251, 77–96. https://doi.org/10.1016/j.quaint.2011.07.001

Cupitò, M., Dalla Longa, E., Donadel, V., Leonardi, G., 2012. Resistance to the 12th century BC crisis in the Veneto Region: the case studies of Fondo Paviani and Montebello Vicentino, in: Kneisel, J., Kirleis, W., Dal Corso, M., Taylor, N., Tiedtke, V. (Eds.), Collapse or Continuity? Environment and Development of Bronze Age Human Landscapes. Habelt, Bonn, pp. 55–70.

Dal Corso, M., 2018. Environmental history and development of the human landscape in a northeastern Italian lowland during the Bronze Age: a multidisciplinary case-study (PhD Thesis). Kiel University.

Davis, B.A.S., Brewer, S., Stevenson, A.C., Guiot, J., 2003. The temperature of Europe during the Holocene reconstructed from pollen data. Quaternary Science Reviews 22, 1701–1716. https://doi.org/10.1016/S0277-3791(03)00173-2

Davis, B.A.S., Zanon, M., Collins, P., Mauri, A., Bakker, J., Barboni, D., Barthelmes, A., Beaudouin, C., Bjune, A.E., Bozilova, E., Bradshaw, R.H.W., Brayshay, B.A., Brewer, S., Brugiapaglia, E., Bunting, J., Connor, S.E., Beaulieu, J.-L. de, Edwards, K., Ejarque, A., Fall, P., Florenzano, A., Fyfe, R., Galop, D., Giardini, M., Giesecke, T., Grant, M.J., Guiot, Jöel, Jahns, S., Jankovská, V., Juggins, S., Kahrmann, M., Karpińska-Kołaczek, M., Kołaczek, P., Kühl, N., Kuneš, P., Lapteva, E.G., Leroy, S.A.G., Leydet, M., Guiot, José, Jahns, S., Jankovská, V., Juggins, S., Kahrmann, M., Karpińska-Kołaczek, M., Kołaczek, P., Kühl, N., Kuneš, P., Lapteva, E.G., Leroy, S.A.G., Leydet, M., Sáez, J.A.L., Masi, A., Matthias, I., Mazier, F., Meltsov, V., Mercuri, A.M., Miras, Y., Mitchell, F.J.G., Morris, J.L., Naughton, F., Nielsen, A.B., Novenko, E., Odgaard, B., Ortu, E., Overballe-Petersen, M.V., Pardoe, H.S., Peglar, S.M., Pidek, I.A., Sadori, L., Seppä, H., Severova, E., Shaw, H., Święta-Musznicka, J., Theuerkauf, M., Tonkov, S., Veski, S., Knaap, W.O. van der, Leeuwen, J.F.N. van, Woodbridge, J., Zimny, M., Kaplan, J.O., 2013. The European Modern Pollen Database (EMPD) project. Veget Hist Archaeobot 22, 521–530. https://doi.org/10.1007/s00334-012-0388-5

de Marinis, R., 2000. Il Museo civico archeologico Giovanni Rambotti di Desenzano del Garda una introduzione alla preistoria del lago di Garda. Città di Desenzano del Garda, Assessorato alla Cultura, Desenzano del Garda.

de Marinis, R., 1999. Towards a Relative and Absolute Chronology for the Bronze Age in Northern Italy. Notizie Archeologiche Bergomensi 7, 23–100.

de Marinis, R.C., 2010. Continuity and discontinuity in northern Italy from the Recent to the Final Bronze Age: a view from north-western Italy, in: Cardarelli, A., Cazzella,

A., Frangipane, M., Peroni, R. (Eds.), Scienze Dell'Antichità. Storia Archeologia Antropologia 15 (2009). Atti Del Convegno Internazionale "Le Ragioni Del Cambiamento/Reasons for Change". Roma, 15-17 Giugno 2006. Edizioni Quasar, pp. 535–545.

De Mulder, G., Leclercq, W., Van Strydonck, M., 2008. Influence from the "groupe Rhin-Suisse-France orientale" on the pottery from the Late Bronze Age urnfields in Western Belgium. A confrontation between pottery building technology, 14C-dates and typochronology, in: Breaking the Mould: Challenging the Past through Pottery. Archaeopress, pp. 105–115.

Downey, S.S., Bocaege, E., Kerig, T., Edinborough, K., Shennan, S., 2014. The Neolithic Demographic Transition in Europe: Correlation with Juvenility Index Supports Interpretation of the Summed Calibrated Radiocarbon Date Probability Distribution (SCDPD) as a Valid Demographic Proxy. PLOS ONE 9, e105730. https://doi.org/10.1371/journal.pone.0105730

Earle, T., Kristiansen, K. (Eds.), 2010. Organizing Bronze Age Societies. Cambridge University Press.

Edinborough, K., Porčić, M., Martindale, A., Brown, T.J., Supernant, K., Ames, K.M., 2017. Radiocarbon test for demographic events in written and oral history. PNAS 201713012. https://doi.org/10.1073/pnas.1713012114

Edinborough, K.S.A., 2009. Population history, abrupt climate change and evolution of arrowhead technology in Mesolithic south Scandinavia, in: Shennan, S.J. (Ed.), Pattern and Process in Cultural Evolution. University of California Press, Berkeley, CA, pp. 191–202.

Edinborough, K.S.A., 2005. Evolution of bow-arrow technology. University of London.

Faure, É., 2012. "Hautes terres" : l'anthropisation des monts d'Aubrac et du Lévezou (Massif Central, France) durant l'holocène : approche palynologique des dynamiques socio-environnementales en moyenne montagne (phdthesis). Université Toulouse le Mirail - Toulouse II.

French, J.C., 2016. Demography and the Palaeolithic Archaeological Record. J Archaeol Method Theory 23, 150–199. https://doi.org/10.1007/s10816-014-9237-4

Gascó, J., 2011. Geographie regionale de l'age du bronze en Languedoc. Quaderns de prehistòria i arqueologia de Castelló 29, 135–151.

Gascó, J., 2000. L'Age du Bronze dans la moitié sud de la France. La maison des roches. éditeur.

Gavin, D.G., Oswald, W.W., Wahl, E.R., Williams, J.W., 2003. A statistical approach to evaluating distance metrics and analog assignments for pollen records. Quaternary Research 60, 356–367. https://doi.org/10.1016/S0033-5894(03)00088-7

Giesecke, T., Davis, B., Brewer, S., Finsinger, W., Wolters, S., Blaauw, M., de Beaulieu, J.-L., Binney, H., Fyfe, R.M., Gaillard, M.-J., Gil-Romera, G., van der Knaap, W.O., Kuneš, P., Kühl, N., van Leeuwen, J.F.N., Leydet, M., Lotter, A.F., Ortu, E., Semmler, M., Bradshaw, R.H.W., 2013. Towards mapping the late Quaternary vegetation change of Europe. Vegetation History and Archaeobotany 23, 75–86. https://doi.org/10.1007/s00334-012-0390-y

Giraud, J.-P., Janin, T., Pons, F. (Eds.), 2003. Nécropoles protohistoriques de la région de Castres (Tarn): Le Causse, Gourjade, Le Martinet, Documents d'archéologie française. La Maison des sciences de l'homme, Paris.

Guilaine, J., 1990. Le Bronze final du midi de la France. Questions d'actualité in La Bretagne et l'Europe préhistoriques. Mémoire en hommage à Pierre-Roland Giot. Revue Archéologique de l'Ouest. Supplément 227–233.

Guiot, J., 2011. Transfer functions. IOP Conference Series: Earth and Environmental Science 14, 012008. https://doi.org/10.1088/1755-1315/14/1/012008

Guiot, J., 1990. Methodology of the last climatic cycle reconstruction in France from pollen data. Palaeogeography, Palaeoclimatology, Palaeoecology 80, 49–69. https://doi.org/10.1016/0031-0182(90)90033-4

Harding, A., Fokkens, H., 2013. The Oxford Handbook of the European Bronze Age. OUP Oxford.

Hijmans, R.J., Cameron, S.E., Parra, J.L., Jones, P.G., Jarvis, A., 2005. Very high resolution interpolated climate surfaces for global land areas. International Journal of Climatology 25, 1965–1978. https://doi.org/10.1002/joc.1276

Hinz, M., Feeser, I., Sjögren, K.-G., Müller, J., 2012. Demography and the intensity of cultural activities: an evaluation of Funnel Beaker Societies (4200–2800 cal BC). Journal of Archaeological Science 39, 3331–3340. https://doi.org/10.1016/j.jas.2012.05.028

Isern, N., Fort, J., Carvalho, A.F., Gibaja, J.F., Ibañez, J.J., 2014. The Neolithic Transition in the Iberian Peninsula: Data Analysis and Modeling. J Archaeol Method Theory 21, 447–460. https://doi.org/10.1007/s10816-013-9193-4

Jalut, G., Esteban Amat, A., Bonnet, L., Gauquelin, T., Fontugne, M., 2000. Holocene climatic changes in the Western Mediterranean, from south-east France to south-east Spain. Palaeogeography, Palaeoclimatology, Palaeoecology 160, 255–290. https://doi.org/10.1016/S0031-0182(00)00075-4

Janin, T., 2009. Jean Guilaine, Mailhac et le Mailhacien, in: De La Méditerranée et d'ailleurs. Mélanges Offerts à Jean Guilaine, Archives d'Écologie Préhistorique. Toulouse, pp. 353–64.

Janin, T., 2000. Le groupe culturel Mailhac I en France méridionale: essai de définition et extension géographique d'apres l'étude des nécropoles du Languedoc occidental, in: Gascó, J., Claustre, F. (Eds.), Habitats, Économies et Sociétés Du Nord-Ouest Méditerranéen de l'Âge Du Bronze Au Premier Âge Du Fer, Actes Du Colloque International, XXIVe Congrès Préhistorique de France (Carcassonne, 26-30 Septembre). Joué-Lès-Tours. pp. 167–74.

Jennings, B., 2014. Breaking with Tradition: Cultural influences for the decline of the Circum-Alpine region lake-dwellings. Sidestone Press.

Jennings, B., 2013. Travelling objects: changing values : trade, exchange, and cultural influences for the decline of the lake-dwelling tradition in the northern Circum-Alpine region during the Late Bronze Age (phd). University of Basel.

Johnson, C.N., Brook, B.W., 2011. Reconstructing the dynamics of ancient human populations from radiocarbon dates: 10 000 years of population growth in Australia. Proc. R. Soc. B 278, 3748–3754. https://doi.org/10.1098/rspb.2011.0343

Juggins, S., 2019. rioja: Analysis of Quaternary Science Data.
Katzenberg, M.A., Saunders, S.R., 2011. Biological Anthropology of the Human Skeleton. John Wiley & Sons.
Kerr, T.R., McCormick, F., 2014. Statistics, sunspots and settlement: influences on sum of probability curves. Journal of Archaeological Science 41, 493–501. https://doi.org/10.1016/j.jas.2013.09.002
Kneisel, J., Kirleis, W., Dal Corso, M., Taylor, N., Tiedtke, V. (Eds.), 2012. Collapse of continuity? Environment and development of bronze age human landscapes. Habelt, Bonn.
Kolář, J., Kuneš, P., Szabó, P., Hajnalová, M., Svobodová, H.S., Macek, M., Tkáč, P., 2016. Population and forest dynamics during the Central European Eneolithic (4500–2000 BC). Archaeological and Anthropological Sciences. https://doi.org/10.1007/s12520-016-0446-5
Kristiansen, K., 2015. The Decline of the Neolithic and the Rise of Bronze Age Society. https://doi.org/10.1093/oxfordhb/9780199545841.013.057
Kristiansen, K., 2000. Europe Before History. Cambridge University Press.
Lavrieux, M., Disnar, J.-R., Chapron, E., Bréheret, J.-G., Jacob, J., Miras, Y., Reyss, J.-L., Andrieu-Ponel, V., Arnaud, F., 2013. 6700 yr sedimentary record of climatic and anthropogenic signals in Lake Aydat (French Massif Central). The Holocene 23, 1317–1328. https://doi.org/10.1177/0959683613484616
Lillios, K.T., Blanco-González, A., Drake, B.L., López-Sáez, J.A., 2016. Mid-late Holocene climate, demography, and cultural dynamics in Iberia: A multi-proxy approach. Quaternary Science Reviews 135, 138–153. https://doi.org/10.1016/j.quascirev.2016.01.011
López-Cachero, F.J., 2011. Cremation Cemeteries in the Northeastern Iberian Peninsula: Funeral Diversity and Social Transformation during the Late Bronze and Early Iron Ages. European Journal of Archaeology 14, 116–132. https://doi.org/10.1179/146195711798369382
López-Cachero, F.J., 2008. Necrópolis de incineración y arquitectura funeraria en el noreste de la Península Ibérica durante el Bronce Final y la Primera Edad del Hierro. Complutum 19, 139–171. https://doi.org/10.5209/CMPL.30433
López-Cachero, F.J., Mercadal, I., Fernàndez, O., 2014. Necròpolis d'incineració, tombes i pràctiques de dipòsit a finals de l'edat del bronze i principis de l'edat del ferro al nord-est peninsular, in: La Transició Bronze Final-1ª Edat Del Ferro En Els Pirineus i Territoris Veïns: XV Colloqui Internacional d'Arqueologia de Puigcerdà. Presented at the Congrés Nacional d'Arqueologia de Catalunya. November 17-19, 2011, Puigcerdà (Spain).
Lull, V., Micó, R., Herrada, C.R., Risch, R., 2013a. Bronze Age Iberia, in: Fokkens, H., Harding, A. (Eds.), The Oxford Handbook of the European Bronze Age. Oxford University Press, Oxford, United Kingdom.
Lull, V., Micó, R., Rihuete, C., Risch, R., 2013b. Political collapse and social change at the end of El Argar, in: Meller, H., Bertemes, F., Bork, H.R., Risch, R. (Eds.), 1600 – Kultureller Umbruch in Schatten Des Thera-Ausbruchs?, Der. 4. Mitteldeutschen Archäologietag, 14–16 Oktober 2011., Tagungen Des Landesmuseums Für

Vorgeschichte Halle. Landesamt für Denkmalpflege und Archäologie in Sachsen-Anhalt, Landesmuseum für Vorgeschichte, Halle (Saale), pp. 283–302.
Magny, M., 2015. Climatic variations in the Circum-Alpine area during the period 4500–2500 cal BP, as reflected by palaeohydrological changes, in: The End of the Lake-Dwellings in the Circum-Alpine Region. Oxbow Books, pp. 85–100.
Magny, M., 2013. Orbital, ice-sheet, and possible solar forcing of Holocene lake-level fluctuations in west-central Europe: A comment on Bleicher. The Holocene 23, 1202–1212. https://doi.org/10.1177/0959683613483627
Magny, M., 2004. Holocene climate variability as reflected by mid-European lake-level fluctuations and its probable impact on prehistoric human settlements. Quaternary International, The record of Human /Climate interaction in Lake Sediments 113, 65–79. https://doi.org/10.1016/S1040-6182(03)00080-6
Magny, M., Combourieu-Nebout, N., de Beaulieu, J.L., Bout-Roumazeilles, V., Colombaroli, D., Desprat, S., Francke, A., Joannin, S., Ortu, E., Peyron, O., Revel, M., Sadori, L., Siani, G., Sicre, M.A., Samartin, S., Simonneau, A., Tinner, W., Vannière, B., Wagner, B., Zanchetta, G., Anselmetti, F., Brugiapaglia, E., Chapron, E., Debret, M., Desmet, M., Didier, J., Essallami, L., Galop, D., Gilli, A., Haas, J.N., Kallel, N., Millet, L., Stock, A., Turon, J.L., Wirth, S., 2013. North–south palaeohydrological contrasts in the central Mediterranean during the Holocene: tentative synthesis and working hypotheses. Clim. Past 9, 2043–2071. https://doi.org/10.5194/cp-9-2043-2013
Matthias, I., Giesecke, T., 2014. Insights into pollen source area, transport and deposition from modern pollen accumulation rates in lake sediments. Quaternary Science Reviews 87, 12–23. https://doi.org/10.1016/j.quascirev.2013.12.015
Mauri, A., Davis, B.A.S., Collins, P.M., Kaplan, J.O., 2015. The climate of Europe during the Holocene: a gridded pollen-based reconstruction and its multi-proxy evaluation. Quaternary Science Reviews 112, 109–127. https://doi.org/10.1016/j.quascirev.2015.01.013
Menotti, F., 2015a. The lake-dwelling phenomenon: myth, reality and...archaeology, in: Menotti, F. (Ed.), The End of the Lake-Dwellings in the Circum-Alpine Region. Oxbow Books.
Menotti, F., 2015b. The 3500-year-long lake-dwelling tradition comes to an end: what is to blame?, in: Menotti, F. (Ed.), The End of the Lake-Dwellings in the Circum-Alpine Region. Oxbow Books.
Menotti, F., 2004. Living on the Lake in Prehistoric Europe: 150 Years of Lake-Dwelling Research. Routledge.
Menotti, F., 2001. "The missing period" : middle bronze age lake-dwellings in the Alps. Archaeopress, Oxford.
Mercuri, A.M., Accorsi, C.A., Mazzanti, M.B., Bosi, G., Cardarelli, A., Labate, D., Marchesini, M., Grandi, G.T., 2006. Economy and environment of Bronze Age settlements – Terramaras – on the Po Plain (Northern Italy): first results from the archaeobotanical research at the Terramara di Montale. Vegetation History and Archaeobotany 16, 43–60. https://doi.org/10.1007/s00334-006-0034-1
Mercuri, A.M., Mazzanti, M.B., Torri, P., Vigliotti, L., Bosi, G., Florenzano, A., Olmi, L., N'siala, I.M., 2012. A marine/terrestrial integration for mid-late Holocene

vegetation history and the development of the cultural landscape in the Po valley as a result of human impact and climate change. Vegetation History and Archaeobotany 21, 353–372. https://doi.org/10.1007/s00334-012-0352-4

Mercuri, A.M., Montecchi, M.C., Pellacani, G., Florenzano, A., Rattighieri, E., Cardarelli, A., 2015. Environment, human impact and the role of trees on the Po plain during the Middle and Recent Bronze Age: Pollen evidence from the local influence of the terramare of Baggiovara and Casinalbo. Review of Palaeobotany and Palynology 218, 231–249. https://doi.org/10.1016/j.revpalbo.2014.08.009

Miras, Y., Beauger, A., Lavrieux, M., Berthon, V., Serieyssol, K., Andrieu-Ponel, V., Ledger, P.M., 2015. Tracking long-term human impacts on landscape, vegetal biodiversity and water quality in the Lake Aydat catchment (Auvergne, France) using pollen, non-pollen palynomorphs and diatom assemblages. Palaeogeography, Palaeoclimatology, Palaeoecology 424, 76–90. https://doi.org/10.1016/j.palaeo.2015.02.016

Miras, Y., Laggoun-Défarge, F., Guenet, P., Richard, H., 2004. Multi-disciplinary approach to changes in agro-pastoral activities since the Sub-Boreal in the surroundings of the "narse d'Espinasse" (Puy de Dôme, French Massif Central). Veget Hist Archaeobot 13, 91–103. https://doi.org/10.1007/s00334-004-0033-z

Mordant, C., 2013. The Bronze Age in France, in: Fokkens, H., Harding, A. (Eds.), The Oxford Handbook of the European Bronze Age. Oxford University Press, Oxford, United Kingdom.

Nychka, D., Furrer, R., Paige, J., Sain, S., 2019. fields: Tools for Spatial Data, R-Package.

Overpeck, J.T., Webb, T., Prentice, I.C., 1985. Quantitative interpretation of fossil pollen spectra: Dissimilarity coefficients and the method of modern analogs. Quaternary Research 23, 87–108. https://doi.org/10.1016/0033-5894(85)90074-2

Palmisano, A., Bevan, A., Shennan, S., 2017. Comparing archaeological proxies for long-term population patterns: An example from central Italy. Journal of Archaeological Science 87, 59–72. https://doi.org/10.1016/j.jas.2017.10.001

Panik, M.J., 2014. Growth Curve Modeling: Theory and Applications. John Wiley & Sons.

Perego, R., Badino, F., Deaddis, M., Ravazzi, C., Vallè, F., Zanon, M., 2011. L'origine del paesaggio agricolo pastorale in nord Italia: espansione di Orlaya grandiflora (L.) Hoffm. nella civiltà palafitticola. Notizie Archeologiche Bergomensi 19, 161–173.

Peros, M.C., Munoz, S.E., Gajewski, K., Viau, A.E., 2010. Prehistoric demography of North America inferred from radiocarbon data. Journal of Archaeological Science 37, 656–664. https://doi.org/10.1016/j.jas.2009.10.029

Pétrequin, P., Magny, M., Bailly, M., 2005. Habitat lacustre, densité de population et climat. L'exemple du Jura français. Wes 4, 143–68.

Peyron, O., Guiot, J., Cheddadi, R., Tarasov, P., Reille, M., de Beaulieu, J.-L., Bottema, S., Andrieu, V., 1998. Climatic Reconstruction in Europe for 18,000 YR B.P. from Pollen Data. Quaternary Research 49, 183–196. https://doi.org/10.1006/qres.1997.1961

Primas, M., 1990. Die Bronzezeit im Spiegel ihrer Siedlungen. Die ersten Bauern 1. Pfahlbaufunde Europas, Band I, Schweiz. Zürich: Sweizerisches Landesmuseum Zürich.

R Core Team, 2015. R: A Language and Environment for Statistical Computing. R Foundation for Statistical Computing, Vienna, Austria.

Ravazzi, C., Marchetti, M., Zanon, M., Perego, R., Quirino, T., Deaddis, M., De Amicis, M., Margaritora, D., 2013. Lake evolution and landscape history in the lower Mincio River valley, unravelling drainage changes in the central Po Plain (N-Italy) since the Bronze Age. Quaternary International 288, 195–205. https://doi.org/10.1016/j.quaint.2011.11.031

Reimer, P.J., Bard, E., Bayliss, A., Beck, J.W., Blackwell, P.G., Bronk Ramsey, C., Buck, C.E., Cheng, H., Edwards, R.L., Friedrich, M., Grootes, P.M., Guilderson, T.P., Haflidason, H., Hajdas, I., Hatté, C., Heaton, T.J., Hoffmann, D.L., Hogg, A.G., Hughen, K.A., Kaiser, K.F., Kromer, B., Manning, S.W., Niu, M., Reimer, R.W., Richards, D.A., Scott, E.M., Southon, J.R., Staff, R.A., Turney, C.S.M., van der Plicht, J., 2013. IntCal13 and Marine13 radiocarbon age calibration curves 0-50,000 years cal BP 55, 1869–1887. https://doi.org/10.2458/azu_js_rc.55.16947

Revelles, J., Antolín, F., Berihuete, M., Burjachs, F., Buxó, R., Caruso, L., López, O., Palomo, A., Piqué, R., Terradas, X., 2014. Landscape transformation and economic practices among the first farming societies in Lake Banyoles (Girona, Spain). Environmental Archaeology 19, 298–310. https://doi.org/10.1179/1749631414Y.0000000033

Revelles, J., Cho, S., Iriarte, E., Burjachs, F., van Geel, B., Palomo, A., Piqué, R., Peña-Chocarro, L., Terradas, X., 2015. Mid-Holocene vegetation history and Neolithic land-use in the Lake Banyoles area (Girona, Spain). Palaeogeography, Palaeoclimatology, Palaeoecology 435, 70–85. https://doi.org/10.1016/j.palaeo.2015.06.002

Risch, R., Meller, H., 2015. Change and Continuity in Europe and the Mediterranean around 1600 bc. Proceedings of the Prehistoric Society 81, 239–264. https://doi.org/10.1017/ppr.2015.10

Roberts, N., Brayshaw, D., Kuzucuoglu, C., Perez, R., Sadori, L., 2011. The mid-Holocene climatic transition in the Mediterranean: Causes and consequences. The Holocene 21, 3–13. https://doi.org/10.1177/0959683610388058

Ruiz Zapatero, G., 2014a. The Urnfields, in: Almagro-Gorbea, M. (Ed.), Iberia. Protohistory of the Far West of Europe: From Neolithic to Roman Conquest. Burgos, pp. 195–215.

Ruiz Zapatero, G., 2014b. Bronce Final - Hierro: la naturaleza de los Campos de Urnas., in: Mercadal, I., Fernàndez, O. (Eds.), La Transició Bronze Final-1ª Edat Del Ferro En Els Pirineus i Territoris Veïns: XV Colloqui Internacional d'Arqueologia de Puigcerdà. Presented at the Congrés Nacional d'Arqueologia de Catalunya. November 17-19, 2011, Puigcerdà (Spain), pp. 635–658.

Shennan, S., 2013. Demographic Continuities and Discontinuities in Neolithic Europe: Evidence, Methods and Implications. J Archaeol Method Theory 20, 300–311. https://doi.org/10.1007/s10816-012-9154-3

Shennan, S., 2009. Pattern and Process in Cultural Evolution. University of California Press.

Shennan, S., Downey, S.S., Timpson, A., Edinborough, K., Colledge, S., Kerig, T., Manning, K., Thomas, M.G., 2013. Regional population collapse followed initial

agriculture booms in mid-Holocene Europe. Nature Communications 4. https://doi.org/10.1038/ncomms3486

Shennan, S., Edinborough, K., 2007. Prehistoric population history: from the Late Glacial to the Late Neolithic in Central and Northern Europe. Journal of Archaeological Science 34, 1339–1345. https://doi.org/10.1016/j.jas.2006.10.031

Stepniak, T.P., 1986. Quantitative aspects of Bronze Age metalwork in western Poland: long-distance exchange and social organization. British Archaeological Reports Ltd.

Stika, H.-P., Heiss, A.G., 2013. Plant cultivation in the Bronze Age, in: Fokkens, H., Harding, A. (Eds.), The Oxford Handbook of the European Bronze Age. Oxford University Press, Oxford, United Kingdom.

Stopp, B., 2015. Animal husbandry and hunting activities in the Late Bronze Age Circum-Alpine region, in: Menotti, F. (Ed.), The End of the Lake-Dwellings in the Circum-Alpine Region. Oxbow Books.

Surmely, F., Miras, Y., Guenet, P., Nicolas, V., Savignat, A., Vannière, B., Walter-Simonnet, A.-V., Servera, G., Tzortzis, S., 2009. Occupation and land-use history of a medium mountain from the Mid-Holocene: A multidisciplinary study performed in the South Cantal (French Massif Central). Comptes Rendus Palevol 8, 737–748. https://doi.org/10.1016/j.crpv.2009.07.002

Surovell, T.A., Brantingham, P.J., 2007. A note on the use of temporal frequency distributions in studies of prehistoric demography. Journal of Archaeological Science 34, 1868–1877. https://doi.org/10.1016/j.jas.2007.01.003

Surovell, T.A., Byrd Finley, J., Smith, G.M., Brantingham, P.J., Kelly, R., 2009. Correcting temporal frequency distributions for taphonomic bias. Journal of Archaeological Science 36, 1715–1724. https://doi.org/10.1016/j.jas.2009.03.029

Tallavaara, M., Pesonen, P., Oinonen, M., 2010. Prehistoric population history in eastern Fennoscandia. Journal of Archaeological Science 37, 251–260. https://doi.org/10.1016/j.jas.2009.09.035

Telford, R.J., Birks, H.J.B., 2009. Evaluation of transfer functions in spatially structured environments. Quaternary Science Reviews 28, 1309–1316. https://doi.org/10.1016/j.quascirev.2008.12.020

Terral, J.-F., Mengüal, X., 1999. Reconstruction of Holocene climate in southern France and eastern Spain using quantitative anatomy of olive wood and archaeological charcoal. Palaeogeography, Palaeoclimatology, Palaeoecology 153, 71–92. https://doi.org/10.1016/S0031-0182(99)00079-6

Timpson, A., Colledge, S., Crema, E., Edinborough, K., Kerig, T., Manning, K., Thomas, M.G., Shennan, S., 2014. Reconstructing regional population fluctuations in the European Neolithic using radiocarbon dates: a new case-study using an improved method. Journal of Archaeological Science 52, 549–557. https://doi.org/10.1016/j.jas.2014.08.011

Torfing, T., 2015. Neolithic population and summed probability distribution of 14C-dates. Journal of Archaeological Science 63, 193–198. https://doi.org/10.1016/j.jas.2015.06.004

Valsecchi, V., Tinner, W., Finsinger, W., Ammann, B., 2006. Human impact during the Bronze Age on the vegetation at Lago Lucone (northern Italy). Vegetation History and Archaeobotany 15, 99–113. https://doi.org/10.1007/s00334-005-0026-6

Vanzetti, A., 2013. 1600? The rise of the Terramare system (Northern Italy), in: Meller, H., Bertemes, F., Bork, H.-R., Rish, R. (Eds.), 1600 – Kultureller Umbruch in Schatten Des Thera-Ausbruchs?, Der. 4. Mitteldeutschen Archäologietag, 14–16 Oktober 2011, Tagungen Del Landesmuseums Für Vorgeschichte Halle. Landesamt für Denkmalpflege und Archäologie in Sachsen-Anhalt, Landesmuseum für Vorgeschichte, Halle (Saale), pp. 267–282.

Vital, J., 2001. Actualités de l'âge du Bronze dans le sud-est de la France. Chronologie, lieux, économie, mobiliers. Documents d'archéologie méridionale. 243–252.

Vital, J., 1999. Identification du Bronze moyen-récent en Provence et en Méditerranée nord-occidentale. Documents d'Archéologie méridionale 22, 7–115.

Vital, J., Convertini, F., Lemercier, O. (Eds.), 2012. Composantes culturelles et Premières productions céramiques du Bronze ancien dans le sud-est de la France. Résultats du Projet Collectif de Recherche 1999-2009. Oxford: BAR International Series.

Ward, G.K., Wilson, S.R., 1978. Procedures for comparing and combining radiocarbon age determinations: a critique. Archaeometry 20, 19–31.

Weckström, J., Seppä, H., Korhola, A., 2010. Climatic influence on peatland formation and lateral expansion in sub-arctic Fennoscandia: Peatland formation in sub-arctic Fennoscandia. Boreas 39, 761–769. https://doi.org/10.1111/j.1502-3885.2010.00168.x

Weninger, B., Clare, L., Jöris, O., Jung, R., Edinborough, K., 2015. Quantum theory of radiocarbon calibration. World Archaeology 47, 543–566. https://doi.org/10.1080/00438243.2015.1064022

Williams, A.N., 2012. The use of summed radiocarbon probability distributions in archaeology: a review of methods. Journal of Archaeological Science 39, 578–589. https://doi.org/10.1016/j.jas.2011.07.014

Zanon, M., Davis, B.A.S., Marquer, L., Brewer, S., Kaplan, J.O., 2018. European Forest Cover During the Past 12,000 Years: A Palynological Reconstruction Based on Modern Analogs and Remote Sensing. Front. Plant Sci. 9. https://doi.org/10.3389/fpls.2018.00253

Zhang, S., Xu, Q., Gaillard, M.-J., Cao, X., Li, J., Zhang, L., Li, Y., Tian, F., Zhou, L., Lin, F., Yang, X., 2016. Characteristic pollen source area and vertical pollen dispersal and deposition in a mixed coniferous and deciduous broad-leaved woodland in the Changbai mountains, northeast China. Vegetation History and Archaeobotany 25, 29–43. https://doi.org/10.1007/s00334-015-0532-0

Zimmermann, A., 2012. Cultural cycles in Central Europe during the Holocene. Quaternary International, Temporal and spatial corridors of Homo sapiens sapiens population dynamics during the Late Pleistocene and Early Holocene 274, 251–258. https://doi.org/10.1016/j.quaint.2012.05.014

Zimmermann, A., Hilpert, J., Wendt, K.P., 2009. Estimations of Population Density for Selected Periods Between the Neolithic and AD 1800. Human Biology 81, 357–380. https://doi.org/10.3378/027.081.0313

PART IV

LAND COVER MODELING: FROM QUALITATIVE POLLEN DATA TO QUANTITATIVE FOREST COVER PERCENTAGES

The pollen record of Bande di Cavriana, presented in Part II, shows how the establishment of a pile-dwelling settlement was accompanied by radical changes in pollen proportions and floristic composition. Similar changes were consistently detected within every single pollen sequence in the Lake Garda area, to the point that a combination of arboreal pollen decline and rise of specific anthropogenic taxa (e.g. *Orlaya grandiflora*) can be considered a reliable biostratigraphic marker for the local transition into the Bronze Age (Zanon et al., 2019). While pollen data depicts a rather dramatic change in vegetational assemblages, the non-linear relation between pollen percentages and actual plant spatial coverage hinders a precise understating of actual variations in land cover (e.g. Gaillard et al., 2010). A common landscape reconstruction algorithm, REVEALS, attempts to correct this complex relationship by modeling the dispersal and deposition of different pollen taxa, taking into account their different pollen productivity and dispersal capabilities (Sugita, 2007a). Yet, the pollen productivity of a given taxon is not constant across space (and time). It might in fact vary depending of multiple factors, including vegetation openness and climate patterns (Broström et al., 2008; Feeser and Dörfler, 2014). For this reason, optimal pollen productivity estimates (PPEs) are region-specific, and currently they have not been investigated across northern Italy. A new methodology that allows to extract PPEs directly from pollen diagrams is currently being tested (Theuerkauf and Couwenberg, 2018), yet it requires precise age-depth models that are not available in the study area.

Given the impossibility to apply REVEALS in a satisfactory manner, a different modeling approach, based on modern pollen analogues, was pursued. The core of this analogue-based method is identical to the modeling technique (i.e. MAT) used in both Zanon et al. (2019) and Capuzzo et al. (2018) to extract climatic information from pollen data. The main difference lies in the composition of the training data set, where modern climate parameters are replaced with land cover information (i.e. in this context, percentages of forest cover).

The capabilities of the MAT concerning climate reconstructions have been widely tested in previous publications (e.g. Davis et al., 2003; Marsicek et al., 2018; Mauri et

al., 2015), while its application to land-cover data was limited to specific vegetation assemblages and time slices across the Northern Hemisphere (Tarasov et al., 2007; Williams et al., 2011). Furthermore, the recent availability of greatly improved calibration datasets (Davis et al., 2013; Hansen et al., 2013) raised the need to re-evaluate entirely the performance of this method across a variety of landscapes.

These are the premises behind the production of the third research paper presented in this dissertation (Zanon et al., 2018), which is reported in its entirety below. As evident from its title ("European Forest Cover During the Past 12,000 Years: A Palynological Reconstruction Based on Modern Analogs and Remote Sensing"), the primary focus of this paper is the application of analogue-based reconstructions to vegetation assemblages occurring across all of Europe since the end of the Pleistocene. This wide spatial and chronological coverage reflects the intentional decision to extend the scope and reach of this modeling exercise in order to increase its relevance for the scientific community. In addition, expanding the study area to a continental scale allowed also to validate the new MAT results against the available REVEALS-based reconstructions, highlighting similarities and differences between the two methodologies and providing a much more solid performance test for the analogue-based model.

Due to its methodological scope and extensive coverage, the content of Zanon et al. (2018) does not specifically address the environmental impact of the pile-dwelling phenomenon. Nonetheless, the methodology developed in this paper was still applied separately to pollen sequences from the Lake Garda area. Data from Bande di Cavriana, Castellaro Lagusello, Lavagnone and Lucone were converted into quantitative forest cover values following Zanon et al. (2018) and presented in poster format at the 52nd meeting of the Italian Institute of Prehistory and Protohistory in 2017. This contribution, titled "Land cover changes across the Copper Age – Bronze Age transition in the Garda Lake region", was authored by M. Zanon, F. Badino, M. Dal Corso, G. Furlanetto and C. Ravazzi. These results are presented and discussed in Part V of this dissertation.

European Forest Cover During the Past 12,000 Years: A Palynological Reconstruction Based on Modern Analogs and Remote Sensing

Marco Zanon[a,b], Basil A. S. Davis[c], Laurent Marquer[d,e,f], Simon Brewer[g] and Jed O. Kaplan[h,i]

a. Institute of Pre- and Protohistoric Archaeology, Christian-Albrechts-Universität zu Kiel, Kiel, Germany
b. Graduate School "Human Development in Landscapes", Christian-Albrechts Universität zu Kiel, Kiel, Germany
c. Institute of Earth Surface Dynamics, University of Lausanne, Lausanne, Switzerland
d. Department of Physical Geography and Ecosystem Science, Lund University, Lund, Sweden
e. GEODE, UMR-CNRS 5602, Université de Toulouse-Jean Jaurès, Toulouse, France
f. Research Group for Terrestrial Palaeoclimates, Max Planck Institute for Chemistry, Mainz, Germany
g. Department of Geography, University of Utah, Salt Lake City, UT, United States
h. ARVE Research SARL, Pully, Switzerland
i. Department of Archaeology, Max Planck Institute for the Science of Human History, Jena, Germany

Original research article published in *Frontiers in Plant Science*, 9, 2018.
https://doi.org/10.3389/fpls.2018.00253

ABSTRACT

Characterization of land cover change in the past is fundamental to understand the evolution and present state of the Earth system, the amount of carbon and nutrient stocks in terrestrial ecosystems, and the role played by land-atmosphere interactions in influencing climate. The estimation of land cover changes using palynology is a mature field, as thousands of sites in Europe have been investigated over the last century. Nonetheless, a quantitative land cover reconstruction at a continental scale has been largely missing. Here, we present a series of maps detailing the evolution of European forest cover during last 12000 years. Our reconstructions are based on the Modern Analog Technique (MAT): a calibration dataset is built by coupling modern pollen samples with the corresponding satellite-based forest-cover data. Fossil reconstructions are then performed by assigning to every fossil sample the average forest cover of its closest modern analogs. The occurrence of fossil pollen

assemblages with no counterparts in modern vegetation represents a known limit of analog-based methods. To lessen the influence of no-analog situations, pollen taxa were converted into plant functional types prior to running the MAT algorithm. We then interpolate site-specific reconstructions for each timeslice using a four-dimensional gridding procedure to create continuous gridded maps at a continental scale. The performance of the MAT is compared against methodologically independent forest-cover reconstructions produced using the REVEALS method. MAT and REVEALS estimates are most of the time in good agreement at a trend level, yet MAT regularly underestimates the occurrence of densely forested situations, requiring the application of a bias correction procedure. The calibrated MAT-based maps draw a coherent picture of the establishment of forests in Europe in the Early Holocene with the greatest forest-cover fractions reconstructed between ~8500 and 6000 calibrated years BP. This forest maximum is followed by a general decline in all parts of the continent, likely as a result of anthropogenic deforestation. The continuous spatial and temporal nature of our reconstruction, its continental coverage, and gridded format make it suitable for climate, hydrological, and biogeochemical modeling, among other uses.

INTRODUCTION

Determining the spatial structure of land cover and its variation through time is essential in order to understand the interplay between biosphere, atmosphere, and human societies. Knowledge of past vegetation dynamics is of great interest to a range of disciplines dealing with landscape, climate, human development, and their reciprocal interactions. For example, information concerning past forest cover influences the archeological narrative (e.g., Kreuz, 2007) and plays a tangible role in defining modern management strategies (Bradshaw et al., 2015; Mitchell, 2005; Vera, 2000); vegetation cover data are a central component of Earth system models dealing with carbon storage and release (e.g., Kaplan et al., 2002) and for investigating the feedbacks between land cover and climate (Gaillard et al., 2010); similarly, the simulation of past human–plants interactions is needed for the understanding of human imprint on ecosystems from early history up to the present day (Kaplan et al., 2009; Pongratz et al., 2008).

Recent landscape history makes use of different mapping technologies, ranging from historical and cartographic sources (e.g., Hohensinner et al., 2013) to satellite imagery (Bossard et al., 2000; DeFries et al., 2000; Hansen et al., 2013). Beyond the reach of these mapping means, our ability to infer past land cover depends on the

interpretation of paleoenvironmental proxies. Past landscape information has been extracted from different archives, such as fossil pollen (e.g., Edwards et al., 2017), plant macrofossils (e.g., tree line studies; Nicolussi et al., 2005), mollusks (e.g., Preece et al., 1986), beetles (e.g., Whitehouse and Smith, 2004), biochemical tracers (e.g., McDuffee et al., 2004) and ancient DNA (Birks and Birks, 2016). Among the diverse sources available, each offering a different point of view on similar questions, the analysis of pollen grains remains unsurpassed in terms of spatial and temporal coverage. The simplest approach in palynology consists of using arboreal versus non-arboreal pollen percentages to estimate forest cover, and in using indicator species (e.g., Behre, 1981) to infer changes in land use. The growing availability of pollen archives at a continental scale has then made it possible to track species expansion/extinction based on isolines and threshold values (e.g., Brewer et al., 2016, 2002; Finsinger et al., 2006; Huntley and Birks, 1983; Ravazzi, 2002). These approaches can be qualified as purely qualitative, as the non-linear relationship between plant abundances and pollen percentages is acknowledged but not corrected for (Gaillard et al., 2008).

Semi-quantitative models have been developed by grouping individual taxa into plant functional types (PFTs) and biomes (Peyron et al., 1998; Prentice et al., 1996), thus providing a consistent methodology to distinguish major vegetation types. The biomisation approach is able to recognize boundaries between plant communities (Williams et al., 2000), although difficulties have emerged at ecotones such as the forest-steppe boundary due to a bias in the method toward arboreal taxa. This bias arose from the original objective of the method to replicate potential natural vegetation (Peyron et al., 1998; Tarasov et al., 1998), and therefore to minimize the role of non-arboreal taxa symptomatic of anthropogenically deforested landscapes. A further problem has been the categorical nature of the biome assignment, leading to difficulties in recognizing gradual ecotonal transitions and producing spatially continuous reconstructions. Often the results have been mapped as point estimates (e.g., Prentice et al., 2000). Continuous spatial fields have been attempted using different techniques, such as in Peng et al. (1995), Collins et al. (2012), and Fyfe et al. (2015). While biomes are distinguished into forest and non-forest types, Collins et al. (2012) also used forest and non-forest PFTs derived from the same biomisation formulae as a more continuous measure of forest cover.

A first attempt to achieve a real quantification was pioneered by Prentice and Parsons (1983), Prentice (1985), and Sugita (1994, 1993), gradually evolving into the Landscape Reconstruction Algorithm (LRA). The LRA models – these are

REVEALS for regional plant abundance and LOVE for local plant abundance (Sugita, 2007a, 2007b) – make use of a comprehensive set of parameters (region-specific pollen productivity estimates, fall speed of pollen, basin size) and assumptions (e.g., wind speed and direction, atmospheric conditions) to simulate pollen dispersal/deposition mechanisms and decrease biases deriving from the non-linear relationships between plant abundances and pollen data.

Pollen-based vegetation reconstructions produced with the LRA are currently available for most of Europe outside of the Mediterranean (e.g., Cui et al., 2014, 2013; Fyfe et al., 2013; Marquer et al., 2017, 2014; Mazier et al., 2015; Nielsen et al., 2012; Nielsen and Odgaard, 2010; Overballe-Petersen et al., 2013; Sugita et al., 2010; Trondman et al., 2015). A wider application of the method to the Mediterranean depends on the collection of reliable pollen productivity estimates for the region, which are not currently available. A different quantitative approach, not requiring pollen productivity estimates demanded by the LRA method, was developed and applied in North America by Williams (2002) and Williams and Jackson (2003). This approach uses instead the Modern Analog Technique (MAT), based on the basic assumption that pollen samples sharing a similar composition are the by-product of comparable vegetation assemblages. Therefore, given two pollen samples – a modern and a fossil one – composed by a similar mixture of taxa, the environmental parameters of the first (e.g., forest cover, climate variables) can be directly transferred to the latter. The relationship between pollen assemblages and forest cover in the Williams method is established using a calibration dataset of modern pollen samples where the forest cover around the pollen site is estimated using satellite remote sensing from the Advanced Very High-Resolution Radiometer (AVHRR). Past forest cover is then reconstructed by assigning to each fossil sample the average forest cover of its closest modern analogs from amongst the modern samples in the calibration dataset. This approach was applied to Northern Eurasia (Kleinen et al., 2011; Tarasov et al., 2007) and to the whole forest-tundra ecotone of the Northern Hemisphere (Williams et al., 2011). Its application in Europe has been so far limited to point reconstructions for a few selected time windows (Williams et al., 2011).

In the present study, we test the capabilities of the MAT for continuous forest-cover reconstructions at a continental scale and from the Pleistocene/Holocene transition to the present day. We follow the methods used by Tarasov et al. (2007) and Williams et al. (2011) but with improved modern calibration and fossil datasets and spatially continuous mapping. The size of modern and fossil pollen data sets have been increased by 80 and 50%, respectively, compared to the European data used by

Williams et al. (2011), while the quality of the metadata and chronological controls for the fossil data have also been greatly improved (Davis et al., 2013; Fyfe et al., 2009; Giesecke et al., 2013). The AVHRR-based forest-cover data (1 km resolution) used in all previous MAT applications has been upgraded with a 30-m resolution dataset (Hansen et al., 2013) based on LANDSAT.

Our results are presented here as both maps for the whole of Europe at 1000-year intervals, and as regional area-average time-series. The full set of 49 maps, each one covering an ~250-year interval, is available as Supplementary Material. Each map displays interpolated forest-cover data with continental coverage at a resolution of five arc-minutes. The predictive ability of our model was assessed though standard statistical indicators based on analysis of the modern training set [r^2 and Root Mean Square Error of Prediction (RMSEP) from cross-validation exercises]. In addition, down core evaluation was also undertaken through a comparison between the MAT and the REVEALS-based forest-cover reconstructions for specific sites, thus testing the performance of our method against methodologically independent forest-cover reconstructions.

MATERIALS AND METHODS

Fossil and modern pollen data

The fossil pollen dataset used in our analysis is the same as presented in Mauri et al. (2015) and based largely on the European Pollen Database (EPD) with some additional data coming from the PANGAEA data archive (www.pangaea.de) and Collins et al. (2012) (Supplementary Fig. S3.1, Appendix III). All age-depth models for all sites used calibrated ^{14}C chronologies, with those for EPD sites based on the latest available chronologies from Giesecke et al. (2013).

The European Modern Pollen Database (EMPD; Davis et al., 2013) was selected as the source for modern palynological data (Supplementary Fig. S3.2, Appendix III). The EMPD includes nearly 5000 samples covering Eurasia and the circum-Mediterranean, which were filtered based on quality-control criteria (see section "Quality Filtering").

Pollen spectra in both the modern and fossil datasets were converted into PFTs following the approach developed by Prentice et al., (1996) and refined by Peyron et al., (1998). Pollen taxa are grouped into PFTs following combinations of plant habit (e.g., woody, herbaceous), phenology (e.g., evergreen, deciduous), leaf form (e.g., broad-leaved, needle-leaved), and climatic range (Prentice, 1985). Differential pollen productivity and dispersal are not accounted for during PFT assignment. The main

steps within the taxa-to-PFTs algorithm are presented in Supplementary Tables S3.1–S3.3, Appendix III. The full procedure is described in Peyron et al., (1998). The capabilities of PFTs in pollen-based climatic and ecological reconstructions have been tested in European contexts through the Holocene (Collins et al., 2012; Davis et al., 2015; Mauri et al., 2015), and were found preferable to taxa approaches in MAT-based climate reconstructions (Davis et al., 2003).

Remote sensing data

Modern forest-cover values were extracted from the Global Forest Change dataset (Hansen et al., 2013), which includes estimates of forest-cover fraction for the year 2000. The forest-cover dataset produced by Hansen et al. (2013) was preferred over the AVHRR-based maps from DeFries et al. (2000) used in previous studies (Tarasov et al., 2007; Williams et al., 2011). While DeFries et al. (2000) offer a wider range of maps covering different vegetation categories, the dataset from Hansen et al. (2013) offers a much higher resolution and a wider range of values. DeFries et al. (2000) provide separate quantitative data on broadleaf, deciduous, evergreen, needle leaf, and total forest cover at a resolution of 1-km. Pixel values are continuous in the range 10–80% of forest cover (woody fraction), with specific codes to mark non-vegetated areas and areas with forest cover lower than 10%. In contrast, Hansen et al. (2013) offer a resolution of 1 arcsecond, equivalent to around 30-m at the equator, and a full range of pixel values from 0 to 100% canopy closure.

The average forest-cover values for the modern pollen data set were extracted by placing a search window around the location of each sample. We applied a general search radius of 50 km to approach a more consistent comparison between MAT and REVEALS estimates, because the REVEALS method suggests that its reconstructions are representative of a 50-km radius around the sites in question (see section "Comparison between MAT and REVEALS Estimates of Past forest cover"). A circular search window was preferred over a square one (used, e.g., in Williams et al., 2011), thus assuming a pollen source area with equal contributions from vegetation from all directions. The forest-cover value of every grid cell falling within the search radius was then distance-weighted using a two-dimensional Gaussian function centered on the pollen sample and subsequently averaged. A Gaussian curve was preferred primarily due to ease of implementation. Future model versions might include more "fat-tailed" distributions (e.g., Dawson et al., 2016). Given the predominance of moss polsters and soil samples in the EMPD, a value of $\sigma = 500$ m was used in order to assign a prevalent weight to the circular region immediately closer

to the sample site (Supplementary Fig. S3.3, Appendix III). A smaller σ value (100 m) was applied only to samples collected in densely forested areas (forest cover > 40% and EMPD sampling context described as "dense forest" or "forest undefined"). In these cases, the 100 m value was preferred over the 500 m one only when it yielded higher forest-cover values, suggesting the presence of denser forests right at the sampling location. A higher distance–weight parameter (σ = 10 km) was applied to samples collected from lakes in order to simulate a wider pollen source area. This σ-value is drawn from the optimal search window half-widths tested in previous studies (Tarasov et al., 2007; Williams et al., 2011; Williams and Jackson, 2003). Similarly to the procedure applied to moss and soil samples, a smaller σ-value (500 m) was applied to small water bodies (surface < 20 ha) surrounded by forested landscapes in order to emphasize the contribution of perilacustrine arboreal vegetation (Matthias and Giesecke, 2014). Since pixels occupied by water bodies were not included in the averaging procedure, weight is automatically added to the outer regions of the search window as both lake size and the number of pixels containing water around the core site increase. Bog sites therefore have the maximum weighting close to the core site. With lakes, the weight given to more distant pixels naturally increases as lake size increases and more pixels containing just water are excluded.

It should be stressed that pollen dispersal mechanisms vary largely from site to site depending on multiple factors (e.g., vegetation density, wind speed, pollen grains size and density, topography). Computational constraints, the wide diversity of the EMPD samples and, above all, the current availability of metadata prevent the calculation of sample-specific search windows and weight factors within this study. The application of narrow distance-weighting parameters (100 m and 500 m) was prompted by empirical and simulation studies on pollen deposition dynamics (e.g. Lavigne et al., 1996; Tinsley and Smith, 1974; Wright, 1952). Local foliage – as an example – might disrupt pollen dispersal, either by acting as a simple physical obstacle (Prentice, 1985) or via electrostatic capture (Bowker and Crenshaw, 2007), causing large amounts of pollen to reach the ground within few meters of the source. Sugita (1994) and Calcote (1995) estimate that between 20 and 60% of the pollen load in forest hollows comes from within a radius of < 100 m. Genetic analysis on plant communities appear to reach similar conclusions despite radically different methodological approaches. DNA paternity tests on *Pinus sylvestris* populations show that as much as ~50% of the pollen reaching female cones may come from individuals located within a 10 m radius, and that more than 90% of the pollen-carried genetic material may come from within a radius of ~200 m (Robledo-Arnuncio and Gil, 2005). When small *Quercus* sp. stands

are considered (ca. ≤6 ha, equivalent – for comparative purposes – to a circular region with r = ~140 m), between ~30 and >80% of successful pollinations were ascribed to pollen coming from within the stand (Gerber et al., 2014; Moracho et al., 2016; Streiff et al., 1999). Surface pollen samples might therefore primarily record a signal from local/extra-local pollen sources (e.g., few dozens to several hundred meters, *sensu* Jacobson and Bradshaw, 1981). In the context of our study, a σ-value = 500 m is meant to stress the importance of nearby pollen sources, while a 100-m value points to a dominant contribution from local dense arboreal cover. Arguably, the LRA could be used to estimate the pollen contribution from vegetation at any given distance from a sample. This effort would at the very least require pollen productivity estimates for all taxa and regions involved in the present study, which are currently not available. As a consequence, the use of only three σ values (100 m, 500 m, and 10 km) represents a necessary simplification.

Definition of forest cover

Study-specific definitions of forest cover should be kept in mind when interpreting and comparing the results from different quantitative approaches. REVEALS-based estimates of forest cover correspond to the overall regional tree abundance expressed in relative percentage cover. Age and size of trees are not assumed to be critical factors influencing the results, although they can have an influence on pollen productivity estimates and pollen dispersal and deposition (Baker et al., 2016; Jackson, 1994; Matthias et al., 2012). Analog-based approaches draw their definition of forest from their respective land cover data sets. Hansen et al. (2013) use a definition comparable to DeFries et al. (2000), describing forest-cover values per pixel as canopy closure percentages for all vegetation taller than 5 m. Significantly, DeFries et al. (2000) point out that a satellite-based mapping approach might identify shrubs as herbaceous vegetation if they are low to the ground, and as woody vegetation if they are taller. In an attempt to address this potential issue, we combined global vegetation height data (Simard et al., 2011) with the CORINE data set (Büttner et al., 2014) in order to detect areas occupied by forests but with a dominant tree height lower than 5 m. Modern samples with a median tree height = 0 m within the area covered by 1σ of the distance–weight function (i.e., the area surrounding the samples that contributes the most to tree cover quantification) were excluded from the analog pool. This filter was applied only to areas covered by the CORINE data set and only to lacustrine samples. The rationale behind the latter discrimination lies in our decision to prioritize the exclusion of easily discernible low-quality samples

while at the same time limiting the occurrence of false positives. In this specific case, the relatively coarse resolution of the tree-height data set (1 km), prompted us to apply a tree-height filter only to samples with σ = 10 km.

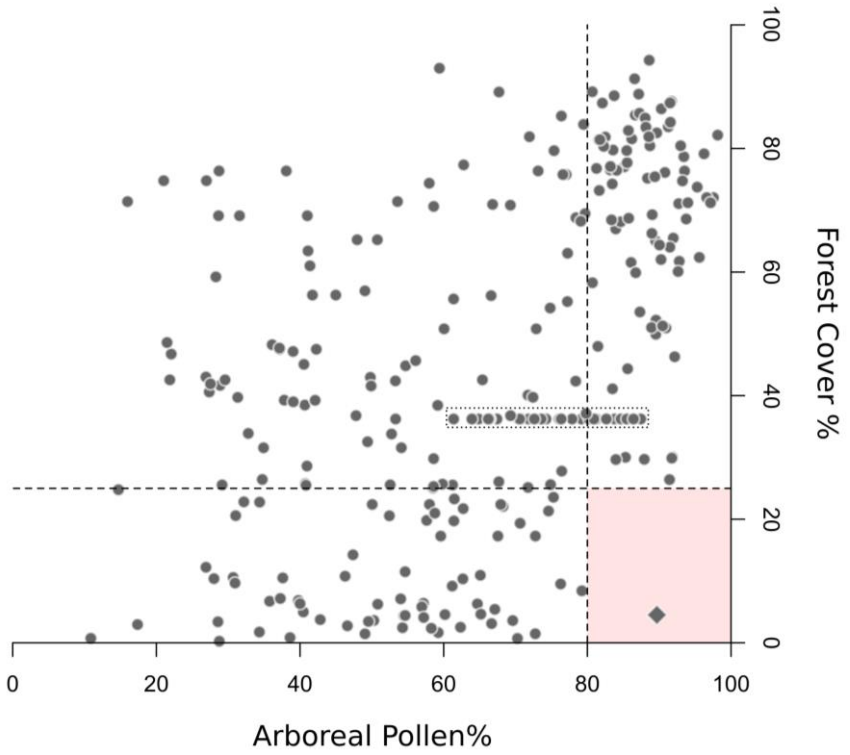

Figure 4.1. *Arboreal pollen vs. forest cover for selected EMPD samples ("high-reliability" samples: location error < 100 m and age < –50 BP). Samples collected from open or species-poor environments are not included (e.g., tundra, sparsely vegetated mountain areas). The dashed lines delineate the boundaries used to detect low quality samples (AP > 80% and forest cover < 25%, see section "Quality Filtering"). Diamond symbol: the only high-reliability sample exceeding both values, located in the Northern Urals (sample name: "Lapteva_a83," longitude 59.08828333, latitude: 59.52495). Despite being labeled as "forest undefined," the sample is located in a treeless area above the local timberline (confirmed by both forest cover and vegetation height data sets). Still, the Globcover 2009 data set identifies its location as "Open (15–40%) needleleaved deciduous or evergreen forest (>5 m)." Nearby pixels are defined as sparsely vegetated. This contradictory information might imply a chronological mismatch between forest cover and pollen data, or inaccurate sample description and Globcover classification (possibly due to ecotonal transitions in the area). In either case, this sample does not invalidate the boundary conditions set by this quality filter. The dotted box includes samples collected in different locations within the same small lake (EMPD names: Kolaczek_f1-32), but with identical geographical coordinates (hence the identical forest-cover values). This situation highlights the need for both accurate sample geolocation and sample-specific pollen source area estimates.*

Quality filtering

The available EMPD metadata were used extensively in conjunction with additional land cover data sets in order to identify pairing inaccuracies between pollen samples and the related vegetation data (e.g., due to location or chronology errors, see section "Sources of Uncertainty") through multiple lines of evidence. After duplicate removal, samples with estimated geolocation errors higher than 100 m were excluded from further elaborations. An additional reliability check was performed by comparing the elevation of each sample as recorded in the EMPD with the elevation for the same latitude and longitude extracted from a high-resolution Digital Elevation Model. Control elevation values were obtained from Mapzen's Elevation Service (mapzen.com), accessed through the R package "elevatr" (Hollister and Shah, 2017). Any difference greater than 200 m resulted in the exclusion of the sample. Samples from riverine or estuarine contexts were excluded too due to the likely presence of pollen floated over long distances. Samples were also filtered to remove those with low pollen counts, retaining only samples with a total sum of terrestrial taxa greater than 100 pollen grains. The Globcover 2009 data set (Arino et al., 2008) was used in addition to the already-mentioned tree height and forest-cover data sets. Samples collected in open landscapes (e.g., sampling context identified as "treeless vegetation," "pasture") but falling in forested Globcover classes and having simultaneously more than 15% forest cover (Globcover lower limit for open forests) and median tree height > 0 were excluded from the analog pool. Similarly, samples collected in forested environments (e.g., "open forest," "closed forest") but falling within open Globcover classes and having at the same time forest cover < 15% and median tree height = 0 were excluded from the training set too. The high-reliability samples (estimated geolocation error < 100 m and estimated age < -50 BP; Fig. 4.1) in the filtered EMPD were then used to find potential inaccuracies in surface samples with insufficient metadata. Any sample with arboreal pollen > 80% associated to forest-cover values < 25% was considered as potentially carrying low-quality information and excluded from the model. Beside geolocation and chronological inaccuracies, this filter addresses also samples collected under isolated trees, or in small thickets not detectable by the forest-cover data set. These threshold values are drawn from Fig. 4.1 and find support in the available literature. As an example, in open or semi-open contexts such as alpine meadows or arid shrublands, AP values are in the range of 40–50% (e.g., Court-Picon et al., 2006; Davies and Fall, 2001). Even above the tree line, in contexts affected by long-distance pollen transport, rare is the case where AP percentages reach values above 80% (e.g., Cañellas-Boltà et al., 2009). Nonetheless,

given the common occurrence of long-distance airborne AP in species-poor environments (e.g., Pardoe, 2014), samples collected in extensive treeless contexts (e.g., tundra, alpine grasslands, deserts) are not included in Fig. 4.1 and are not affected by this filter. A comparable filter was not applied to situations with low AP and high forest cover values due to difficulties in identifying equally distinctive boundaries. See the discussion for additional considerations on data selection.

The filtering process led to the removal of ~52% of the EMPD content, resulting in 2526 usable samples (Supplementary Fig. S3.2, Appendix III). Of these, 211 samples were distance-weighted using a σ-value = 100 m, 1894 samples using a σ-value = 500 m, and 421 samples using a σ-value = 10 km.

Past forest-cover reconstruction

Forest-cover reconstructions are based on the MAT (Guiot, 1990; Jackson and Williams, 2004; Overpeck et al., 1985). The basic assumption behind the MAT is that pollen samples sharing similar combinations of taxa originate from comparable plant assemblages. The vegetation parameters of a modern pollen sample can therefore be transferred to any fossil sample sharing a similar palynological composition. In order to define how different two samples are, the floristic assemblages of both the fossil and the training sample are reduced to a single coefficient of dissimilarity. Squared-chord distance was selected as the dissimilarity index of choice because of its ability to differentiate between vegetation types (Gavin et al., 2003; Overpeck et al., 1985). Analog computations were performed using the R package 'rioja' (Juggins, 2019). The optimal maximum number of analogs, k = 8, was determined via leave-one-out (LOO) cross-validation. Reconstructed forest-cover percentages were then recalculated as the weighted average of the forest-cover values of the best analogs whose chord distance did not exceed a threshold T. The value of T is not straightforward to define since it is data dependent (Davis et al., 2015). We opted for a value of T = 0.3, as it has proved sufficient to discriminate between major vegetation assemblages in Europe (Huntley, 1990).

The fossil dataset was divided into 49 timeslices ranging from 12000 to 0 calibrated years BP (years before AD 1950; hereafter BP). Each timeslice covers a 250-year window with the exception of the most recent one, which is asymmetric as it cannot project into the future, and therefore covers an interval of 185 years centered on 0 BP.

Mapping procedure

The reconstructed forest covers from each pollen record (i.e., point estimates) within each timeslice have been interpolated onto a uniform spatial and temporal grid using a four-dimensional (longitude, latitude, elevation, and time) Thin Plate Spline algorithm (TPS) fitted to a Digital Elevation Model (five arc-minutes resolution) using the R package 'fields' (Furrer et al., 2013). A three-dimensional TPS (latitude, longitude, elevation) was applied to the 0 BP timeslice in order to limit skewed results due to its unbalanced sample distribution around the 0 BP mark. This follows the same procedure used in mapping Holocene climate and vegetation used by Mauri et al. (2015), Collins et al. (2012) and Davis et al. (2003).

The maps of forest cover also include changes in European coastlines and ice sheets throughout the Holocene following Mauri et al. (2015). Small inland bodies of water are ignored in the reconstructed maps. Areas with low site/sample density over several time-windows have been excluded from our reconstruction, a process that was also used to define the borders of the study region. The results for some marginal areas (i.e., western North Africa and the eastern portion of the study area) are included but are not addressed in the paper, which focuses on the data-rich area of Europe north of the Mediterranean and west of 44°E.

To provide a comparison with traditional approaches based on the interpretation of arboreal pollen (AP) percentages, we also applied the same interpolation procedure to AP values (sum of woody taxa percentages, excluding dwarf shrubs and vines) for every fossil timeslice. The complete series of 49 forest-cover maps and 49 AP maps is included in the Supplementary Materials (Supplementary Fig. S3.4, S3.5, Appendix III). All maps were produced using GMT 4.5.15 (Wessel et al., 2013).

Forest-cover error estimates were calculated for each timeslice by interpolating the standard error of the analog-based reconstruction for every fossil sample. The standard error itself was calculated as the standard deviation of the n best analogs (after applying the chord threshold) divided by the square root of n. This first interpolated error estimate was then added to the standard error generated by the interpolation process itself (Furrer et al., 2013; Mauri et al., 2015). For computational reasons, error estimates are provided in gridded form at a resolution of 1° (Supplementary Fig. S3.6, Appendix III). Additional errors deriving from non-quantifiable uncertainties within data sources (see section "Sources of Uncertainty") or from methodological limits (e.g., use of PFTs, lack of distinction between species-specific pollen productivity/dispersal; see section "No-Analog Situations and the PFT

Approach") can't be quantified with the available data or technical knowledge. Therefore, these error sources are not accounted for in the calculation of error estimates.

In order to provide regional summaries of forest cover and AP changes, the study area was divided into eight regions (Fig. 4.2) and area-average estimates of forest cover were calculated for each region based on the gridded maps. The region borders are loosely based on the European biogeographic areas proposed by Rivas-Martínez et al. (2004). The area-average estimates of forest cover and AP percentages were then summarized in the form of time-series graphs covering the whole set of 49 time-slices.

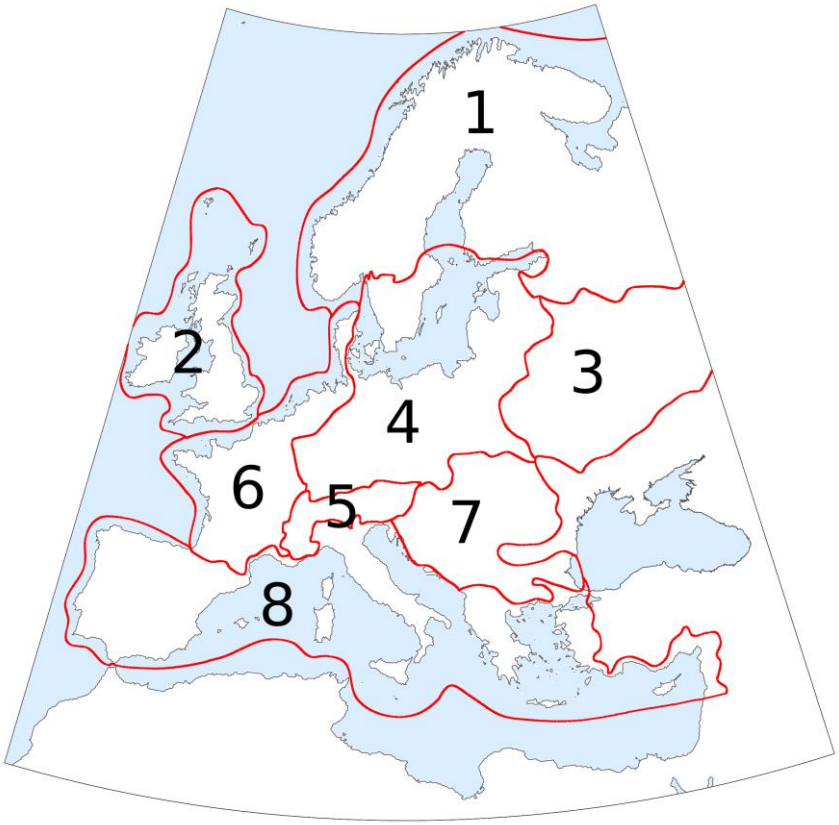

Figure 4.2. *Study area divided into 8 regions to provide regional summaries of forest-cover changes. Names used in the text: 1. Boreal region; 2. British Isles; 3. Eastern European plain; 4. Central Europe; 5. Alpine region; 6. Atlantic region; 7. Dinaro-Carpathian region; 8. Mediterranean region. Region borders are loosely based on the European biogeographic areas proposed by Rivas-Martínez et al. (2004).*

Evaluation of the reconstruction method

Performance of the transfer function and interpolation using modern data. The ability of MAT to reconstruct forest cover for the present time was first assessed using a two-fold cross-validation exercise. The modern pollen dataset was randomly split into two separate sets of equal size, subsequently using one as a training dataset to reconstruct the forest cover of the other and vice-versa. The whole process was repeated 999 times. The resulting r^2, RMSEP, plus a simple reading of the residuals, were used to assess the basic performance of the method. The RMSEP has the same unit as the environmental variable, and is therefore expressed as percentages of forest cover.

An h-block cross-validation test (Telford and Birks, 2009) was not performed. With the h-block test, all samples within a distance h of a test sample are omitted from analog selection. This test is generally applied to climate reconstructions, in order to exclude or mitigate the effects of spatial autocorrelation in the training set. The European land cover is much less uniform than the European climate, being instead characterized by high fragmentation and spatial diversity even over short distances (Kallimanis and Koutsias, 2013; Palmieri et al., 2011). Due to the high spatial variability of pollen spectra/parent vegetation pairings, the h-block test might not represent an optimal solution for land cover reconstructions.

Additionally, we tested the joint ability of MAT and interpolation algorithms to reproduce the modern forest-cover patterns visible in Hansen et al. (2013). For this purpose, modern forest-cover values were reconstructed under less restrictive conditions via simple LOO cross validation. LOO-derived modern forest-cover values were then interpolated using the procedure described in Section "Mapping Procedure." The same procedure was applied to AP percentages derived from the EMPD.

Reconstruction of Holocene forest cover in the Alps. The Alpine region provides an excellent context to test the performance of the 4-D interpolation due to its high topographic variability, the abundance of fossil pollen archives, and the numerous studies concerning local tree line and timberline dynamics. Therefore, as an additional test, we compared the MAT-based forest-cover values reconstructed at different elevations in the Alpine region with the data from Hansen et al. (2013) for the present and with independent macrofossil-based timberline/treeline reconstructions for the Holocene. To achieve this result, we grouped all the pixels

(grid cells) falling within the Alpine region (n. 5 in Fig. 4.2) into 200-vertical-meter elevation bands, except for those below 400 m which were grouped into a single band. This process was repeated for each of the 49 paleo-timeslices, as well as for the present day using both the LOO-based reconstruction and the map from Hansen et al. (2013).

As with the maps, areas with low site/sample density were excluded from the analysis. A lack of pollen sites at the very highest altitudes meant that for this test the analysis was limited to below 2800 m throughout the Holocene, with a slightly lower limit of 2400 m before 11000 BP and 2600 m from 10000 to 11000 BP when there were fewer sites above those altitudes.

A basic definition of "forest" in alpine contexts includes a minimum canopy cover above 40% (e.g., Burga and Perret, 2001) or 50–60% (Szerencsits, 2012). We adopt an intermediate threshold, following the upper altitudinal boundary of forest cover values >50% in our reconstruction. We interpret this minimum value as an indicator of widespread forested environments across the whole region, and use it as a simplistic threshold to track forest behavior in our reconstructions around the timberline ecotone (maximum vertical extent of alpine forests).

Comparison between MAT and REVEALS estimates of past forest cover. Forest-cover reconstructions based on MAT have been evaluated against methodologically independent REVEALS reconstructions for selected fossil pollen records (five large lakes, >50 ha surface) in central and northern Europe. The REVEALS model (Sugita, 2007a) provides pollen-based estimates of regional plant abundances for 25 taxa (trees, shrubs, and herbs) in percentage cover and associated standard errors. Note that REVEALS estimates inferred from large lakes give the most reliable reconstructions of regional plant abundance (Marquer et al., 2017; Trondman et al., 2015).

We used five REVEALS target sites published in Marquer et al. (2014) for the method-independent evaluation of the MAT-based forest-cover reconstructions. These five pollen records were selected because the data was publicly available from EPD, and because the sites are all located in central and northern Europe, where pollen-productivity estimates are available to run REVEALS for the major pollen taxa (Broström et al., 2008; Mazier et al., 2012). For further details about the pollen records, see Marquer et al. (2014).

Several tests have been done to decrease the 500-year time intervals of the reconstructions in Marquer et al. (2014) to the lowest reliable time intervals: 400-,

300-, 200-, and 100-year time intervals were used for reconstructions and the results show that 200-year time intervals provide a good compromise between the size and number of the time intervals available and good REVEALS standard errors. The REVEALS model was therefore run for 200-year time windows covering the last 11700 years: the number of time windows is dependent on the length of the record at each target site. The protocol for running REVEALS follows Marquer et al. (2017, 2014) and Trondman et al. (2015). For this test, the time resolution of the MAT estimates matches the REVEALS parameters.

The REVEALS estimates for the 25 taxa were grouped into open-land and forest categories, and the associated standard errors were calculated again. The REVEALS forest covers include covers of *Abies*, *Alnus*, *Betula*, *Carpinus*, *Corylus*, *Fagus*, *Fraxinus*, *Juniperus*, *Picea*, *Pinus*, *Quercus*, *Salix*, *Tilia*, and *Ulmus*, and represent the regional cover within 50 km around each target site.

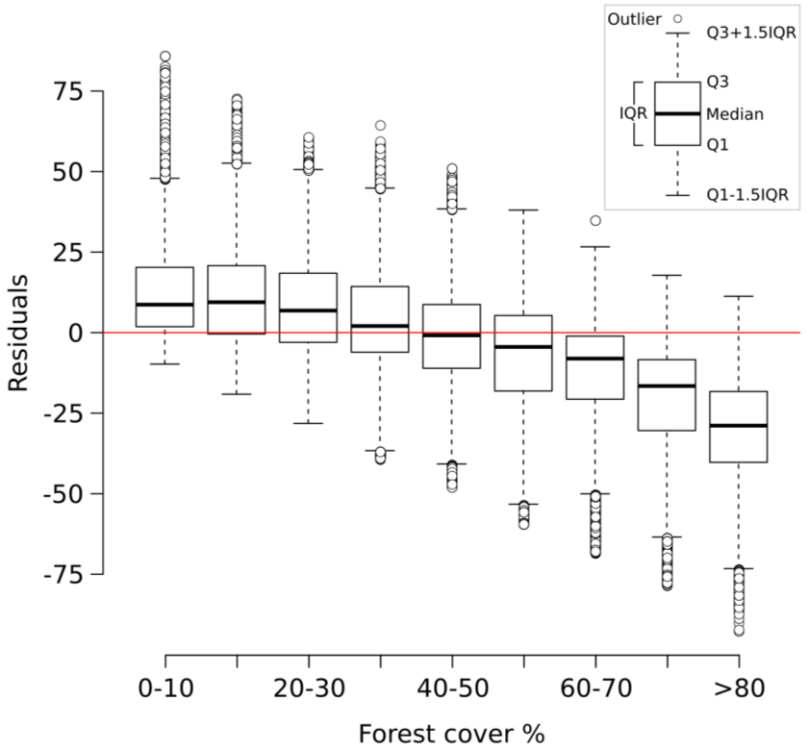

Figure 4.3. *Box-and-whisker plot showing the residuals of the two-fold cross validation exercise (999 iterations) grouped into discrete forest-cover classes. Residuals are expressed as reconstructed minus observed forest-cover values. Q1 = first quartile; Q3 = third quartile; IQR = interquartile range.*

RESULTS

Model validation

Performance of the cross-validation exercise. The two-fold cross-validation exercise shows that the MAT-based forest-cover model is able to account for close to 50% of the variance ($r^2 = 0.49$) and that the RMSEP (20.7%) is lower than the standard deviation of the data set (29%). These values reflect the wide array of uncertainties affecting the model (see sections "Sources of Uncertainty", "No-analog Situations and the PFT Approach", "forest-cover Underestimation"), yet they suggest that it can identify and reproduce a relationship between remote sensing data and pollen percentages. An analysis of the residuals of the two-fold cross-validation (Fig. 4.3) highlights negligible bias in the 0–70% forest-cover range, with the median error lying well in the range of ±10% points. A larger discrepancy between observations and the reconstruction is especially visible at sites with very high forest cover (>80%), where the median reconstructed values tend to be more than 25% points lower than the observed forest cover. These differences might depend on a combination of factors. For instance, high-forest-cover samples (>80%) are the least represented in the calibration dataset, likely making them more prone to be affected by poor analogs. The lowest residuals are concentrated in southern Europe (Supplementary Fig. S3.7, Appendix III) probably reflecting the limited representation in the modern dataset of large units of Mediterranean forest. These issues are revisited in the discussion section.

MAT–REVEALS comparison. The comparison between MAT and REVEALS estimates (Fig. 4.4) shows generally similar trends (overall correlation coefficient: $r = 0.75$; Fig. 4.5a). This level of agreement is notable, considering the quite different approaches of the two methodologies toward landscape reconstruction. Disagreements in absolute values constitute the main difference between the two models. The MAT assigns lower forest covers to early pioneering pine and birch woodlands (~12000–10000 BP); during this phase, most of the closest modern analogs are chosen within the tundra biome or in proximity of the forest-tundra ecotone (Supplementary Fig. S3.8, Appendix III). Differences between the models might then depend on a combination of factors, including potential forest-cover overestimation by REVEALS in Early Holocene contexts, and tree-height detection limits for MAT estimates. Major differences in terms of absolute values persist across all pairs after 10000 BP, with the full development of mixed deciduous woodlands.

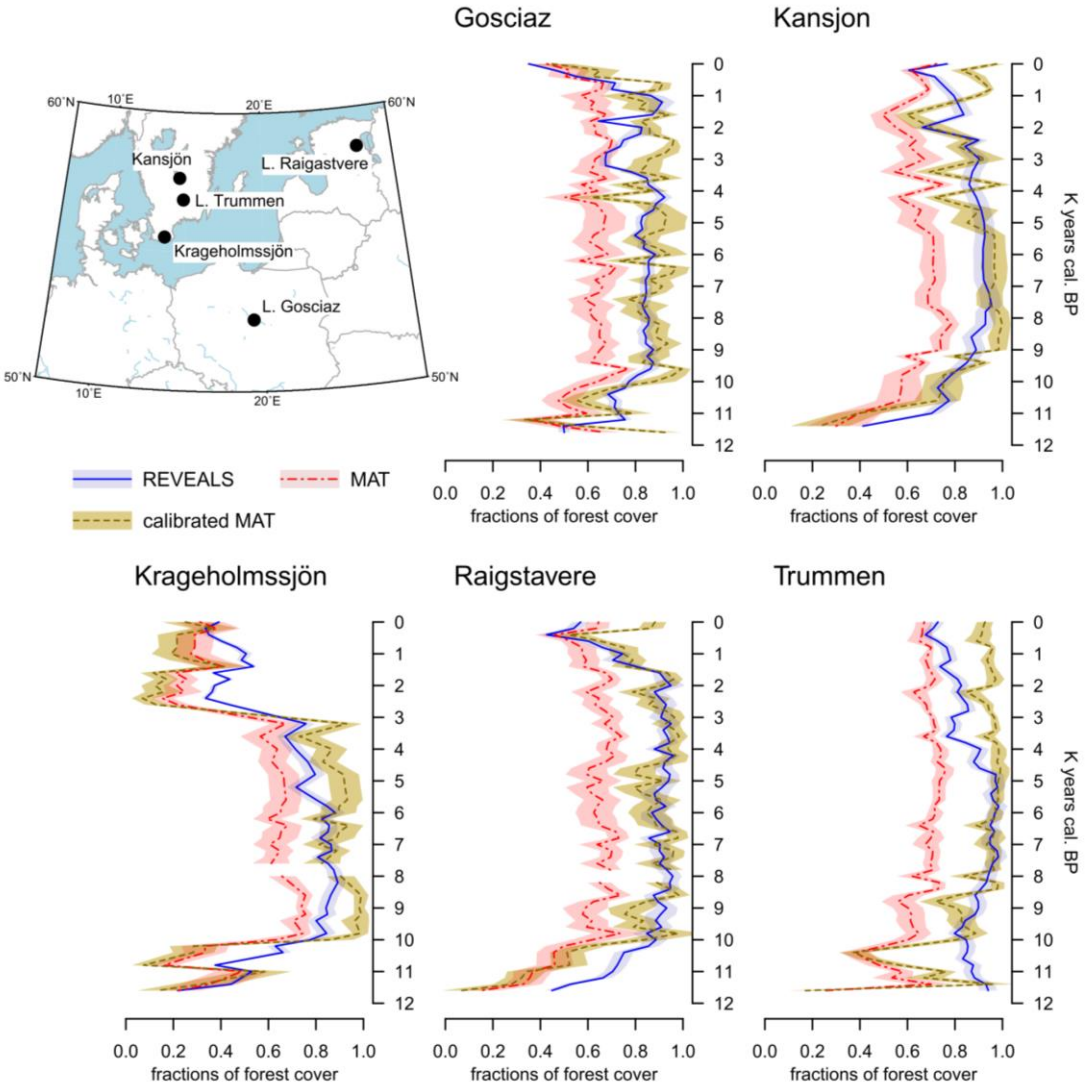

Figure 4.4. *Location of five target sites and reconstructed forest-cover values based on MAT (calibrated and uncalibrated) and REVEALS estimates. The shaded area represents the standard error of each reconstruction. Calibrated values are obtained via the bias correction procedure detailed in Section "Bias Correction".*

The REVEALS curves rise to values higher than 85–90% before acquiring an overall stable neutral trend. After a comparable initial positive trend, the MAT curves stabilize at around 60–70%. Differences of ~18–25 percentage points persist across the whole Mid-Holocene (Supplementary Table S3.4, Appendix III). This consistent behavior reinforces the results of the cross-validation exercise (Fig. 4.3), pointing to a limited performance of the MAT in densely forested contexts. As noted in section "Performance of the Cross-validation Exercises," the reasons behind this behavior might depend on a lack of suitable analogs in the training data set, in turn resulting from the low residual forest cover across present-day Europe. Different approaches

toward forest-cover quantification might play a notable role too, i.e., sum of all forest-forming taxa, regardless of their habitus (REVEALS) vs. tree-height detections limits of the underlying forest cover map (MAT). Undetectable trees lower than 5 m might then account for at least part of the difference between the MAT and REVEALS curves.

Consistently, the only two no-analog situations (gaps in the MAT curves of Krageholmssjön and Raigstavere) are recorded at around 8000 BP, testifying further to limits in the training data set concerning the reconstruction of early Mid-Holocene forests. The occurrence of no-analog situations in our reconstructions is addressed in section "Quantification of No-analog Occurrences."

The agreement between MAT and REVEALS curves improves in the Late Holocene, when forest-cover decline brings the REVEALS values below 80%. The average difference in absolute values between the two reconstructions is reduced to ~10–17 percentage points in the last 4000 years of the sequences (Supplementary Table S3.4, Appendix III).

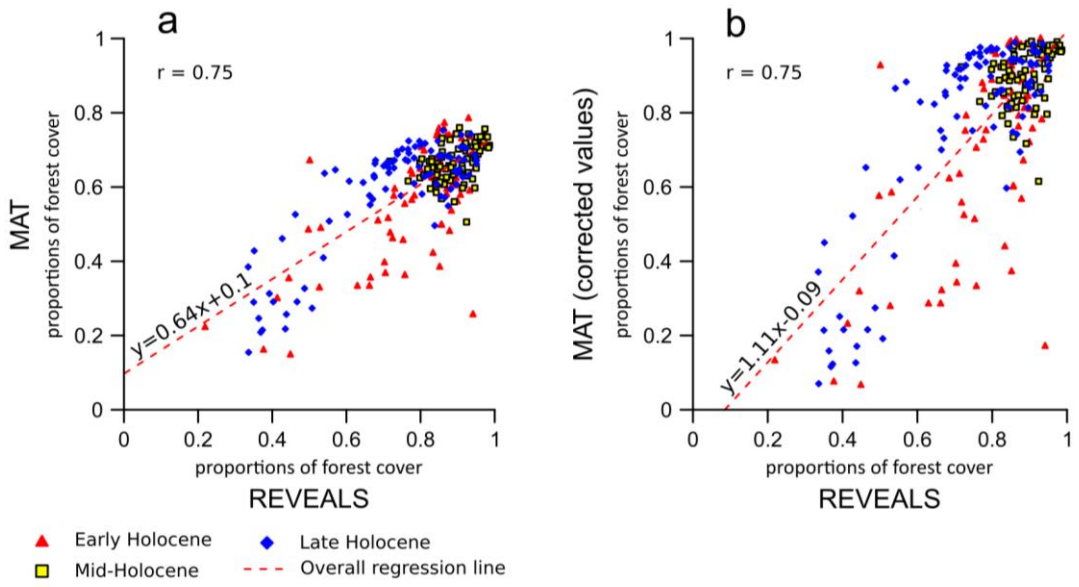

Figure 4.5. *MAT–REVEALS comparison. (a) REVEALS vs. uncalibrated MAT values. (b) Reveals vs. calibrated MAT values. Overall statistical correlation values referred to Figure 4.4. Study time-window subdivision: Early Holocene: 11700–8100 BP. Mid-Holocene: 8100–4100 BP. Late Holocene: 4100–0 BP.*

Quantification of no-analog occurrences. The MAT–REVEALS comparison shows few gaps in the MAT-based curves (sites of Krageholmssjön and Raigstavere, Fig. 4.4), highlighting the occurrence of missing analogs and prompting

us to explore the extent of this issue. For an appropriate comparison, we ran the MAT algorithm for the whole fossil and modern data sets using selected pollen taxa (i.e., without any transformation into PFT scores) and PFT scores (as described in section "Fossil and Modern Pollen Data") separately. The full list of taxa used in this simulation is presented in Supplementary Table S3.5, Appendix III. The occurrence of no-analog samples for every timeslice is presented in Fig. 4.6. Consistently with the parameters of our model, a no-analog situation is detected when the closest analog to a fossil sample has a squared chord distance higher than 0.3 (Huntley, 1990).

The taxa-based approach results in large portions of the fossil data sets presenting no-analog situations (Fig. 4.6a). The period between ~9000 and 6000 BP shows the highest values, with over 30% of the samples in each timeslice having no close analogs in the training set. The effect of the PFT approach is visible in Fig. 4.6b: the highest no-analog percentages are still concentrated between ~9000 and 6000 BP, but with values rarely exceeding 2%. A more detailed region-by-region subdivision is presented in Supplementary Fig. S3.9, Appendix III.

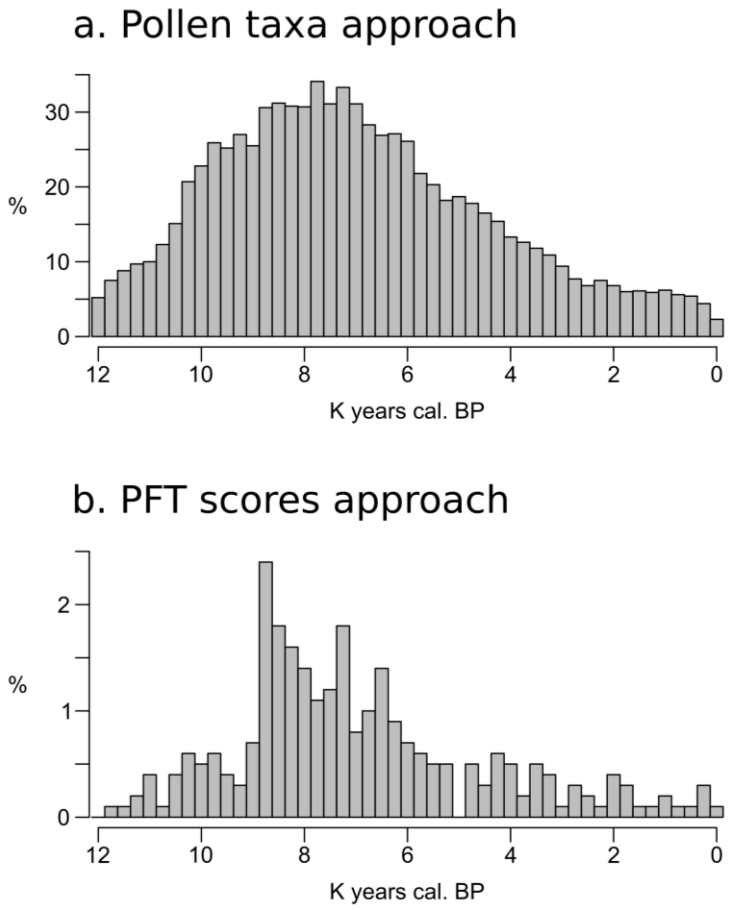

Figure 4.6. *(a,b) Percentage of fossil samples with no close analogs in the training data set calculated for each time slice.*

Bias correction. The results of the two-fold cross-validation exercise highlight a mild overestimation of forest cover at values $\lesssim$ 30% and, above all, a growing bias for values $\gtrsim$ 50%. This systematic underrepresentation of high forest-cover values is clearly visible in the MAT–REVEALS downcore comparison, possibly suggesting a comparable bias spread across all Holocene reconstructions. Considering the seemingly systematic occurrence of this modeling error, we employ an empirical distribution correction approach (Lafon et al., 2013) to rectify the forest-cover reconstructions in our model.

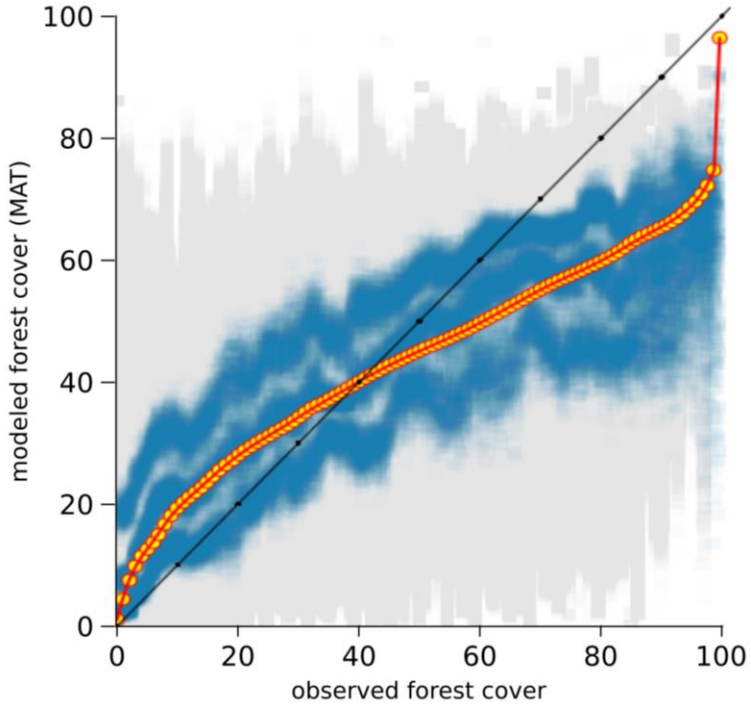

Figure 4.7. *Calibration curve used to correct the modeled forest-cover values. Gray squares: modeled vs. observed forest-cover values from the two-fold ross-validation exercise. Blue squares: resampled first, second, and third quartiles. Yellow circles: modeled vs. fitted empirical quantiles. Red line: regression curve used for calibration of the modeled values.*

The results of the two-fold cross-validation exercise (999 iterations) were resampled using randomly distributed 5%-wide windows (10 randomly placed windows for every iteration) in order to address the predominance of low forest-cover samples in the training set. The first, second, and third quartile were extracted within each window. Robust empirical quantiles for modeled vs. observed forest cover were estimated via Quantile Mapping (R package 'qmap,' Gudmundsson, 2016), based on every second

percentile between 1 and 100. A smooth spline regression curve was fitted to the resulting quantile–quantile plot (Fig. 4.7) and used as a calibration curve for the modeled forest-cover values. The resampling strategy and regression parameters were tested via trial-and-error, opting for a solution that minimizes the bias for high forest-cover classes. The application of the bias correction curve to the two-fold cross-validation iterations is visible in Fig. 4.8, where it shows a largely corrected median bias across all forest-cover classes. The correction of MAT values in the MAT–REVEALS comparison (Fig. 4.4) shows how the calibration curve succeeds in closing the gaps between the two models during the Mid-Holocene (Supplementary Table S3.4, Appendix III), while at the same time preserving the relative trend between timeslices.

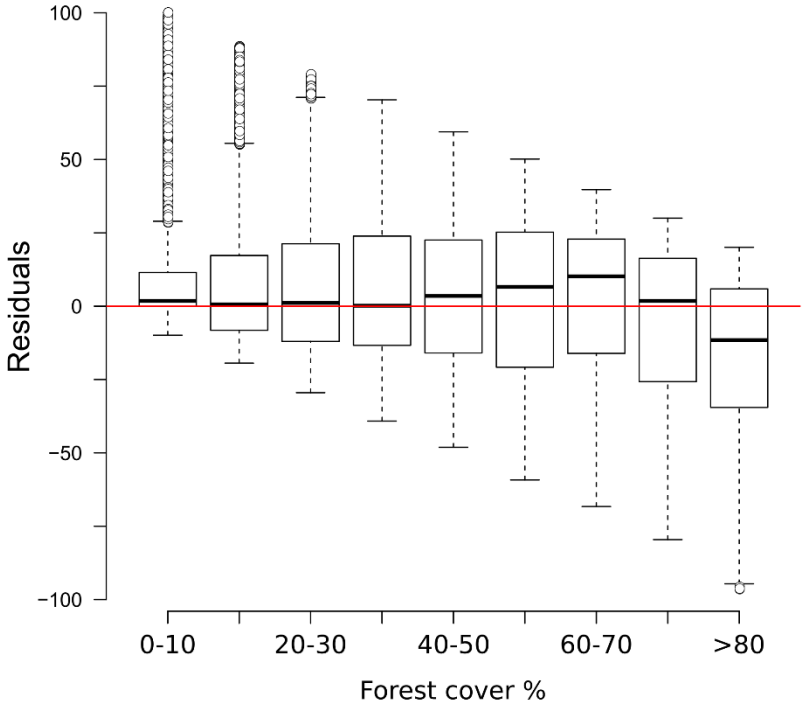

Figure 4.8. *Box-and-whisker plot showing the residuals of the two-fold cross validation exercise (Figure 4.3) after the application of the calibration curve.*

It should still be noted that the bias-correction procedure is applied mechanically to all samples regardless of their age, composition or location. As a consequence, this simple calibration approach might result in an over- or under-correction of forest-cover values. Any decrease in agreement between MAT and REVEALS might be ascribed to these effects. Examples include the exacerbation of low forest-cover values in the Late Holocene section of Krageholmssjön, or marked shifts from 60–70% (uncalibrated) to >90% (calibrated) forest-cover values within the most recent timeslices of Kansjon and Raigstavere. Similarly, the monotonic behavior that characterizes most of the MAT-based Trummen curve results in a growing discrepancy between MAT and REVEALS from ~5000 BP onward. These differences are nonetheless counterbalanced by a general and notable improvement in the correlation between MAT and REVEALS (overall regression line with slope = 1.11 and intercept = -0.09; Fig. 4.5b). The forest-cover reconstructions presented in the following sections are based on the application of this bias correction procedure.

Evaluation of the interpolation procedure. A visual comparison between actual modern cover from Hansen et al. (2013) (Fig. 4.9a) and the MAT-based, interpolated modern forest-cover map (obtained via LOO method, Fig. 4.9b) is used to evaluate the ability of the interpolation procedure to reproduce the main patterns in forest cover at the European scale. Higher forest densities are correctly reconstructed in mountain areas, notably at mid-low elevations in the Alps and along the Apennines, in the Balkan Peninsula and in the Carpathians, and partly in northern Iberia. In northern Europe, extensive forested areas are reconstructed around the Gulf of Bothnia and in western Russia. By comparison, the interpolated AP map displays similar distributions in central and southeastern Europe, but differs substantially in the remaining areas. Particularly visible is the pattern in northern Europe, where high AP values are present well beyond the northernmost limit of densely forested areas and show a generally limited spatial variability. A region-by-region comparison is presented in Fig. 4.10, together with the full extent of the fossil-database reconstructions. The synthesis in Fig. 4.10 highlights how a combination of MAT and interpolation succeeds in producing forest-cover values that are within the range derived from Hansen et al. (2013), while AP values regularly exceed it. Non-overlapping values are produced only for the British Isles, presumably due to the relatively poor spatial distribution of modern samples available for this specific region (Supplementary Fig. S3.2, Appendix III).

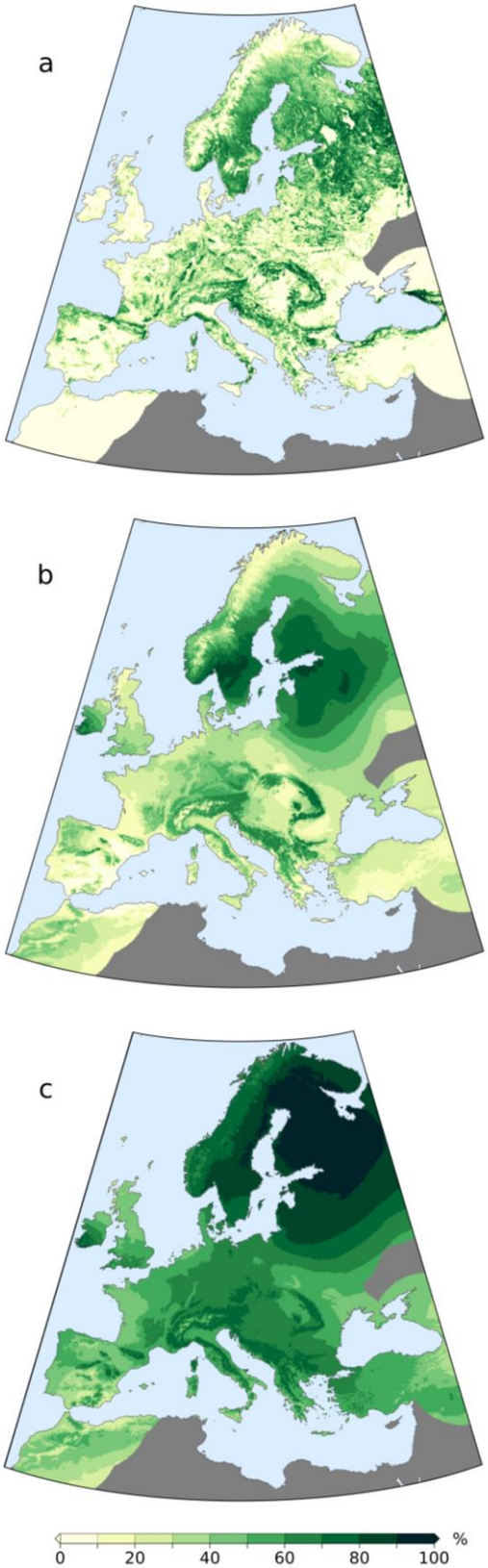

Figure 4.9. *a) Map of the study area with present day forest cover from Hansen et al., 2013; (b) Present-day forest cover reconstructed via MAT (LOO cross validation, calibrated) and 3D interpolation; (c) Interpolated present day arboreal pollen (AP) percentages from the EMPD and 3D interpolation. Dark gray areas are excluded from the analysis due to low site density.*

Forest-Cover elevation in the Alpine environment. A summary of the average MAT-derived forest cover in the Alps at different altitudes during the Holocene is presented in Fig. 4.11. The overall lowest forest-cover values are reconstructed at the end of the Younger Dryas period, before 11700 BP, when values > 50% are not recorded in the regional synthesis. A sharp increase in forest-cover percentages is immediately visible after 11500 BP, rapidly leading to the maximum altitudinal development of dense Alpine forests in our reconstruction (~10000–7000 BP). A gradual negative trend is then recorded between ~7000 and 2250 BP, lowering the 50% threshold from ~2600 m to ~1800 m. Eventually, after ~500 BP, values below 800 m decrease noticeably too, bringing the overall forest-cover situation close to the modern one across all elevation bands. In Fig. 4.11, the 50% boundary in both the 0 BP timeslice and LOO-based modern timeslice is located at 1800 m. By comparison, the satellite-based modern forest cover is placed 400 m lower, at 1400 m. It should be noted that the satellite-based 1400–1600-m elevation class has a forest cover value only slightly lower than the threshold value (48.9%), causing a seemingly abrupt difference in elevation between the satellite-based and MAT-based forest covers. Comparing the 0 BP timeslice with the satellite-based and the LOO-based forest covers returns a correlation coefficient r = 0.98 in both cases. Similarly, comparing the satellite-based and LOO data results in r = 0.97.

Forest-cover reconstructions

Late Pleistocene and Holocene onset (Figs. 4.10, 4.12a-b). During the last stage of the Pleistocene, the average forest-cover ranges from ~6% (British Isles) to ~48% (Central Europe), with an overall study area average of ~25%. The highest percentages are reconstructed along a diagonal belt spanning from the circum-alpine area to central-eastern Europe (Fig. 4.12a). The beginning of the Holocene is marked by a general increase in forest cover, with particularly steep trajectories in the British Isles, in the Atlantic region and, resulting in an isolated peak, in Eastern Europe.

First half of the Holocene (Figs. 4.10, 4.12c–g). Maximum forest development is reached between ~8500 and 6000 BP, with intensity and timing varying from area to area. Only the Atlantic region displays an early and isolated maximum around 10500 BP. Wide standard deviations are visible across most regions within the same time slice. Positive forest-cover trends last until 6250 BP in the Eastern European plain.

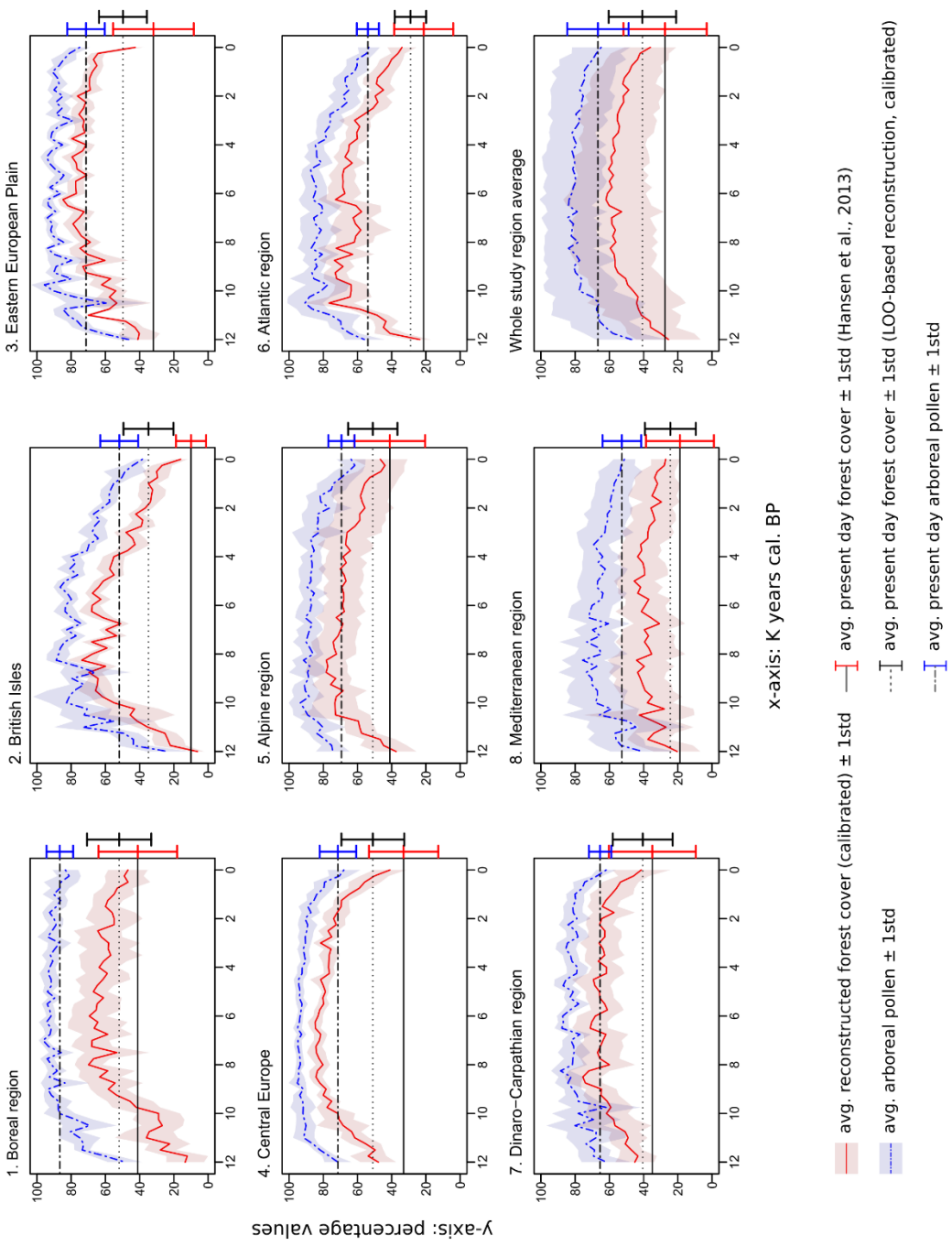

Figure 4.10. *Time series for the whole study area and the eight regions (time vs. percentages of reconstructed forest cover and percentage of arboreal pollen). Areas covered by water or ice are not included in the calculation of average forest-cover/AP values and their relative standard deviation. The deviation from the mean does not represent the error of the reconstruction but is simply a measure of inter-regional variability. The horizontal lines provide a comparison with present-day values for each region, i.e., modern forest cover from Hansen et al. (2013) (Figure 4.9a), interpolated LOO-based modern forest cover (Figure 4.9b) and interpolated percentage of arboreal pollen (Figure 4.9c).*

The highest average values are recorded in Central Europe, with percentages often above 80%. The least forested region is the Mediterranean, where forest cover rarely exceeds 40%. A phase of decline and stagnation lasting from ~8250 to 6500 BP is visible in the British Isles, in the Atlantic and Dinaro-Carpathian regions, and in the Mediterranean. With the end of this phase, forest cover values recover and return approximately to pre-decline levels. A similar decline begins in the Alps after 8250 BP, but is not followed by forest recovery.

Second half of the Holocene (Figs. 4.10, 4.12h–l). The negative trend observed in the Alps since 8250 BP continues during the second half of the Holocene. A comparable stable decline is visible across most regions generally from 6000 BP. The contraction of forested areas varies across Europe in terms of intensity and timing, but invariably leads from Early/Mid-Holocene maxima to present-day values without any interposed major recovery phase. Only the Dinaro-Carpathian region shows a predominant neutral trend until ~1500 BP, then followed by a rather steep decline to present-day values. A notable increase in steepness occurs in Central Europe after 1500 BP too, while in the British Isles, in the Easter European Plain and in the Alps occurs after ~750 BP.

DISCUSSION

We reconstruct for the first time spatially continuous fields of forest cover over the entire European continent for the last 12000 years based on quantitative criteria. The large spatial and long temporal scale of the study and the hundreds of individual sites on which it is based preclude a detailed analysis of individual local areas, so we restrict our discussion here to the main strengths and weaknesses of the model. It should be remembered that the reconstruction is based on aggregate results from several sites, and it is to be expected that individual site reconstructions may show different trends when viewed in isolation.

Sources of uncertainty

Williams and Jackson (2003), Jackson and Williams (2004), and Mauri et al. (2015) present an extensive summary of potential error sources affecting models based on pollen and modern analogs. These include the quantity and quality of the fossil and modern pollen data, chronological uncertainties, and the completeness and accuracy of attendant metadata.

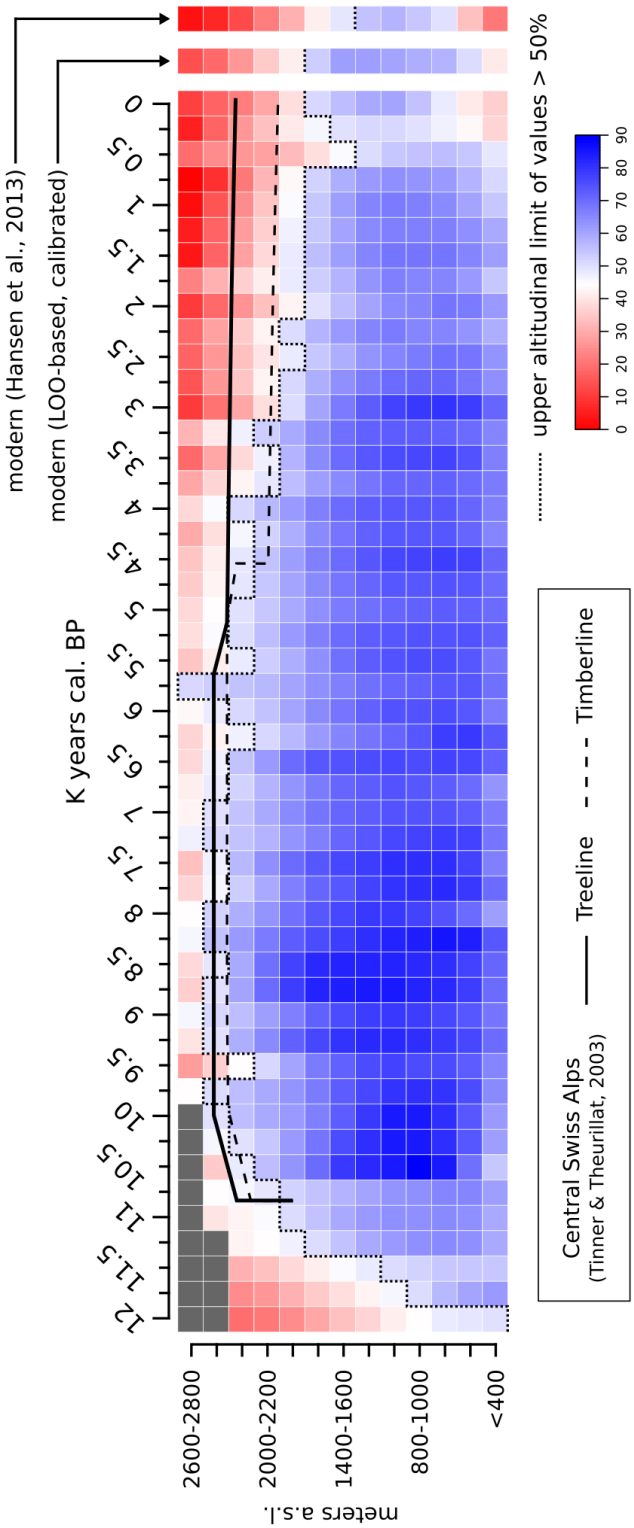

Figure 4.11. *MAT-based forest cover values (calibrated) for the end of the Younger Dryas and the Holocene in the Alpine region grouped in discrete elevation classes. forest-cover data from Hansen et al. (2013) and LOO-based from the same region (derived from Figure 4.9) are added as a modern reference. Gray colored pixels and pixels above 2800 m are masked due to lack of local pollen archives. Holocene macrofossil-based treeline and timberline curves from the central Swiss Alps are juxtaposed for comparison (digitized from Tinner and Theurillat, 2003).*

Whilst it is possible to apply rigorous quality control criteria, there is a direct trade-off in terms of the number of samples, and consequently the spatial, temporal, and ecological coverage. This can be particularly important for instance for the size of the modern pollen training set, and therefore the number of analogs that are available to the MAT. For instance, a sample count of 400–600 pollen grains belonging to terrestrial species is generally considered a safe minimum threshold to minimize statistical fluctuations of taxa percentages within a sample (Birks and Birks, 1980), with lower pollen counts being occasionally imposed by the sample nature itself (e.g., bad preservation, low volume). Applying a minimum pollen count (terrestrial taxa only) of 600 grains would lead to a >60% sample loss in both the training and the fossil databases, affecting the spatial coverage and the general variability of both data sets. In our reconstruction we used a smaller sub-set of taxa selected from the total terrestrial count, and therefore we chose a smaller threshold of 100 terrestrial pollen grains as the minimum count.

The size of the count influences the taxonomic diversity of the sample, as does the skill of the analyst. Furthermore, additional vegetation parameters, such as habitus-related aspects are not always inferable from pollen data. Even when two species exhibit clearly different growth habits, their pollen grains might prove difficult to differentiate, as exemplified is exemplified by the *Betula* genus. Dwarf birch (*Betula nana*), an arctic/cool temperate low shrub, is not distinguishable from arboreal birches through grain size alone, requiring instead to calculate the ratio of equatorial diameter to pore height (Birks, 1968). It is not possible to ascertain to which extent this distinction constitutes a common practice among analysts (e.g., it is admittedly avoided in Solovieva et al., 2015). This specific issue is at least partly mitigated by the PFT approach: *B. nana* pollen grains are assigned to the arctic-alpine PFT, while undifferentiated *Betula* pollen may be categorized as either boreal summer-green or arctic-alpine depending on the remaining floristic assemblage of a given sample (Peyron et al., 1998 and Supplementary Tables S3.1–S3.3, Appendix III). Woody vegetation growth habit and size might be variously affected by environmental properties too, such as water availability and soil composition. These variables are not accounted for in the analog selection process, and can lead to associate fossil pollen spectra to incorrect modern vegetation parameters.

An additional source of uncertainty stems from the definition of forest in the Hansen et al. (2013) forest-cover dataset, which specifies that "forest" has a minimum height of 5 m. However, the LANDSAT sensors used to create the dataset do not detect tree height.

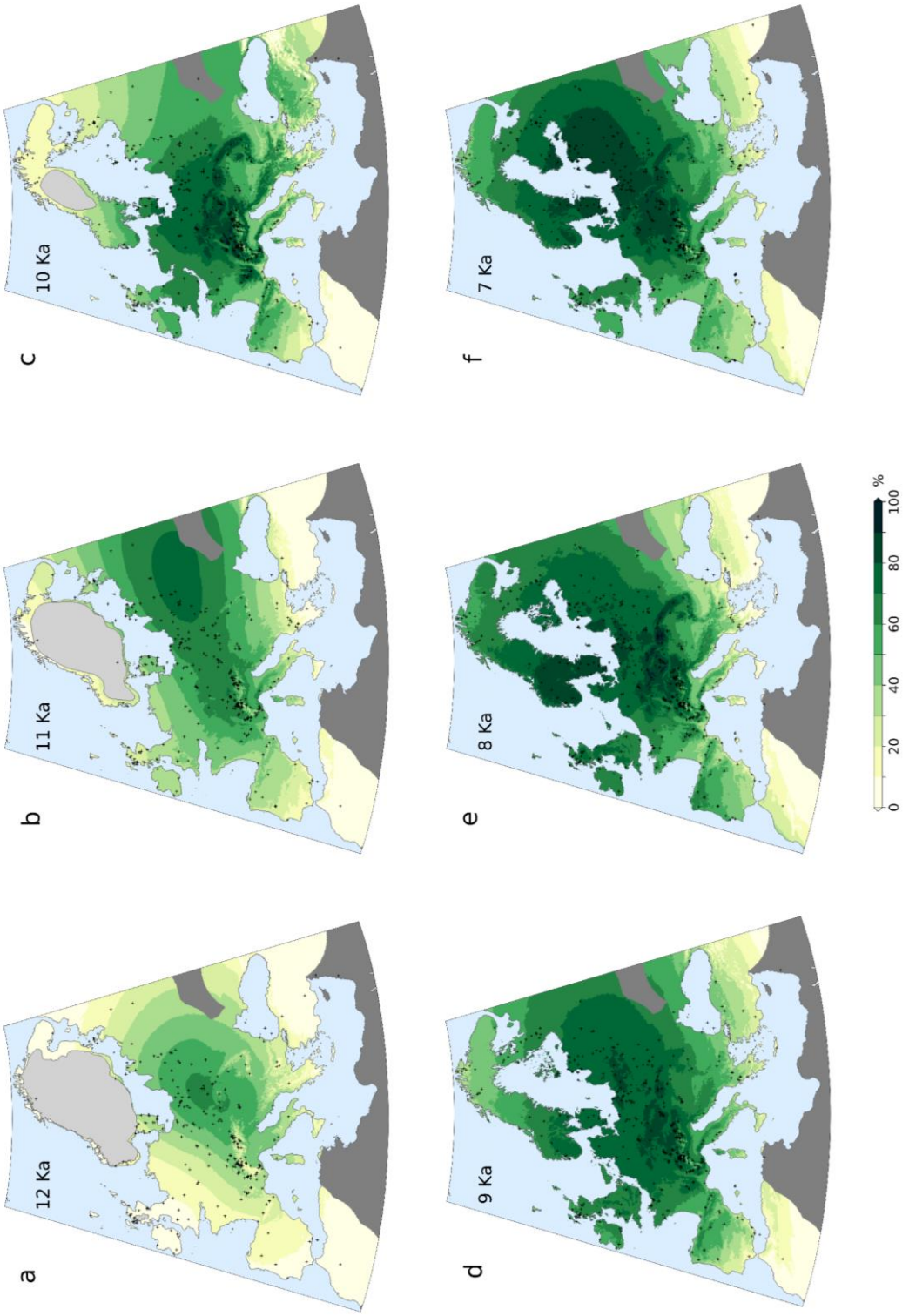

Figure 4.12. *MAT-based forest-cover values (calibrated) for selected time slices during the past 12000 years (a–l). Gray crosses represent pollen sites locations. Light gray areas over northern Europe and Scotland represent Early Holocene ice cover. Dark gray areas are excluded from the analysis due to low site density.*

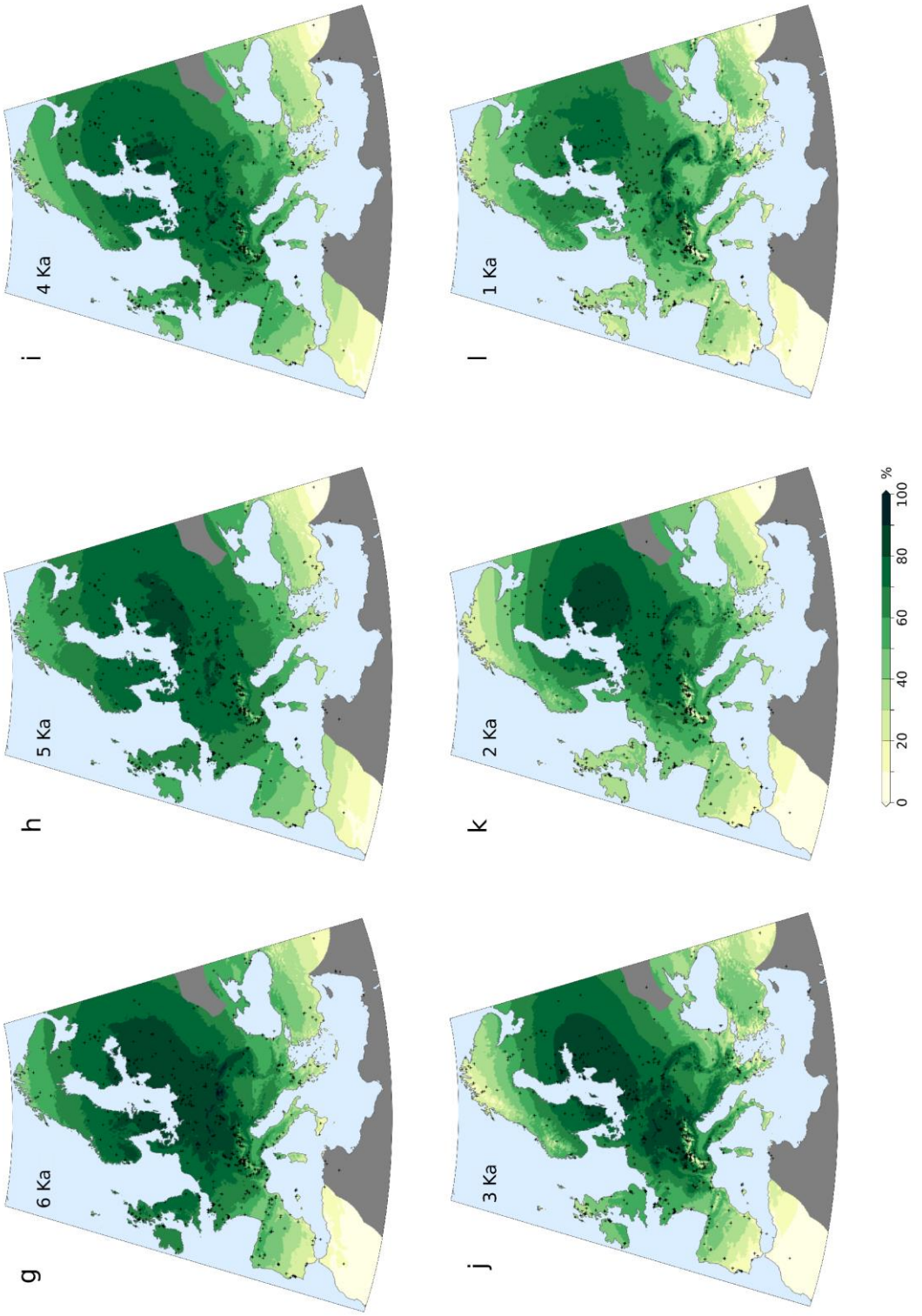

Figure 4.12. *(Continued)*

Therefore, "forest" cover mapped in this dataset is subject to uncertainty and areas mapped as forest could in reality be something else, which would lead to irreconcilable differences between pollen spectra and tree cover. For example, forest could be mapped in the dataset when the vegetation cover is in fact rather a dense, tall shrubland, e.g., in the arctic. While indistinguishable to a satellite-based sensor, an arctic shrubland might have a very different floristic composition than, e.g., boreal forest, and this difference would be obvious in a pollen spectrum. This mismatch between observations from satellites and modern pollen samples would result in calibration uncertainty, where areas with similar forest cover have different pollen spectra, and vice versa.

Sample misplacement is another source for incorrect matches between pollen and satellite data. The high grid resolution of the remote sensing data and the small σ-value of the pixel-weighting equation result in a high sensitivity of the search window to shifts in its position. The EMPD provides reliability estimates for sample geolocation, which – combined with randomized location checks – have been used in the present work to exclude samples with known large uncertainties. This information is not available for the whole dataset, especially for older samples, due to gaps in the documentation or specific limitations (e.g., lack of GPS logging devices during fieldwork operations). Surface samples with unknown location reliability amount to >50% of the total. Despite this lack of metadata, they were included in the elaboration in order not to depopulate the analog pool.

An additional issue revolves around the availability of remote-sensing data. While satellite-based forest-cover data are available only for selected time periods, i.e., the year 2000 for Hansen et al. (2013) and years 1992–1993 in the case of DeFries et al. (2000), during the past decades European forest cover experienced a general increase, with localized areas of forest loss (Lambrechts et al., 2009; Potapov et al., 2015). For comparison, the EMPD samples with known age were collected mostly between the years 1978 and 2010. As a consequence, pollen spectra might be paired with non-contemporary vegetation patterns. The relevance of this issue can be proportional to the age difference between the two data sets, as a wider gap would simply leave more time for landscape transformations to take place. Nonetheless, chronology-based filters were explicitly avoided, since wide chronological differences do not necessarily imply significant vegetation changes.

All of these examples are meant to highlight how surface-pollen datasets would benefit from both enhanced sample density and metadata quality, ideally not only

covering a wider range of vegetation assemblages, but also containing redundancy that would allow for stricter and task-oriented selection of samples. Furthermore, improvements in remotely sensed land-cover data would be desirable, e.g., using new sensors that directly integrate the spectral and physical characteristics of the vegetation into a single dataset. It is important to remember that good transfer function performance may equally be dependent on having a reliable calibration dataset as on having good pollen data.

No-analog situations and the PFT approach

The ability of MAT to find a proper set of analogs is challenged by the many factors influencing plant biology and distribution through time (Jackson and Williams, 2004). Pollen production and dispersal can be influenced by the age of the plant, with younger specimens producing less pollen than older ones (Jackson, 1994; Matthias et al., 2012). Similarly, varying concentrations of atmospheric CO_2 have a direct effect on the production of flowering shoots, leading to an increase in pollen production with growing CO_2 values (Ladeau and Clark, 2006; Ziska and Caulfield, 2000). Growth-speed limitations and interspecies competition might result in a lagged expansion within a potential bioclimatic space (e.g., Gardner and Willis, 1999). Furthermore, a growing human influence on the landscape in the second half of the Holocene played a role in the expansion of disturbance-dependent taxa outside of their niches (e.g., Perego et al., 2011), and possibly also contributed to early extinction events (Wick and Möhl, 2006). A combination of these and other factors led to the rise and decline of plant communities that potentially have no close parallels in contemporary vegetation.

Changes in pollen productivity within the same species represent an issue that is difficult to address and common to all pollen-based models. On the other hand, the sensitivity of the MAT to migration lags, extinction events, and gaps in the training data set can be lessened by avoiding a taxa-based approach. The use of PFT scores, as used in the present study, groups pollen taxa in broader classes defined by physical, phenological and climatic factors. The absence of specific taxa from an area does not hinder the performance of a PFT-based reconstruction as long as their potential bioclimatic space is occupied by species with comparable traits. The low occurrence of no-analog situations in our reconstructions (Fig. 4.6b) proves the effectiveness of the PFT approach, and suggests that no-analogs do not affect the performance of the model. Yet a concentration of no-analogs between ~9000 and 6000 BP remains notable. It occurs during the phase of maximum European forest development and

highlights from a different perspective the noted model weakness with dense forest covers.

Still, the use of PFTs should not be regarded as a complete solution to the no-analog issue, but more as a viable and more robust alternative to taxa-based approaches. In fact, notable differences between taxa remain unaccounted for within the PFT method and contribute to the overall uncertainty of the model. As an example, beech (*Fagus*), lime (*Tilia*), and elm (*Ulmus*) share the same PFT (Cool-temperate summer-green; Peyron et al., 1998) despite having widely different pollen productivity estimates (beech: 0.76–6.7; lime: 1.3; elm: 0.8. Values are relative to the pollen productivity of Poaceae; Broström et al., 2008). Two samples with the same proportion of cool-temperate summer-green taxa (e.g., one composed primarily of beech and one of lime/elm) might then still be the product of different vegetation patterns. Beech spread gradually across Europe during the Holocene and is well represented in modern pollen diagrams (e.g., Magri, 2008). On the other hand, lime and elm are minor components of the present-day pollen landscape, having reached their palynological peak during the Early/Mid-Holocene (e.g., Huntley and Birks, 1983). Modern samples with beech might then be selected as best analogs for fossil samples lacking this taxon but containing lime and elm. The occurrence of such pairings – considering the potentially much higher pollen productivity of beech – could contribute too to the underestimation of Early/Mid-Holocene forest cover.

Forest-cover underestimation

The results of the two-fold cross-validation exercise and the MAT–REVEALS comparison (see sections "Performance of the Cross-validation Exercise and MAT–REVEALS Comparison") highlight a distinct issue with the reconstruction of high forest covers. A visible contribution to this issue is given by the limited availability of EMPD samples from highly forested contexts, but additional factors could play important roles too. Notably, the modern European landscape is largely deforested. As a consequence, any sample misplacement or incorrect distance-weighting could more likely lead to pair pollen samples with low forest-cover values. The use of PFTs could impact the model performance too, as noted in section "No-Analog Situations and the PFT Approach." Most importantly, the MAT does not have any intrinsic ability to differentiate between local pollen sources and long-distance transport, an issue exacerbated by the generally poor pollen dispersal capabilities of open-landscape species (i.e., –simplifying –most herbaceous taxa). The under-representation of non-arboreal species results in samples with comparably high AP values but widely

different forest-cover percentages (e.g., Broström et al., 1998 and Fig. 4.1 in the present paper), likely hindering a fine distinction between moderately and highly forested contexts.

These issues could be addressed by driving the analog selection process through a series of constraints. An example might involve calculating the average pollen productivity estimates of all PFTs, and reducing the analog pool to samples with comparable traits. Similarly, pollen accumulation rates could be used to detect predominant long-distance transport. Testing these solutions is currently prevented by a lack of necessary information, as pollen productivity estimates for the whole study area and for all taxa involved are currently not available. Similarly, the EMPD does not contain information concerning pollen accumulation rates. These limits led us to tackle the forest underestimation issue through a single correction equation applied to all sampling contexts and vegetation assemblages (see section "Bias Correction").

Comparison with current land-cover change narratives

Unraveling the fine reasons behind the regionally diverse forest cover trends remains beyond the scope of this paper. We will mostly constrain our analysis to a comparison between our data and the land cover dynamics emerging from qualitative interpretations and quantitative models. The interpolated results of our reconstruction draw a coherent picture of forest advancement and retreat spanning the last 12 millennia. While the limits of the method constitute an undeniable source of approximation, it is important to note that the reconstructions are often consistent with existing narratives of vegetation development from a regional to a continental scale, although these have virtually all been based on a qualitative interpretation of pollen data.

Late Pleistocene. The average forest cover across most of Europe just before the onset of Holocene warming points to a landscape dominated by non-arboreal vegetation. In agreement with this reconstruction, the traditional interpretation of pollen data describes a steppe-like environment with prevalent shrub and xerophytic vegetation covering most of the deglaciated areas of Western and Southern Europe (Bakels, 1995; Guiter et al., 2005; Walker and Lowe, 1990). Similarly, the presence of a steppic landscape matches several interpretations of Central Mediterranean (e.g., Bordon et al., 2009; Combourieu-Nebout et al., 2013; Tinner et al., 2009) and Eastern Mediterranean archives (e.g., Langgut et al., 2011; Roberts et al., 2001; Rossignol-

Strick, 1995). In contrast, Lawson et al. (2004) point to a limited woodland contraction phase inserted in a context of gradual postglacial forest recovery. The expansion of an unforested environment during the Younger Dryas period is a phenomenon acknowledged in the Iberian Peninsula as well (Carrión et al., 2010). Here, the treeless conditions reconstructed in Fig. 4.12a appear to be fitting for high-elevation sites and areas affected by a decrease in precipitation (Carrión, 2002; Carrión and Van Geel, 1999; Muñoz Sobrino et al., 2004), but might underestimate the presence of pine and oak woodlands growing in more favorable locations (Rubiales et al., 2010).

The higher forest-cover percentages emerging in central Europe probably reflect the presence of surviving Allerød pine/birch woodlands stretching from the Alpine piedmont (Wick, 2000) to Central Europe (Andres et al., 2001; Bos, 2001; Sobkowiak-Tabaka et al., 2017). Moving northward to the Baltic coast, the conditions inferred from pollen diagrams describe increasingly open birch and pine forests (Jahns, 2007; Nelle and Dörfler, 2008) gradually giving way to tundra-like conditions (Kihno et al., 2011)). The relatively high forest cover values reconstructed around the Baltic Ice Lake may appear excessive considering the local importance of heliophilous taxa and the low pollen accumulation rates of forest species (Veski et al., 2012). Reworked pollen grains of thermophilous trees (e.g., Jahns, 2007) might arguably inflate model estimates. Nonetheless, macrofossil remains and pollen threshold values point to persistent populations of birch, pine, and spruce even at high latitudes and close to the ice margin (Heikkilä et al., 2009; Kullman, 2002).

Post-glacial forest recovery. The beginning of the Holocene is marked by warmer temperatures and greater moisture availability that promoted a rapid, wholesale transformation of land cover. The rise of forest-cover values over most of Europe is in line with the vegetation changes inferred from pollen diagrams. Existing woodlands densified and patchy tree stands replaced tundra parkland vegetation (e.g., Nelle and Dörfler, 2008; Robin et al., 2011). Growing forest density across Southern and Central Europe reflects the rapid expansion of thermophilous trees in pollen diagrams (Brewer et al., 2002; Giesecke et al., 2011). The 10500 BP timeslice is characterized by an unusually high land-cover variability (high standard deviations in Fig. 4.10), occurring together with visibly higher error estimates (Supplementary Fig. S3.6, Appendix III). Significantly, this time window envelops the abrupt rise of hazel in central and southern European pollen diagrams (~10600 BP, Giesecke et al., 2011). This synchronous and fast paced event possibly resulted in widespread forest-cover

differences at both intra-site (sudden palynological change between adjacent samples) and inter-site level (neighboring sites having different forest covers due to chronological factors – i.e., limits of their respective age–depth models), ultimately producing inflated error estimates propagating through site-poor areas. Peak levels of forest development are generally reconstructed between ~8500 and 6000 BP, following the maximum extent reached by mixed deciduous forests (Brewer et al., 2002). Rising forest-cover values in Scandinavia reflect the colonizing wave of pioneering birch woodlands over the newly deglaciated landscapes (Bjune et al., 2004). Values higher than 50% are reconstructed in Northern Scandinavia after 8000 BP, reflecting the widespread occurrence of birch and pine-birch forests at high latitudes (Barnekow, 2000; Bjune et al., 2004; Seppa, 1998).

Compared to other regions, there is only a modest increase in forest cover density in the Mediterranean between Late Pleistocene and Early and Mid-Holocene. These low values possibly reflect a combination of denser forests spreading inland and at upland sites (Carrión et al., 2010; Sadori et al., 2011), and the contemporary development of coastal matorral/maquis shrublands (Calò et al., 2012; Carrión and Dupré, 1996; Pantaléon-Cano et al., 2003; Tinner et al., 2009).

Middle/Late Holocene forest cover decline. During the second half of the Holocene, forest-cover percentages are characterized by negative trends that bring the curves to present-day values. Increasing human pressure is regarded as the primary driver behind such behavior (Davis et al., 2015; Fyfe et al., 2015; Kaplan et al., 2009), although the role of climate should not be dismissed (Marquer et al., 2017). Forest cover over Northern Europe will have been influenced by the Early Holocene rise in temperatures and later Holocene cooling after the Mid-Holocene thermal optimum, whilst forests in Southern Europe were more influenced by similar trends in moisture (Davis et al., 2003). The estimated increase in carrying capacity of early agricultural societies implies an expansion of productive surfaces (croplands, pastures) at the expense of woodlands and wetlands. A growing exploitation of forest resources, primarily timber and fuel, must be accounted for as well, contributing to the general widespread and growing forest-cover reduction. The average picture described by our model is spatially and chronologically comparable to the synthesis presented by Fyfe et al. (2015), based on the categorization (Pseudobiomization, PBM) of Europe's land surface into aggregated land-cover classes (e.g., forest, semi-open vegetation, open vegetation). At a pan-European scale, both models reproduce a period of maximum forest extent between ~8500 and 6000 BP. Notably, this phase of relative stability is

followed in both models by a very gradual forest decline. This negative trend then accelerates after 1400 BP in Fyfe et al. (2015) and after 1500 BP in our model (study area average, Fig. 4.10). Additional similarities between the PBM and MAT can be found at a smaller scale too. Fyfe et al. (2015) describe a clear distinction between Western and Eastern Europe, with the first displaying consistently lower forest values. This East-West distinction is also visible in REVEALS estimates by Nielsen et al. (2012) and Trondman et al. (2015), and in the multi-model comparison by Pirzamanbein et al. (2014), confirming it as a robust feature of European land-cover history. The same pattern is clearly visible in our reconstruction since the Early Holocene, placing its origin before the expansion of Neolithic agriculture (Fyfe et al., 2015), and possibly reflecting – at least in part – an interplay of continentality and soil texture gradients (Nielsen et al., 2012).

The differences between Eastern and Western Europe are not limited to absolute land-cover values: the two regions show different forest-loss dynamics too. Fyfe et al. (2015) show a visible negative trend across their Western region (Western France) from ~4500 BP. On the other hand, Eastern Europe (Czech/Slovakia) presents only a very mild decline between ~6000 and 1500 BP, then followed by a sudden and much sharper forest collapse. The Western France trajectory shares clear similarities with our Atlantic region curve, including a forest decline and recovery episode between ~8000 and 6000 BP. The Czech/Slovakia situation matches forest-decline patterns in both Central Europe and in the Dinaro-Carpathian region (sudden decline after ~1500 BP) in the MAT-based model.

It is worth noting that quantitative landscape reconstructions by Nielsen et al. (2012), Pirzamanbein et al. (2014), and Trondman et al. (2015) agree on producing widespread Open Landscape values between ~0 and 30% at 6000 BP for central and northern Europe (i.e., ~70–100% forest cover). These values are matched by the MAT-based reconstruction for the same area and time slice (range 60–90%), confirming further the validity of the MAT calibration algorithm.

In the British Isles, Woodbridge et al. (2014) set the onset of Neolithic land use in Britain at ~6,000 BP; this is also when our MAT-based forest cover begins its negative trend. A notable difference consists in a re-afforestation event detected by Woodbridge et al. (2014) between 5400 and 4200 BP which temporarily interrupts the overall negative Late Holocene decline. This event is not visible in the MAT-based curve, possibly due to a non-perfect comparability between the PBM land cover classes and the continuous MAT reconstruction.

The Mediterranean region shows an overall weak and gradual increase in open areas when compared with other more dramatic regional dynamics. The largely open landscape reconstructed during the Early/Middle Holocene is likely to play a primary role in lessening any evidence of radical human impact, yet other factors might contribute to this modest change in land cover too. As an example, even severe disturbance events (e.g., Cremaschi et al. 2006) might simply not be visible due to the spatial and temporal coverage of the underlying fossil database.

Vertical performance of the interpolation procedure in the Alpine region. It has been widely argued that pollen percentages alone are not sufficient to infer the local presence of tree populations in extreme environments at the limits of tree growth (e.g. Ali et al., 2003; Ponel et al., 1992; Tinner et al., 1996). Under these conditions, flowering season is negatively affected and trees tend to propagate via vegetative multiplication and not through sexual reproduction (Black and Bliss, 1980; Charalampopoulos et al., 2013; Kullman, 1992), likely altering their palynological signature. The combined interpretation of pollen percentages and influx may help in identifying clearer vegetation thresholds (Hicks, 1994), potentially countering the effect of upslope and long distance pollen transport. Still, the presence of macrofossils is considered the most solid piece of evidence to reconstruct vegetation history across the timberline (e.g., Birks and Birks, 2000). Considering the limits of pollen data in high-elevation contexts, in the present section we evaluate the capabilities of our model to detect much broader forest dynamics. Importantly, it again should be remembered that we reconstruct the area-average forest cover of the entire Alpine region, and that this might variously differ from individual site records and smaller regional studies.

By end of the Younger Dryas period (11700 BP), alpine forests became rather open even in the lowlands (Ammann et al., 2007; Vescovi et al., 2007). This situation appears to be broadly compatible with our model, which does not produce values >50% before 11750 BP. The following abrupt positive shift of the 50% threshold matches well the upward movement of forests at the transition into the Holocene (Tinner and Kaltenrieder, 2005). In their simulation of alpine biomass, Heiri et al. (2006) detect a short-lived dieback event around 10500 BP. Notably, the MAT-based model records a mild stagnation episode of the 50% threshold approximately around the same period, between ~11250 and 10500 BP (Fig. 4.11). Differences in the scale of the reconstructions, chronological uncertainties and temporal interpolation might explain the slight offset between the two events. Speculatively, the forest-cover

stagnation seen in our model could be ascribed to the combined effects of the cool Preboreal oscillation (11363/11100 BP; Schwander et al., 2000) on alpine forests (Gobet et al., 2005), and to the dieback identified by Heiri et al. (2006). Major dieback events are described by Heiri et al. (2006) also between ~9500–9300 BP and ~6500–6000 BP, both matching mild – but not necessarily significant – elevation drops of the 50% threshold in our reconstruction. The prominent dieback described by Heiri et al. (2006) at 8000 BP does not appear to be resolved in Fig. 4.11, probably because of the temporal resolution of samples in the underlying pollen dataset. An overall regional change is anyway visible in Fig. 4.10, where alpine forest-cover values drop noticeably after ~8250 BP. Between 9750 and ~7000 BP the 50% threshold fluctuates mostly between 2400 and 2600 m. The lower value is in good agreement with the timberline elevation proposed by Tinner and Theurillat (2003) for the Swiss Central Alps, based on macrofossil analysis (Fig. 4.11). Notably, estimates for maximum forest limits range from 2500 m (Tessier et al., 1993) to 2800 m (Talon, 2010) in the French Alps. After ~7000 BP, the upper limit of the 50% threshold begins to drop quite steadily, likely reflecting the contribution of different local forest dynamics to our regional average. Treeline decline is visible as early as 6350 BP in the Austrian Alps (Nicolussi et al., 2005), while it is recorded after ~5750 in the Central Swiss Alps (Fig. 4.11 and Tinner and Theurillat, 2003). The abrupt timberline drop reconstructed by Tinner and Theurillat (2003) between 4750 and 4250 BP appears to be diluted in time in our reconstruction (Fig. 4.11). The 50% threshold never exceeds 2400 m after 5750 BP, possibly reflecting the origin of anthropogenic pastures above 2300 m during the Copper Age (~5600 BP, Pini et al., 2017) and a subsequent continuous and growing exploitation of the high alpine landscape.

Ultimately, a comparison between our model and independent palaeo-ecological studies suggests that a combination of MAT and interpolation can reproduce broad vertical vegetation patterns (i.e., fluctuations of the upper limit of region-wide dense forests) at a resolution sufficient for large-scale vegetation models. The reconstruction of sharper forest-vs.-no-forest cutoffs remains beyond the capability of the interpolation procedure. Finer results could be achieved through the incorporation of complementary proxy data (i.e., plant macro remains, charcoal), although with the caveat that such data remain much less widely available than pollen records.

CONCLUSION

In this study we applied the MAT to generate a continuous, continental-scale reconstruction of European forest-cover spanning the last 12000 years. Our

reconstruction follows the general methodology published by Tarasov et al. (2007) and Williams et al. (2011). When compared with these studies, our work presents a series of improvements that extend the reliability and spatial/temporal coverage of the reconstruction. An increased number of samples in the modern database allows for stricter quality control and provides a better representation of different vegetation types. A larger fossil database allows for higher spatial density and better dating control. The satellite-based forest-cover data set used in previous studies (DeFries et al., 2000) was replaced with a higher resolution map (Hansen et al., 2013), leading to more reliable pairings between vegetation and modern pollen data. Furthermore, pollen taxa were aggregated into PFTs in order to reduce the occurrence of no-analog situations. The main improvement in mapping our results is the use of four-dimensional spatial interpolation (Mauri et al., 2015). This procedure extrapolates reconstructed vegetation data between a grid of fossil sites in both space and time, producing a set of forest-cover maps with continuous coverage and regular time-step at a continental scale. These characteristics represent a rather unique feature within the category of pollen-based quantitative vegetation reconstructions, and make these maps suitable for comparison with vegetation models and anthropogenic land-cover change scenarios.

The reliability of our reconstructions is supported by a comparison with methodologically independent data sets. Forest-cover reconstructions based on the MAT (this study) and on the LRA were compared for selected sites (Marquer et al., 2014) in the circum-Baltic area. Both methodologies present widely comparable trends. Notable divergences are visible especially during the Mid-Holocene, with REVEALS consistently producing higher values. The limits of the MAT concerning the reconstruction of high forest covers can be ascribed to limitations within both the available training data set and the method itself. A visible role is played by the scarce representation of densely forested areas in the EMPD, an issue furtherly exacerbated by the averaging nature of the MAT. Furthermore, the MAT does not have any intrinsic capability to correct for differential pollen productivity, or identify samples largely affected by long-distance pollen transport. These problems could be addressed through targeted sampling campaigns, aimed at improving the coverage of specific vegetation patterns in the EMPD, and possibly by introducing constraints based on pollen productivity and accumulation rates. Given the systematic occurrence of biased MAT results and the current inapplicability of constraint-based procedures, we opted to tackle this issue through a statistical approach to bias correction. We used Quantile Mapping to extract a calibration curve from the output of the cross-validation

exercise. The effectiveness of this calibration approach is testified by a visible reduction of the overall bias in both the cross-validation test and the comparison with REVEALS data.

The resulting continental-scale maps draw a coherent picture of vegetation development across Europe since the end of the Younger Dryas period. Forest cover trends fit well in accepted narratives based on qualitative and quantitative interpretations of palaeovegetation data.

As a further test, we evaluated the vertical performance of the interpolation procedure against macrofossil-based tree line/timberline studies in the Alps. Detecting ecotones in alpine environments via pollen percentages is a task affected by wide margins of error. Consequently, we focused our comparison on broader vegetation patterns (i.e., variations in the upper limit of region-wide dense forests). A combination of MAT and spatio-temporal interpolation proved able to track major tree cover fluctuations in proximity of the timberline, thus reinforcing the broad reliability of the interpolation algorithm across a highly dynamic landscape.

FUNDING

This research has been supported by grants from the Italian Ministry of Research and Education (FIRB RBID08LNFJ), the Swiss National Science Foundation (PP0022_119049), the European Research Council (COEVOLVE 313797), the Graduate School "Human Development in Landscapes" at Kiel University (GSC 208/2), and by the DFG Collaborative Research Centre SFB 1266.

ACKNOWLEDGMENTS

This study depends on the resources provided by the European Pollen Database and the PANGAEA data archive. The work of the data contributors and the EPD and PANGEA communities is gratefully acknowledged.

Bibliography

Ali, A.A., Carcaillet, C., Guendon, J.-L., Quinif, Y., Roiron, P., Terral, J.-F., 2003. The Early Holocene treeline in the southern French Alps: new evidence from travertine formations. Global Ecology and Biogeography 12, 411–419.

Ammann, B., Birks, H., Walanus, A., Wasylikowa, K., 2007. Late Glacial Multidisciplinary Studies, in: Elias, S.A. (Ed.), Encyclopedia of Quaternary Science. Elsevier, Amsterdam, pp. 2475–2486. https://doi.org/10.7892/boris.30415

Andres, W., Bos, J.A., Houben, P., Kalis, A.J., Nolte, S., Rittweger, H., Wunderlich, J., 2001. Environmental change and fluvial activity during the Younger Dryas in central Germany. Quaternary International 79, 89–100.

Arino, O., Bicheron, P., Achard, F., Latham, J., Witt, R., Weber, J.-L., 2008. GlobCover. The most detailed portrait of Earth (No. 136), ESA Bulletin. ESA.

Bakels, C.C., 1995. Late Glacial and Holocene pollen records from the Aisne and Vesle valleys, Northern France: the pollen diagrams Maizy-Cuiry and Bazoches. Mededelingen Rijks Geologische Dienst 223–234.

Baker, A.G., Zimny, M., Keczyński, A., Bhagwat, S.A., Willis, K.J., Latałowa, M., 2016. Pollen productivity estimates from old-growth forest strongly differ from those obtained in cultural landscapes: Evidence from the Białowieża National Park, Poland. The Holocene 26, 80–92. https://doi.org/10.1177/0959683615596822

Barnekow, L., 2000. Holocene regional and local vegetation history and lake-level changes in the Torneträsk area, northern Sweden. Journal of Paleolimnology 23, 399–420.

Behre, K.-E., 1981. The interpretation of anthropogenic indicators in pollen diagrams. Pollen et spores 23, 225–245.

Birks, H.H., Birks, H.J.B., 2000. Future uses of pollen analysis must include plant macrofossils. Journal of Biogeography 27, 31–35. https://doi.org/10.1046/j.1365-2699.2000.00375.x

Birks, H.J.B., 1968. The Identification of Betula Nana Pollen. New Phytologist 67, 309–314. https://doi.org/10.1111/j.1469-8137.1968.tb06386.x

Birks, H.J.B., Birks, H.H., 2016. How have studies of ancient DNA from sediments contributed to the reconstruction of Quaternary floras? New Phytol 209, 499–506. https://doi.org/10.1111/nph.13657

Birks, H.J.B., Birks, H.H., 1980. Quaternary palaeoecology. Edward Arnold London.

Bjune, A., Birks, H.J.B., Seppä, H., 2004. Holocene vegetation and climate history on a continental-oceanic transect in northern Fennoscandia based on pollen and plant macrofossils. Boreas 33, 211–223. https://doi.org/10.1080/03009480410001244

Black, R.A., Bliss, L.C., 1980. Reproductive Ecology of Picea Mariana (Mill.) BSP., at Tree Line Near Inuvik, Northwest Territories, Canada. Ecological Monographs 50, 331–354. https://doi.org/10.2307/2937255

Bordon, A., Peyron, O., Lézine, A.-M., Brewer, S., Fouache, E., 2009. Pollen-inferred Late-Glacial and Holocene climate in southern Balkans (Lake Maliq). Quaternary International 200, 19–30. https://doi.org/10.1016/j.quaint.2008.05.014

Bos, J.A., 2001. Lateglacial and Early Holocene vegetation history of the northern Wetterau and the Amöneburger Basin (Hessen), central-west Germany. Review of Palaeobotany and Palynology 115, 177–204.

Bossard, M., Feranec, J., Otahel, J., 2000. CORINE Land Cover Technical Guide: Addendum 2000. Report No. 40. European Environment Agency, Copenhagen.

Bowker, G.E., Crenshaw, H.C., 2007. Electrostatic forces in wind-pollination—Part 2: Simulations of pollen capture. Atmospheric environment 41, 1596–1603.

Bradshaw, R.H., Jones, C.S., Edwards, S.J., Hannon, G.E., 2015. Forest continuity and conservation value in Western Europe. The Holocene 25, 194–202. https://doi.org/10.1177/0959683614556378

Brewer, S., Cheddadi, R., De Beaulieu, J.L., Reille, M., 2002. The spread of deciduous Quercus throughout Europe since the last glacial period. Forest Ecology and Management 156, 27–48.

Brewer, S., Giesecke, T., Davis, B.A.S., Finsinger, W., Wolters, S., Binney, H., Beaulieu, J.-L. de, Fyfe, R., Gil-Romera, G., Kühl, N., Kuneš, P., Leydet, M., Bradshaw, R.H., 2016. Late-glacial and Holocene European pollen data. Journal of Maps 0, 1–8. https://doi.org/10.1080/17445647.2016.1197613

Broström, A., Gaillard, M.-J., Ihse, M., Odgaard, B., 1998. Pollen-landscape relationships in modern analogues of ancient cultural landscapes in southern Sweden — a first step towards quantification of vegetation openness in the past. Veget Hist Archaebot 7, 189–201. https://doi.org/10.1007/BF01146193

Broström, A., Nielsen, A.B., Gaillard, M.-J., Hjelle, K., Mazier, F., Binney, H., Bunting, J., Fyfe, R., Meltsov, V., Poska, A., Räsänen, S., Soepboer, W., von Stedingk, H., Suutari, H., Sugita, S., 2008. Pollen productivity estimates of key European plant taxa for quantitative reconstruction of past vegetation: a review. Vegetation History and Archaeobotany 17, 461–478. https://doi.org/10.1007/s00334-008-0148-8

Burga, C.A., Perret, R., 2001. Monitoring of Eastern and Southern Swiss Alpine Timberline Ecotones, in: Biomonitoring: General and Applied Aspects on Regional and Global Scales, Tasks for Vegetation Science. Springer, Dordrecht, pp. 179–194. https://doi.org/10.1007/978-94-015-9686-2_11

Büttner, G., Soukup, T., Kosztra, B., 2014. CLC2012 Addendum to CLC2006 Technical Guidelines. Final Draft. EEA, Copenhagen.

Calcote, R., 1995. Pollen Source Area and Pollen Productivity: Evidence from Forest Hollows. Journal of Ecology 83, 591–602. https://doi.org/10.2307/2261627

Calò, C., Henne, P.D., Curry, B., Magny, M., Vescovi, E., La Mantia, T., Pasta, S., Vannière, B., Tinner, W., 2012. Spatio-temporal patterns of Holocene environmental change in southern Sicily. Palaeogeography, Palaeoclimatology, Palaeoecology 323–325, 110–122. https://doi.org/10.1016/j.palaeo.2012.01.038

Cañellas-Boltà, N., Rull, V., Vigo, J., Mercadé, A., 2009. Modern pollen—vegetation relationships along an altitudinal transect in the central Pyrenees (southwestern Europe). The Holocene 19, 1185–1200. https://doi.org/10.1177/0959683609345082

Carrión, J.S., 2002. Patterns and processes of Late Quaternary environmental change in a montane region of southwestern Europe. Quaternary Science Reviews 21, 2047–2066. https://doi.org/10.1016/S0277-3791(02)00010-0

Carrión, J.S., Dupré, M., 1996. Late Quaternary vegetational history at Navarrés, Eastern Spain. A two core approach. New Phytologist 134, 177–191.

Carrión, J.S., Fernández, S., González-Sampériz, P., Gil-Romera, G., Badal, E., Carrión-Marco, Y., López-Merino, L., López-Sáez, J.A., Fierro, E., Burjachs, F., 2010. Expected trends and surprises in the Lateglacial and Holocene vegetation history of the Iberian Peninsula and Balearic Islands. Review of Palaeobotany and Palynology 162, 458–475. https://doi.org/10.1016/j.revpalbo.2009.12.007

Carrión, J.S., Van Geel, B., 1999. Fine-resolution Upper Weichselian and Holocene palynological record from Navarrés (Valencia, Spain) and a discussion about factors of Mediterranean forest succession. Review of Palaeobotany and Palynology 106, 209–236.

Charalampopoulos, A., Damialis, A., Tsiripidis, I., Mavrommatis, T., Halley, J.M., Vokou, D., 2013. Pollen production and circulation patterns along an elevation gradient in Mt Olympos (Greece) National Park. Aerobiologia 29, 455–472. https://doi.org/10.1007/s10453-013-9296-0

Collins, P.M., Davis, B.A.S., Kaplan, J.O., 2012. The mid-Holocene vegetation of the Mediterranean region and southern Europe, and comparison with the present day: Mid-Holocene Mediterranean vegetation. Journal of Biogeography 39, 1848–1861. https://doi.org/10.1111/j.1365-2699.2012.02738.x

Combourieu-Nebout, N., Peyron, O., Bout-Roumazeilles, V., Goring, S., Dormoy, I., Joannin, S., Sadori, L., Siani, G., Magny, M., 2013. Holocene vegetation and climate changes in the central Mediterranean inferred from a high-resolution marine pollen record (Adriatic Sea). Climate of the Past 9, 2023–2042. https://doi.org/10.5194/cp-9-2023-2013

Court-Picon, M., Buttler, A., Beaulieu, J.-L. de, 2006. Modern pollen/vegetation/land-use relationships in mountain environments: an example from the Champsaur valley (French Alps). Veget Hist Archaeobot 15, 151. https://doi.org/10.1007/s00334-005-0008-8

Cremaschi, M., Pizzi, C., Valsecchi, V., 2006. Water management and land use in the terramare and a possible climatic co-factor in their abandonment: The case study of the terramara of Poviglio Santa Rosa (northern Italy). Quaternary International 151, 87–98. https://doi.org/10.1016/j.quaint.2006.01.020

Cui, Q.-Y., Gaillard, M.-J., Lemdahl, G., Stenberg, L., Sugita, S., Zernova, G., 2014. Historical land-use and landscape change in southern Sweden and implications for present and future biodiversity. Ecol Evol 4, 3555–3570. https://doi.org/10.1002/ece3.1198

Cui, Q.-Y., Gaillard, M.-J., Lemdahl, G., Sugita, S., Greisman, A., Jacobson, G.L., Olsson, F., 2013. The role of tree composition in Holocene fire history of the hemiboreal and southern boreal zones of southern Sweden, as revealed by the application of the Landscape Reconstruction Algorithm: Implications for biodiversity and climate-change issues. The Holocene 23, 1747–1763. https://doi.org/10.1177/0959683613505339

Davies, C.P., Fall, P.L., 2001. Modern pollen precipitation from an elevational transect in central Jordan and its relationship to vegetation: Modern vegetation and pollen in

Jordan. Journal of Biogeography 28, 1195–1210. https://doi.org/10.1046/j.1365-2699.2001.00630.x

Davis, B.A.S., Brewer, S., Stevenson, A.C., Guiot, J., 2003. The temperature of Europe during the Holocene reconstructed from pollen data. Quaternary Science Reviews 22, 1701–1716. https://doi.org/10.1016/S0277-3791(03)00173-2

Davis, B.A.S., Collins, P.M., Kaplan, J.O., 2015. The age and post-glacial development of the modern European vegetation: a plant functional approach based on pollen data. Vegetation History and Archaeobotany 24, 303–317. https://doi.org/10.1007/s00334-014-0476-9

Davis, B.A.S., Zanon, M., Collins, P., Mauri, A., Bakker, J., Barboni, D., Barthelmes, A., Beaudouin, C., Bjune, A.E., Bozilova, E., Bradshaw, R.H.W., Brayshay, B.A., Brewer, S., Brugiapaglia, E., Bunting, J., Connor, S.E., Beaulieu, J.-L. de, Edwards, K., Ejarque, A., Fall, P., Florenzano, A., Fyfe, R., Galop, D., Giardini, M., Giesecke, T., Grant, M.J., Guiot, Jöel, Jahns, S., Jankovská, V., Juggins, S., Kahrmann, M., Karpińska-Kołaczek, M., Kołaczek, P., Kühl, N., Kuneš, P., Lapteva, E.G., Leroy, S.A.G., Leydet, M., Guiot, José, Jahns, S., Jankovská, V., Juggins, S., Kahrmann, M., Karpińska-Kołaczek, M., Kołaczek, P., Kühl, N., Kuneš, P., Lapteva, E.G., Leroy, S.A.G., Leydet, M., Sáez, J.A.L., Masi, A., Matthias, I., Mazier, F., Meltsov, V., Mercuri, A.M., Miras, Y., Mitchell, F.J.G., Morris, J.L., Naughton, F., Nielsen, A.B., Novenko, E., Odgaard, B., Ortu, E., Overballe-Petersen, M.V., Pardoe, H.S., Peglar, S.M., Pidek, I.A., Sadori, L., Seppä, H., Severova, E., Shaw, H., Święta-Musznicka, J., Theuerkauf, M., Tonkov, S., Veski, S., Knaap, W.O. van der, Leeuwen, J.F.N. van, Woodbridge, J., Zimny, M., Kaplan, J.O., 2013. The European Modern Pollen Database (EMPD) project. Veget Hist Archaeobot 22, 521–530. https://doi.org/10.1007/s00334-012-0388-5

Dawson, A., Paciorek, C.J., McLachlan, J.S., Goring, S., Williams, J.W., Jackson, S.T., 2016. Quantifying pollen-vegetation relationships to reconstruct ancient forests using 19th-century forest composition and pollen data. Quaternary Science Reviews 137, 156–175. https://doi.org/10.1016/j.quascirev.2016.01.012

DeFries, R.S., Hansen, M.C., Townshend, J.R.G., Janetos, A.C., Loveland, T.R., 2000. A new global 1-km dataset of percentage tree cover derived from remote sensing. Global Change Biology 6, 247–254.

Edwards, K.J., Fyfe, R.M., Jackson, S.T., 2017. The first 100 years of pollen analysis. Nature Plants 3, 17001. https://doi.org/10.1038/nplants.2017.1

Feeser, I., Dörfler, W., 2014. The glade effect: Vegetation openness and structure and their influences on arboreal pollen production and the reconstruction of anthropogenic forest opening. Anthropocene 8, 92–100. https://doi.org/10.1016/j.ancene.2015.02.002

Finsinger, W., Tinner, W., Vanderknaap, W., Ammann, B., 2006. The expansion of hazel (Corylus avellana L.) in the southern Alps: a key for understanding its early Holocene history in Europe? Quaternary Science Reviews 25, 612–631. https://doi.org/10.1016/j.quascirev.2005.05.006

Furrer, R., Nychka, D., Sain, S., 2013. fields: Tools for Spatial Data, R-Package.

Fyfe, R.M., de Beaulieu, J.-L., Binney, H., Bradshaw, R.H.W., Brewer, S., Le Flao, A., Finsinger, W., Gaillard, M.-J., Giesecke, T., Gil-Romera, G., Grimm, E.C., Huntley,

B., Kunes, P., Kühl, N., Leydet, M., Lotter, A.F., Tarasov, P.E., Tonkov, S., 2009. The European Pollen Database: past efforts and current activities. Vegetation History and Archaeobotany 18, 417–424. https://doi.org/10.1007/s00334-009-0215-9

Fyfe, R.M., Twiddle, C., Sugita, S., Gaillard, M.-J., Barratt, P., Caseldine, C.J., Dodson, J., Edwards, K.J., Farrell, M., Froyd, C., Grant, M.J., Huckerby, E., Innes, J.B., Shaw, H., Waller, M., 2013. The Holocene vegetation cover of Britain and Ireland: overcoming problems of scale and discerning patterns of openness. Quaternary Science Reviews 73, 132–148. https://doi.org/10.1016/j.quascirev.2013.05.014

Fyfe, R.M., Woodbridge, J., Roberts, N., 2015. From forest to farmland: pollen-inferred land cover change across Europe using the pseudobiomization approach. Global Change Biology 21, 1197–1212. https://doi.org/10.1111/gcb.12776

Gaillard, M.-J., Sugita, S., Bunting, J., Dearing, J., Bittmann, F., 2008. Human impact on terrestrial ecosystems, pollen calibration and quantitative reconstruction of past land-cover. Veget Hist Archaeobot 17, 415–418. https://doi.org/10.1007/s00334-008-0170-x

Gaillard, M.-J., Sugita, S., Mazier, F., Trondman, A.-K., Broström, A., Hickler, T., Kaplan, J.O., Kjellström, E., Kokfelt, U., Kuneš, P., Lemmen, C., Miller, P., Olofsson, J., Poska, A., Rundgren, M., Smith, B., Strandberg, G., Fyfe, R., Nielsen, A.B., Alenius, T., Balakauskas, L., Barnekow, L., Birks, H.J.B., Bjune, A., Björkman, L., Giesecke, T., Hjelle, K., Kalnina, L., Kangur, M., van der Knaap, W.O., Koff, T., Lagerås, P., Latałowa, M., Leydet, M., Lechterbeck, J., Lindbladh, M., Odgaard, B., Peglar, S., Segerström, U., von Stedingk, H., Seppä, H., 2010. Holocene land-cover reconstructions for studies on land cover-climate feedbacks. Climate of the Past 6, 483–499. https://doi.org/10.5194/cp-6-483-2010

Gardner, A.R., Willis, K.J., 1999. Prehistoric farming and the postglacial expansion of beech and hornbeam: a comment on Küster. The Holocene 9, 119–121.

Gavin, D.G., Oswald, W.W., Wahl, E.R., Williams, J.W., 2003. A statistical approach to evaluating distance metrics and analog assignments for pollen records. Quaternary Research 60, 356–367. https://doi.org/10.1016/S0033-5894(03)00088-7

Gerber, S., Chadœuf, J., Gugerli, F., Lascoux, M., Buiteveld, J., Cottrell, J., Dounavi, A., Fineschi, S., Forrest, L.L., Fogelqvist, J., Goicoechea, P.G., Jensen, J.S., Salvini, D., Vendramin, G.G., Kremer, A., 2014. High Rates of Gene Flow by Pollen and Seed in Oak Populations across Europe. PLOS ONE 9, e85130. https://doi.org/10.1371/journal.pone.0085130

Giesecke, T., Bennett, K.D., Birks, H.J.B., Bjune, A.E., Bozilova, E., Feurdean, A., Finsinger, W., Froyd, C., Pokorný, P., Rösch, M., Seppä, H., Tonkov, S., Valsecchi, V., Wolters, S., 2011. The pace of Holocene vegetation change – testing for synchronous developments. Quaternary Science Reviews 30, 2805–2814. https://doi.org/10.1016/j.quascirev.2011.06.014

Giesecke, T., Davis, B., Brewer, S., Finsinger, W., Wolters, S., Blaauw, M., de Beaulieu, J.-L., Binney, H., Fyfe, R.M., Gaillard, M.-J., Gil-Romera, G., van der Knaap, W.O., Kuneš, P., Kühl, N., van Leeuwen, J.F.N., Leydet, M., Lotter, A.F., Ortu, E., Semmler, M., Bradshaw, R.H.W., 2013. Towards mapping the late Quaternary

vegetation change of Europe. Vegetation History and Archaeobotany 23, 75–86. https://doi.org/10.1007/s00334-012-0390-y

Gobet, E., Tinner, W., Bigler, C., Hochuli, P.A., Ammann, B., 2005. Early-Holocene afforestation processes in the lower subalpine belt of the Central Swiss Alps as inferred from macrofossil and pollen records. The Holocene 15, 672–686. https://doi.org/10.1191/0959683605hl843rp

Gudmundsson, L., 2016. qmap: Statistical Transformations for Post-Processing Climate Model Output.

Guiot, J., 1990. Methodology of the last climatic cycle reconstruction in France from pollen data. Palaeogeography, Palaeoclimatology, Palaeoecology 80, 49–69. https://doi.org/10.1016/0031-0182(90)90033-4

Guiter, F., Andrieu-Ponel, V., Digerfeldt, G., Reille, M., de Beaulieu, J.-L., Ponel, P., 2005. Vegetation history and lake-level changes from the Younger Dryas to the present in Eastern Pyrenees (France): pollen, plant macrofossils and lithostratigraphy from Lake Racou (2000 m a.s.l.). Vegetation History and Archaeobotany 14, 99–118. https://doi.org/10.1007/s00334-005-0065-z

Hansen, M.C., Potapov, P.V., Moore, R., Hancher, M., Turubanova, S.A., Tyukavina, A., Thau, D., Stehman, S.V., Goetz, S.J., Loveland, T.R., Kommareddy, A., Egorov, A., Chini, L., Justice, C.O., Townshend, J.R.G., 2013. High-Resolution Global Maps of 21st-Century Forest Cover Change. Science 342, 850–853. https://doi.org/10.1126/science.1244693

Heikkilä, M., Fontana, S.L., Seppä, H., 2009. Rapid Lateglacial tree population dynamics and ecosystem changes in the eastern Baltic region. Journal of Quaternary Science 24, 802–815. https://doi.org/10.1002/jqs.1254

Heiri, C., Bugmann, H., Tinner, W., Heiri, O., Lischke, H., 2006. A model-based reconstruction of Holocene treeline dynamics in the Central Swiss Alps. Journal of Ecology 94, 206–216. https://doi.org/10.1111/j.1365-2745.2005.01072.x

Hicks, S., 1994. Present and past pollen records of Lapland forests. Review of Palaeobotany and Palynology, Modern Pollen Rain and Fossil Pollen Spectra 82, 17–35. https://doi.org/10.1016/0034-6667(94)90017-5

Hohensinner, S., Sonnlechner, C., Schmid, M., Winiwarter, V., 2013. Two steps back, one step forward: reconstructing the dynamic Danube riverscape under human influence in Vienna. Water Hist 5, 121–143. https://doi.org/10.1007/s12685-013-0076-0

Hollister, J., Shah, T., 2017. elevatr: Access Elevation Data from Various APIs.

Huntley, B., 1990. Dissimilarity mapping between fossil and contemporary pollen spectra in Europe for the past 13,000 years. Quaternary Research 33, 360–376.

Huntley, B., Birks, H.J.B., 1983. An Atlas of Past and Present Pollen Maps for Europe, 0-13,000 Years Ago. Cambridge University Press. https://doi.org/10.1016/0034-6667(86)90044-8

Jackson, S.T., 1994. Pollen and spores in Quaternary lake sediments as sensors of vegetation composition: theoretical models and empirical evidence, in: Traverse, A. (Ed.), Sedimentation of Organic Particles. Cambridge University Press, Cambridge, pp. 253–286. https://doi.org/10.1017/CBO9780511524875.015

Jackson, S.T., Williams, J.W., 2004. MODERN ANALOGS IN QUATERNARY PALEOECOLOGY: Here Today, Gone Yesterday, Gone Tomorrow? Annual Review of Earth and Planetary Sciences 32, 495–537. https://doi.org/10.1146/annurev.earth.32.101802.120435

Jacobson, G.L., Bradshaw, R.H., 1981. The selection of sites for paleovegetational studies. Quaternary research 16, 80–96.

Jahns, S., 2007. Palynological investigations into the Late Pleistocene and Holocene history of vegetation and settlement at the Löddigsee, Mecklenburg, Germany. Vegetation History and Archaeobotany 16, 157–169. https://doi.org/10.1007/s00334-006-0074-6

Juggins, S., 2019. rioja: Analysis of Quaternary Science Data.

Kallimanis, A.S., Koutsias, N., 2013. Geographical patterns of Corine land cover diversity across Europe: The effect of grain size and thematic resolution. Progress in Physical Geography 37, 161–177. https://doi.org/10.1177/0309133312465303

Kaplan, J.O., Krumhardt, K.M., Zimmermann, N., 2009. The prehistoric and preindustrial deforestation of Europe. Quaternary Science Reviews 28, 3016–3034. https://doi.org/10.1016/j.quascirev.2009.09.028

Kaplan, J.O., Prentice, I.C., Knorr, W., Valdes, P.J., 2002. Modeling the dynamics of terrestrial carbon storage since the Last Glacial Maximum. Geophys. Res. Lett. 29, 2074. https://doi.org/10.1029/2002GL015230

Kihno, K., Saarse, L., Amon, L., 2011. Late Glacial vegetation, sedimentation and ice recession chronology in the surroundings of Lake Prossa, central Estonia. Estonian Journal of Earth Sciences 60, 147. https://doi.org/10.3176/earth.2011.3.03

Kleinen, T., Tarasov, P., Brovkin, V., Andreev, A., Stebich, M., 2011. Comparison of modeled and reconstructed changes in forest cover through the past 8000 years: Eurasian perspective. The Holocene 21, 723–734. https://doi.org/10.1177/0959683610386980

Kreuz, A., 2007. Closed forest or open woodland as natural vegetation in the surroundings of Linearbandkeramik settlements? Vegetation History and Archaeobotany 17, 51–64. https://doi.org/10.1007/s00334-007-0110-1

Kullman, L., 2002. Boreal tree taxa in the central Scandes during the Late-Glacial: implications for Late-Quaternary forest history. Journal of Biogeography 29, 1117–1124.

Kullman, L., 1992. The ecological status of grey alder (Alnus incana (L.) Moench) in the upper subalpine birch forest of the central Scandes. New phytologist 120, 445–451.

Ladeau, S.L., Clark, J.S., 2006. Pollen production by Pinus taeda growing in elevated atmospheric CO2. Functional Ecology 20, 541–547. https://doi.org/10.1111/j.1365-2435.2006.01133.x

Lafon, T., Dadson, S., Buys, G., Prudhomme, C., 2013. Bias correction of daily precipitation simulated by a regional climate model: a comparison of methods. Int. J. Climatol. 33, 1367–1381. https://doi.org/10.1002/joc.3518

Lambrechts, C., Wilkie, M., Rucevska, I., Sen, M., Conrad, K.M., Joshi, M., Laestadius, L., Løvold, L., Martin, C., Päivinen, R., Smith Olsen, C. (Eds.), 2009. Vital forest graphics. UNEP/GRID-Arendal.

Langgut, D., Almogi-Labin, A., Bar-Matthews, M., Weinstein-Evron, M., 2011. Vegetation and climate changes in the South Eastern Mediterranean during the Last Glacial-Interglacial cycle (86 ka): new marine pollen record. Quaternary Science Reviews 30, 3960–3972. https://doi.org/10.1016/j.quascirev.2011.10.016

Lavigne, C., Godelle, B., Reboud, X., Gouyon, P.H., 1996. A method to determine the mean pollen dispersal of individual plants growing within a large pollen source. TAG Theoretical and Applied Genetics 93, 1319–1326.

Lawson, I., Frogley, M., Bryant, C., Preece, R., Tzedakis, P., 2004. The Lateglacial and Holocene environmental history of the Ioannina basin, north-west Greece. Quaternary Science Reviews 23, 1599–1625. https://doi.org/10.1016/j.quascirev.2004.02.003

Magri, D., 2008. Patterns of post-glacial spread and the extent of glacial refugia of European beech (Fagus sylvatica). Journal of Biogeography 35, 450–463. https://doi.org/10.1111/j.1365-2699.2007.01803.x

Marquer, L., Gaillard, M.-J., Sugita, S., Poska, A., Trondman, A.-K., Mazier, F., Nielsen, A.B., Fyfe, R.M., Jönsson, A.M., Smith, B., Kaplan, J.O., Alenius, T., Birks, H.J.B., Bjune, A.E., Christiansen, J., Dodson, J., Edwards, K.J., Giesecke, T., Herzschuh, U., Kangur, M., Koff, T., Latałowa, M., Lechterbeck, J., Olofsson, J., Seppä, H., 2017. Quantifying the effects of land use and climate on Holocene vegetation in Europe. Quaternary Science Reviews 171, 20–37. https://doi.org/10.1016/j.quascirev.2017.07.001

Marquer, L., Gaillard, M.-J., Sugita, S., Trondman, A.-K., Mazier, F., Nielsen, A.B., Fyfe, R.M., Odgaard, B.V., Alenius, T., Birks, H.J.B., Bjune, A.E., Christiansen, J., Dodson, J., Edwards, K.J., Giesecke, T., Herzschuh, U., Kangur, M., Lorenz, S., Poska, A., Schult, M., Seppä, H., 2014. Holocene changes in vegetation composition in northern Europe: why quantitative pollen-based vegetation reconstructions matter. Quaternary Science Reviews 90, 199–216. https://doi.org/10.1016/j.quascirev.2014.02.013

Marsicek, J., Shuman, B.N., Bartlein, P.J., Shafer, S.L., Brewer, S., 2018. Reconciling divergent trends and millennial variations in Holocene temperatures. Nature 554, 92–96. https://doi.org/10.1038/nature25464

Matthias, I., Giesecke, T., 2014. Insights into pollen source area, transport and deposition from modern pollen accumulation rates in lake sediments. Quaternary Science Reviews 87, 12–23. https://doi.org/10.1016/j.quascirev.2013.12.015

Matthias, I., Nielsen, A.B., Giesecke, T., 2012. Evaluating the effect of flowering age and forest structure on pollen productivity estimates. Veget Hist Archaeobot 21, 471–484. https://doi.org/10.1007/s00334-012-0373-z

Mauri, A., Davis, B.A.S., Collins, P.M., Kaplan, J.O., 2015. The climate of Europe during the Holocene: a gridded pollen-based reconstruction and its multi-proxy evaluation. Quaternary Science Reviews 112, 109–127. https://doi.org/10.1016/j.quascirev.2015.01.013

Mazier, F., Broström, A., Bragée, P., Fredh, D., Stenberg, L., Thiere, G., Sugita, S., Hammarlund, D., 2015. Two hundred years of land-use change in the South Swedish Uplands: comparison of historical map-based estimates with a pollen-

based reconstruction using the landscape reconstruction algorithm. Veget Hist Archaeobot 24, 555–570. https://doi.org/10.1007/s00334-015-0516-0

Mazier, F., Gaillard, M.-J., Kuneš, P., Sugita, S., Trondman, A.-K., Broström, A., 2012. Testing the effect of site selection and parameter setting on REVEALS-model estimates of plant abundance using the Czech Quaternary Palynological Database. Review of Palaeobotany and Palynology 187, 38–49. https://doi.org/10.1016/j.revpalbo.2012.07.017

McDuffee, K.E., Eglinton, T.I., Sessions, A.L., Sylva, S., Wagner, T., Hayes, J.M., 2004. Rapid analysis of ^{13}C in plant-wax *n*-alkanes for reconstruction of terrestrial vegetation signals from aquatic sediments: ANALYSIS OF ^{13}C IN PLANT-WAX *N*-ALKANES. Geochemistry, Geophysics, Geosystems 5, n/a-n/a. https://doi.org/10.1029/2004GC000772

Mitchell, F.J.G., 2005. How open were European primeval forests? Hypothesis testing using palaeoecological data. Journal of Ecology 93, 168–177. https://doi.org/10.1111/j.1365-2745.2004.00964.x

Moracho, E., Moreno, G., Jordano, P., Hampe, A., 2016. Unusually limited pollen dispersal and connectivity of Pedunculate oak (*Quercus robur*) refugial populations at the species' southern range margin. Molecular Ecology 25, 3319–3331. https://doi.org/10.1111/mec.13692

Muñoz Sobrino, C., Ramil-Rego, P., Gómez-Orellana, L., 2004. Vegetation of the Lago de Sanabria area (NW Iberia) since the end of the Pleistocene: a palaeoecological reconstruction on the basis of two new pollen sequences. Vegetation History and Archaeobotany 13, 1–22. https://doi.org/10.1007/s00334-003-0028-1

Nelle, O., Dörfler, W., 2008. A summary of the late-and post-glacial vegetation history of Schleswig-Holstein. Mitteilungen der Arbeitsgemeinschaft Geobotanik in Schleswig-Holstein und Hamburg 65, 45–68.

Nicolussi, K., Kaufmann, M., Patzelt, G., Plicht van der, J., Thurner, A., 2005. Holocene tree-line variability in the Kauner Valley, Central Eastern Alps, indicated by dendrochronological analysis of living trees and subfossil logs. Vegetation History and Archaeobotany 14, 221–234. https://doi.org/10.1007/s00334-005-0013-y

Nielsen, A.B., Giesecke, T., Theuerkauf, M., Feeser, I., Behre, K.-E., Beug, H.-J., Chen, S.-H., Christiansen, J., Dörfler, W., Endtmann, E., Jahns, S., de Klerk, P., Kühl, N., Latałowa, M., Odgaard, B.V., Rasmussen, P., Stockholm, J.R., Voigt, R., Wiethold, J., Wolters, S., 2012. Quantitative reconstructions of changes in regional openness in north-central Europe reveal new insights into old questions. Quaternary Science Reviews 47, 131–149. https://doi.org/10.1016/j.quascirev.2012.05.011

Nielsen, A.B., Odgaard, B.V., 2010. Quantitative landscape dynamics in Denmark through the last three millennia based on the Landscape Reconstruction Algorithm approach. Veget Hist Archaeobot 19, 375–387. https://doi.org/10.1007/s00334-010-0249-z

Overballe-Petersen, M.V., Nielsen, A.B., Bradshaw, R.H.W., 2013. Quantitative vegetation reconstruction from pollen analysis and historical inventory data around a Danish small forest hollow. Journal of Vegetation Science 24, 755–771. https://doi.org/10.1111/jvs.12007

Overpeck, J.T., Webb, T., Prentice, I.C., 1985. Quantitative interpretation of fossil pollen spectra: Dissimilarity coefficients and the method of modern analogs. Quaternary Research 23, 87–108. https://doi.org/10.1016/0033-5894(85)90074-2

Palmieri, A., Dominici, P., Kasanko, M., Martino, L., 2011. Diversified landscape structure in the EU Member States. Eurostat. Statistics in focus 21.

Pantaléon-Cano, J., Yll, E.-I., Pérez-Obiol, R., Roure, J.M., 2003. Palynological evidence for vegetational history in semi-arid areas of the western Mediterranean (Almería, Spain). The Holocene 13, 109–119. https://doi.org/10.1191/0959683603hl598rp

Pardoe, H.S., 2014. Surface pollen deposition on glacier forelands in southern Norway II: Spatial patterns across the Jotunheimen–Jostedalsbreen region. The Holocene 24, 1675–1685.

Peng, C.H., Guiot, J., Campo, E.V., Cheddadi, R., 1995. Temporal and Spatial Variations of Terrestrial Biomes and Carbon Storage Since 13 000 yr BP in Europe: Reconstruction from Pollen Data and Statistical Models, in: Boreal Forests and Global Change. Springer, Dordrecht, pp. 375–390. https://doi.org/10.1007/978-94-017-0942-2_36

Perego, R., Badino, F., Deaddis, M., Ravazzi, C., Vallè, F., Zanon, M., 2011. L'origine del paesaggio agricolo pastorale in nord Italia: espansione di Orlaya grandiflora (L.) Hoffm. nella civiltà palafitticola. Notizie Archeologiche Bergomensi 19, 161–173.

Peyron, O., Guiot, J., Cheddadi, R., Tarasov, P., Reille, M., de Beaulieu, J.-L., Bottema, S., Andrieu, V., 1998. Climatic Reconstruction in Europe for 18,000 YR B.P. from Pollen Data. Quaternary Research 49, 183–196. https://doi.org/10.1006/qres.1997.1961

Pini, R., Ravazzi, C., Raiteri, L., Guerreschi, A., Castellano, L., Comolli, R., 2017. From pristine forests to high-altitude pastures: an ecological approach to prehistoric human impact on vegetation and landscapes in the western Italian Alps. Journal of Ecology. https://doi.org/10.1111/1365-2745.12767

Pirzamanbein, B., Lindström, J., Poska, A., Sugita, S., Trondman, A.-K., Fyfe, R., Mazier, F., Nielsen, A.B., Kaplan, J.O., Bjune, A.E., Birks, H.J.B., Giesecke, T., Kangur, M., Latałowa, M., Marquer, L., Smith, B., Gaillard, M.-J., 2014. Creating spatially continuous maps of past land cover from point estimates: A new statistical approach applied to pollen data. Ecological Complexity 20, 127–141. https://doi.org/10.1016/j.ecocom.2014.09.005

Ponel, P., de Beaulieu, J.L., Tobolski, K., 1992. Holocene paleoenvironment at the timberline in the Taillefer Massif: pollen analysis, study of plant and insect macrofossils. The Holocene 2, 117–130.

Pongratz, J., Reick, C., Raddatz, T., Claussen, M., 2008. A reconstruction of global agricultural areas and land cover for the last millennium. Global Biogeochem. Cycles 22, GB3018. https://doi.org/10.1029/2007GB003153

Potapov, P.V., Turubanova, S.A., Tyukavina, A., Krylov, A.M., McCarty, J.L., Radeloff, V.C., Hansen, M.C., 2015. Eastern Europe's forest cover dynamics from 1985 to 2012 quantified from the full Landsat archive. Remote Sensing of Environment 159, 28–43. https://doi.org/10.1016/j.rse.2014.11.027

Preece, R.C., Coxon, P., Robinson, J.E., 1986. New Biostratigraphic Evidence of the Post-Glacial Colonization of Ireland and for Mesolithic Forest Disturbance. Journal of Biogeography 13, 487. https://doi.org/10.2307/2844814

Prentice, C., Guiot, J., Huntley, B., Jolly, D., Cheddadi, R., 1996. Reconstructing biomes from palaeoecological data: a general method and its application to European pollen data at 0 and 6 ka. Climate Dynamics 12, 185–194.

Prentice, I.C., 1985. Pollen representation, source area, and basin size: toward a unified theory of pollen analysis. Quaternary Research 23, 76–86.

Prentice, I.C., Jolly, D., BIOME 6000 participants, 2000. Mid-Holocene and glacial-maximum vegetation geography of the northern continents and Africa. Journal of Biogeography 27, 507–519. https://doi.org/10.1046/j.1365-2699.2000.00425.x

Prentice, I.C., Parsons, R.W., 1983. Maximum Likelihood Linear Calibration of Pollen Spectra in Terms of Forest Composition. Biometrics 39, 1051–1057. https://doi.org/10.2307/2531338

Ravazzi, C., 2002. Late Quaternary history of spruce in southern Europe. Review of Palaeobotany and palynology 120, 131–177.

Rivas-Martínez, S., Penas, A., Díaz, T.E., 2004. Biogeographic and bioclimatic maps of Europe. Serviços Cartográficos da Universidade de Léon.

Roberts, N., Reed, J.M., Leng, M.J., Kuzucuoğlu, C., Fontugne, M., Bertaux, J., Woldring, H., Bottema, S., Black, S., Hunt, E., others, 2001. The tempo of Holocene climatic change in the eastern Mediterranean region: new high-resolution crater-lake sediment data from central Turkey. The Holocene 11, 721–736.

Robin, V., Rickert, B.-H., Nadeau, M.-J., Nelle, O., 2011. Assessing Holocene vegetation and fire history by a multiproxy approach: The case of Stodthagen Forest (northern Germany). The Holocene 22, 337–346. https://doi.org/10.1177/0959683611423687

Robledo-Arnuncio, J.J., Gil, L., 2005. Patterns of pollen dispersal in a small population of *Pinus sylvestris* L. revealed by total-exclusion paternity analysis. Heredity 94, 13. https://doi.org/10.1038/sj.hdy.6800542

Rossignol-Strick, M., 1995. Sea-land correlation of pollen records in the eastern Mediterranean for the glacial-interglacial transition: biostratigraphy versus radiometric time-scale. Quaternary Science Reviews 14, 893–915.

Rubiales, J.M., García-Amorena, I., Hernández, L., Génova, M., Martínez, F., Manzaneque, F.G., Morla, C., 2010. Late Quaternary dynamics of pinewoods in the Iberian Mountains. Review of Palaeobotany and Palynology 162, 476–491. https://doi.org/10.1016/j.revpalbo.2009.11.008

Sadori, L., Jahns, S., Peyron, O., 2011. Mid-Holocene vegetation history of the central Mediterranean. The Holocene 21, 117–129. https://doi.org/10.1177/0959683610377530

Schwander, J., Eicher, U., Ammann, B., 2000. Oxygen isotopes of lake marl at Gerzensee and Leysin (Switzerland), covering the Younger Dryas and two minor oscillations, and their correlation to the GRIP ice core. Palaeogeography, Palaeoclimatology, Palaeoecology 159, 203–214. https://doi.org/10.1016/S0031-0182(00)00085-7

Seppa, H., 1998. Postglacial trends in palynological richness in the northern Fennoscandian tree-line area and their ecological interpretation. The Holocene 8, 43–53. https://doi.org/10.1191/095968398674096317

Simard, M., Pinto, N., Fisher, J.B., Baccini, A., 2011. Mapping forest canopy height globally with spaceborne lidar. J. Geophys. Res. 116, G04021. https://doi.org/10.1029/2011JG001708

Sobkowiak-Tabaka, I., Kubiak-Martens, L., Okuniewska-Nowaczyk, I., Ratajczak-Szczerba, M., Kurzawska, A., Kufel-Diakowska, B., 2017. Reconstruction of the Late Glacial and Early Holocene landscape and human presence in Lubrza, Western Poland, on the basis of multidisciplinary analyses. Environmental Archaeology 0, 1–14. https://doi.org/10.1080/14614103.2016.1268993

Solovieva, N., Klimaschewski, A., Self, A.E., Jones, V.J., Andrén, E., Andreev, A.A., Hammarlund., D., Lepskaya, E.V., Nazarova, L., 2015. The Holocene environmental history of a small coastal lake on the north-eastern Kamchatka Peninsula. Global and Planetary Change 134, 55–66. https://doi.org/10.1016/j.gloplacha.2015.06.010

Streiff, Ducousso, Lexer, Steinkellner, Gloessl, Kremer, 1999. Pollen dispersal inferred from paternity analysis in a mixed oak stand of Quercus robur L. and Q. petraea (Matt.) Liebl. Molecular Ecology 8, 831–841. https://doi.org/10.1046/j.1365-294X.1999.00637.x

Sugita, S., 2007a. Theory of quantitative reconstruction of vegetation I: pollen from large sites REVEALS regional vegetation composition. The Holocene 17, 229–241. https://doi.org/10.1177/0959683607075837

Sugita, S., 2007b. Theory of quantitative reconstruction of vegetation II: all you need is LOVE. The Holocene 17, 243–257. https://doi.org/10.1177/0959683607075838

Sugita, S., 1994. Pollen Representation of Vegetation in Quaternary Sediments: Theory and Method in Patchy Vegetation. Journal of Ecology 82, 881–897. https://doi.org/10.2307/2261452

Sugita, S., 1993. A Model of Pollen Source Area for an Entire Lake Surface. Quaternary Research 39, 239–244. https://doi.org/10.1006/qres.1993.1027

Sugita, S., Parshall, T., Calcote, R., Walker, K., 2010. Testing the Landscape Reconstruction Algorithm for spatially explicit reconstruction of vegetation in northern Michigan and Wisconsin. Quaternary Research 74, 289–300. https://doi.org/10.1016/j.yqres.2010.07.008

Szerencsits, E., 2012. Swiss Tree Lines - a GIS-Based Approximation. Landscape Online. https://doi.org/10.3097/LO.201228

Talon, B., 2010. Reconstruction of Holocene high-altitude vegetation cover in the French southern Alps: evidence from soil charcoal. The Holocene 20, 35–44. https://doi.org/10.1177/0959683609348842

Tarasov, P., Williams, J.W., Andreev, A., Nakagawa, T., Bezrukova, E., Herzschuh, U., Igarashi, Y., Müller, S., Werner, K., Zheng, Z., 2007. Satellite- and pollen-based quantitative woody cover reconstructions for northern Asia: Verification and application to late-Quaternary pollen data. Earth and Planetary Science Letters 264, 284–298. https://doi.org/10.1016/j.epsl.2007.10.007

Tarasov, P.E., Cheddadi, R., Guiot, J., Bottema, S., Peyron, O., Belmonte, J., Ruiz-Sanchez, V., Saadi, F., Brewer, S., 1998. A method to determine warm and cool steppe biomes from pollen data; application to the Mediterranean and Kazakhstan regions. J. Quaternary Sci. 13, 335–344. https://doi.org/10.1002/(SICI)1099-1417(199807/08)13:4<335::AID-JQS375>3.0.CO;2-A

Telford, R.J., Birks, H.J.B., 2009. Evaluation of transfer functions in spatially structured environments. Quaternary Science Reviews 28, 1309–1316. https://doi.org/10.1016/j.quascirev.2008.12.020

Tessier, L., Beaulieu, J.-L.D., Couteaux, M., Edouard, J.-L., Ponel, P., Rolando, C., Thinon, M., Thomas, A., Tobolski, K., 1993. Holocene palaeoenvironments at the timberline in the French Alps—a multidisciplinary approach. Boreas 22, 244–254. https://doi.org/10.1111/j.1502-3885.1993.tb00184.x

Theuerkauf, M., Couwenberg, J., 2018. ROPES Reveals Past Land Cover and PPEs From Single Pollen Records. Front. Earth Sci. 6. https://doi.org/10.3389/feart.2018.00014

Tinner, W., Ammann, B., Germann, P., 1996. Treeline fluctuations recorded for 12,500 years by soil profiles, pollen, and plant macrofossils in the Central Swiss Alps. Arctic and Alpine Research 131–147.

Tinner, W., Kaltenrieder, P., 2005. Rapid responses of high-mountain vegetation to early Holocene environmental changes in the Swiss Alps. Journal of Ecology 93, 936–947. https://doi.org/10.1111/j.1365-2745.2005.01023.x

Tinner, W., Theurillat, J.-P., 2003. Uppermost Limit, Extent, and Fluctuations of the Timberline and Treeline Ecocline in the Swiss Central Alps during the Past 11,500 Years. Arctic, Antarctic, and Alpine Research 35, 158–169. https://doi.org/10.1657/1523-0430(2003)035[0158:ULEAFO]2.0.CO;2

Tinner, W., van Leeuwen, J.F.N., Colombaroli, D., Vescovi, E., van der Knaap, W.O., Henne, P.D., Pasta, S., D'Angelo, S., La Mantia, T., 2009. Holocene environmental and climatic changes at Gorgo Basso, a coastal lake in southern Sicily, Italy. Quaternary Science Reviews 28, 1498–1510. https://doi.org/10.1016/j.quascirev.2009.02.001

Tinsley, H.M., Smith, R.T., 1974. Surface Pollen Studies Across a Woodland/Heath Transition and Their Application to the Interpretation of Pollen Diagrams. New Phytologist 73, 547–565. https://doi.org/10.1111/j.1469-8137.1974.tb02132.x

Trondman, A.-K., Gaillard, M.-J., Mazier, F., Sugita, S., Fyfe, R., Nielsen, A.B., Twiddle, C., Barratt, P., Birks, H.J.B., Bjune, A.E., Björkman, L., Broström, A., Caseldine, C., David, R., Dodson, J., Dörfler, W., Fischer, E., van Geel, B., Giesecke, T., Hultberg, T., Kalnina, L., Kangur, M., van der Knaap, P., Koff, T., Kuneš, P., Lagerås, P., Latałowa, M., Lechterbeck, J., Leroyer, C., Leydet, M., Lindbladh, M., Marquer, L., Mitchell, F.J.G., Odgaard, B.V., Peglar, S.M., Persson, T., Poska, A., Rösch, M., Seppä, H., Veski, S., Wick, L., 2015. Pollen-based quantitative reconstructions of Holocene regional vegetation cover (plant-functional types and land-cover types) in Europe suitable for climate modelling. Global Change Biology 21, 676–697. https://doi.org/10.1111/gcb.12737

Vera, F.W.M., 2000. Grazing ecology and forest history. CABI Pub, Wallingford, Oxon ; New York, NY.

Vescovi, E., Ravazzi, C., Arpenti, E., Finsinger, W., Pini, R., Valsecchi, V., Wick, L., Ammann, B., Tinner, W., 2007. Interactions between climate and vegetation during the Lateglacial period as recorded by lake and mire sediment archives in Northern Italy and Southern Switzerland. Quaternary Science Reviews 26, 1650–1669. https://doi.org/10.1016/j.quascirev.2007.03.005

Veski, S., Amon, L., Heinsalu, A., Reitalu, T., Saarse, L., Stivrins, N., Vassiljev, J., 2012. Lateglacial vegetation dynamics in the eastern Baltic region between 14,500 and 11,400calyrBP: A complete record since the Bølling (GI-1e) to the Holocene. Quaternary Science Reviews 40, 39–53. https://doi.org/10.1016/j.quascirev.2012.02.013

Walker, M.J., Lowe, J.J., 1990. Reconstructing the environmental history of the last glacial-interglacial transition: evidence from the Isle of Skye, Inner Hebrides, Scotland. Quaternary Science Reviews 9, 15–49.

Wessel, P., Smith, W.H.F., Scharroo, R., Luis, J., Wobbe, F., 2013. Generic Mapping Tools: Improved Version Released. Eos Trans. AGU 94, 409–410. https://doi.org/10.1002/2013EO450001

Whitehouse, N.J., Smith, D.N., 2004. "Islands" in Holocene Forests: Implications for Forest Openness, Landscape Clearance and'Culture-Steppe'Species. Environmental Archaeology 9, 199–208.

Wick, L., 2000. Vegetational response to climatic changes recorded in Swiss Late Glacial lake sediments. Palaeogeography, Palaeoclimatology, Palaeoecology 159, 231–250.

Wick, L., Möhl, A., 2006. The mid-Holocene extinction of silver fir (Abies alba) in the Southern Alps: a consequence of forest fires? Palaeobotanical records and forest simulations. Vegetation History and Archaeobotany 15, 435–444. https://doi.org/10.1007/s00334-006-0051-0

Williams, J.W., 2002. Variations in tree cover in North America since the last glacial maximum. Global and Planetary Change 35, 1–23.

Williams, J.W., Jackson, S.T., 2003. Palynological and AVHRR observations of modern vegetational gradients in eastern North America. The Holocene 13, 485–497. https://doi.org/10.1191/0959683603hl613rp

Williams, J.W., Tarasov, P., Brewer, S., Notaro, M., 2011. Late Quaternary variations in tree cover at the northern forest-tundra ecotone. Journal of Geophysical Research 116. https://doi.org/10.1029/2010JG001458

Williams, J.W., Webb, T., Richard, P.H., Newby, P., 2000. Late Quaternary biomes of Canada and the eastern United States. Journal of Biogeography 27, 585–607. https://doi.org/10.1046/j.1365-2699.2000.00428.x

Woodbridge, J., Fyfe, R.M., Roberts, N., Downey, S., Edinborough, K., Shennan, S., 2014. The impact of the Neolithic agricultural transition in Britain: a comparison of pollen-based land-cover and archaeological 14C date-inferred population change. Journal of Archaeological Science 51, 216–224. https://doi.org/10.1016/j.jas.2012.10.025

Wright, J.W., 1952. Pollen dispersion of some forest trees. Forest Service, U.S. Dept. of Agriculture, Northeastern Forest Experiment Station, Station Paper 46.

Ziska, L.H., Caulfield, F.A., 2000. Rising CO2 and pollen production of common ragweed (Ambrosia artemisiifolia L.), a known allergy-inducing species: implications for public health. Functional Plant Biology 27, 893–898.

PART V

HUMAN-ENVIRONMENT DYNAMICS BETWEEN MIDDLE AND LATE HOLOCENE: AN OVERVIEW OF THE RESULTS

Unraveling climate trajectories

The results presented in Parts II, III and IV offer new opportunities to test the solidity of current archaeological and environmental narratives concerning the northern Italian Bronze Age and neighboring periods. This new data availability is well exemplified by the work conducted at Bande di Cavriana (Part II; Zanon et al., 2019), which represents the very first extensive multi-disciplinary investigation conducted in the southern Lake Garda area for the Mid/Late-Holocene. Multiple similarities between the Bande di Cavriana record (Fig. 5.1), the lake-level curves from Lake Ledro and Lake Accesa (Magny et al., 2012), and southern-alpine flood data (Wirth et al., 2013) provided additional evidences that the transition between Copper and Bronze Age was characterized by marked hydrogeological instability affecting the whole central and northern Italian peninsula. This situation leads to two main observations concerning the onset of the pile-dwelling phenomenon. Primarily, it is apparent that the establishment of a sharp and stable cold/wet downturn occurred already during the final part of the Copper Age and therefore it preceded the mass establishment of lake dwellings. Additionally, the supra-regional nature of this climate shift may exclude that the Lake Garda area was selected by Bronze Age settlers due to its different, more stable climate conditions. Given these considerations, it can be stated that an initial and sudden change in climatic trajectories did not constitute a triggering factor in the emergence of the pile-dwelling phenomenon. Nonetheless, the persistence of fast and steadily changing conditions might have over time led to a tipping point in the residual resilience of local societies, ultimately leading to a radical change in settlement strategies. Give the preference for lacustrine locations, it is reasonable to assume that the presence of water played a role in in the formation of this new settlement system. Yet, the establishment of new pile dwellings appears to be regularly associated with strong eutrophication processes in the hosting water bodies (i.e. sharp transition from calcareous lacustrine sedimentation to fine organic deposits), likely caused by mass dumping of organic waste material directly in the basins (Badino et al., 2011; Dal Corso, 2018; Perego, 2015; Zanon et al., 2019). This practice undoubtedly affected water quality, but it is currently not possible to

determine if and how it affected the health of the local dwellers. The lacustrine settlement of Lavagnone persisted on the same ~10 ha basin for the whole duration of the Bronze Age (de Marinis et al., 2005), suggesting that water quality might not have been a limiting factor. Living in close proximity to water sources might have been desirable for crop cultivation and animal husbandry, therefore accessing this resource through small water bodies -although polluted with organic waste material- could have been more desirable than living in areas more affected by potential hydrogeological instability (e.g. riverside settlements).

The Bande di Cavriana record shows also that the agreement visible between multiple proxies at the Copper Age-Bronze Age transition does not necessarily extend to other parts of the Holocene. A clear example is represented by the warm/arid shift recorded at Bande di Cavriana between ca. 6300 and 6100 years cal. BP (4350-4150 years BC; Fig. 5.1) which, as reported in Part II, is not clearly identifiably in other palaeoclimatic records. In addition, this trend change overlaps with the Rotmoos I cold oscillation (6300-6100 years cal. BP; 4350–4150 years BC) detected in the Central and Eastern Alps (Segnana et al., 2019). The Rotmoos I phase is regarded as equivalent to the western-alpine Piora I cold oscillation (Burga et al., 2001; Segnana et al., 2019) which is dated approximately between 6100 and 5800/5700 years cal. BP (4150 and 3850/3750 years BC; Martinetto et al., 2018; Wick and Möhl, 2006). The importance of the Piora I oscillation within this discussion lies in the fact that it affected vegetation development along part of the southern alpine margin, just 100 km North-West of Bande di Cavriana (Wick and Möhl, 2006). At Bande di Cavriana, the 6300-6100 years cal. BP warm/dry shift is followed by a rather minor cold/wet event between 6100 and 5800 year cal. BP (4150-3850 years BC). This succession of opposite trends and their overlap with the Rotmoos I/Piora I age estimates make it difficult to determine whether the area surrounding Bande di Cavriana behaved consistently with other proxies (i.e. with a cold/wet shift, although rather minor) or if it reacted to this general cold/wet episode with a distinctly opposite trend. A closer agreement should still be noticed concerning the Rotmoos II (5600-5100 years cal. BP; 3650–3150 years BC) and Piora II (5400-4900 years cal. BP; 3450-2950 years BC) cold oscillations (Martinetto et al., 2018; Segnana et al., 2019), both broadly fitting within an accelerating colder/wetter trend at Bande di Cavriana (Fig. 5.1).

While the occurrence and timing of any of these event are not directly relevant to discuss Bronze Age dynamics, they highlight quite convincingly the main pitfalls of correlating distant climate proxies. Dating uncertainties can alter significantly the

interpretation of climate dynamics between neighboring areas, influencing archaeological narratives as a result.

Exploring these intra- and inter-regional climate patterns is one of the primary research targets of Capuzzo et al. (2018), presented in Part III. The approach followed in Capuzzo et al. (2018) is not too dissimilar from the multi-proxy validation procedure conducted at Bande di Cavriana. A primary difference lies in the fact that reference palaeoclimatic curves in Capuzzo et al. (2018) are built from the combination of multiple regional archives rather than from a single site.

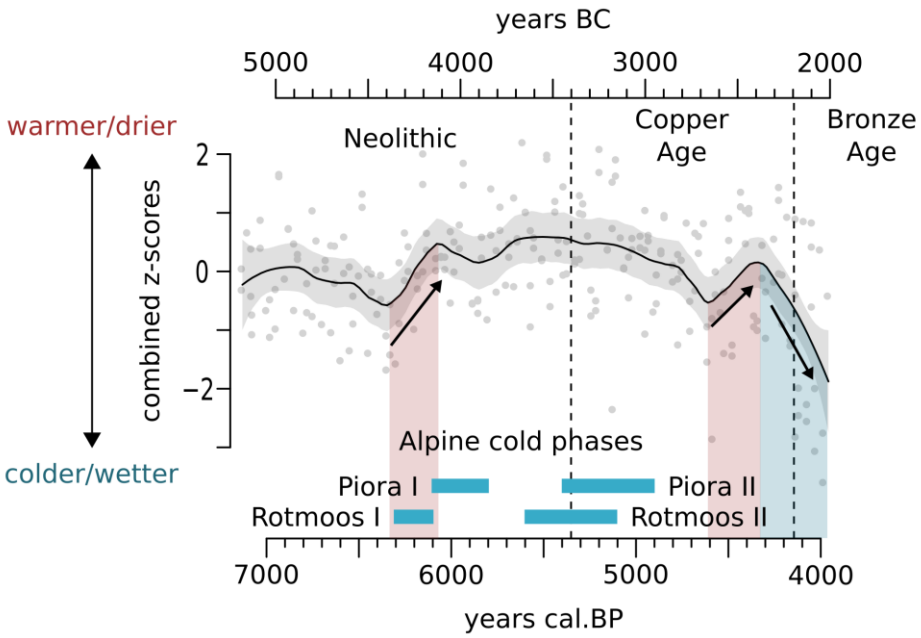

Figure 5.1. *Climate curve from Bande di Cavriana produced from the combination of multiple proxies. The arrows and corresponding vertical shaded areas highlight sharp trend changes. Modified from Zanon et al., (2019). The ages of the Rotmoos and Piora oscillations are taken from Martinetto et al. (2018) and Segnana et al. (2019).*

The results emerging from Capuzzo et al. (2018) cover a wide variety of research topics. From a modeling perspective, they show that simple pollen-based climate reconstructions display visible similarities with independent palaeoenvironmental proxies, and therefore may indeed represent a useful sources of climatic information in contexts where other proxies are not available (provided that good quality data is available, and that vegetation in the target area was sufficiently sensitive to climate fluctuations). Importantly, the consistent behavior of different palaeoclimatic

indicators within central/northern Italy adds more evidences that climate in this area behaved rather homogeneously across both the rise and fall of Bronze Age networks. The comparison with other European regions is particularly valuable, since it makes use of a consistent methodology to show how "climatic deteriorations" might be expressed by different combinations of temperature and precipitation patterns across Europe. These regional differences effectively show how the use of extra-local or extra-regional proxies should always be evaluated with care in the construction of archaeological narratives. Vice-versa, the interpretation of modeled data should always incorporate a critical assessment of the archaeological evidence. The importance of this pairing emerges clearly from the behavior of the Po Plain demographic curve (Fig. 5.2a). Comments on this reconstruction were already included in Part III, yet it might be useful to complement them with a few more considerations. A superficial interpretation of this model may suggest that population decline in the study area began already around 3400 years cal. BP (1450 years BC), within the Middle Bronze Age. This negative trend is indeed tracking a decline in archaeological features, i.e. a steady settlement abandonment. Yet the central Po Plain was far from being devoid of settlements during this period. What does not emerge from the demographic curve is the contemporaneous growth of central dwelling places, which suggests instead a reorganization of the settlement network. In fact, the larger surface occupied by the surviving settlements points to rising population numbers, i.e. the opposite of what the monodimensional demographic model suggests. This aggregation phase is still marked by a shift in climate patterns, as suggested by the onset of a negative precipitation trend (Fig. 5.2b) and by evidence for lowering water tables (Dal Corso, 2018; Dalla Longa et al., 2019; Perego et al., 2011). Climate change might then still have played a role in determining and directing population fluxes, although not (initially) in a destructive way. Mass movements towards central places could be interpreted as evidences for an increased cohesion and social cooperation in order to better face less favorable conditions. This solution lasted until approximately 3150-3100 years cal. BP (1200-1150 years BC), when apparently the carrying capacity of the central Po Plain decreased drastically. The flat behavior of the demographic curve visible in Fig. 5.2a after this date reflects indeed the demise of the Bronze Age settlement networks. The increasingly arid conditions emerging from Fig. 5.2b-c are much in agreement with the current archaeological interpretation (Cremaschi et al., 2016). Yet, alternative and/or aggravating triggers remain currently unexplored. While evidence of conflict/social unrest are currently lacking, a possible role played by epidemics –possibly in relation to high population

densities and active exchange networks- has yet to be investigated. Addressing this issue might help clarifying both the triggers of the Bronze Age collapse and how it unraveled, i.e. whether it resulted in population displacements over long distances or in widespread population die-offs (or both).

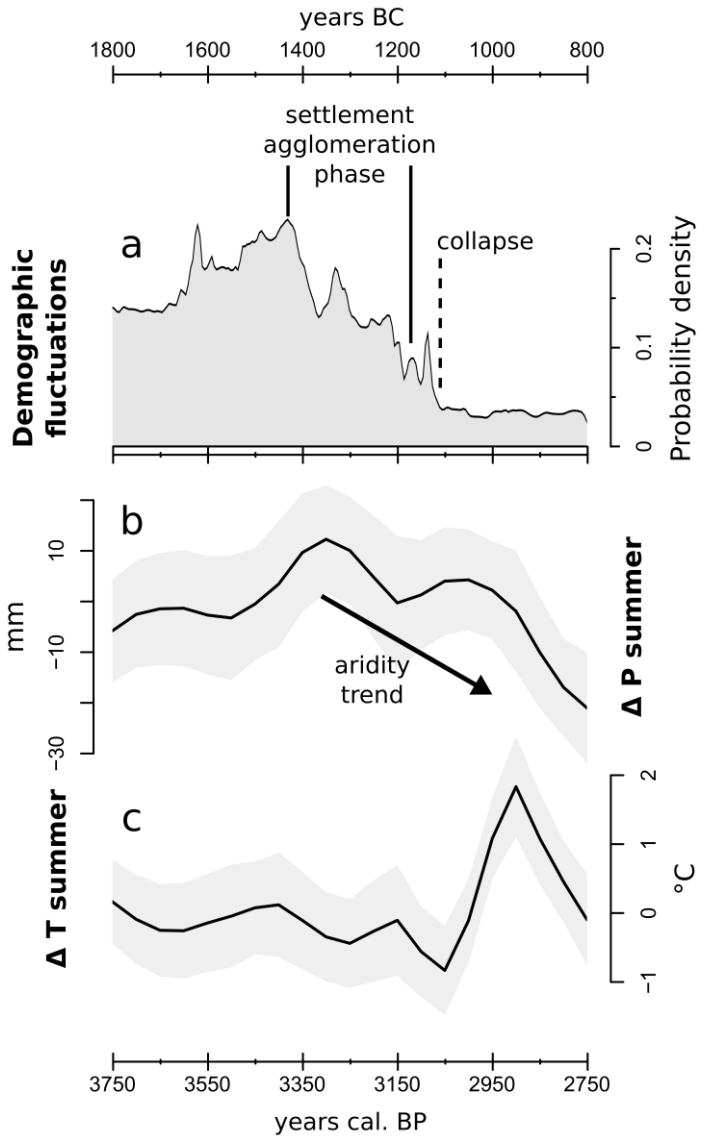

Figure 5.2. *(**a**) Radiocarbon-based demographic curve for the Western and Central Po Plain (N-Italy). Precipitation (**b**) and temperature (**c**) curves derived from northern-Italian pollen data. Modified from Capuzzo et al., (2018).*

Investigating land cover and land use changes

The suitability of a given environment to human occupation is surely not determined by climate alone: resource availability in relation to population growth represents another potential driver of change. The availability of natural resources is not a static parameter across time. Besides 'natural' factors, such as climate and ecological competition, it is widely influenced by access to knowledge, adequate technology (e.g. appropriate hunting, fishing, and farming implements) and availability of human labor (i.e. possibility to accomplish multiple subsistence-related tasks more efficiently and simultaneously). Understanding how and to what scale past societies could exploit their surrounding opens the possibility to investigate new questions, such as to what extent they understood their impact on the environment (e.g. soil erosion and depletion), what measures they put in place to favor sustainable practices (e.g. field rotation, coppicing) and how they understood and protected themselves against unexpected unfavorable circumstances (e.g. repeated harvest failures).

Addressing this complex set of intersecting open issues requires breaking them down into more accessible research questions. A first approach involves understanding how land cover changed through time in relation to human presence in a given area. This information can be readily accessed in qualitative form through pollen analysis, as exemplified by the rise in cropland and pasture indicators at Bande di Cavriana. The expansion of these pollen taxa can be easily interpreted as a reasonable need to establish productive areas to fulfill basic subsistence requirements, yet this relatively superficial reading of the data offers limited information concerning the degree of human impact on the landscape. Specific plant taxa can offer a more complete ecological picture. The rise of *Orlaya grandiflora*, as reported in Part II, represents a fitting example. The preference of this taxon for coarse, well drained substrates does not only suggest a reduction in forested areas. More importantly, it can be linked to increasing soil erosion. Its rising presence might then point to decreasing soil fertility and to the expansion of poor grazing areas for livestock in proximity of the settlement.

Extracting this information from pollen data represent a useful additional step towards a better understanding of possible human-induced stress triggers, yet it remains part of a prominently *qualitative* approach. The construction and evaluation of a *quantitative* land-cover algorithm was pursued extensively in Part IV.

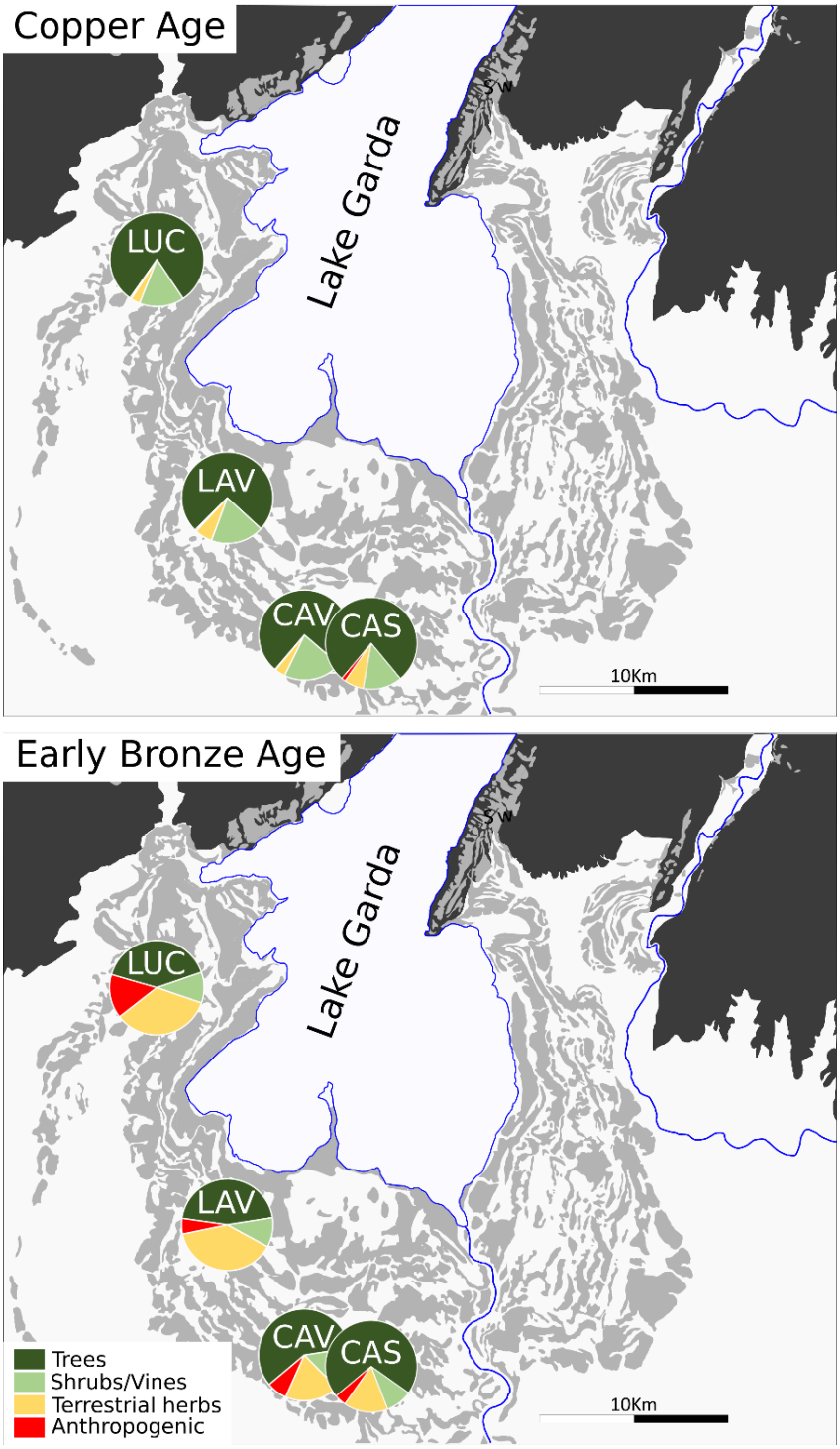

Figure 5.3. *Percentage values of broad palynological classes at four different sites within the southern Lake Garda area. LUC = Lucone di Polpenazze. LAV = Lavagnone di Desenzano del Garda, CAV = Bande di Cavriana, CAS = Castellaro Lagusello. See Fig. 5.4 for the time span covered by each window.*

This modeling method was then applied to four pollen sequences from the Lake Garda area: Bande di Cavriana, Castellaro Lagusello, Lavagnone di Desenzano del Garda and Lucone di Polpenazze. Pollen data from Castellaro Lagusello was provided by M. Dal Corso (Kiel University), while C. Ravazzi, F. Badino and G. Furlanetto (CNR-IDPA, Milano, Italy) provided pollen counts from Lucone and Lavagnone. The pollen diagrams from Lucone and Lavagnone have been only partially published and can't be presented in full within this dissertation. For this reason, pollen data from all locations are shown only in condensed form in Fig. 5.3. As with Bande di Cavriana, all these sites show a pre-Bronze Age situation dominated by arboreal pollen species, with only minimal anthropic interference. The establishment of pile-dwelling settlements, occurring with slightly different timing at each site, is consistently marked by a rapid change in floristic composition. In order to investigate this abrupt transition, forest cover modeling was performed for each site using all samples dated between 5350 and 3500 years cal. BP (3400-1550 years BC). All modeled data was then aggregated and LOESS-smoothed to obtain a regional forest cover curve. The results of this elaboration are presented in Fig. 5.4. A notable difference is indeed visible between the Copper Age, with value between 70% and 90%, and the Bronze Age, where forest cover drops sharply to 10-30%. This abrupt change is consistent with the hypothesis that the expansion of pile-dwelling villages had unprecedented effects on the regional land cover, yet any conclusion derived from this modeling exercise should be taken with due caution. Any land-cover reconstruction model can be applied rather mechanically and acritically to a give set of data. Modeling algorithms are not intrinsically able to discriminate between different depositional contexts, sampling procedures or anomalous pollen assemblages. It is up to the analyst to determine whether the quality of fossil and/or training samples is appropriate to reconstruct a desired environmental parameter. External constraints and filters, such as those based on minimum pollen counts or appropriate sampling contexts, can be incorporated in the modeling algorithm in order to improve its reliability. Yet, the extent to which such procedures can be applied depends entirely on the quality of any accompanying metadata available for each sample. This issue is particularly relevant for the forest-cover reconstruction attempted in Fig. 5.4, since multiple uncertainties concerning local pollen deposition still remain to be addressed. All Bronze Age pollen sequences available in the Lake Garda area were collected at a relatively short distance from archeological dwelling layers. It might then be reasonable to assume that at least part of the pollen contained in these records is not a product of 'natural' transport (e.g. atmospheric deposition or carried by runoff water), but a result of near-site

anthropic activities (e.g. cereal processing, dumping of waste material; Karg, 1996; Robinson and Hubbard, 1977). Non-arboreal pollen represents the main component of these anthropic pollen sources, possibly leading to an under-representation of arboreal taxa. From a modeling perspective, this situation would result in an inflated reconstruction of non-forested areas. The production of such spurious results, stemming directly from "tainted" raw pollen counts, would not depend on the modeling algorithm used and therefore should not be regarded as affecting exclusively the analogue-based approach presented in Part IV.

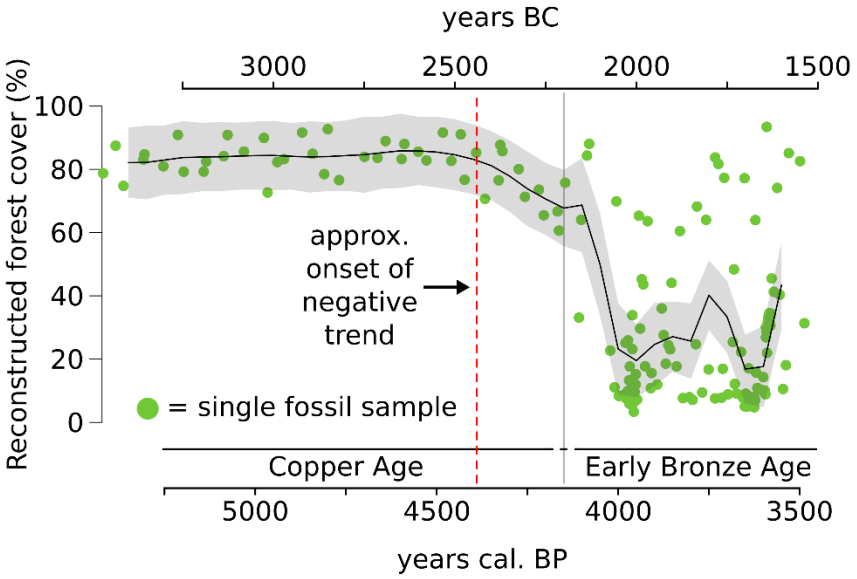

Figure 5.4. *Forest cover in the southern Lake Garda region reconstructed via Modern Analogue Technique.*

It is currently not possible to determine to which extent this issue may have affected the pollen records included in Fig. 5.4. The massive drop in forest cover does not represent an unrealistic reconstruction, since Bronze Age dwellers undoubtedly had need for timber, pastures and croplands. Yet it should be more cautiously regarded as a sort of "worst case scenario". This land-cover model, although not conclusive, represents a valuable starting point to initiate a discussion on quantitative vegetation reconstructions in the area. Possible future developments might involve targeted pollen analysis conducted at variable distances from Bronze Age settlement layers in order to determine how proximity to the settlements affects pollen deposition. Ideally, these near-site investigations should be complemented by off-site data (i.e. from

basins that did not host villages along their shores or immediate vicinities) in order to test the modeling algorithm in contexts with negligible human interference. Importantly, the value of the forest cover model presented in Fig. 5.4 is not limited to its application to Bronze Age samples. The absence of (known) Copper Age settlements along the shores of the investigated basins makes them suitable to discuss modeled vegetation dynamics for this period with a higher degree of confidence. Most notably, forest cover percentages appear to acquire a slight negative trend already from ca. 4300 years cal. BP (2350 years BC). This boundary coincides with the onset of cold/wet conditions visible at the Bande di Cavriana (Fig. 5.1), suggesting that climate change had a visible effect on vegetation density. This newly documented behavior adds a new and unexplored layer of complexity to the onset of the pile-dwelling phenomenon. Speculatively, it is possible that a gradual reduction in arboreal vegetation cover over time might have contributed to make the area more accessible to Bronze Age settlers. This factor, combined with others (e.g. self-evident preference for wetland sites), might have promoted the widespread rise of lake-dwellings in the Lake Garda area.

Bibliography

Badino, F., Baioni, M., Castellano, L., Martinelli, N., Perego, R., Ravazzi, C., 2011. Foundation, development and abandoning of a Bronze Age pile-dwelling ("Lucone d", Garda Lake) recorded in the palynostratigraphic sequence of the pond offshore the settlement. Il Quaternario e Italian Journal of Quaternary Sciences 24.

Burga, C.A., Perret, R., Zoller, H., 2001. Swiss localities of early recognized Holocene climate oscillations Characterization and significance. Vierteljahrsschrift der Naturforschenden Gesellschaft in Zürich.

Capuzzo, G., Zanon, M., Dal Corso, M., Kirleis, W., Barceló, J.A., 2018. Highly diverse Bronze Age population dynamics in Central-Southern Europe and their response to regional climatic patterns. PLOS ONE 13, e0200709. https://doi.org/10.1371/journal.pone.0200709

Cremaschi, M., Mercuri, A.M., Torri, P., Florenzano, A., Pizzi, C., Marchesini, M., Zerboni, A., 2016. Climate change versus land management in the Po Plain (Northern Italy) during the Bronze Age: New insights from the VP/VG sequence of the Terramara Santa Rosa di Poviglio. Quaternary Science Reviews 136, 153–172. https://doi.org/10.1016/j.quascirev.2015.08.011

Dal Corso, M., 2018. Environmental history and development of the human landscape in a northeastern Italian lowland during the Bronze Age: a multidisciplinary case-study (PhD Thesis). Kiel University.

Dalla Longa, E., Dal Corso, M., Vicenzutto, D., Nicosia, C., Cupitò, M., 2019. The Bronze Age settlement of Fondo Paviani (Italy) in its territory. Hydrography, settlement distribution, environment and in-site analysis. Journal of Archaeological Science: Reports 28, 102018. https://doi.org/10.1016/j.jasrep.2019.102018

de Marinis, R.C., Rapi, M., Ravazzi, C., Arpenti, E., Deaddis, M., Perego, R., 2005. Lavagnone (Desenzano del Garda): new excavations and palaeoecology of a Bronze Age pile dwelling site in northern Italy, in: Della Casa, Ph., Trachsel, M. (Eds.), Wetland Economies and Societies. Proceeding of the International Conference in Zurich, Zurich, 10-13 March 2004. Collectio Archæologica 3, 221-232.

Karg, S., 1996. Winter- and Spring-foddering of Sheep/Goat in the Bronze Age Site of Fiavè-Carera, Northern Italy. Environmental Archaeology 1, 87–94. https://doi.org/10.1179/146141096790605786

Magny, M., Joannin, S., Galop, D., Vannière, B., Haas, J.N., Bassetti, M., Bellintani, P., Scandolari, R., Desmet, M., 2012. Holocene palaeohydrological changes in the northern Mediterranean borderlands as reflected by the lake-level record of Lake Ledro, northeastern Italy. Quaternary Research 77, 382–396. https://doi.org/10.1016/j.yqres.2012.01.005

Martinetto, E., Peduzzi, R., Ajassa, R., Buffa, G., Castellano, S., Gianotti, F., Vescovi, E., 2018. Scoperta di macrofossili vegetali (4.8-4.7 ka cal BP) al Lago Cadagno nell'ambito delle attività dei Naturalisti dell'Università di Torino in Val Piora (Canton Ticino, Svizzera). Bollettino della Società ticinese di scienze naturali 106, 12.

Perego, R., 2015. Contribution to the development of the Bronze Age plant economy in the surrounding of the Alps: an archaeobotanical case study of two Early and Middle Bronze Age sites in northern Italy (Lake Garda region). University of Basel.

Perego, R., Badino, F., Deaddis, M., Ravazzi, C., Vallè, F., Zanon, M., 2011. L'origine del paesaggio agricolo pastorale in nord Italia: espansione di Orlaya grandiflora (L.) Hoffm. nella civiltà palafitticola. Notizie Archeologiche Bergomensi 19, 161–173.

Robinson, M., Hubbard, R.N.L.B., 1977. The transport of pollen in the bracts of hulled cereals. Journal of Archaeological Science 4, 197–199. https://doi.org/10.1016/0305-4403(77)90067-X

Segnana, M., Oeggl, K., Poto, L., Gabrieli, J., Festi, D., Kofler, W., Cesco Frare, P., Zaccone, C., Barbante, C., 2019. Holocene vegetation history and human impact in the eastern Italian Alps: a multi-proxy study on the Coltrondo peat bog, Comelico Superiore, Italy. Veget Hist Archaeobot. https://doi.org/10.1007/s00334-019-00749-y

Wick, L., Möhl, A., 2006. The mid-Holocene extinction of silver fir (Abies alba) in the Southern Alps: a consequence of forest fires? Palaeobotanical records and forest simulations. Vegetation History and Archaeobotany 15, 435–444. https://doi.org/10.1007/s00334-006-0051-0

Wirth, S.B., Glur, L., Gilli, A., Anselmetti, F.S., 2013. Holocene flood frequency across the Central Alps – solar forcing and evidence for variations in North Atlantic atmospheric circulation. Quaternary Science Reviews 80, 112–128. https://doi.org/10.1016/j.quascirev.2013.09.002

Zanon, M., Unkel, I., Andersen, N., Kirleis, W., 2019. Palaeoenvironmental dynamics at the southern Alpine foothills between the Neolithic and the Bronze Age onset. A multi-proxy study from Bande di Cavriana (Mantua, Italy). Quaternary Science Reviews 221, 105891. https://doi.org/10.1016/j.quascirev.2019.105891

Appendix I

The site of Bande di Cavriana, presented in Part II, was not the only location probed for sediment samples. Coring operations were conducted at four other sites within the southern Lake Garda area: Grezze, Polecra pond, Ca' Nove and Lake Frassino (Fig. S1.1). Following an initial assessment, none of these location were chosen for comprehensive palaeoecological investigations. The reasons behind these choices are presented here together with a synthesis of the data collected at each site.

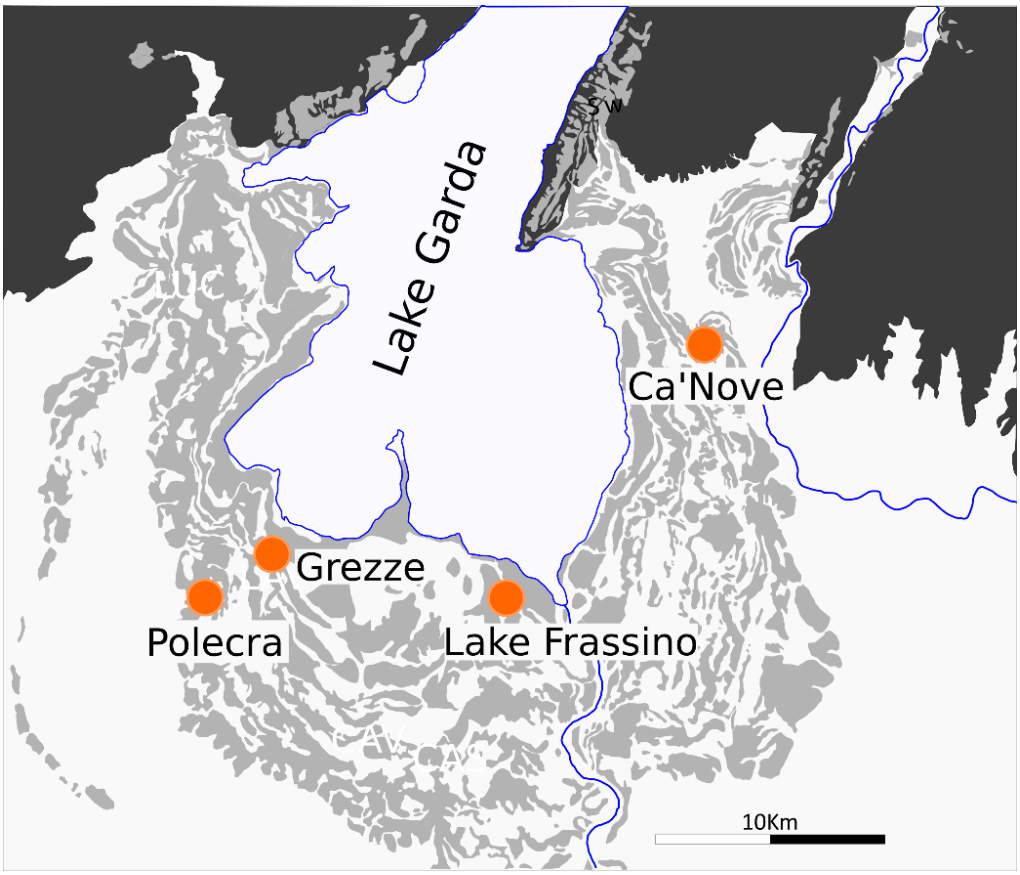

Figure S1.1. *Position of additional coring sites within the southern Lake Garda area.*

Grezze

Coordinates (WGS84): Latitude: 45.4539° - Longitude: 10.5369°

This name identifies here a small, unnamed wetland located on the outskirts of the municipality of Desenzano del Garda, along Via Grezze (Fig. S1.2). Several characteristics made Grezze a desirable location for palaeoecological analysis within this project. This wetland does not hosts (known) Bronze Age dwelling remains, suggesting that it may have been a suitable location for off-sites pollen analysis. Its proximity to the site of Lavagnone (located ca. 2 km to the south of Grezze) would have made it also optimal to investigate land use in the immediate neighborhood of a major pile-dwelling settlement.

Figure S1.2. *Coring location at the site of Grezze, within the municipality of Desenzano del Garda. Photo source: GoogleEarth.*

Corings at Grezze took place in 2013. Approximately 1.5 m or stratigraphy were recovered before reaching the coarse substrate of glacial origin. The bottom 10 cm of the sequence are composed by gray/light blue clay. This layer is followed by ca. 65 cm of silty fine organic deposits with varying concentrations of woody root remains. The most superficial portion was composed by topsoil abundantly disturbed by modern root systems. Eight sediment samples were prepared for pollen analysis following the same procedure described in Part II for Bande di Cavriana.

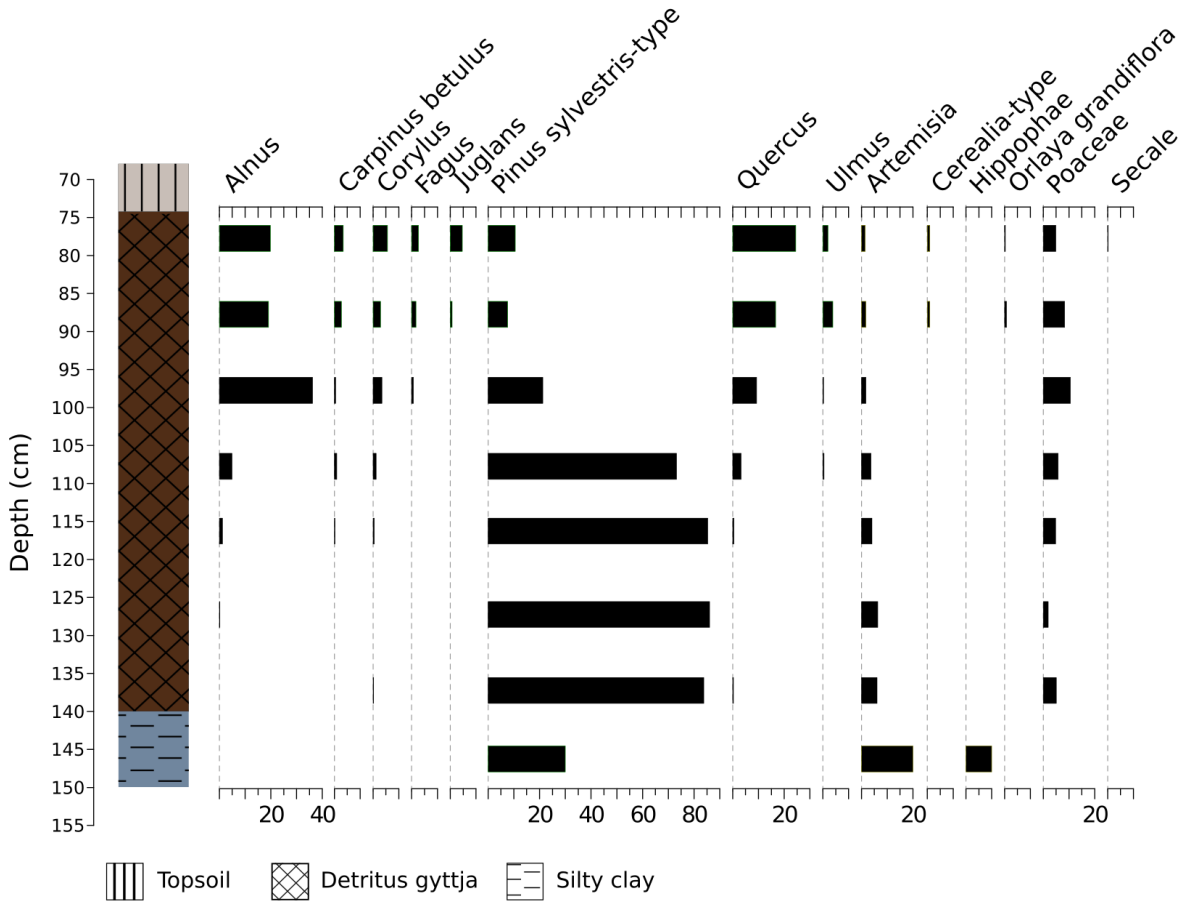

Figure S1.3. *Grezze pollen diagram. Simplified lithology and percentage values of selected taxa.*

A minimum of 400 pollen grains of terrestrial taxa were counted for samples collected from the organic sediment layer. The only sample coming from the basal clay deposit revealed an extremely poor pollen content, therefore the counting procedure was halted after 20 grains.

The percentages of the most diagnostic taxa recoded along the sequence are presented in Fig. S1.3. The initial dominance of *Pinus* in the bottom half of the organic layer suggests a Late Pleistocene origin, as visible in the Lucone and Manerba sequences (Ravazzi et al., 2014; Valsecchi et al., 2006), followed then by the Holocene rise of mixed deciduous forest taxa (e.g. *Alnus*, *Quercus* and *Corylus)*. The two most superficial samples are characterized by the expansion of *Carpinus betulus* and *Juglans*, and by traces of *Orlaya grandiflora* and *Secale*. These indicator taxa, as discussed in Part II, suggest that the top ca. 20 cm of this sequence might envelop a time span ranging from the onset of the Copper age to the Roman period, i.e. more than 3000 years. Such a low sedimentation rate, coupled with the high amount of woody rots clumps, made the sequence unsuitable for high-resolution sampling and analysis.

Polecra Pond

Coordinates (WGS84): Latitude: 45.436543° - Longitude: 10.495638°

Polecra Pond (Italian: *Laghetto di Polecra*) is a small water body located approximately 2-3 km South of the municipality of Lonato (Fig. S1.4). The old age of the pond is possibly supported by three distinct areas with Upper-Paleolithic artefacts discovered along the northwestern part of the basin (de Marinis, 2000). A noteworthy characteristic of this water body lies in the fact that, despite being located at the summit of a moraine ridge, its water level does not appear to vary significantly during the year (Frattini, 2008). These characteristics, together with the absence of other (known) archaeological traces along its shores, made Polecra Pond a possible candidate for the recovery of a pollen sequence unaffected by human disturbance during the Bronze Age. Corings at Polecra Pond took place in 2013. Multiple test corings were conducted right on the shoreline, all of which either resulted in the recovery of clearly reworked material or were interrupted by unpassable coarse deposits.

Figure S1.4. *Approximate outline of Polecra Pond. Photo source: GoogleEarth.*

After being informed more precisely about the nature of palynological investigations (i.e. specifically mentioning the need for undisturbed stratigraphic sequences), the

owner of Polecra Pond recalled that in the recent past (second half of the last century) the lake was temporarily drained in an attempt to identify its water source and exploit it for agricultural purposes. In the (unsuccessful) pursuit of this task, the infilling of the lake was removed with a mechanical excavator. Furthermore, a paved road -now entirely covered by soil- was build around the shore in order to consolidate it and to allow driving cars right around the lake. These previously unknown details are reported here to prevent similar unsuccessful coring attempts during future field campaigns. Frattini (2008) reports that until few decades ago the pond had a much wider and elliptic outline, with the current conformation being the result of reclamation processes. The exact timing of all these disturbance events has not been investigated further within this project. Given the available information, it is possible that part of the basin infilling might still lay intact beneath the reclamation layer.

Ca' Nove

Coordinates (WGS84): Latitude: 45.534899° - Longitude: 10.771809°

The Ca' Nove wetland is located South of the municipality of Cavaion Veronese (Fig. S1.5). This site was selected as a potential candidate to investigate Bronze Age man-environment interactions along the Eastern side of the Lake Garda moraine complex, given that no palynological sequences are currently available from this area. Bronze Age pile-dwelling remains were discovered within this basin towards the end of the last century (Salzani et al., 1988). Contextual stratigraphic investigations and preliminary palynological data suggested a good potential for more detailed palaeoecological analysis (Salzani et al., 1988).

Figure S1.5. *Coring location at the site of Ca' Nove, right South of the municipality of Cavaion Veronese. Photo source: GoogleEarth.*

In more recent times, large portions of the stratigraphy were damaged during an extensive attempt at making the basin exploitable for economic purposes (reportedly, due to reclamation procedures or during the excavation of an artificial fishing pond). A strip of land extending from the shoreline towards the center of the wetland was consolidated with coarse materials and used as a base for a mechanical excavator, leaving the stratigraphy underneath it allegedly untouched (information provided by M. Parolotti, discoverer of the Bronze Age dwelling and director of the local

archaeological museum). A test coring (code: CAN1) was performed in this residual area in 2014, leading to the recovery of ca. 2 m of sediment. Coring operations were interrupted before reaching the coarse moraine deposits.

The stratigraphy of core CAN1 can be described as follows:

0-55 cm: reworked gravel and silt

55-90 cm: sandy silt

90-121 cm: minerogenic mud with high organic component

121-151 cm: clay with sparse pebbles

151-185 cm: peat at varying stages of decomposition

185-200 cm: highly decomposed peat/fine detritus gyttja

200-205 cm: peat layer

205-258 cm: coarse detritus gyttja with abundant mollusk remains

This sequence bears some similarities with core S2 from Salzani et al. (1988), which was collected approximately in the same area, although it was not possible to determine its precise location.

Six pollen samples were analyzed along the CAN1 sequence, with a minimum pollen sum ranging between 100 and 250 grains of terrestrial species. Sample preparation and identification followed the methodology described in Part II. Percentage values of the most diagnostic taxa are presented in Fig. S1.6. The pollen assemblage of the bottom three samples is compatible with the composition of Early/Mid Holocene mixed deciduous forests (Valsecchi et al., 2006). The *Carpinus betulus* content of the following sample (164 cm), paired with its lack of anthropogenic indicators, would conservatively place it between 6000 and 4150 years cal. BP (4050-2200 years BC). Highly indicative is the presence of *Orlaya grandiflora* in the two most superficial samples, which strongly points to a transition into the Bronze Age (see Part II for specific considerations on *Carpinus, Orlaya* and other local biostratigraphic markers). These two topmost samples are also characterized by diluted pollen content and poor preservation. The mineral deposits between 121 and 151 cm can be compared with a distinctly anthropogenic layer described approximately at the same depth by Salzani et al. (1988) in their S2 core. Contrary to the situation in core S2, no visible cultural remains were detected in CAN1, yet an anthropic origin of the clay layer might reasonably explain its high percentages of *O. grandiflora* and Cerealia-type grains.

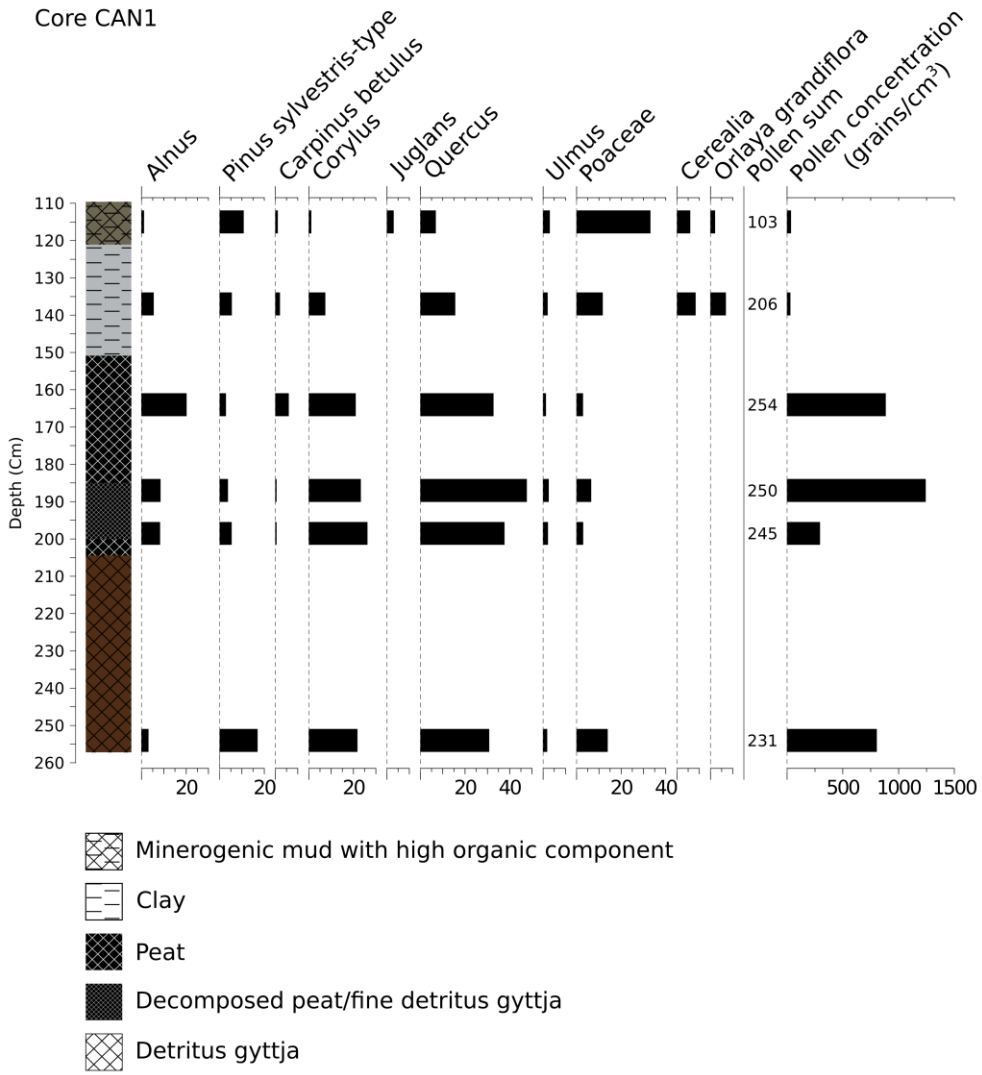

Figure S1.6. *Ca' Nove pollen diagram. Simplified lithology, percentages of selected taxa, pollen sum and concentration values.*

The Bronze Age layers of core CAN1 might then potentially reflect an on-site situation, rather than a near-site one. On-site contexts are more challenging to investigate compared to near- or off-site situations. Human activities which occurred directly at the sampling site might have variously interfered with pollen and sediment accumulation (e.g. with removal of material due to periodic cleaning of dwelling areas, or through abrupt accumulation of material in order to consolidate the damp ground). Given the poor pollen preservation of the Bronze Age layers from core CAN1, and considering the challenges involved in determining their formation processes, the site of Ca' Nove was not selected for more detailed investigations within this project.

Lake Frassino

Coordinates (WGS84): Latitude: 45.432635° - Longitude: 10.662750°

Lake Frassino is the largest lake in the area after Lake Garda itself. Neolithic remains are documented in proximity of its northern shore (Spadoni, 1973), yet this site is mostly known for its Bronze Age record. The earlies pile-dwelling remains within the basin are dendrochronology dated to 3659 ± 10 years cal. BP (1709 ± 10 years BC; Martinelli, 2007). Given the excellent preservation of its waterlogged cultural layers, the Bronze Age settlement from Lake Frassino was among those included in the serial UNESCO World Heritage site "Prehistoric Pile Dwellings around the Alps" (World Heritage Committee, 2011).

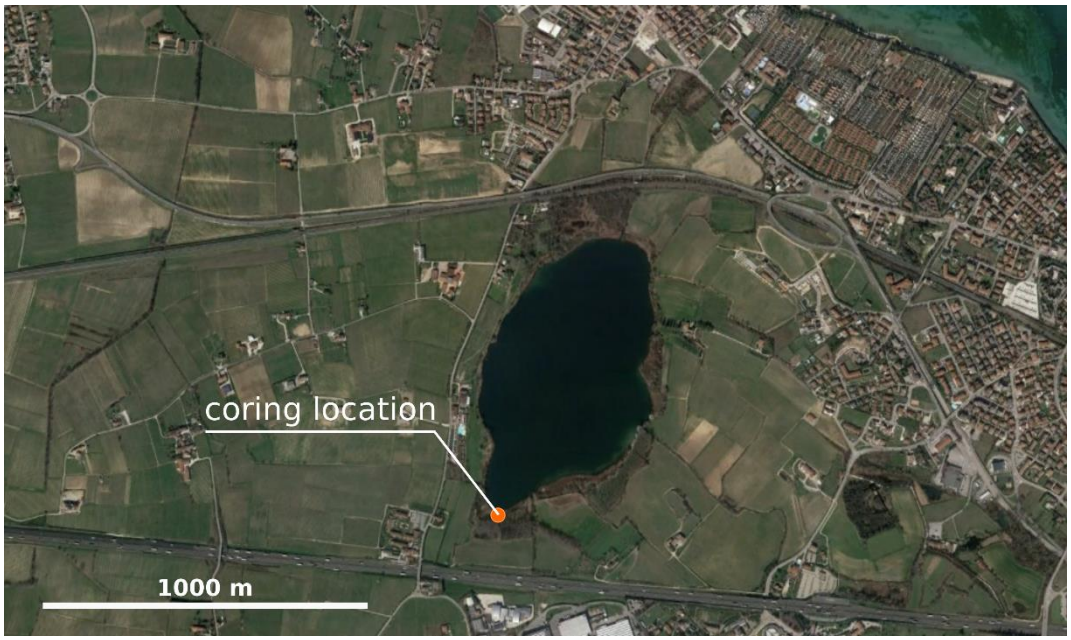

Figure S1.7. *Coring location at Lake Frassino. Photo source: GoogleEarth.*

The stratigraphy of Lake Frassino was described by Baroni et al. (2006). The documented presence of an interrupted sedimentary sequence extending from the Lateglacial to the present day made this site a particularly attractive location for palaeoenvironmental analysis. Exploratory corings were performed in 2014 in the southernmost part of the basin (Fig. S1.7), approximately in the same area investigated in Baroni et al. (2006). Two sequences, FRA1 and FRA2, were retrieved, reaching a maximum depth of four meters. The maximum depth achievable was determined uniquely by time constraints. The sedimentary sequence is primarily composed by

carbonate deposits and detritus gyttja layers. A composite stratigraphic column based on both cores is presented in Fig. S1.8. Pollen analysis was performed on 16 samples. Sediment preparation and pollen identification procedures followed the methodology presented in Part II. Fig. S1.8 shows a selection of the most diagnostic pollen taxa, together with the position of radiocarbon dated materials collected along the cores. Radiocarbon dating results are listed in Tab. S1.1. No other datable material was retrieved. The bottom of the sequence is dated to the first part of the Middle Bronze Age, approximately only one and a half century after the establishment of the Frassino pile-dwelling.

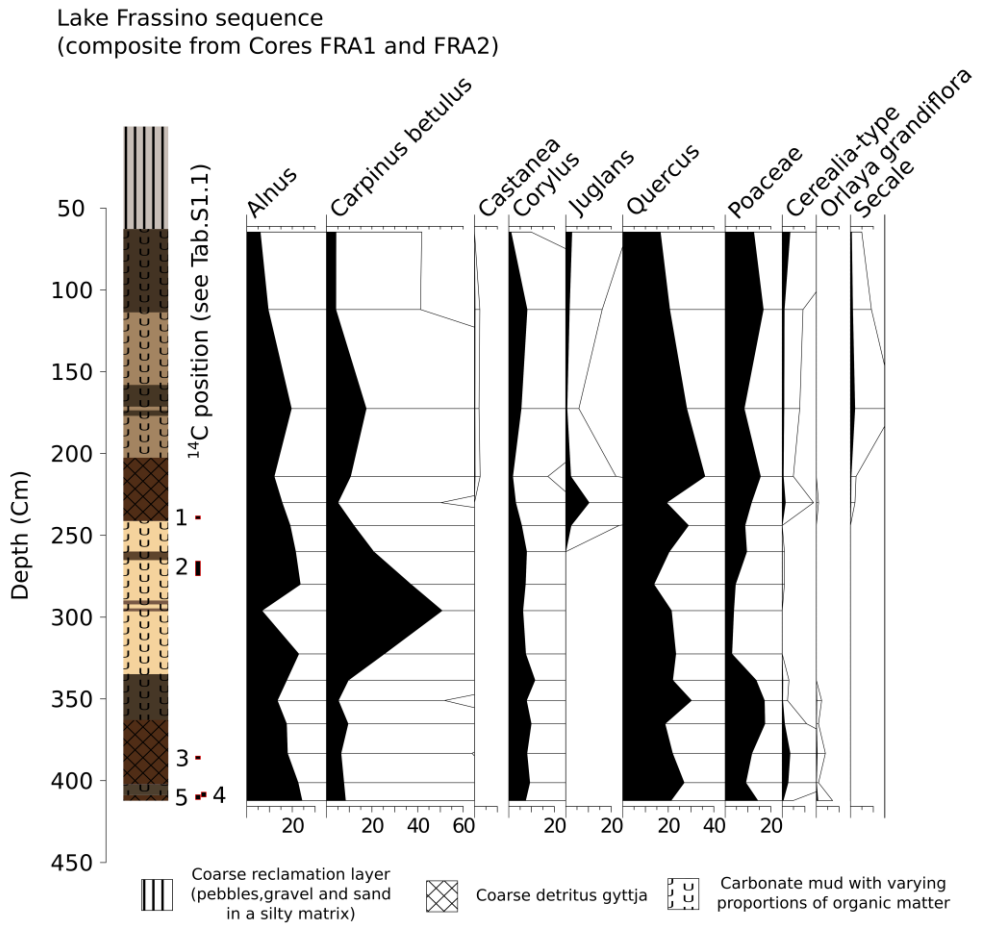

Figure S1.8. *Lake Frassino sequence. Simplified lithology, percentages of selected taxa, and position of dated material.*

The pollen curves in Fig. S1.8 clearly show a decline in anthropogenic taxa (Cerealia-type and *Orlaya grandiflora*) after ca. 380 cm, possibly linked to the abandonment of the Frassino settlement and to the end of the Bronze Age pile-dwelling phenomenon.

The relatively limited number of available datings allowed to produce only a basic linear age-depth model across this abandonment phase. Such solution was considered not sufficiently reliable, given that the many lithological changes suggest instead a succession of rather different sedimentation rates. In addition. it is unclear whether dating number 3, which is considerably older than datings 1 and 2, belongs to a littoral woody taxon affected by hard-water effect, or if it should be interpreted as reworked material. Given these challenges, it was judged not possible to insert any land-cover/land-use narrative into a convincing chronological framework.

Table S1.1. *Radiocarbon dating from the Lake Frassino cores.*

Number in Fig. S1.8	Lab. Code	Uncalibrated ^{14}C Age	Calibrated Age cal. BP (2σ range)	Median age (years cal. BP)	Material
1	Poz-66042	1920 ± 35 BP	1948-1740	1868	Leaf fragments. *Alnus* twigs, *Alnus* catkin fragments, *Alnus* seeds.
2	Poz-73742	2225 ± 35 BP	2330-2152	2230	*Rubus sp.* seeds
3	Poz-66252	3395 ± 35 BP	3811-3563	3640	Twig
4	Poz-69226	3280 ± 35 BP	3586-3407	3510	*Alnus* sp. twig
5	Poz-66251	3270 ± 35 BP	3575-3403	3502	Twig, probably *Alnus* sp.

This sequence was not selected for more detailed investigations, yet the available data contain nonetheless precious information. The onset of a stable occurrence of multiple marker taxa, such as *Juglans*, *Castanea* and *Secale,* is not well documented or well dated so far in the Lake Garda area. Their rise is clearly traceable in the Frassino diagram. This sequence might offer the opportunity to trace the local vegetation history with a resolution not achievable at any other know site.

Bibliography

Baroni, C., Zanchetta, G., Fallick, A.E., Longinelli, A., 2006. Mollusca stable isotope record of a core from Lake Frassino, northern Italy: hydrological and climatic changes during the last 14 ka. The Holocene 16, 827–837. https://doi.org/10.1191/0959683606hol975rp

de Marinis, R., 2000. Il Museo civico archeologico Giovanni Rambotti di Desenzano del Garda una introduzione alla preistoria del lago di Garda. Città di Desenzano del Garda, Assessorato alla Cultura, Desenzano del Garda.

Frattini, S., 2008. Zone umide della pianura bresciana e degli antiteatri morenici dei laghi d'Iseo e di Garda (Provincia di Brescia, Regione Lombardia), Monografie di "Natura Bresciana." Museo civico di scienze naturali di Brescia.

Martinelli, N., 2007. Dendrocronologia delle palafitte dell'area gardesana: situazione delle ricerche e prospettive. Contributi di archeologia in memoria di Mario Mirabella Roberti. Atti del XVI Convegno Archeologico Benacense (Cavriana, 15–16 October 2005). Annali Benacensi XIII–XIV 103–20.

Ravazzi, C., Pini, R., Badino, F., De Amicis, M., Londeix, L., Reimer, P.J., 2014. The latest LGM culmination of the Garda Glacier (Italian Alps) and the onset of glacial termination. Age of glacial collapse and vegetation chronosequence. Quaternary Science Reviews 105, 26–47. https://doi.org/10.1016/j.quascirev.2014.09.014

Salzani, L., Balista, C., Leonardi, G., D'Alessandro, M., Chelidonio, G., Belluzzo, G., Rizzetto, G., 1988. Prime indagini archeologiche, geoarcheologiche e paleoambientali a Ca'Nove di Cavaion Veronese. Quaderni di Archeologia del Veneto 4, 203–229.

Spadoni, F., 1973. Laghetto del Frassino. Materiali neoliti ci (Peschiera-Verona). Preistoria Alpina 9, 265–267.

Valsecchi, V., Tinner, W., Finsinger, W., Ammann, B., 2006. Human impact during the Bronze Age on the vegetation at Lago Lucone (northern Italy). Vegetation History and Archaeobotany 15, 99–113. https://doi.org/10.1007/s00334-005-0026-6

World Heritage Committee, 2011. Decisions adopted by the World Heritage Committee at its 35th session (No. WHC-11/35.COM/20). UNESCO, Paris.

Appendix II

This section contains the supplementary material for the research article "Palaeoenvironmental dynamics at the southern Alpine foothills between the Neolithic and the Bronze Age onset. A multi-proxy study from Bande di Cavriana (Mantua, Italy)", presented in Part II.

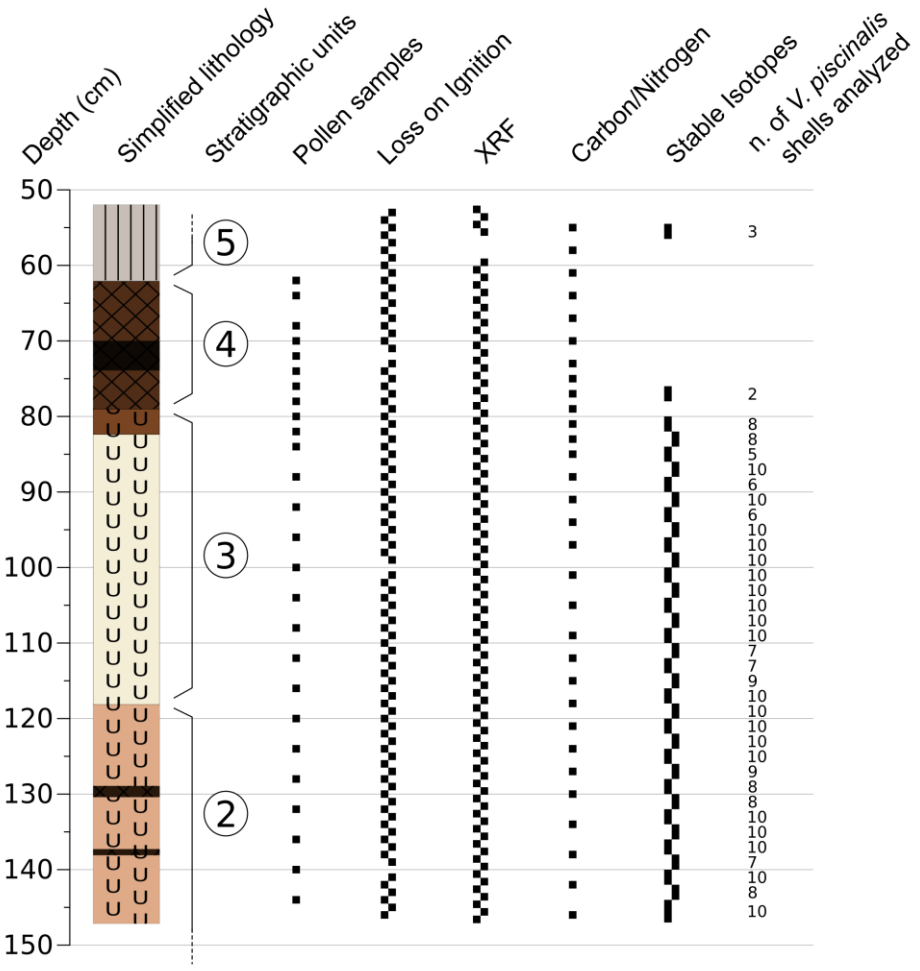

Figure S2.1. *Sampling resolution for different proxies along core CAV4*

Appendix III

This section collects all supplementary figures and tables for the research article "European forest cover during the past 12,000 years: a palynological reconstruction based on modern analogs and remote sensing", presented in Part IV.

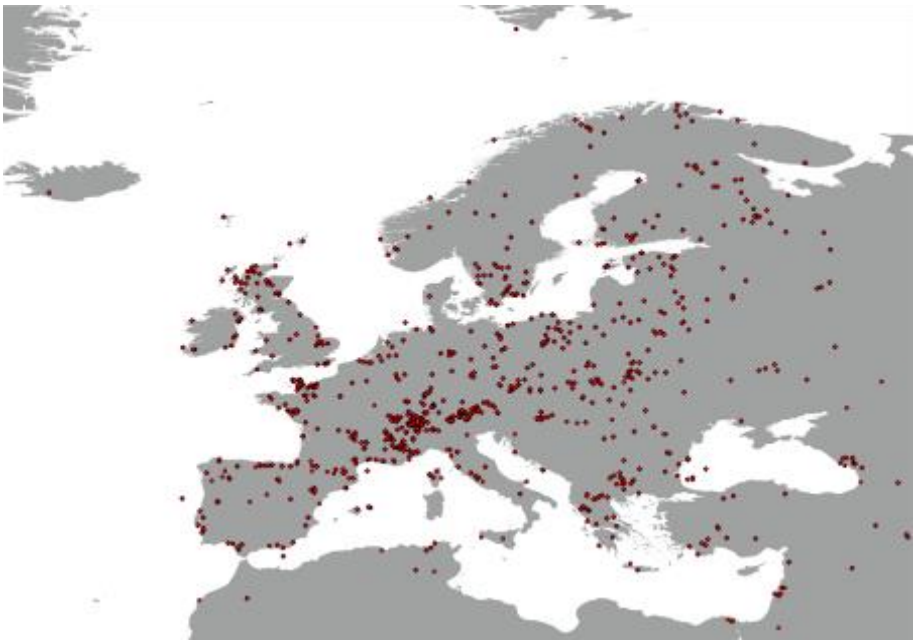

Figure S3.1*. Distribution of fossil pollen sequences used in the present paper.*

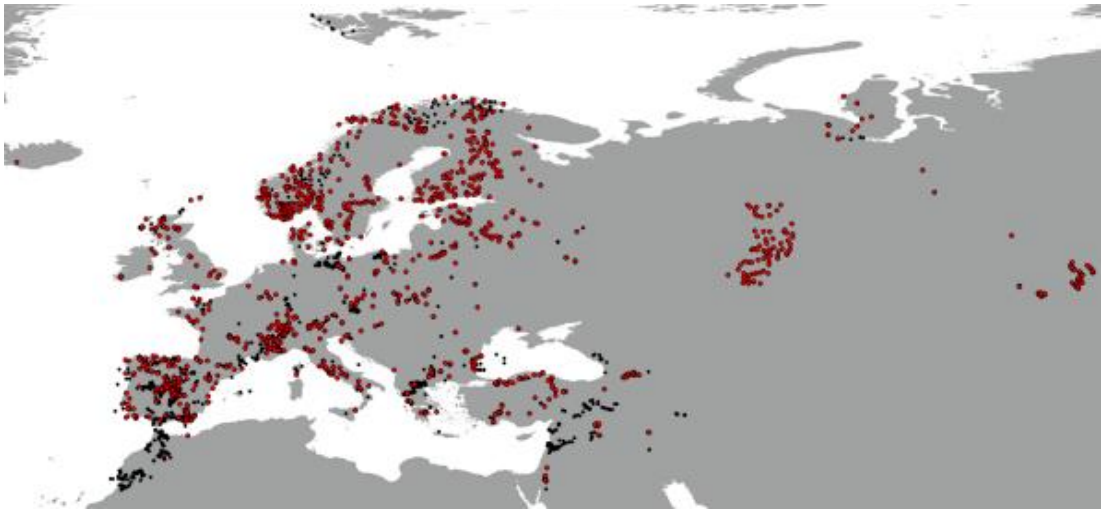

Figure S3.2. *Distribution of surface samples in the European Modern Pollen Database (all dots). Red dots: extent of the database after quality filtering (see section 2.4 in the manuscript).*

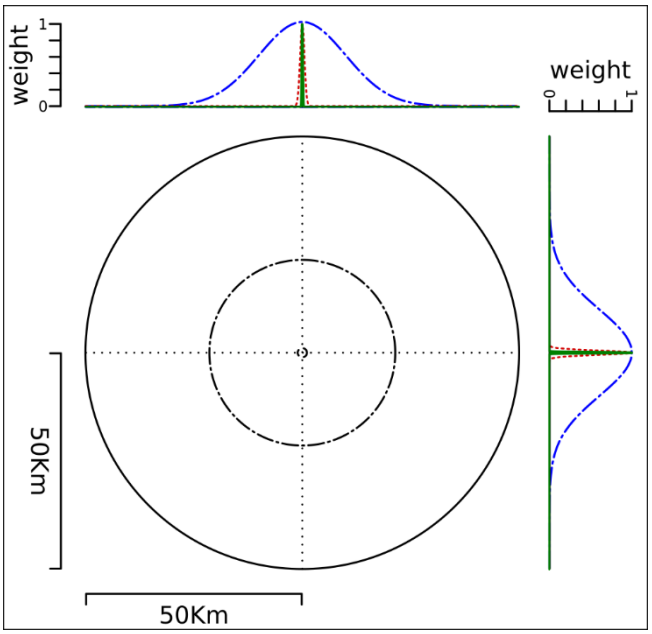

Figure S3.3. *Exemplification of weight distribution using a 2d Gaussian function with a range of 50 Km (solid-line outer circle). Dash-dots blue line: σ = 10km. Dotted red line: σ = 500m. Solid green line: σ = 100m. For reference, the inner dot-dash circle shows the limits of the 0.1 weight threshold for σ = 10km (ca. 21.5Km radius). The small central dashed circle shows the same weight threshold for σ = 500m (ca. 1km radius). During the extraction of forest cover values, all weights falling within each search radius were scaled to a sum of 1.*

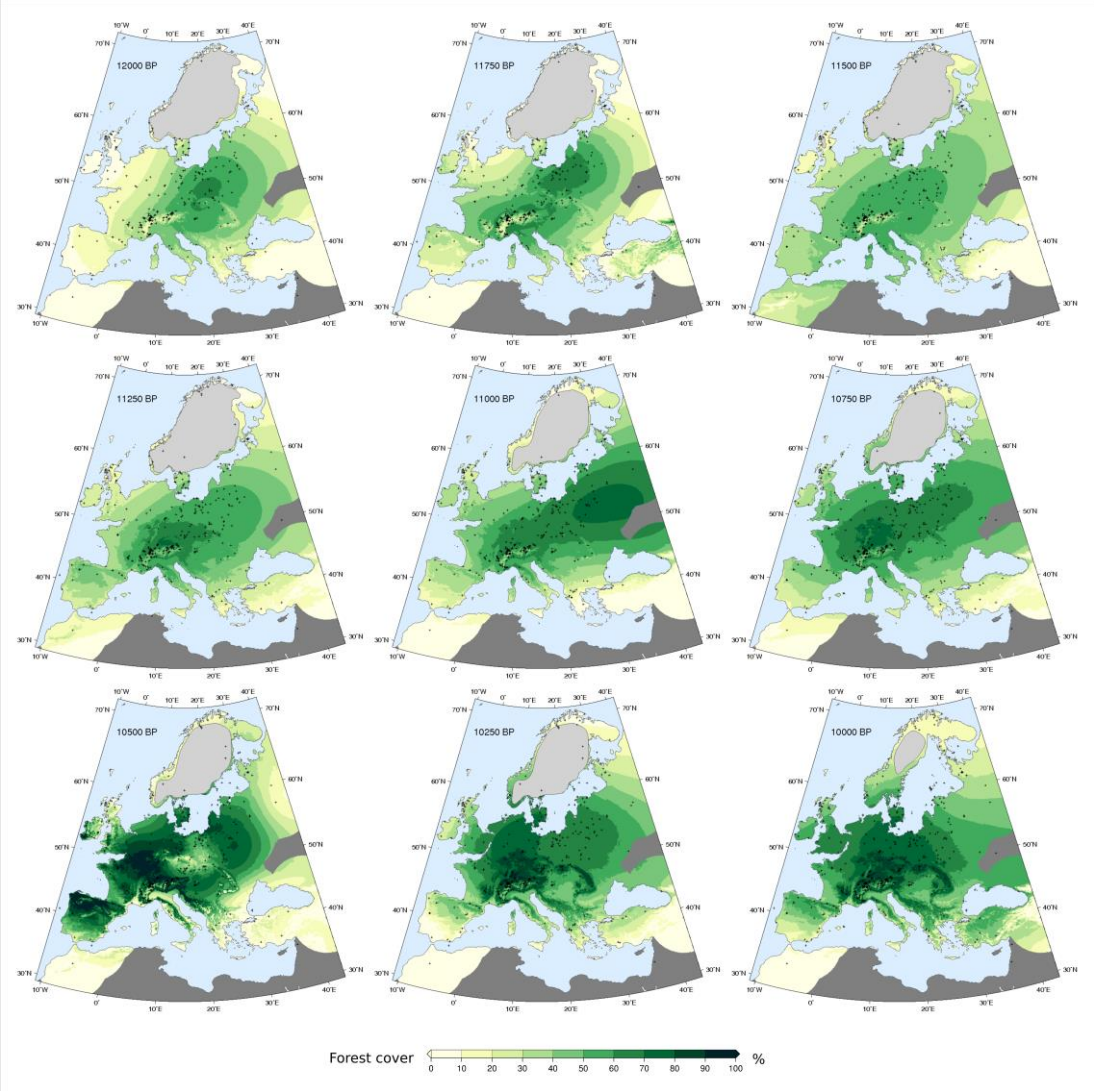

Figure S3.4. *Holocene interpolated tree cover maps. Light grey area over northern Europe represent Early Holocene ice cover. Dark grey areas are excluded from the analysis due to low site density. Grey crosses represent the location of pollen site used for the interpolation.*

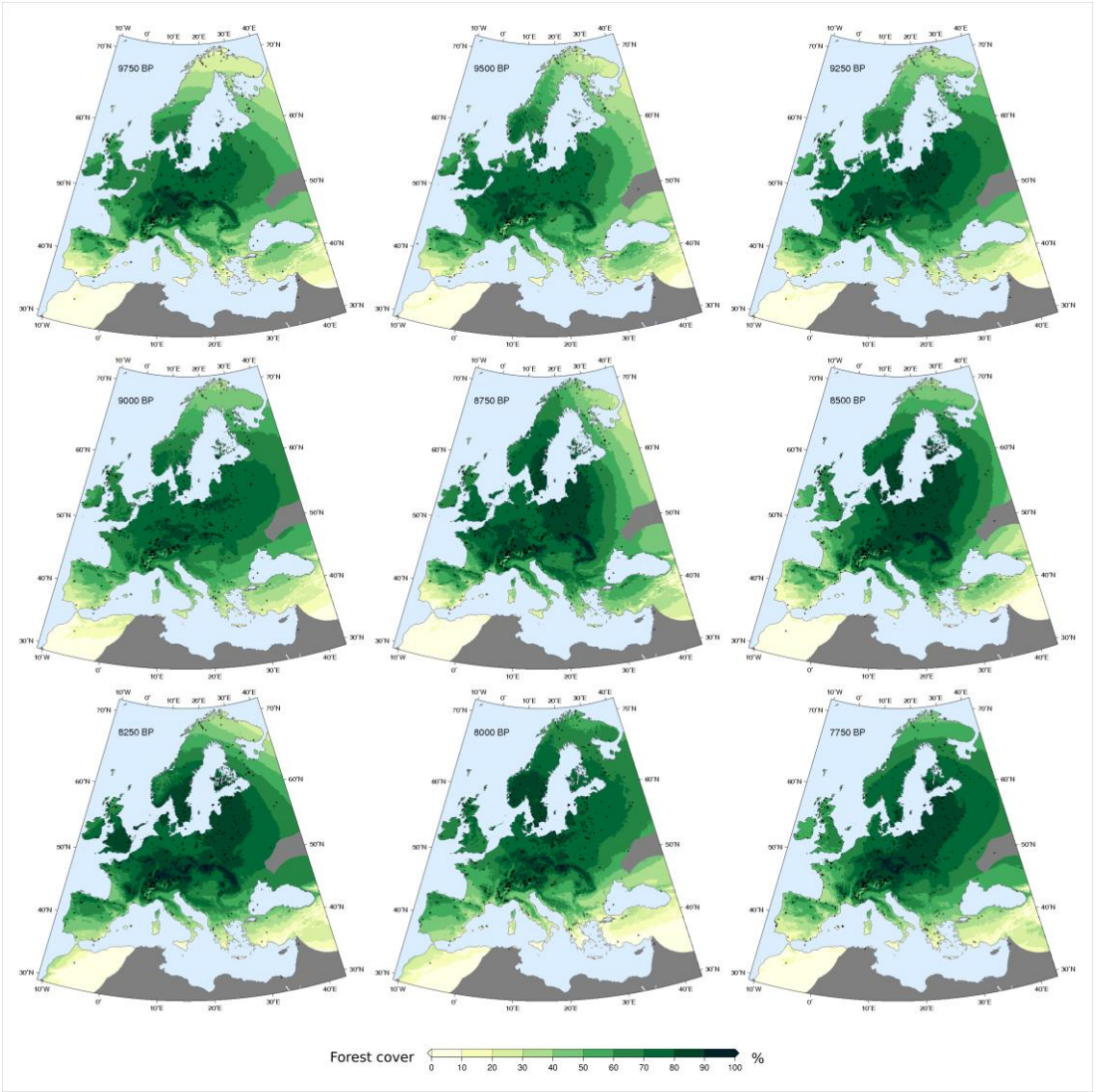

(Continues from Fig. S3.4)

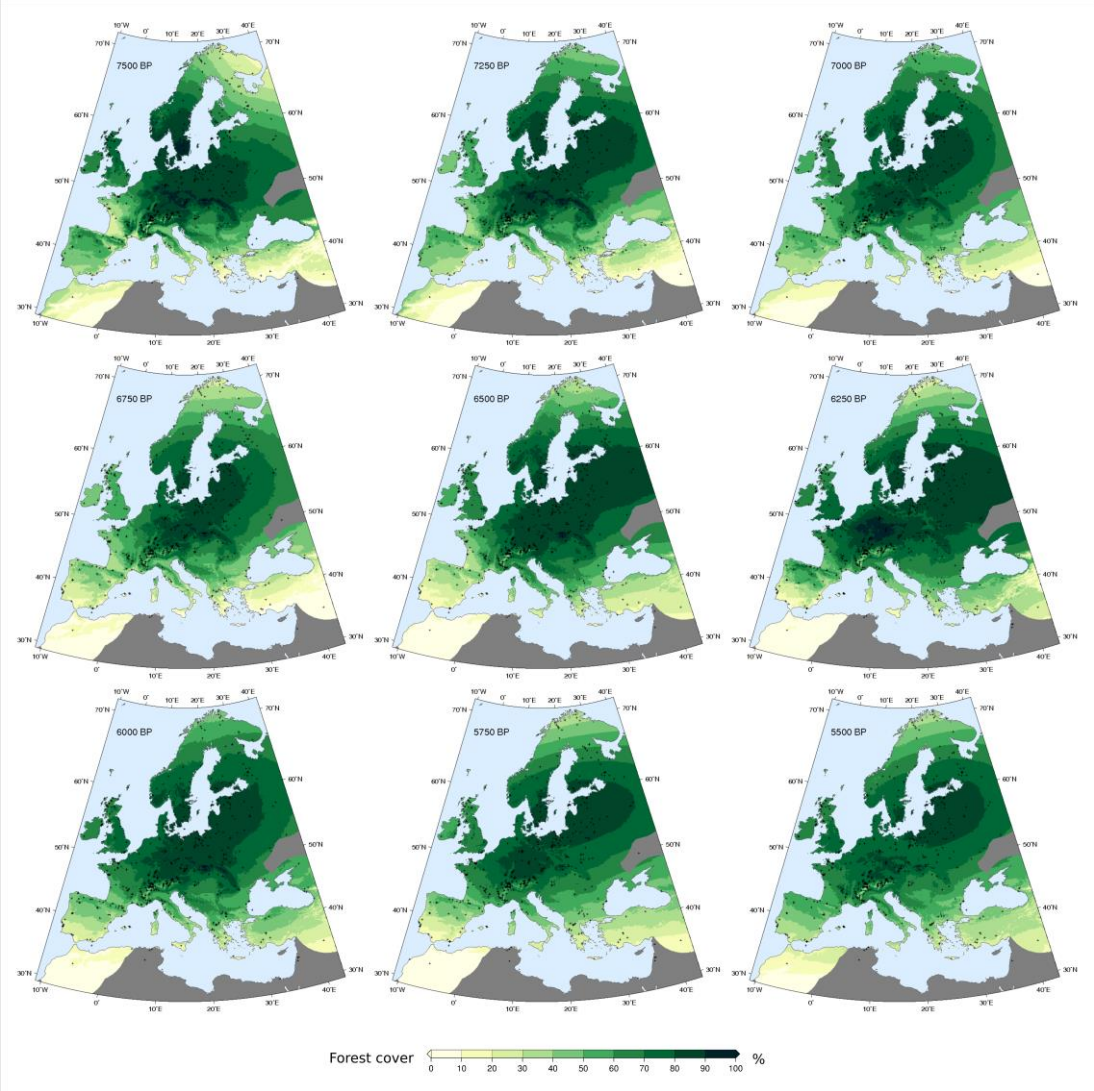

(Continues from Fig. S3.4)

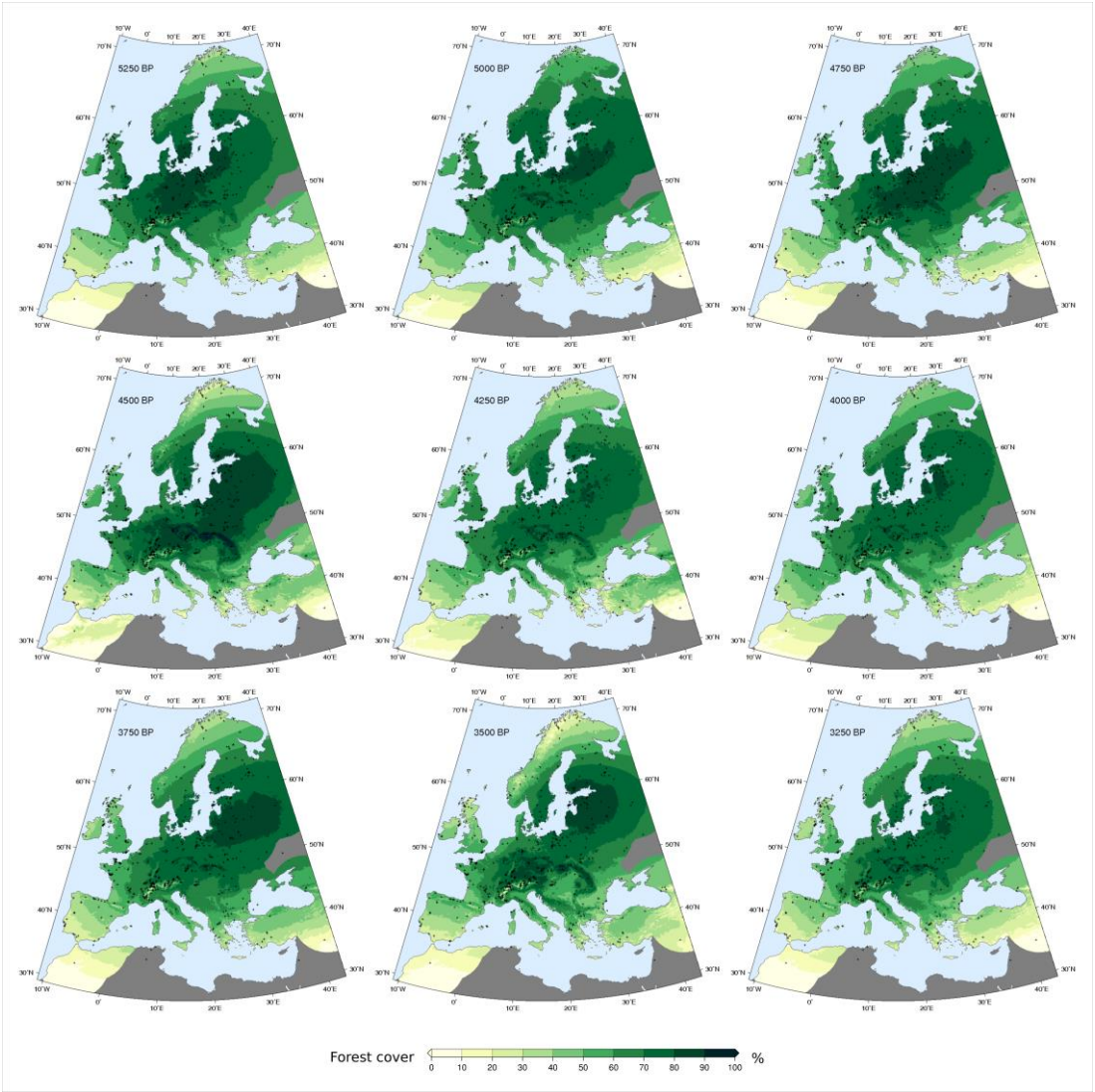

(Continues from Fig. S3.4)

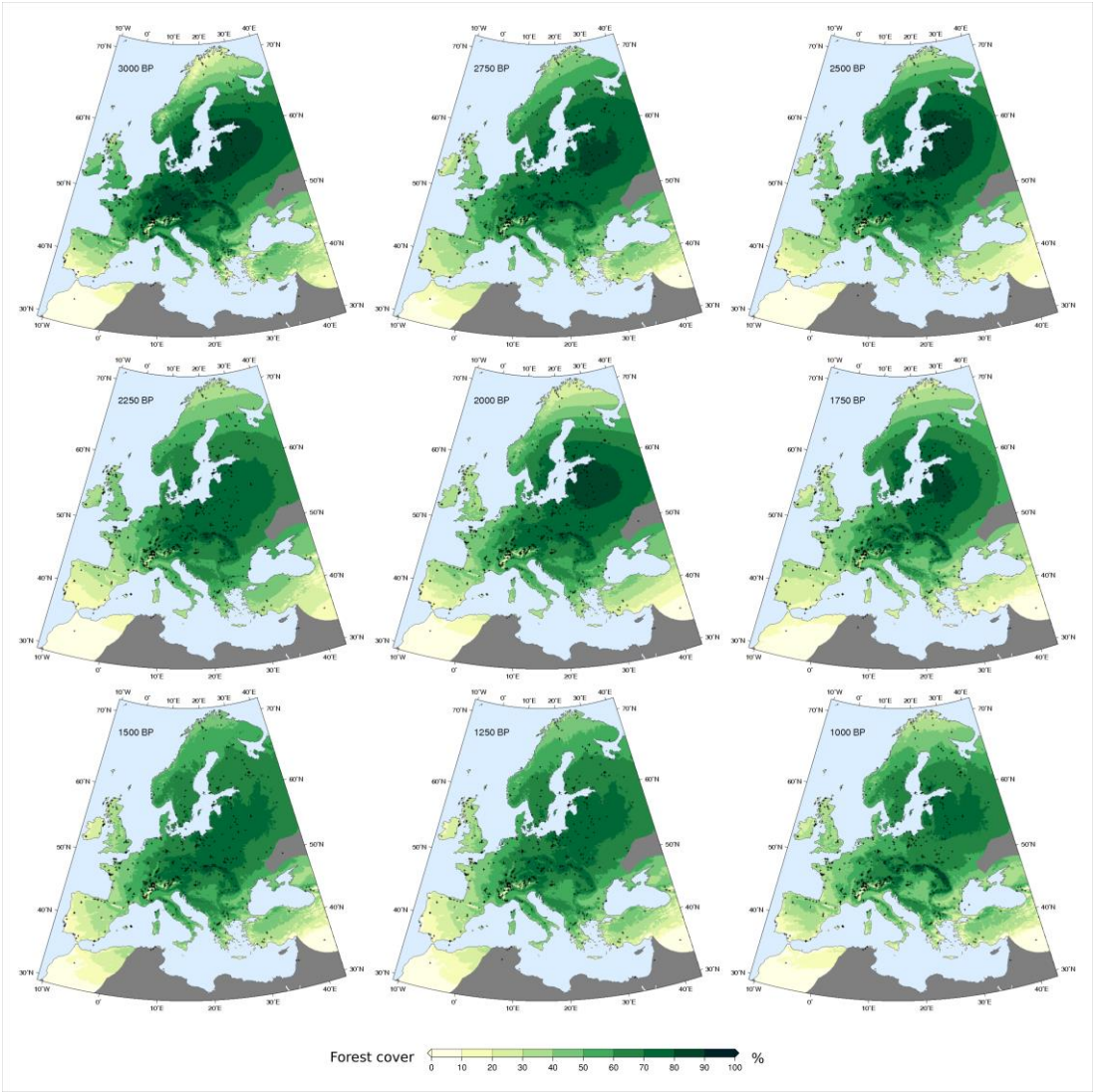

(Continues from fig. S3.4)

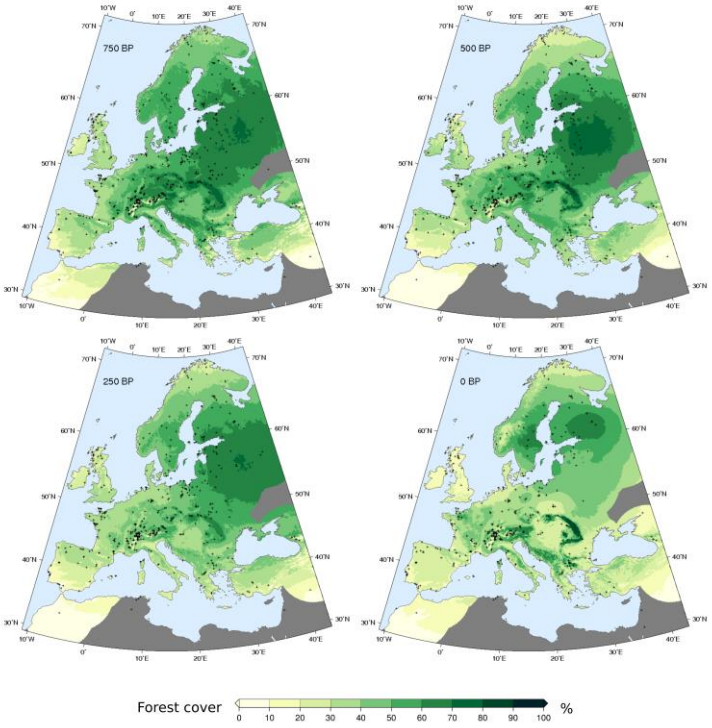

(Continues from fig. S3.4)

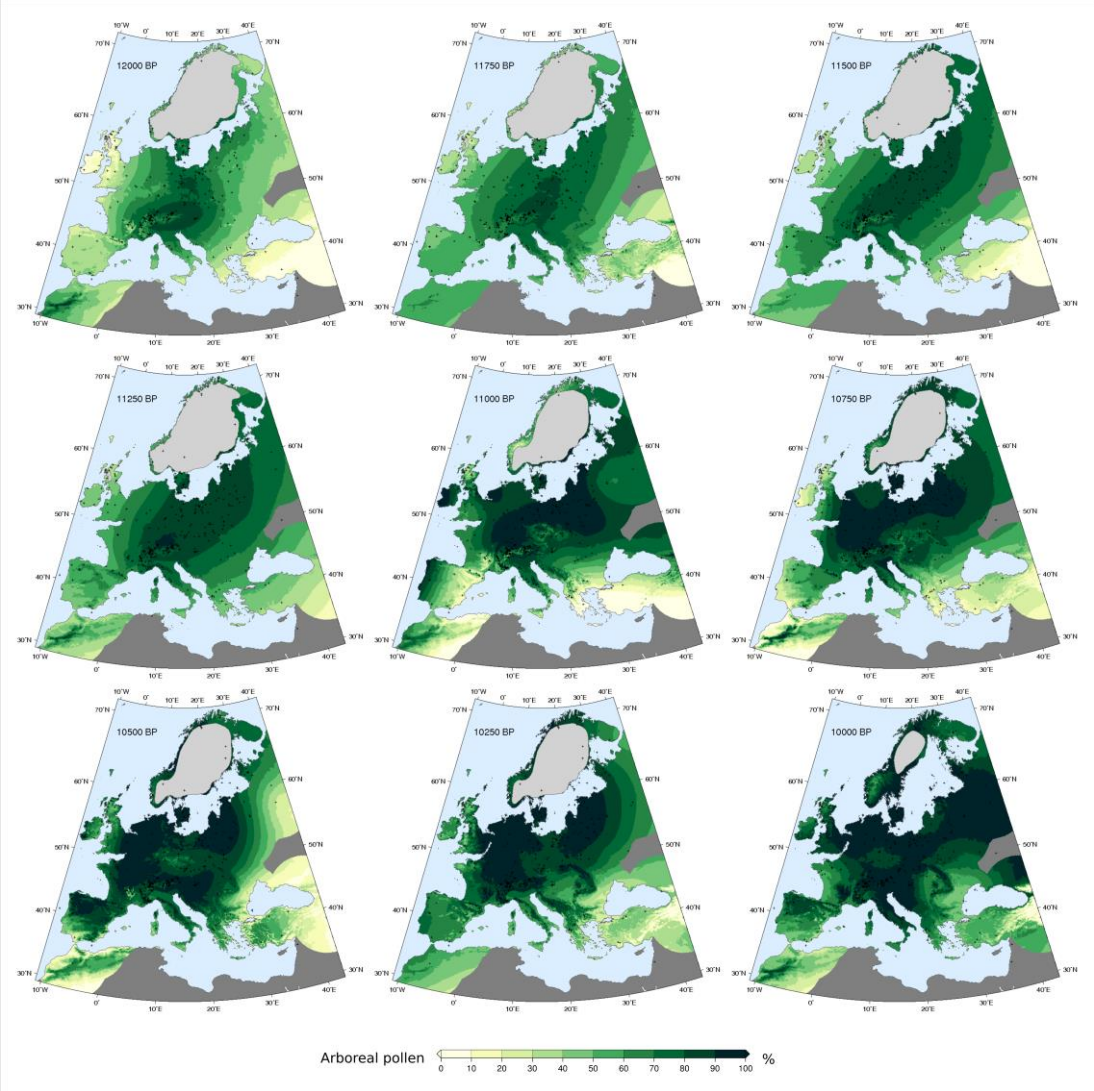

Figure S3.5. *Holocene interpolated arboreal pollen maps. Light grey area over northern Europe represent Early Holocene ice cover. Dark grey areas are excluded from the analysis due to low site density. Grey crosses represent the location of pollen site used for the interpolation.*

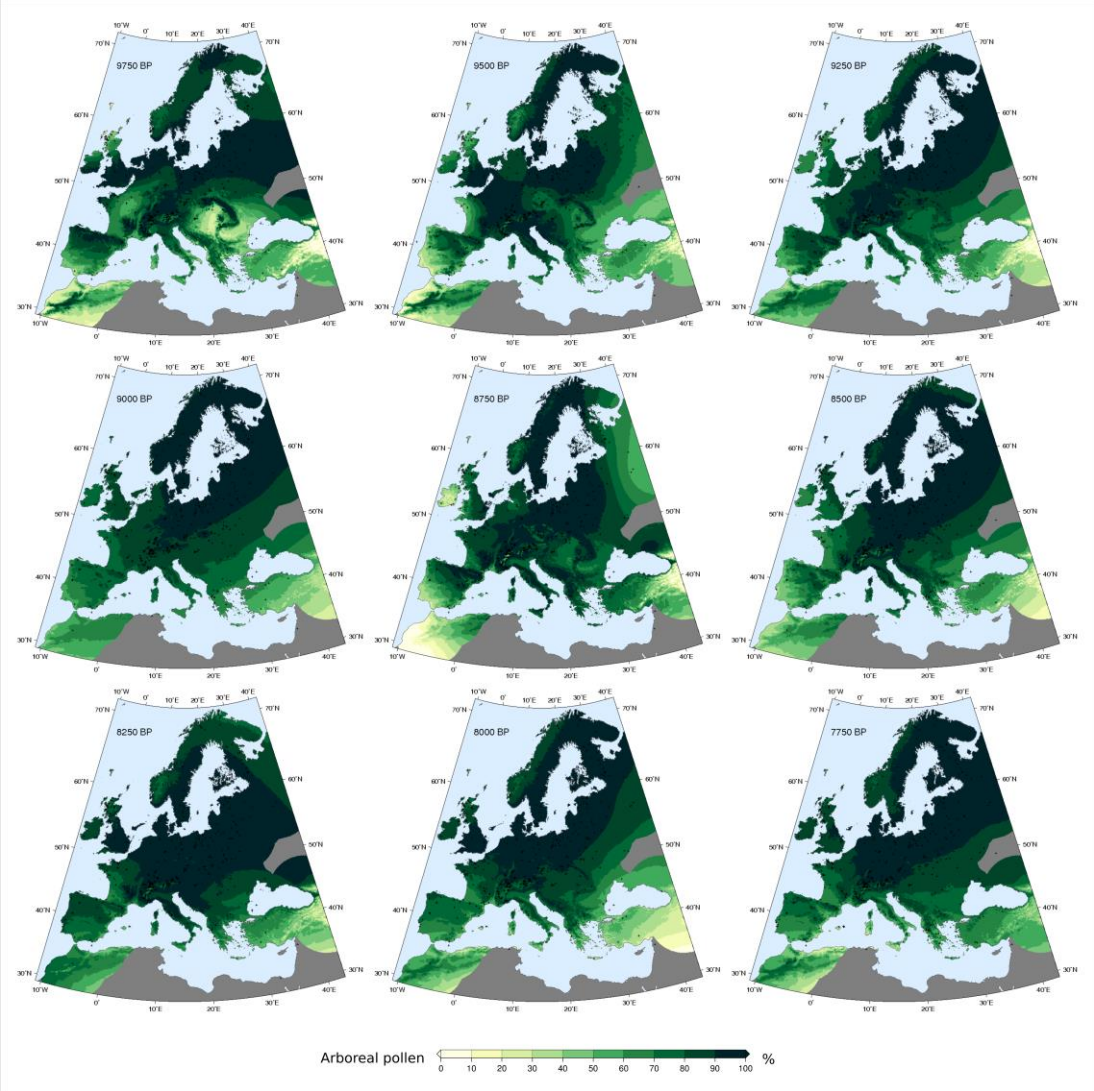

(Continues from fig. S3.5)

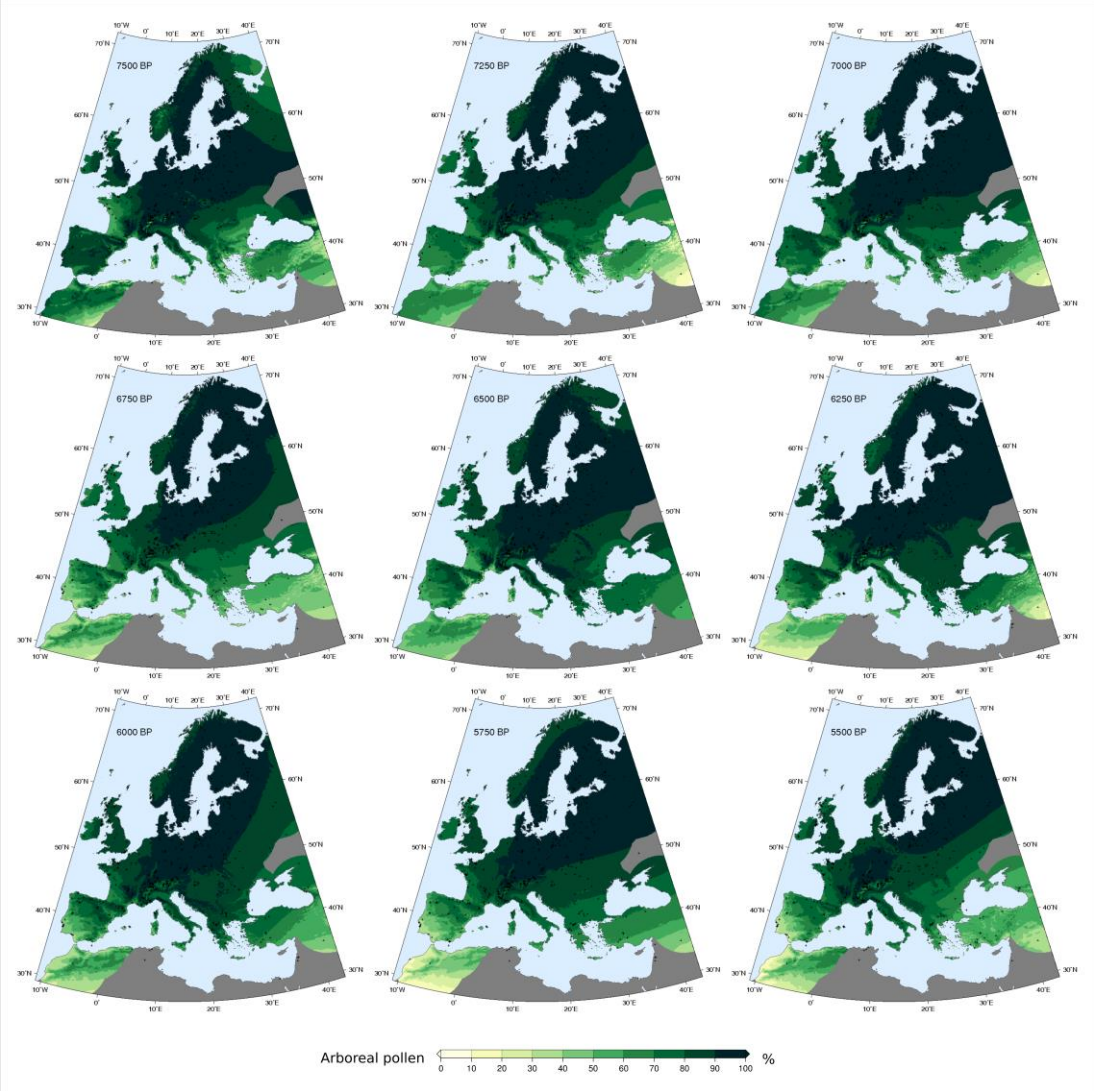

(Continues from fig. S3.5)

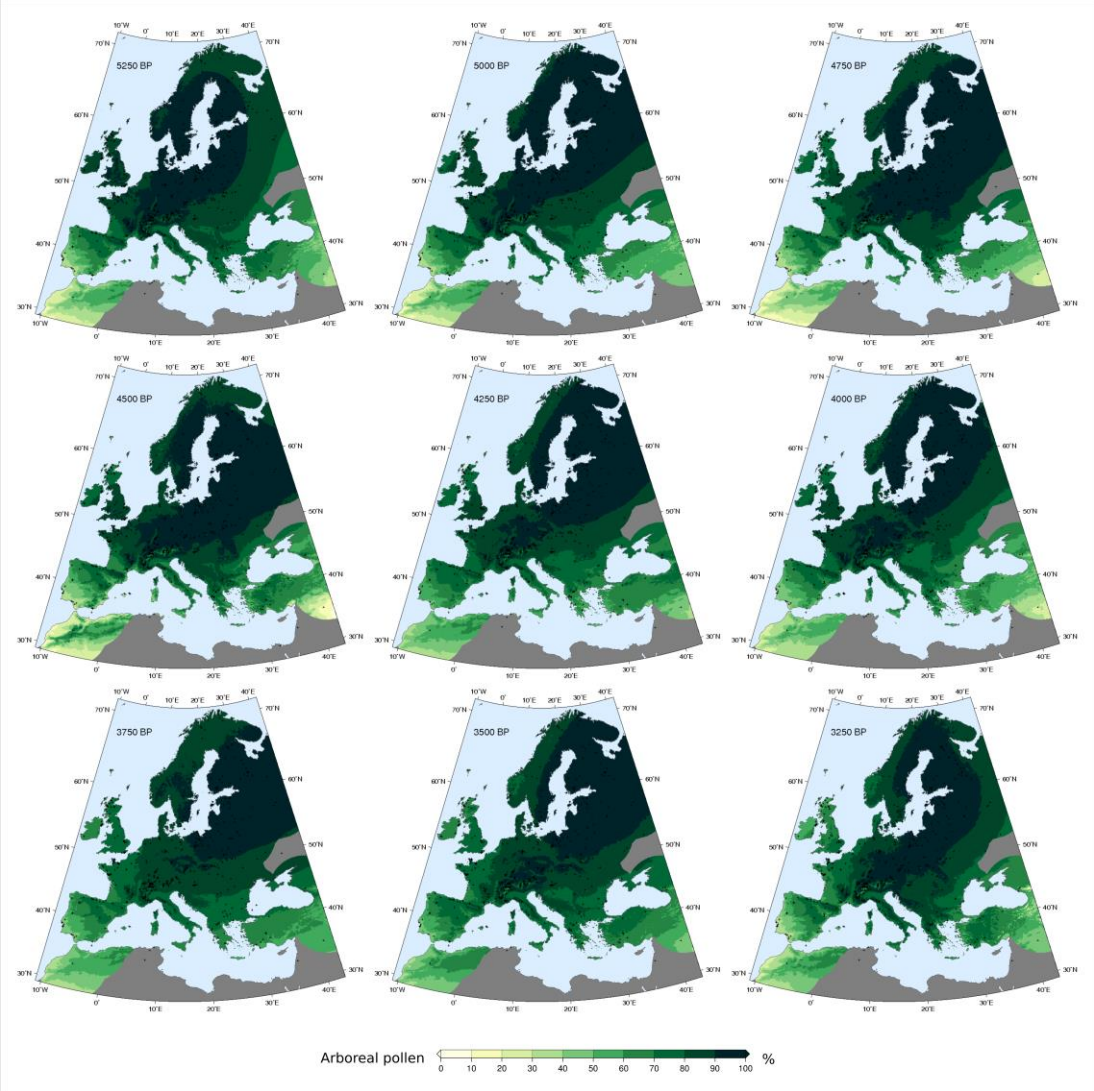

(Continues from fig. S3.5)

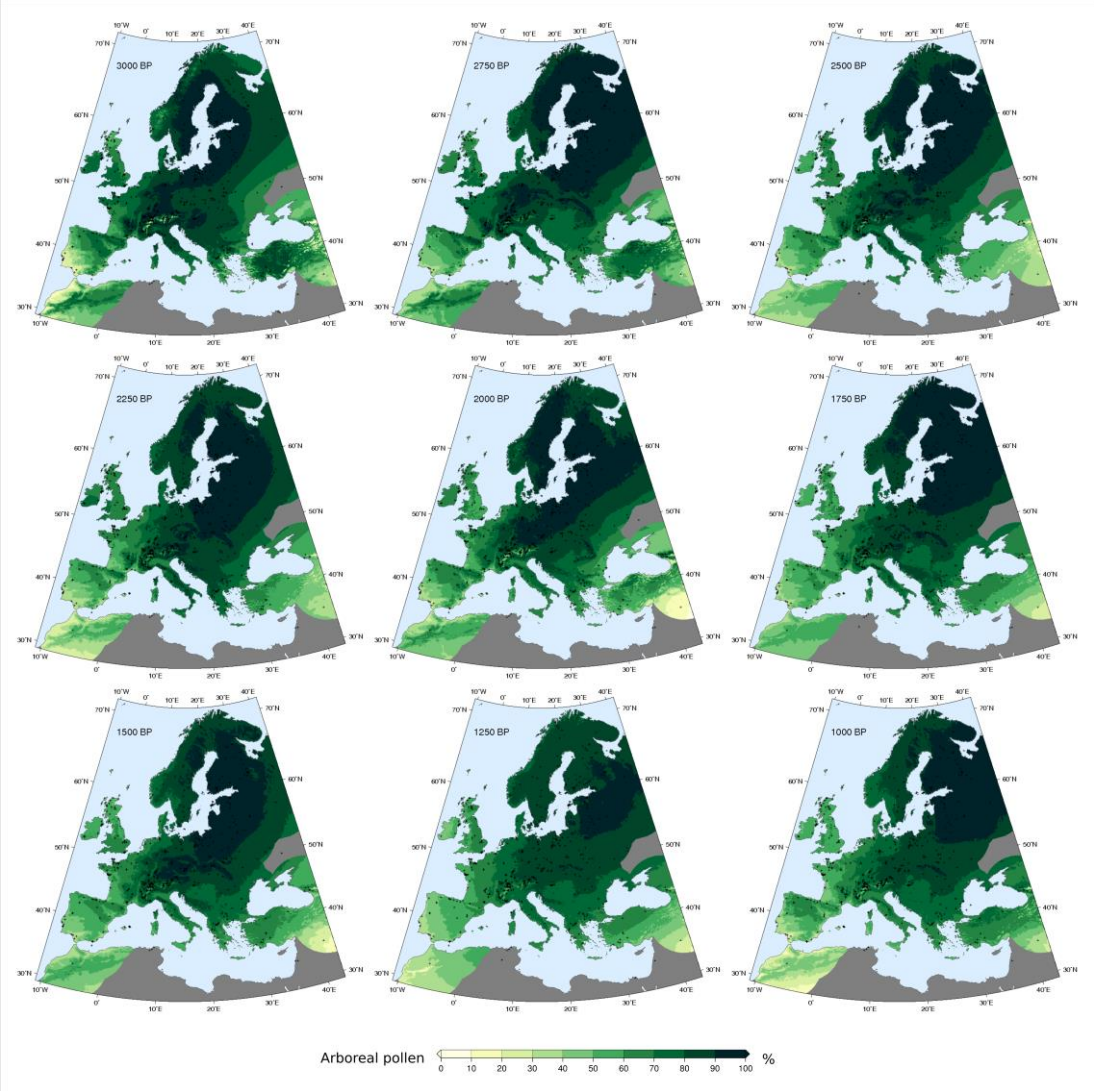

(Continues from fig. S3.5)

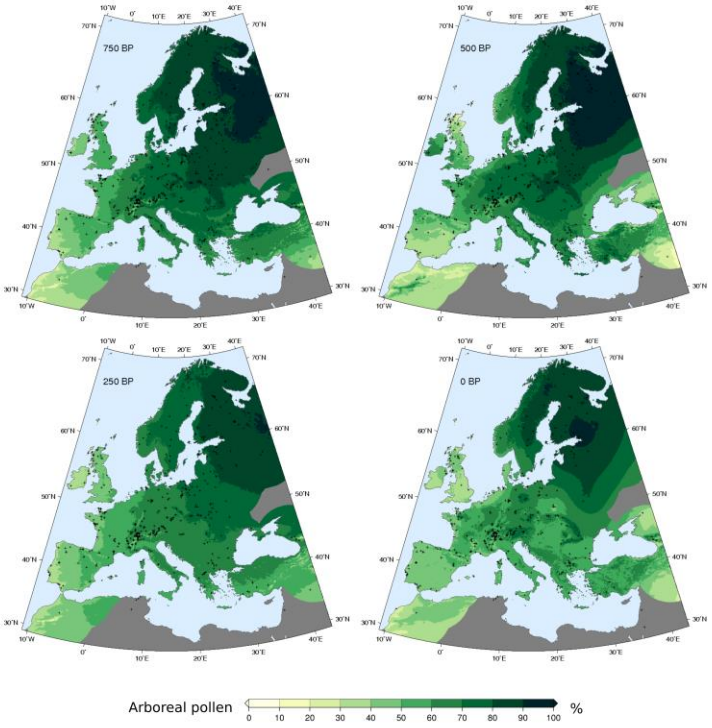

(Continues from fig. S3.5)

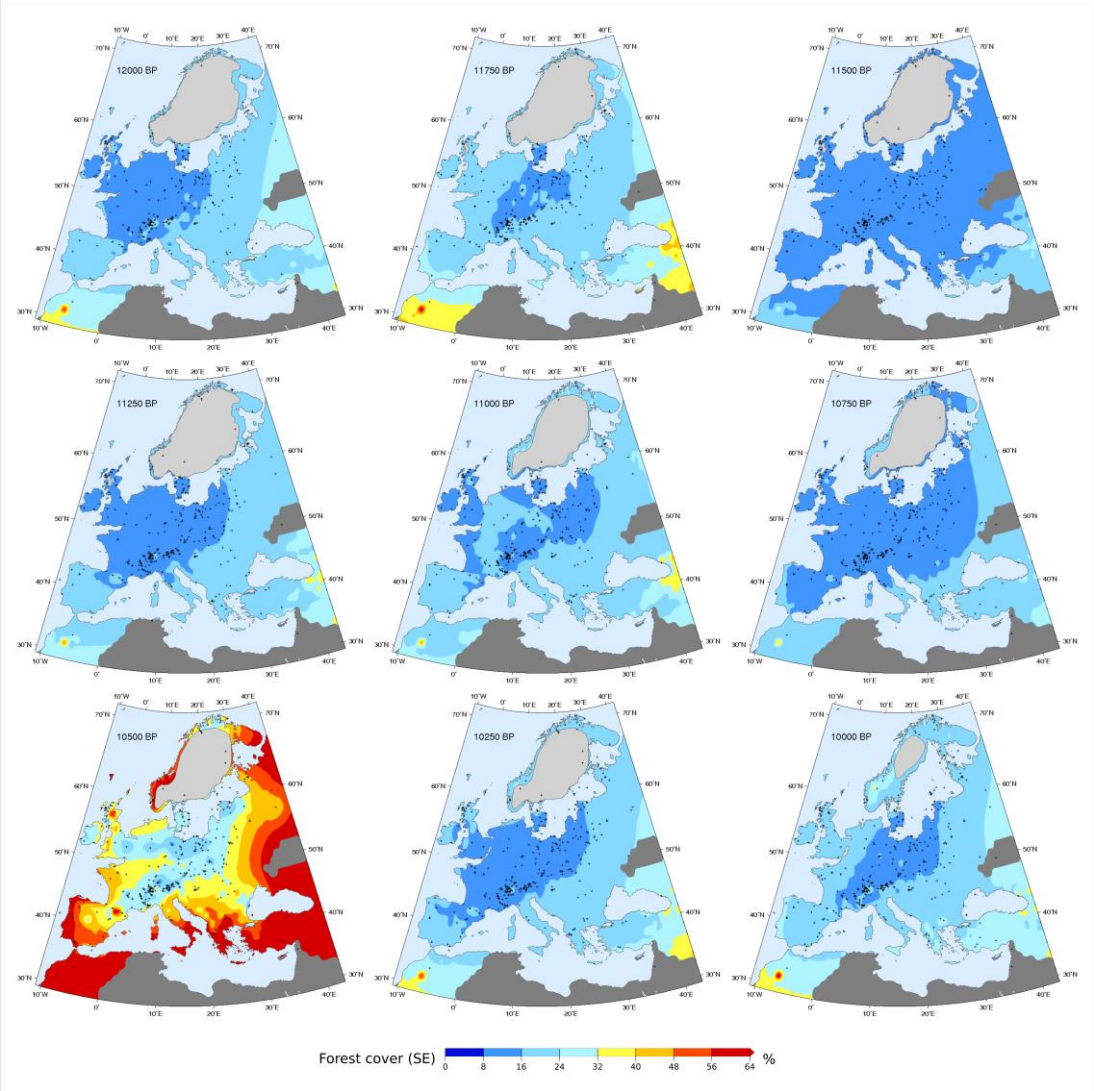

Figure S3.6. *Standard Error estimates for the forest cover reconstruction. Light grey area over northern Europe represent Early Holocene ice cover. Dark grey areas are excluded from the analysis due to low site density. Grey crosses represent the location of pollen site used for the interpolation.*

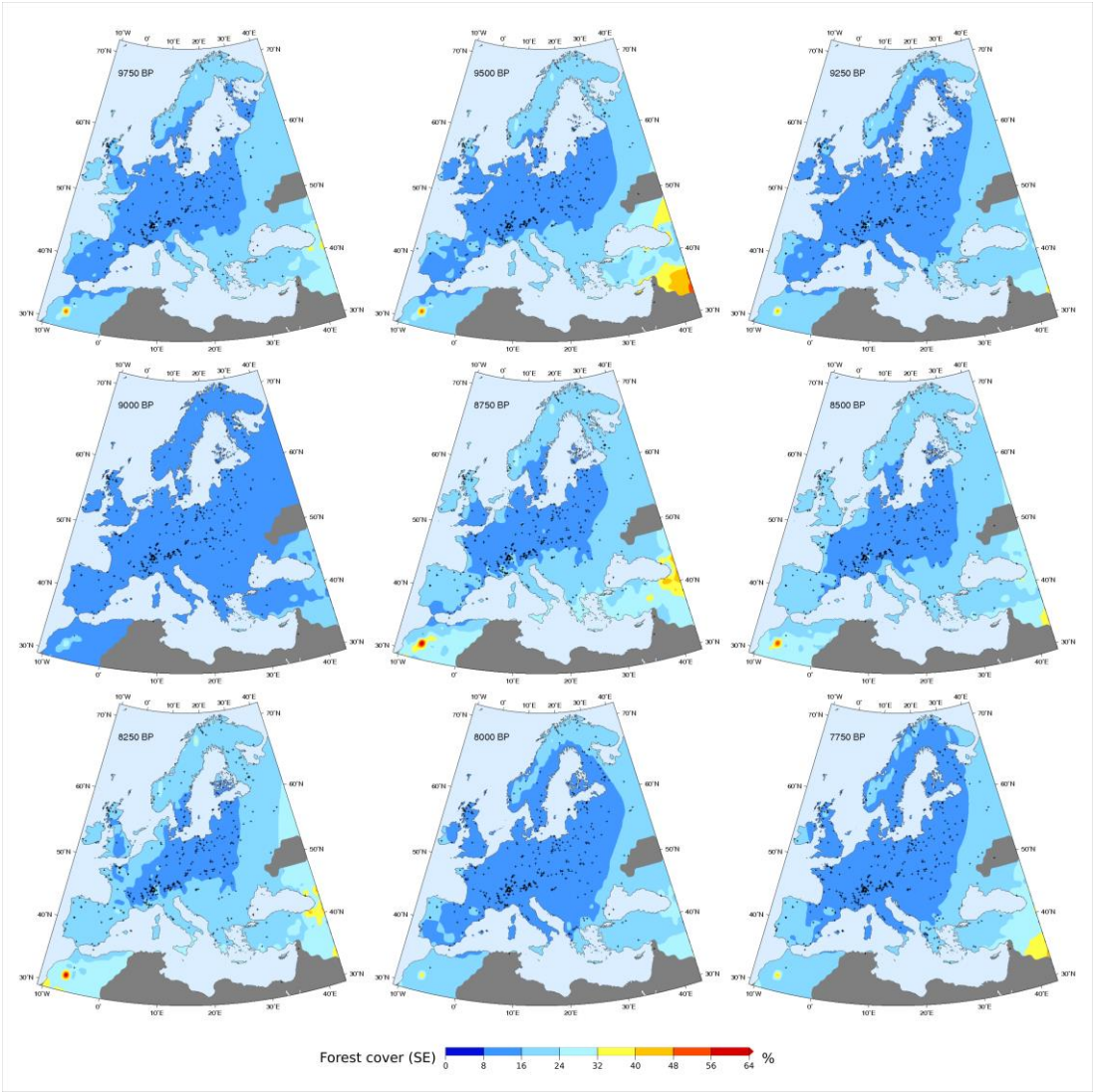

(Continues from fig. S3.6)

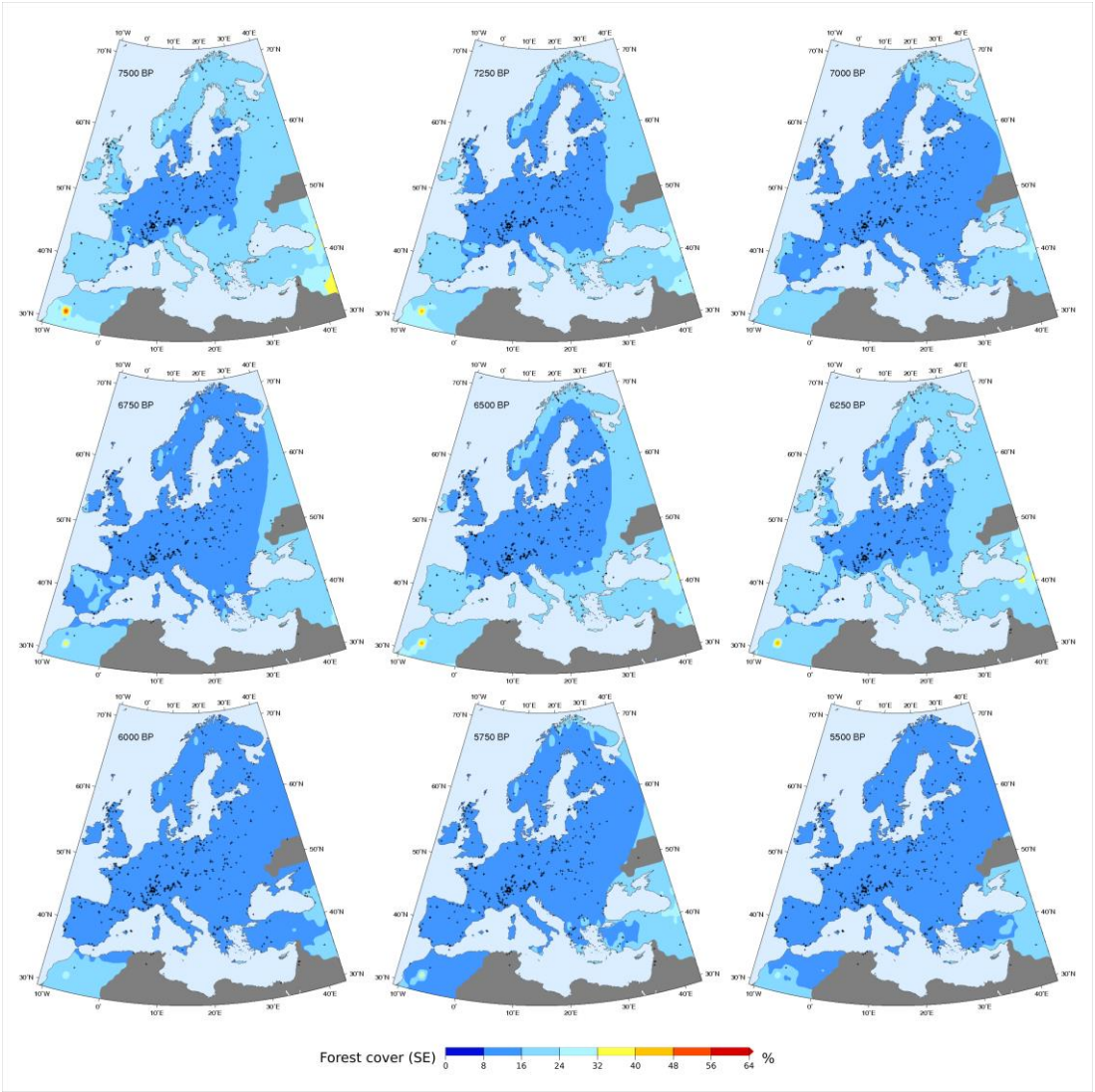

(Continues from fig. S3.6)

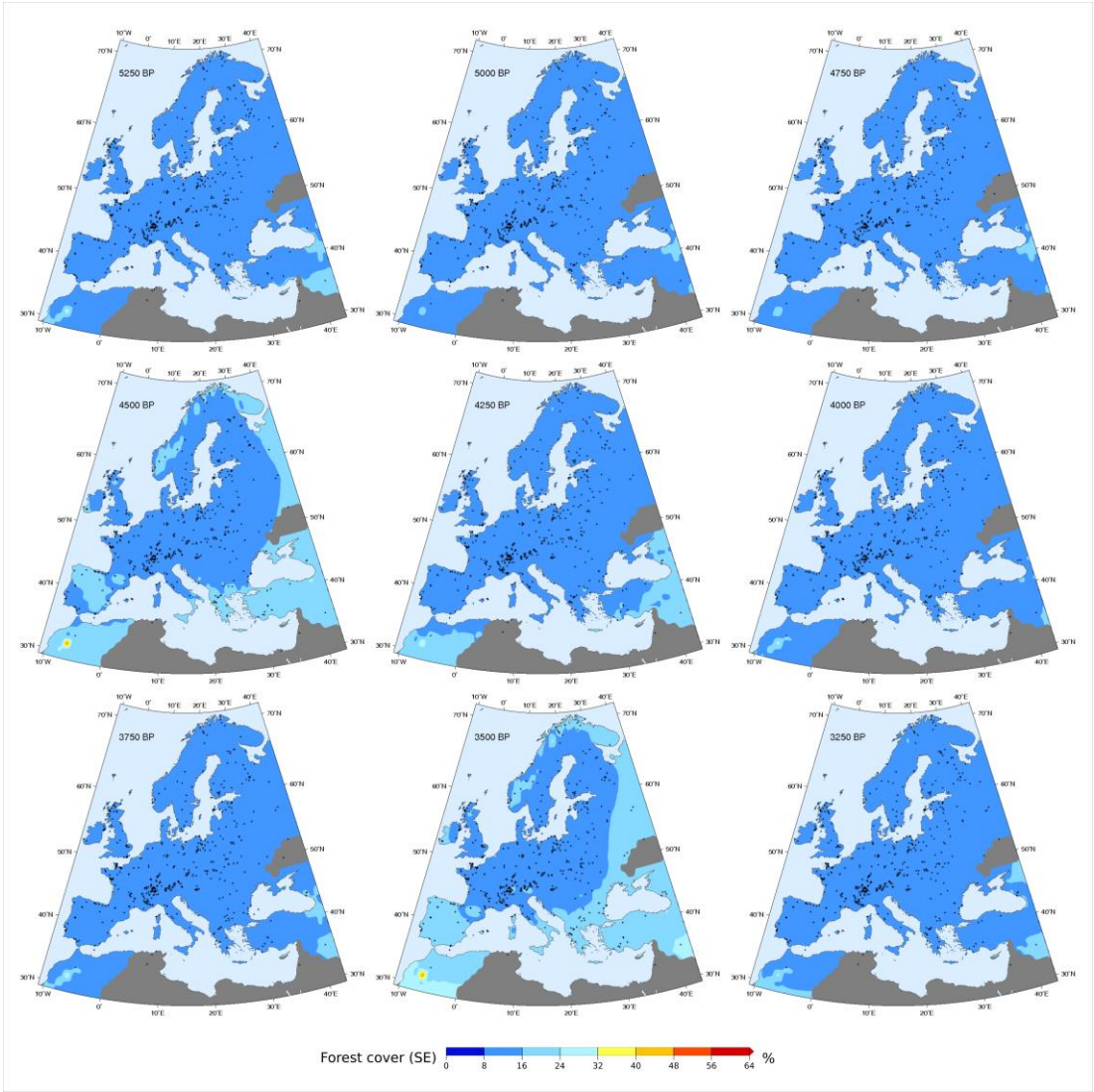

(Continues from fig. S3.6)

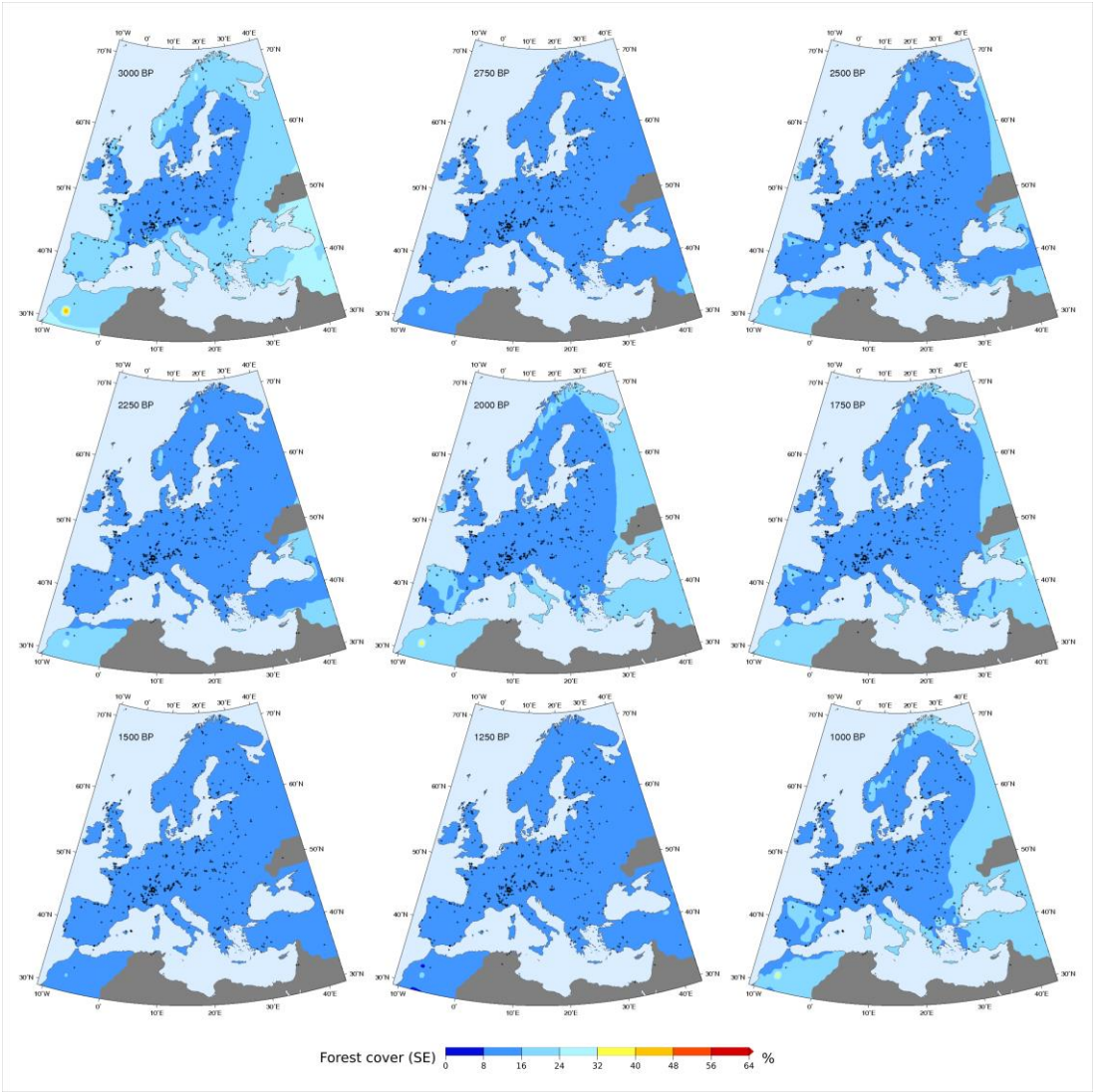

(Continues from fig. S3.6)

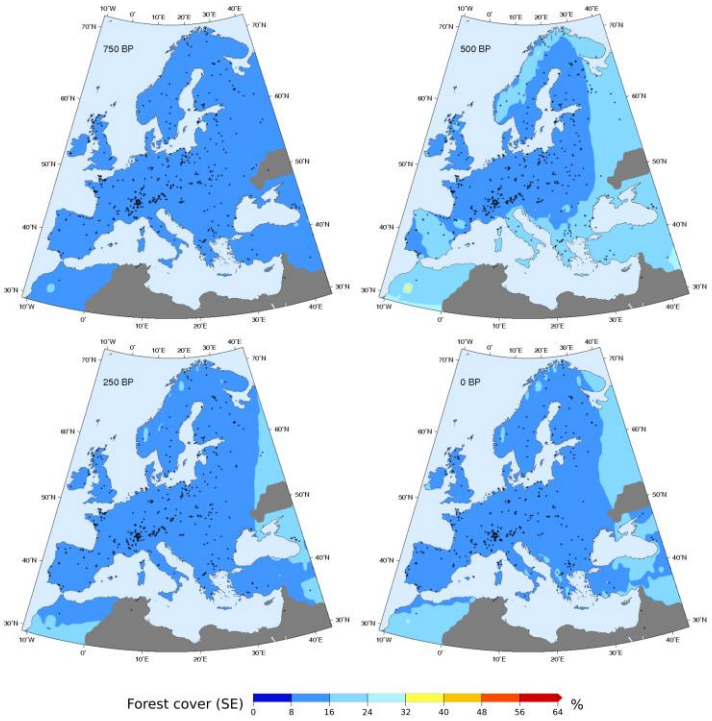

(Continues from fig. S3.6)

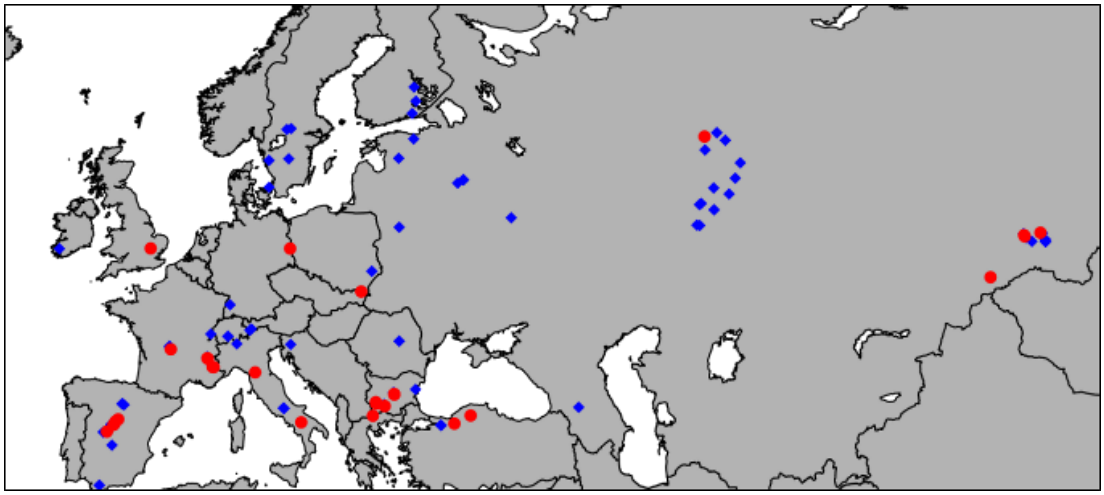

Figure S3.7. *Map displaying sites with modern tree cover higher than 80%. Blue diamonds: sites with residual values higher than -40. Red circles: sites with residual values lower than -40.*

Figure S3.8. *Location of the closest modern analogues (yellow diamonds, single closest analogue for each fossil sample) for the five sites involved in the MAT-REVEALS comparison (fig. 4.4) within the 12000 – 10000 BP period. The extent of the tundra biome (Olson et al., 2001) is highlighted in red.*

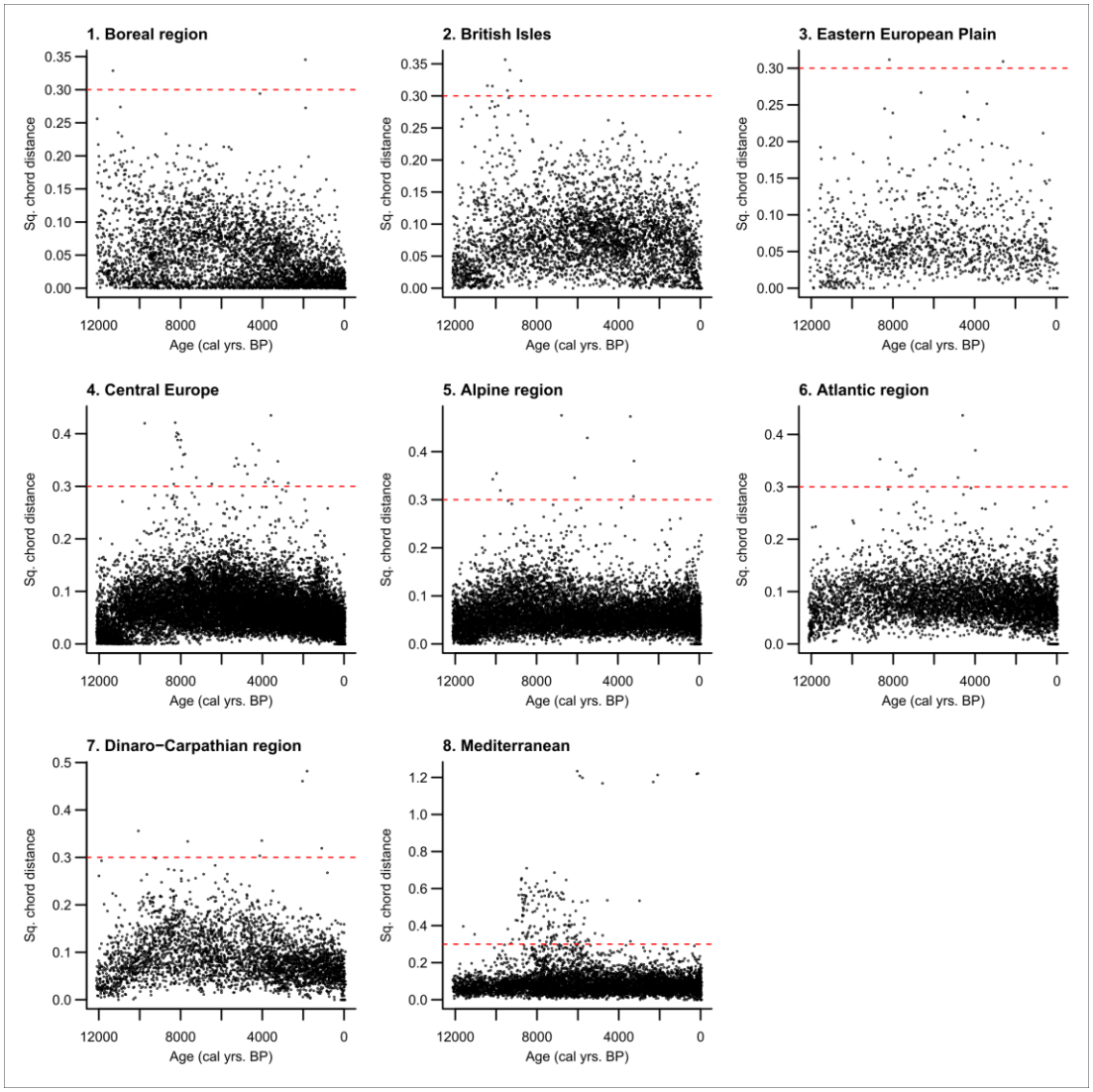

Figure S3.9. *Minimum squared chord distances for each region across the whole fossil data set. The horizontal dashed red line marks the 0.3 value used as a threshold in the present study following Huntley (1990). The Mediterranean region emerges as having the highest occurrence of no-analogue samples, likely connected to the low representation of extensive Mediterranean forests in the training data set.*

Table S3.1. *Conversion of pollen counts into Plant Functional Types (PFTs) taken from Peyron et al. (1998). Pollen taxa within each pollen sample are grouped in PFTs according to shared climatic ranges and biological traits. Some taxa can belong to multiple PFTs. The complete taxa-to-PFTs procedure is described in Peyron et al. (1998).*

Pollen Taxa	PFT	Code
Larix	Boreal summergreen	bs
Betula	Boreal summergreen arctic-alpine	bs/aa
Picea, *Pinus* subgen. *Haploxylon*	Boreal evergreen conifer	bec
Abies	Boreal evergreen/cool-temperate conifer	bec/ctc
Cedrus, *Taxus*	Intermediate temperate conifer	ctc1
Juniperus, *Pinus* subgen. *Diploxylon*	Eurythermic conifer	ec
Alnus, *Salix*	Temperate/boreal summergreen/arctic-alpine	ts/bs/aa
Populus	Temperate/boreal summergreen	ts/bs
Acer, *Fraxinus excelsior*, *Quercus* (deciduous)	Temperate summergreen	ts
Carpinus, *Ulmus*, *Corylus*, *Fagus*, *Frangula*, *Tilia*,	Cool-temperate summergreen	ts1
Castanea, *Platanus*, *Ostrya*, *Fraxinus ornus*, *Vitis*, *Juglans*	Warm-temperate summergreen	ts2
Quercus (evergreen)	Warm-temperate broad-leaved evergreen	wte
Buxus, *Hedera*, *Ilex*	Cool-temperate broad-leaved evergreen	wte1
Acacia, *Cistus*, *Rhus*, *Myrtus*, *Olea*, *Phillyrea*, *Pistacia*, *Ceratonia*	Warm-temperate sclerophyll trees/shrub	wte2
Hippophae, *Polygonum*	Cold grass shrub	cgs
Fabaceae, *Zizyphus,* Scrophulariaceae, *Ephedra fragilis,* Brassicaceae, Crassulaceae	Warm grass shrub	wgs
Apiaceae, Asteraceae, *Armeria,* Boraginaceae, Campanulaceae, Caryophyllaceae, *Centaurea,* Dipsacaceae, *Helianthemum, Plantago,* Plumbaginaceae, *Ranunculus,* Rosaceae, Rubiaceae, *Rumex, Sanguisorba, Thalictrum*	Steppe forb/shrub	sf
Artemisia, Chenopodiaceae	Steppe/desert forb/shrub	sf/df
Ephedra, Zygophyllaceae	Desert forb/shrub	df
Alnus fruticosa, Betula nana, Saxifraga, Empetrum, Dryas, Rhododendron, Vaccinium	Arctic-alpine dwarf shrub	aa
Poaceae	Grass	g
Ericaceae, *Calluna*	Heath	h

Table S3.2. *Biome assignment based on PFT scores as reported by Peyron et al. (1998). Biome scores for each sample are calculated by summing all the PFTs belonging to each biome. PFT assignment follows tab. S3.1. The biome having the highest score is then assigned to the corresponding sample. The complete taxa-to-PFTs procedure is described in Peyron et al. (1998). *=the presence of code bctc in Peyron et al (1998) is likely a typo, as it does not correspond to any PFT described in the paper. In the present paper, it was replaced with bec/ctc (i.e. Abies, tab. S3.1) following Prentice et al. (1996), which include Abies in the Temperate Deciduous biome. **= Peyron et al. (1998) do not include the ts PFT in the Temperate Deciduous biome. This missing PFT is likely a typo, as ts includes the taxon Quercus (deciduous), which is an important component of the Temperate Deciduous biome. In the present paper, we included the ts PFT in the composition of the Temperate Deciduous biome following Prentice et al. (1996).*

Biome	PFT combination
Cold deciduous forest	bs+bs/aa+ts/bs/aa+ts/bs+h
Taiga	bs+bs/aa+bec+bec/ctc+ts/bs/aa+ts/bs+ec+h
Cold mixed forest	bs+bs/aa+bec/ctc+ctc1+ts/bs/aa+ts/bs+ts1+ec+h
Cool conifer forest	bs+bs/aa+bec+bec/ctc+ts/bs/aa+ts/bs+ts1+ec+h
Temperate deciduous	bs+bs/aa+bctc*+ctc1+ts/bs/aa+ts/bs+ts**+ts1+ts2+wte1+ec+h
Cool mixed forest	bs+bs/aa+bec+bec/ctc+ts/bs/aa+ts/bs+ts+ts1+ts2+ec+h
Warm mixed forest	ts/bs/aa+ts/bs+ts+ts1+ts2+wte/+wte1+ec+h
Xerophytic wood/scrub	wte+wte2+ec+g
Desert (hot or cold)	df+sf/df
Cool steppe	cgs+sf+sf/df+g
Warm steppe	wgs+sf+sf/df+g
Tundra	bs/aa+ts/bs/aa+aa+h+g

Table S3.3. *PFT refinement based on biome scores as presented by Peyron et al. (1998). Some of the initial PFT scores defined in tab. S3.1 are reassigned (initial PFTs changed into final PFTs) according to the biome selected in tab. S3.2. This step refines the attribution of certain taxa to more specific PFTs. As an example, in tab. S3.1 Betula is assigned to PFT bs/aa. If the overall pollen content places a sample in the tundra biome, then any Betula pollen in that specific sample is reassigned to PFT aa. The complete taxa-to-PFTs procedure is described in Peyron et al. (1998).*

Biomes	Initial PFT	Final PFT
Cold deciduous forest and Taiga	bs/aa, ts/bs/aa, ts/bs	bs
	ec	bec
Cold mixed forests and Cool conifer forests	ts/bs/aa, ts/bs	tsbs
	ec	bec/ctc
Temperate deciduous and Cool mixed forest	bs/aa	bs
	ts/bs/aa, ts/bs	ts
	ec	bec/ctc
Warm mixed forest	ts/bs/aa, ts/bs	ts
	ec, h	wte
Xerophytic woods/scrubs	ec	wte
Tundra	bs/aa, ts/bs/aa, h, g	aa
Cool steppe	sf, sf/df	cgs
	g	aa
Warm steppe	sf, sf/df	wgs
	g	cgs
Cold desert and hot desert	sf/df	df

Table S3.4. *MAT-REVEALS comparison. Site-by-site statistical correlation values referred to fig. 4.4. Time-window subdivision: Late Pleistocene-Early Holocene: 11700 - 8100 BP. Mid- Holocene: 8100 - 4100 BP. Late Holocene: 4100 - 0 BP.*

Site	Period	Difference MAT-REVEALS (proportions of forest cover*100)	
		Uncalibrated	Calibrated
Gosciaz	Early Holocene	-16.5±11.5	2.2±16.6
	Mid-Holocene	-21.3±6.2	1.3±9.8
	Late Holocene	-12.1±11.8	8.8±11.7
Kansjon	Early Holocene	-18.7±6.3	-2.8±13.5
	Mid-Holocene	-24.3±4.6	-0.1±7.2
	Late Holocene	-16.2±11.5	5±15
Krageholmssjön	Early Holocene	-13.4±9.8	-3.2±20.8
	Mid-Holocene	-18.2±5.5	5.3±6.9
	Late Holocene	-12.8±6.8	-14.7±15.7
Raigstavere	Early Holocene	-27.4±6.8	-14.2±15.3
	Mid-Holocene	-25.4±4.7	-1.7±6.4
	Late Holocene	-17.3±11.9	4.6±10.4
Trummen	Early Holocene	-31±12.6	-15.2±22.3
	Mid-Holocene	-24.1±4.6	0.8±4.6
	Late Holocene	-10±4.9	15.3±5.3

Table S3.5. *Selection of taxa used in the taxa-based MAT test for no-analogue situations (fig.4.6). The wide taxonomical variability of the modern and fossil databases was simplified by grouping taxa into distinctive genera, generally following the guidelines of Beug (2004) and Moore et al. (1991). The selected pollen taxa include the most frequently occurring taxa recorded in both the modern and fossil databases. Additional, less frequent pollen taxa were also taken into account due to their potential help in discriminating between vegetation assemblages (e.g. Cedrus, Olea/Phillyrea for distinctively circum-Mediterranean communities).*

1. *Abies*	24. *Fraxinus*
2. *Acer*	25. *Hedera*
3. *Alnus*	26. *Hippophae*
4. Apiaceae	27. *Ilex*
5. *Artemisia*	28. *Juglans*
6. Asteraceae	29. Lamiaceae
7. *Betula*	30. *Larix/Pseudotsuga*
8. *Carpinus*	31. *Olea/Phillyrea*
9. Caryophyllaceae	32. *Ostrya* type
10. *Castanea*	33. *Picea*
11. *Cedrus*	34. *Pinus*
12. Cerealia	35. *Pistacia*
13. Chenopodiaceae	36. Plantaginaceae
14. Cichorioideae	37. Poaceae
15. Cistaceae	38. *Quercus*
16. *Corylus*	39. Ranunculaceae
17. Cruciferae	40. Rosaceae
18. Cupressaceae	41. *Rumex*
19. Dipsacaceae	42. *Salix*
20. *Ephedra*	43. *Tilia*
21. Ericaceae	44. *Ulmus/Zelkova*
22. Fabaceae	45. Urticaceae
23. *Fagus*	46. *Vitis*

Bibliography

Beug, H.-J. (2004). *Leitfaden der Pollenbestimmung für Mitteleuropa und angrenzende Gebiete*. Verlag Dr. Friedrich Pfeil.

Huntley, B. (1990). Dissimilarity mapping between fossil and contemporary pollen spectra in Europe for the past 13,000 years. *Quat. Res.* 33, 360–376.

Moore, P. D., Webb, J. A., and Collison, M. E. (1991). *Pollen analysis.* Blackwell scientific publications.

Olson, D. M., Dinerstein, E., Wikramanayake, E. D., Burgess, N. D., Powell, G. V. N., Underwood, E. C., et al. (2001). Terrestrial Ecoregions of the World: A New Map of Life on Earth. *BioScience* 51, 933–938.

Peyron, O., Guiot, J., Cheddadi, R., Tarasov, P., Reille, M., de Beaulieu, J.-L., et al. (1998). Climatic Reconstruction in Europe for 18,000 YR B.P. from Pollen Data. *Quat. Res.* 49, 183–196. doi:10.1006/qres.1997.1961.

Prentice, C., Guiot, J., Huntley, B., Jolly, D., and Cheddadi, R. (1996). Reconstructing biomes from palaeoecological data: a general method and its application to European pollen data at 0 and 6 ka. *Clim. Dyn.* 12, 185–194.